

**AMMONIUM AMPHIPHILES CARRYING
MESOGENIC UNITS**

SYNTHESIS · PROPERTIES · APPLICATIONS

Marcel D. Everaars

1517 937647

Promotor: dr. E.J.R. Sudhölter,
hoogleraar in de fysisch-organische chemie

Co-promotor: dr. A.T.M. Marcelis,
universitair docent in de organische chemie

Marcel D. Everaars

**AMMONIUM AMPHIPHILES CARRYING
MESOGENIC UNITS**

SYNTHESIS · PROPERTIES · APPLICATIONS

Proefschrift
ter verkrijging van de graad van doctor
op gezag van de rector magnificus
van de Landbouwwuniversiteit Wageningen,
dr. C.M. Karssen,
in het openbaar te verdedigen
op vrijdag 21 maart 1997
des namiddags te vier uur in de Aula

Isn: 937647

ISBN 90-5485-656-4

BIBLIOTHEEK
LANDBOUWUNIVERSITEIT
WAGENINGEN

The cover shows a nematic liquid crystalline phase as observed by polarization microscopy (magnification 1000x).

Stellingen

- 1) In tegenstelling tot fasecontrastmicroscopie wordt helderveldlichtmicroscopie ten onrechte niet geschikt geacht om 'giant vesicles' te observeren.
Menger, F. M.; Gabrielson, K. D. *Angew. Chem.* **1995**, *107*, 2260.
- 2) De regioselectieve cyclisatie van verschillende laurediolen onder invloed H_2O_2 , NaBr en lactoperoxidase in DMSO wordt door Ishihara *et al.* ten onrechte toegeschreven aan de conformatie van het actieve centrum van het enzym.
Ishihara, J.; Kanoh, N.; Murai, A. *Tetrahedron Lett.* **1995**, *36*, 737.
- 3) Bij de verklaring van het verdwijnen van de blauwverschuiving van het UV absorptiemaximum van benzylideeniline-bevattende ammonium amfifielen in bilaagstructuren bij verhoging van de temperatuur wordt voorbij gegaan aan het feit dat onder deze condities de kritische bilaagconcentratie stijgt waardoor wel eens een aanzienlijk deel van de moleculen als monomeer aanwezig kan zijn.
Nishimi, T.; Ishikawa, Y.; Ando, R.; Kunitake, T. *Recl. Trav. Chim. Pays Bas* **1994**, *113*, 201.
- 4) De waargenomen verschuivingen in het UV absorptiespectrum na het mengen van azobenzeen-bevattende ammonium vesikels en didodecyldimethylammonium bromide vesikels worden door Shimomura *et al.* terecht toegeschreven aan de vorming van gemengde bilagen. Ongelukkigerwijs wordt dit proces door hen 'membrane fusion' genoemd.
Shimomura, M.; Kunitake, T. *Chem. Lett.* **1981**, 1001.
- 5) In tegenstelling tot wat soms beweerd wordt vormen dioctadecyldimethylammonium bromide^a en dihexadecylfosfaat^b geen gesloten vesikels door ultrasoon trillen in respectievelijk water en in een 25 mM Tris buffer (pH = 8; 25 °C). Men dient hiermee rekening te houden bij het bestuderen van trans-membraan processen.^a

^aAndersson, M.; Hammarström, L.; Edwards, K. *J. Phys. Chem.* **1995**, *99*, 14531.

^aOkahata, Y.; Ando, R.; Kunitake, T. *Ber. Bunsenges. Phys. Chem.* **1981**, *85*, 789.

^bHammarström, L.; Velikjan, I.; Karlsson, G.; Katarina, E. *Langmuir* **1995**, *11*, 408.

- 6) Voor de hypothese dat interdigitering van mesogene eenheden in vloeibaar-kristallijne fasen wordt gedreven door gunstige electrostatische interacties tussen de permanente dipoolmomenten van de mesogene eenheden kunnen zowel bevestigende als ontkennende voorbeelden worden aangedragen.
- Dit proefschrift.
Imrie, C. T.; Schlee, T.; Karasz, F. E.; Attard, G. S. *Macromolecules* 1993, 26, 539.
- 7) Bij de verslaggeving van grote rampen in het buitenland wordt vaak expliciet vermeld dat er geen Nederlandse slachtoffers zijn. Dit wekt de indruk dat de ramp daardoor minder ernstig is.
- 8) De bestrijding van het broeikas-effect is in eerste instantie geen probleem voor chemici, fysici of biologen maar wel voor sociologen en politici.
- 9) Het is koren op de molen van de Amerikaanse presidenten dat Saddam Hoessein zijn militaire expansiedrift altijd vlak voor de Amerikaanse presidentsverkiezingen plant.
- 10) Doordat in de statistieken over de werkgelegenheid onder chemici ook de mensen op een 'Kenniss Instandhouding Plaats' tot de werkenden worden gerekend wordt een te optimistisch beeld geschetst.
- 11) Als de sportfederaties strengere dopingcontroles zouden houden dan betekent dit dat er jaarlijks minder records worden verbroken waardoor het bekijken van sport voor het publiek minder aantrekkelijk wordt.
- 12) Je kunt beter in een 'drugsstaat' wonen dan in een land dat kernproeven uitvoert.

Stellingen behorende bij het proefschrift

"Ammonium Amphiphiles Carrying Mesogenic Units: Synthesis • Properties • Applications"

Wageningen, 21 maart 1997

Marcel D. Everaars

Voorwoord

Voor u ligt het resultaat van vier jaar sleutelen en meten aan schizofrene moleculen. Iedereen binnen de vakgroep Organische Chemie heeft wel op zijn of haar manier een steentje bijgedragen aan het tot stand komen van dit proefschrift. De behulpzaamheid en collegialiteit van alle medewerkers maken dat ik nu kan terugkijken op vier zeer leuke en leerzame jaren. Ik wil iedereen hiervoor hartelijk bedanken. Enkele personen wil ik nog met name noemen. In de eerste plaats Ernst Sudhölter die mij in de gelegenheid stelde om dit promotieonderzoek uit te voeren. Ik heb de vrijheid die jij mij hebt gegeven om mijn eigen ideeën uit te werken altijd zeer gewaardeerd.

Ton Marcelis, ik ken weinig mensen die zoveel geduld hebben als jij. Bij jou kon ik altijd terecht voor raad en daad, hoe druk je het ook had. De talloze discussies, nuttige suggesties en de kritische beoordeling van de manuscripten hebben in belangrijke mate bijgedragen aan het verschijnen van dit proefschrift in zijn huidige vorm. Bedankt voor de zeer plezierige begeleiding.

Arie Koudijs, van jou heb ik de fijne kneepjes van het synthesevak geleerd. De tijd bij jou op zaal roept nog altijd goede herinneringen op.

Alle studenten die mij zoveel werk uit handen hebben genomen, Alma Kuijpers, Emilie Laverdure, Zanna Koronova en Solenne Denis.

De mensen van de analyse-afdeling, Beb, Hugo en Rien voor de snelle analyses waardoor het onderzoek in vlot tempo kon doorlopen. Ronald, Pleun, Gert en Jurrie voor het aanleveren van de benodigde chemicaliën en het glaswerk. De dames van het secretariaat, Ineke, Elly en Ien voor alle bewezen diensten.

Buiten de vakgroep gaat mijn dank uit naar Nico Sommerdijk (KUN), Blandine Jérôme en prof. dr. W.H. de Jeu (FOM) voor de Röntgendiffractiemetingen en Rob Koehorst (LUW, moleculaire fysica) voor de fluorescentiemetingen. De electronenmicroscopische opnamen zijn gemaakt door Joop Groenewegen (LUW, virologie) en door Jan van Breemen en prof. dr. A. Brisson (RUG). Buiten Nederland hebben prof. dr. G.J. Ashwell (Cranfield, UK) en prof. dr. O.N. de Oliveira Jr. (São Paulo, Brazilië) hun steentje bijgedragen.

Ook de leden van de promotiecommissie prof. dr. J.B.F.N. Engberts, prof. dr. R.J.M. Nolte, prof. dr. Æ. de Groot en prof. dr. M.A. Cohen Stuart wil ik bedanken voor hun inzet.

Mijn speciale dank gaat verder uit naar Gert Jan Kuiper voor het koffiezetten, het wassen van het vuile glaswerk en het destilleren van oplosmiddelen, wanneer het eigenlijk mijn beurt was. Jij deed daar niet moeilijk over en zei dan altijd "ach, ik heb toch niks beters te doen".

Tenslotte wil ik een bijzondere collega bedanken, Cindy, voor jouw steun en behulpzaamheid door de jaren heen. Vooral toen promoveren, solliciteren, verhuizen en een nieuwe baan zich tegelijkertijd aandienen is jouw hulp van groot belang geweest. Bedankt hiervoor.

Marcel

Science is based on facts in much the same way that a house is erected from bricks, but a mere collection of facts is no more a science than a pile of bricks a house.

Henri Poincaré (1854-1912)

CONTENTS

Chapter 1 General introduction

1.1	Lyotropic mesomorphism	2
1.1.1	Self-aggregation	2
1.1.2	Aggregate morphology	4
1.1.3	Krafft temperature	7
1.1.4	Vesicle formation and stability	7
1.1.5	Langmuir monolayers	8
1.2	Thermotropic mesomorphism	10
1.2.1	Thermotropic phase behavior	10
1.2.2	Exciton coupling	12
1.3	Amphotropic mesomorphism	14
1.3.1	General properties	14
1.3.2	Bilayer properties	15
1.3.3	Metal ion binding amphotropes	18
1.3.4	Effects of trans-cis isomerization	19
1.3.5	Amphotrope-polyelectrolyte complexes	20
1.3.6	Langmuir-Blodgett films	20
1.3.7	Second harmonic generation	23
1.4	Outline of the thesis	24
1.5	References	25

Chapter 2 Single chained amphotropes:

Effects of incorporation of mesogenic units in ammonium amphiphiles

Abstract	32	
2.1	Introduction	33
2.2	Results and discussion	33
2.2.1	Lyotropic aggregation behavior	34
2.2.2	Ion-pair amphiphiles	39
2.3	Conclusions	41
2.4	Experimental section	42
2.4.1	Synthesis	42
2.4.2	Methods	43
2.5	References	43

Chapter 3 Metal ion binding amphotrope:

Single chained amphiphile carrying an *o*-hydroxyazobenzene unit

Abstract	46
3.1 Introduction	47
3.2 Results and discussion	47
3.3 Conclusions	52
3.4 Experimental section	52
3.4.1 Synthesis	52
3.4.2 Methods	53
3.5 References	53

Chapter 4 Double chained amphiphiles carrying one mesogen

Abstract	56
4.1 Introduction	57
4.2 Results and discussion	57
4.2.1 Thermotropic properties	57
4.2.2 Aggregate morphology and phase behavior	58
4.2.3 Substituent effects on the phase transition temperatures	62
4.2.4 Monomer exchange experiments	65
4.2.5 Monolayer stability	66
4.2.6 Perfluorinated amphotrope	67
4.3 Conclusions	69
4.4 Experimental section	70
4.4.1 Synthesis	70
4.4.2 Methods	71
4.5 References	72

Chapter 5 Double chained amphiphiles carrying two mesogens

Abstract	74
5.1 Introduction	75
5.2 Results and discussion	75
5.2.1 Thermotropic properties	75
5.2.2 Aggregation behavior in water	78
5.2.3 Mixed amphiphile systems	80
5.2.4 Fluorescence studies	82
5.2.5 Formation of monolayers	84
5.3 Conclusions	87
5.4 Experimental section	87

5.4.1	Synthesis	87
5.4.2	Methods	90
5.5	References	90

Chapter 6 Polymerizable amphotropes

	Abstract	92
6.1	Introduction	93
6.2	Results and discussion	93
6.2.1	Thermotropic properties	93
6.2.2	Lyotropic properties	96
6.3	Conclusions	101
6.4	Experimental section	101
6.4.1	Synthesis	101
6.4.2	Methods	103
6.5	References	103

Chapter 7 Monomer transfer and solubilization of vesicles

	Abstract	106
7.1	Introduction	107
7.2	Results and discussion	108
7.2.1	Vesicle forming properties	108
7.2.2	Monomer transfer between vesicles	109
7.2.3	Solubilization of bilayers	115
7.3	Conclusions	117
7.4	Experimental section	118
7.5	References	119

Chapter 8 Effects of mesogen orientation on self-organization

	Abstract	122
8.1	Introduction	123
8.2	Results and discussion	123
8.2.1	Thermotropic properties	123
8.2.2	Lyotropic properties	124
8.2.3	Monolayer behavior	128
8.3	Conclusions	131
8.4	Experimental section	132
8.4.1	Synthesis	132

8.4.2	Methods	135
8.5	References	136
Chapter 9	Surfactant-polyelectrolyte complexes	
	Abstract	138
9.1	Introduction	139
9.2	Results and discussion	139
	9.2.1 Superstructures from didodecyldimethylammonium bromide and poly(acrylic acid)	139
	9.2.2 Ionically complexed side chain liquid crystalline polymers	145
9.3	Conclusions	146
9.4	Experimental section	147
9.5	References	147
Chapter 10	Triple chained amphotropes	
	Abstract	150
10.1	Introduction	151
10.2	Results and discussion	151
	10.2.1 Thermotropic properties	151
	10.2.2 Monolayer properties	154
	10.2.3 Langmuir-Blodgett films	157
10.3	Conclusions	161
10.4	Experimental section	162
	10.4.1 Synthesis	162
	10.4.2 Methods	163
10.5	References	163
	Summary	165
	Samenvatting	167
	Curriculum vitae	169
	List of publications	171

Chapter 1



General Introduction

1 GENERAL INTRODUCTION

The spontaneous aggregation of molecules to form ordered supramolecular structures is one of the most fundamental processes in the chemistry of life. The biomembrane is perhaps the most well known product of the self-assembly of molecules. The fluid character of the molecules constituting the biomembrane combined with the high degree of orientational order clearly illustrates why this structure is called a liquid crystalline phase or mesophase.

Mesophases which are formed by solvent induced molecular aggregation, water in the case of the biomembrane, are called lyotropic liquid crystalline phases. Mesophases which are induced by temperature effects are referred to as thermotropic liquid crystals. Compounds that combine the properties of lyotropic and thermotropic liquid crystals are the so-called amphotropic liquid crystals.* This intriguing class of compounds is the subject of this thesis.

1.1 Lyotropic mesomorphism

1.1.1 Self-aggregation

The term 'amphiphile' indicates that one part of the molecule likes a polar solvent while the other does not. This causes these molecules to concentrate at the solvent-air interface which usually lowers the surface tension of the solvent. Therefore amphiphiles are often called SURFace ACTive AgeNTS or briefly surfactants.

Self-assembled structures of amphiphiles arise from a delicate interplay between solute-solvent, solvent-solvent and solute-solute interactions. Besides water, self-aggregation has been documented in polar solvents like hydrazine¹, ethyl ammonium nitrate², formamide³, ethylene glycol⁴ and molten pyridinium chloride.⁵ A molecule is amphiphilic in polar solvents when a polar or ionic headgroup region and an apolar tail region are present. There are many chemicals that meet this description. Indeed the organic chemist and nature itself provide us with all thinkable variations on this theme. Variations are found in the number and length of the hydrophobic chains, linear or branched chains, charge of the headgroups *i.e.* cationic, anionic, zwitterionic or nonionic. Also the number of headgroups can be varied. Bola-amphiphiles possess two headgroups at both termini of the hydrophobic part of the molecule. Also dimeric⁶⁻⁸ and trimeric⁹ ammonium surfactants have been reported containing two or three alkyl chains and two or three ammonium headgroups connected by alkyl spacers (Figure 1). These amphiphilic molecules self-assemble to create a microphase in which the hydrocarbon chains sequester themselves inside the aggregate and the headgroups orient themselves towards the polar solvent.

* 'Amphotropic' is also used for a subclass of retroviruses that affect both murine and non-murine cells.

Lyotropic aggregation is not restricted to polar solvents. Fluorocarbons and hydrocarbons are also mutually immiscible. In a perfluorinated solvent a partially fluorinated long chain hydrocarbon behaves as an amphiphilic molecule and aggregates to form micelles with a hydrocarbon core and fluorocarbon headgroups.¹⁰ This solvophobic/solvophilic relationship may be reversed since bilayer assemblies of fluorocarbon amphiphiles have also been observed in aprotic organic media like cyclohexane.¹¹ The common driving force for the molecular assembly is the solute/solvent immiscibility, an enthalpic force that arises from differences in cohesive energy between solute and solvent.

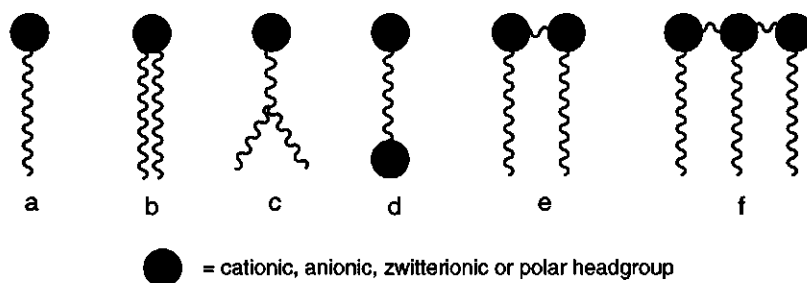


Figure 1. Schematic representation of amphiphilic molecules; a = single chained amphiphile, b = double chained amphiphile, c = branched amphiphile, d = bola-amphiphile, e = dimeric amphiphile, f = trimeric amphiphile.

The forces that govern the attraction between two or more molecules in water are not yet well understood. During the past 50 years there has been much controversy about the driving force for these hydrophobic interactions. A popular interpretation is the 'iceberg model' proposed by Frank and Evans¹² in 1945. The unusually large and negative entropy of dissolution of apolar molecules in water is explained by assuming a 'structuring of the water molecules' in the hydration sphere of the molecule, accompanied by the formation of extra and stronger hydrogen bonds. The association of the apolar molecules is then accompanied by a release of structured hydration water. The gain in entropy (ΔS) is assumed to be the driving force for hydrophobic interactions.

Recently a different interpretation evolved.¹³⁻¹⁵ At more elevated temperatures the hydrogen bond network of water weakens considerably but aggregation of apolar molecules still occurs and is mainly enthalpy (ΔH) driven. The change in Gibbs free energy (ΔG) for aggregation is almost temperature independent. This $\Delta H/\Delta S$ compensation effect upon changing the temperature indicates that changes in the hydrogen bond network do not govern the aggregation. The hydrogen bond network of water seems to be hardly disturbed by the apolar solute. Furthermore, hydrophobic hydration is an enthalpically favorable process. A tangential orientation of the O-H bonds of the water molecules relative to an apolar surface is most favorable. Possibly, the reduced rotational freedom and a compression of the water molecules

in the hydration sphere, without the formation of new hydrogen bonds, contribute to the negative entropies of dissolution. The small size of water molecules makes that many water molecules are involved in the hydration spheres. Besseling and Scheutjens^{15a} support the view that the hydrogen bond network has to stretch slightly in order to accomodate the intruder. In analogy to a polymer network this stretching will cost entropy.

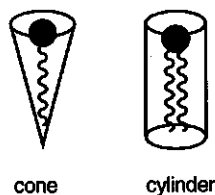
When the concentration of the solute increases, the hydration spheres start to overlap. This occurs when there is not sufficient water to complete the hydrophobic hydration spheres. This leads to a loss in hydrogen bonds and induces hydrophobic interactions. Consequently, the apolar molecules start to aggregate and London dispersion interactions between the apolar parts induce the formation of micelles or bilayer structures. The concentration at which aggregation is induced is called critical hydrophobic interaction concentration (chic).^{15b} For amphiphiles this concentration is equal to the critical micelle concentration (cmc) or critical bilayer concentration.

1.1.2 Aggregate morphology

For amphiphiles the aggregate morphology is determined by very delicate attractive interactions between the hydrophobic parts and repulsive interactions between the hydrated headgroups. Very important are also the molecular packing constraints within the core of the aggregate.¹⁰ A qualitative prediction of the aggregate morphology of an amphiphile in water can be given using the so-called surfactant parameter, P , introduced by Israelachvili, Mitchell and Ninham.¹⁶ P is defined by the ratio between the volume of the hydrophobic moiety of the surfactant molecule ($v = 27.5 + 27n_c$) and the product of the length of the tail ($l_c = 1.5 + 1.27n_c$) and the headgroup area of the surfactant a_0 (n_c is the number of carbon atoms in the tail). This last quantity, a_0 , can be determined by experiments or be estimated. The P values are linked to a preferential molecule packing which then determines the aggregate morphology. Cone shaped molecules ($P < 1/3$) can easily pack to form aggregates with high curvatures like micelles whereas cylindrical molecules ($P = 1$) prefer to form flat bilayer structures.

$$P = \frac{v}{a_0 l_c}$$

spherical micelles	$P < 1/3$
worm-like micelles	$1/3 < P < 1/2$
bilayers	$1/2 < P < 1$
inverted micelles	$P > 1$



Factors such as solvent ionic strength, temperature, degree of hydrogen bonding between the headgroups, headgroup hydration and hydrocarbon chain extension and unsaturation will all

affect the monomer shape. The influence of these factors cannot always be measured and is therefore not incorporated into the equation.

The most popular model for micelles nowadays is the model proposed by Gruen¹⁷ (see Figure 2). The micelle can be divided into two regions, namely the core of the micelle which contains the chains of the surfactant and the Stern layer in which the headgroups, part of the counter ions and water are located. Chain bending is allowed resulting in chain looping and partial exposure of the chain termini to the water. However, there is almost no water penetration into the micellar core.

Double chained surfactants tend to form bilayer structures. The idea that lipids in a cell membrane are arranged in a bilayer was first proposed in 1925 by Gorter and Grendel.¹⁸ In 1972 Singer and Nicolson¹⁹ proposed the fluid mosaic model in which the membrane is depicted as a fluid-like lipid bilayer containing freely diffusing proteins (see Figure 2). In 1977 Kunitake and Okahata²⁰ reported that the synthetic amphiphile didodecyldimethylammonium bromide would also form bilayer vesicles upon sonication in water. Since then the number of synthetic bilayer forming amphiphiles has increased enormously.

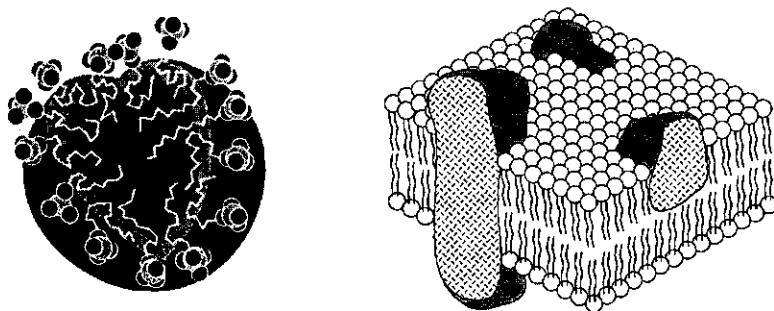


Figure 2. Gruen's micelle (left) and the fluid mosaic model for a bilayer membrane (right). Taken from reference 22a.

Like biomembranes these synthetic membranes exist in a gel phase (L_β) at low temperatures, with all trans rotamers in the alkyl chains. When the temperature is increased and exceeds a critical value which is characteristic for each amphiphile, the alkyl chains melt into the liquid crystalline phase (L_α) which contains some gauche rotamers.^{21,22} The temperature at which this transition occurs is defined as the phase transition temperature T_c . Generally, the T_c value decreases with decreasing chain length and increasing asymmetry of the alkyl chains.^{23,24} Differential scanning calorimetry is an extremely suitable method to measure the phase transition temperature and enthalpy change. From the phase transition enthalpy the patch number^{25,26} can be calculated. The patch number is the number of monomers in the bilayer that undergo the phase transition simultaneously.

The formation of bilayer structures is not limited to the conventional amphiphiles. In the 1950s S. W. Fox reported that random thermal copolymerization of amino acids yields products which resemble proteins. These so-called proteinoids form cell-like spherules composed of bilayer membranes in water.²⁷⁻³¹ According to the author these structures might have played an important role in the evolution of life.

Besides normal micelles and bilayer vesicles a number of other lyotropic phases are known like rod-shaped micelles, inverted micelles, hexagonal phases and cubic and lamellar phases. A schematic representation of these phases is given in Figure 3.

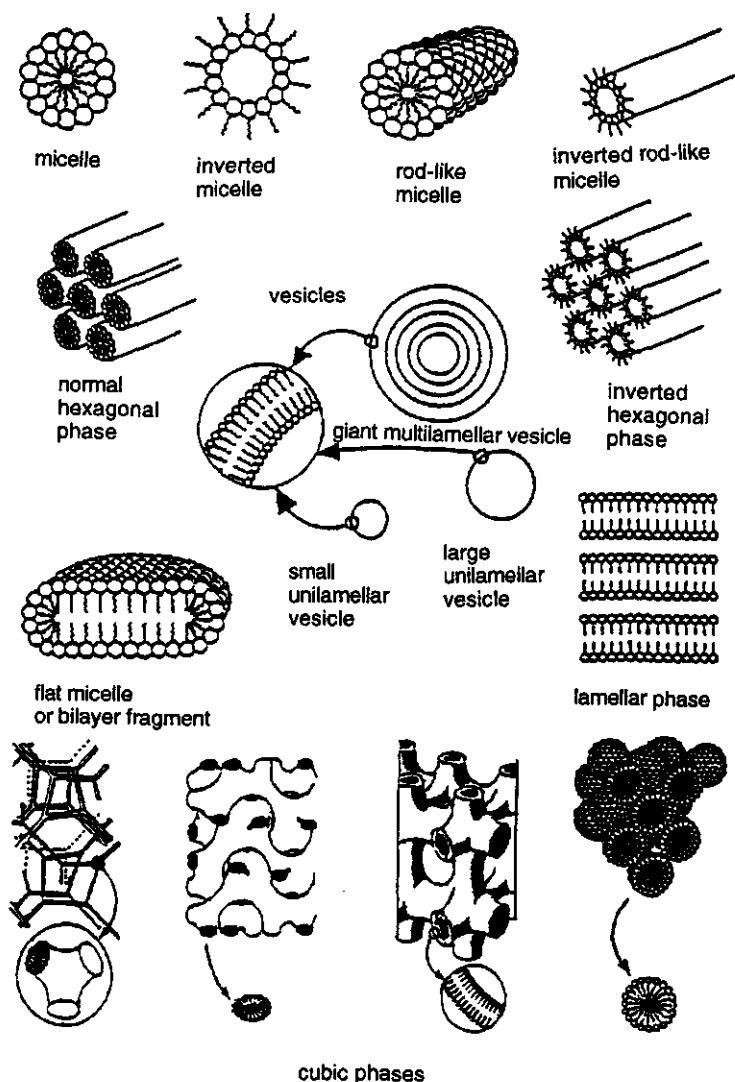


Figure 3. Schematic representation of various lyotropic phases. Taken from ref. 49.

1.1.3 Krafft temperature

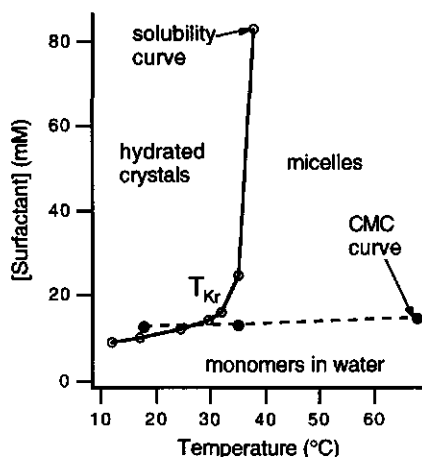


Figure 4. The Krafft phenomenon for surfactants.

The temperature at which the surfactant solubility equals the critical aggregation concentration is called the Krafft temperature (T_{Kr}). Just above this point the surfactant solubility increases rapidly and a homogeneous dispersion of surfactant aggregates is formed.¹⁰ The Krafft phenomenon reflects the equilibrium between surfactants in solution and in hydrated crystals and can be regarded as the melting point of the hydrated crystals.³² Surfactant solutions below their T_{Kr} can remain in a metastable state for days before crystallization occurs. The T_{Kr} is determined by the packing of the molecules in a crystal lattice. Within a homologous series of surfactants T_{Kr} increases with increasing chain

length and an odd-even effect has been observed.^{33,34} The T_{Kr} is also influenced by the choice of the counter ion and by branching or unsaturation of the alkyl chains.

1.1.4 Vesicle formation and stability

Literature overwhelmingly reports the spontaneous formation of thermodynamically stable vesicles.³⁵⁻³⁷ Most of these claims are, however, erroneous.³⁸ When lipid films or surfactant crystals are hydrated the lamellae swell and grow into myelin structures which in general do not spontaneously detach from the crystal, with the exception of a few particles formed as the result of crystal imperfections. The energy needed for the formation of myelin structures is provided by the exothermic hydration reaction. The hydrated layers at the surface of the crystal however prevent the hydration of the molecules in the interior of the crystal. Only mechanical agitation provided by swirling, shaking or vortexing causes the bilayer tubules to break and to reseal the exposed hydrocarbon edges, and this results in the formation of (multilamellar) vesicles.^{39,40} Without external energy input no vesicles will be formed. In order to produce smaller or unilamellar vesicles, additional energy has to be dissipated into the system. This can be done mechanically (sonication, extrusion), electrochemically (changes of pH, ionic strength, surface potential etc.) or chemically (change of solubility conditions, dissolving or adsorbing molecules into the outer leaflet of the bilayers). The higher the energy input, the smaller and more numerous the vesicles become. This explains why different preparation procedures yield different size distributions of the vesicles.

The vesicles so formed may be stable for months or years but they are not thermodynamically stable. With time passing they aggregate, fuse and eventually precipitate as stacks of flat, fully

hydrated bilayers, so-called flocculae. With every vesicle fusion the energy associated with the curvature of the membrane is halved. Eventually lamellar phases will be formed and vesicles can be regarded as high energy intermediates between the crystalline state and the fully hydrated lamellar phase. Spontaneous formation of thermodynamically stable vesicles is only possible in the case that a bilayer adopts a spontaneous curvature. For practically all single component bilayers this is not the case.

Most vesicles are in a metastable state but locked in a kinetic trap. Vesicle aggregation is prevented, apart from entropy contributions, by mutual repulsive forces between the hydration spheres, thermal fluctuations of the bilayers and electrostatic repulsions (for ionic surfactants).⁴¹ Vesicle fusion can be induced by the addition of fusogenic agents, usually divalent ions. A prerequisite for induced fusion is however that the bilayer is in its liquid-crystalline phase.^{42,43}

The stability of vesicles can be increased by using polymerizable amphiphiles and polymerization of the monomers in the vesicles.⁴⁴ Also polymerizable counter ions have been used to prepare 'vesicles in a net'.⁴⁵⁻⁴⁷ The adsorption of polymers to vesicle surfaces can also increase their stability.⁴⁴

Vesicles have been proposed as vehicles for drug targeting. However, the utilization of vesicles for delivering encapsulated therapeutic agents is severely limited by the rapid removal of these particles from the blood stream by specialized phagocytic cells in the liver and spleen. When lipids which are modified with poly(ethyleneglycol) are incorporated into vesicles a steric barrier is formed outside the membrane. These so-called 'stealth vesicles' remain in the blood up to 100 times longer than conventional vesicles.⁴⁸⁻⁵⁰

As stated before large vesicles are obtained when little energy is dissipated into the system. In this way so-called giant vesicles can be made. These vesicles can reach diameters up to 100 μm and can readily be observed by light microscopy. Didodecyldimethylammonium bromide is especially prone to the formation of these large structures. This finding led to the development of 'cytomimetic chemistry' by Menger *et al.*⁵¹⁻⁵⁵ The giant vesicles exhibit a number of cell-like processes like osmotic activity, fission, fusion, endocytosis, birthing and foraging. Also autocatalytic self-reproduction of giant vesicles has been reported.⁵⁶

1.1.5 Langmuir monolayers

Molecular films at the water-air interface are denoted as Langmuir films. Using a trough with movable barriers allows manipulation of the film at the water-air interface and simultaneous recording of the so-called surface pressure-area (π -A) isotherm. The surface pressure is defined as the difference between the surface tension of the pure subphase and the monolayer covered subphase. The monolayers are usually spread from volatile organic solvents. The different spreading kinetics of different solvents can influence the monolayer morphology.⁵⁷ The general method to record π -A isotherms is to use a constant rate of compression. This implies that the

strain rate of compression increases during the experiment. It has been suggested that it would be better to use a constant strain rate of compression. Then differences between isotherms using different strain rates can be correlated with relaxation times of molecular processes in the monolayer.⁵⁸

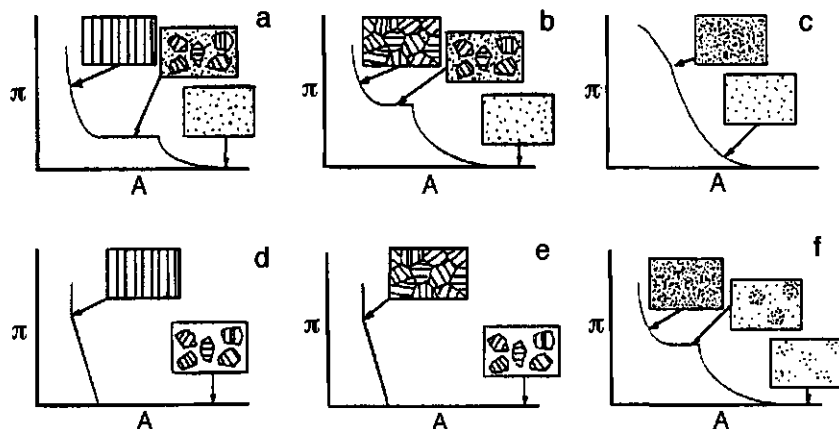


Figure 5. π - A isotherms for a compound with a strong (a,b,c) and a weak (d,e,f) headgroup repulsion at different temperatures. The temperature increases from left to right. The monolayer can be amorphous or crystalline. The crystalline domains have elastic properties at low temperature (a,d) and viscoelastic properties at more elevated temperatures (b,e). Taken from ref. 58b.

The isotherms give information about the molecular cross-section and orientational behavior of the amphiphiles as well as about interactions with substances dissolved in the subphase. Depending on the available area per molecule, the temperature and composition of the subphase, and the nature of the compound the molecules in the monolayer can be in different phases (Figure 5). At large molecular areas molecules with strong headgroup repulsions are in a liquid expanded phase. Upon compression the molecules adopt a liquid condensed or crystalline phase. This phase can, below a certain temperature, coexist with the liquid expanded phase over a certain range of molecular areas. When all molecules are in the condensed or crystalline phase the surface pressure increases steeply upon further compression. At high surface pressures the monolayer collapses. This collapse is often described as a cooperative folding over to generate an organized trilayer.^{59,60a} After expansion and subsequent recompression of the monolayer the initial isotherm can be restored sometimes.

Stable monolayers can often be transferred onto solid substrates by dipping the substrate vertically or horizontally through the monolayer. Commonly used substrates are glass and quartz slides, silicon wafers and mica. Upon vertical dipping of hydrophilic substrates (water meniscus points upward) the first monolayer is deposited in the receding mode, on hydrophobic substrates (water meniscus points downward) in the advancing mode. Depending

on the polarity of the substrate surface after deposition of each subsequent monolayer, three different multilayer assemblies can be obtained.

X-type: head-to-tail arrangement with the headgroups pointing away from the substrate.

Y-type: the molecules are arranged head-to-head and tail-to-tail.

Z-type: head-to-tail arrangement with the headgroups pointing toward the substrate.

The Y-type deposition is the most commonly observed deposition mode and yields the most stable multilayers. X- and Z-type multilayers often transform into Y-type structures due to molecular turnaround.^{60b} So far only few monomeric materials have shown to give stable X- or Z-type structures.

The organization of the monolayer at the water-air interface can be visualized by either fluorescence or Brewster angle microscopy. The molecular orientation of the molecules at the water-air interface and in the deposited films has been studied with polarized Fourier-transform infrared spectroscopy, UV-VIS absorption spectroscopy, X-ray diffraction and second harmonic generation.

1.2 Thermotropic mesomorphism

1.2.1 Thermotropic phase behavior

Thermotropic liquid crystalline phases or mesophases are usually formed by rod-like (calamitic) or disk-like (discotic) molecules.⁶¹⁻⁶³ The presence of a rigid core is essential and is therefore referred to as 'mesogenic unit'. The molecules in these phases have orientational order but reduced positional order. Globular compounds can form plastic crystalline phases. The molecules in these phases have positional order but no orientational order.

Rod-like molecules can form smectic or (chiral) nematic phases (Figure 6). Disk-like molecules can form columnar discotic or nematic phases. The mesophase is called 'enantiotropic' if the mesophase is formed both upon heating the crystalline phase and upon cooling from the isotropic phase. Mesophases are referred to as 'monotropic' if they are solely formed upon cooling from the isotropic phase. Monotropic mesophases are therefore not thermodynamically stable and will crystallize sooner or later.

In the *nematic phase* there is a high degree of order with regard to the orientation of the molecules although the molecules have rotational and translational freedom. The only difference with the isotropic phase is thus that the molecules are oriented with their long axes more or less parallel to each other. Between crossed polarizers the nematic phase is characterized by thread-like, marbled or Schlieren textures (see Figure 7a). Upon cooling from the isotropic phase the nematic phase appears first as droplets.⁶¹

According to the 'swarm hypothesis' proposed by Bose⁶⁴ not all molecules in the nematic phase have the same orientation but they are grouped in aggregates or swarms. The molecules

within a swarm lie parallel to each other but in an orientation which is random with respect to molecules in other swarms. These swarms give rise to the typical patterns observed between crossed polarizers. The turbid appearance of the mesophase is attributed to light scattering caused by the swarms. The swarm hypothesis also explains the strong orientational effect of electric and magnetic fields on the nematic phase.

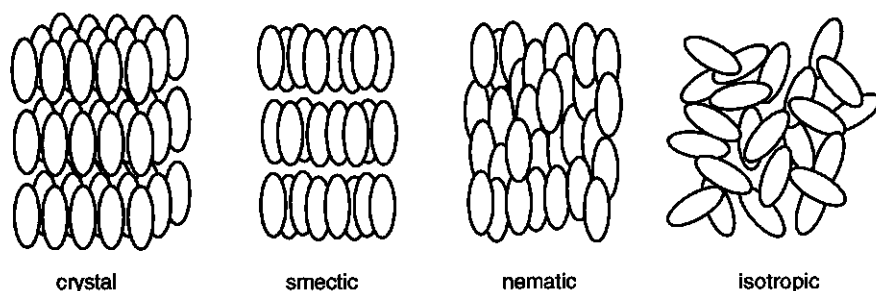


Figure 6. Schematic representation of different thermotropic phases.

The *chiral nematic* or *cholesteric phase* is a nematic phase that is composed of optically active molecules. As a consequence a spontaneous twist in the phase is induced about an axis normal to the preferred molecular direction. In racemates both enantiomers counteract each other which results in the formation of a normal nematic phase. If the nematic phase is doped with a small fraction of chiral molecules, a cholesteric ordering can be induced. The helical superstructure is responsible for some unique optical properties such as selective reflection of circularly polarized light and an optical rotation which is approximately 1000 times larger than for a normal optically active compound.

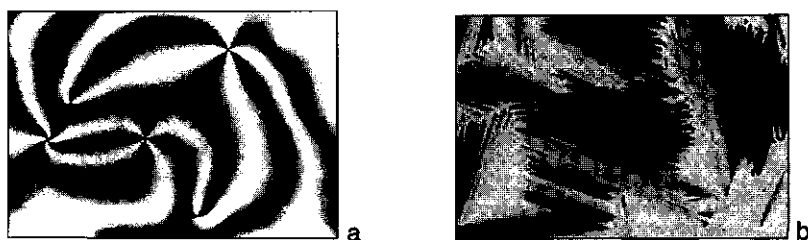


Figure 7. (a) Nematic Schlieren texture. (b) smectic fan-shaped focal-conic texture viewed between crossed polarizers.

Smectic mesophases have layered structures. The attractive forces between the layers are weak compared to the lateral attraction between the molecules. Therefore the layers can slide over one another quite easily. This gives the smectic phase fluid properties although it is usually more viscous than a nematic phase. Within these layers the ordering of the molecules is variable. In

smectic A the molecules are oriented, on average, perpendicular to the layer plane but are irregularly distributed over the layer, without long range order. Smectic B differs from smectic A because the molecules are hexagonally packed. Smectic C resembles smectic A but the molecules are inclined with respect to the layer normal. A dozen more smectic phases have been identified. Between crossed polarizers the smectic A phase is characterized by a fan-shaped focal-conic texture. A homeotropically aligned (*i.e.* layers parallel to the supporting glass) smectic C phase shows Schlieren textures. Upon cooling from the isotropic phase a smectic phase appears first as bâtonnettes.⁶¹

The layer spacing can be determined by X-ray diffraction. When mesogens have large dipole moments the neighboring molecules can minimize their unfavorable dipole interaction by assuming an antiparallel orientation.⁶¹

Discotic mesophases are formed by disk-like molecules which are arranged into columnar stacks. These columnar stacks are hexagonally packed. Also disordered nematic phases are found for disk-like molecules.

1.2.2 Exciton coupling

Excitons are mobile excited states in an molecular array of organic materials. In regularly ordered molecular arrays the excited state can hop from molecule to molecule without separation of the electron-hole pair (Frenkel exciton). Kasha developed a simple theory to explain exciton coupling in dimers.⁶⁵⁻⁶⁹ It explains qualitatively the observed spectral properties of dimers and higher aggregates. This theory is based on the assumption that the transition moment for an electronic transition can be considered to be localized in the center of a chromophore and has its polarization axis parallel to the long axis of the chromophore. The interaction between two molecules causes the excited state in the monomer to split into two states in the bichromophoric complex. If there is no direct overlap between the molecular orbitals of the chromophores, the exciton splitting energy is given by:

$$E_{\text{ex}} = \frac{\mathbf{M}_a \cdot \mathbf{M}_b}{r^3} - \frac{3(\mathbf{M}_a \cdot \mathbf{r})(\mathbf{M}_b \cdot \mathbf{r})}{r^5}$$

where \mathbf{M}_a and \mathbf{M}_b are the transition moments of the electronic excitations in the chromophores a and b respectively. \mathbf{r} is the vector between the centers of two chromophores and r is its magnitude. Because the transition moment is a vector, the magnitude of the interaction depends not only on the distance r but also on the relative orientation of the chromophores a and b. The energies of the resulting two states relative to the monomer excited state (E_m) are given by:

$$E^{\pm} = E_m \pm E_{\text{ex}} + D$$

where D is the dispersion or Van der Waals interaction energy.

For parallel transition moment dipoles the out-of-phase transition dipole arrangement corresponds electrostatically to a lowering of energy (E^-). Because the transition dipoles cancel each other the transition to this lower energy level is forbidden. Only the transition to the higher energy level corresponding to the in-phase dipoles is allowed (E^+). Parallel chromophore aggregation, also called H-aggregation, therefore results in a shift of the UV absorption maximum to lower wavelengths (blue shift) with respect to the monomer absorption maximum. For in-line transition dipoles the in-phase transition dipole arrangement corresponds to the lowest energy level and the out-of-phase arrangement to the highest level. This means that only the transition to the lowest energy level is allowed. This results in a shift of the UV absorption maximum to higher wavelengths (red shift). This type of aggregates is also called J-aggregates. The shift of the absorption maximum (in wavenumber $\Delta\nu$) for an aggregate consisting of N monomers with respect to the monomer absorption is given by⁵⁷:

$$\Delta\nu = \frac{2}{hc} \frac{N-1}{N} \frac{\mu^2}{r^3} (1-3\cos^2\alpha)$$

in which μ is the magnitude of the transition moment, r the magnitude of the center-to-center distance between the chromophores and α the angle between the chromophore long axes and the chromophore center-to-center line.

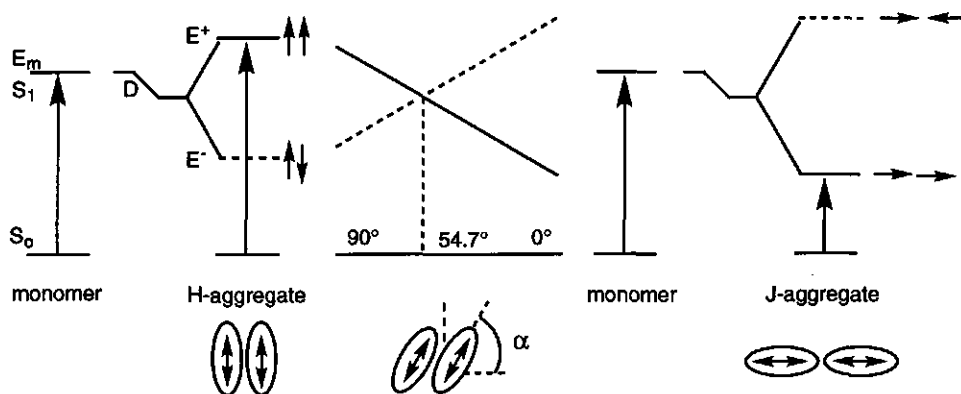


Figure 8. Schematic representation of the exciton splitting of the excited state in a bichromophoric complex according to Kasha.

Fluorescence always occurs from the lowest excited state level. Exciton fluorescence will thus be red shifted with respect to the monomer emission. Because the transition from the lowest excited level to the ground state is forbidden for H-aggregates, the fluorescence of these aggregates is considerably quenched.

1.3 Amphotropic mesomorphism

1.3.1 General properties

Liquid crystalline phases are characterized by a combination of specific ordering and mobility of the molecules in the system. Whereas in lyotropic mesophases this is induced by the solvent, the formation of thermotropic mesophases is caused by temperature induced mobility of form anisotropic molecules. Amphotropic molecules (αμφι = both, τρεπεν = to align) are molecules which, because of their structure, can be ordered according to both principles. Amphotropic behavior has for example been observed for some phospholipids,⁷⁰ alkylated monosaccharides⁷¹ and for amphiphilic metal salts.⁷² These compounds have the structure of normal amphiphiles but nevertheless show thermotropic mesomorphic behavior.

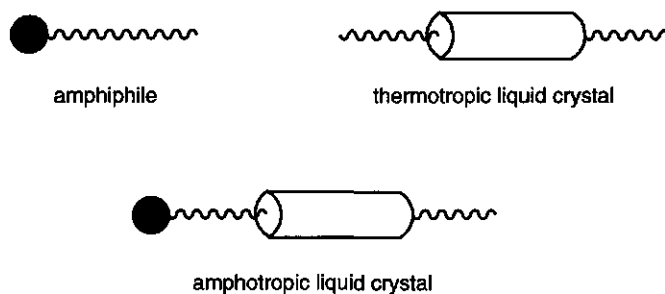
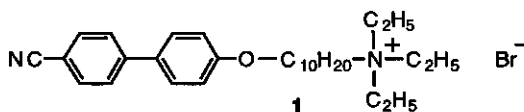


Figure 9. Schematic representation of amphiphiles, liquid crystals and amphotropes.

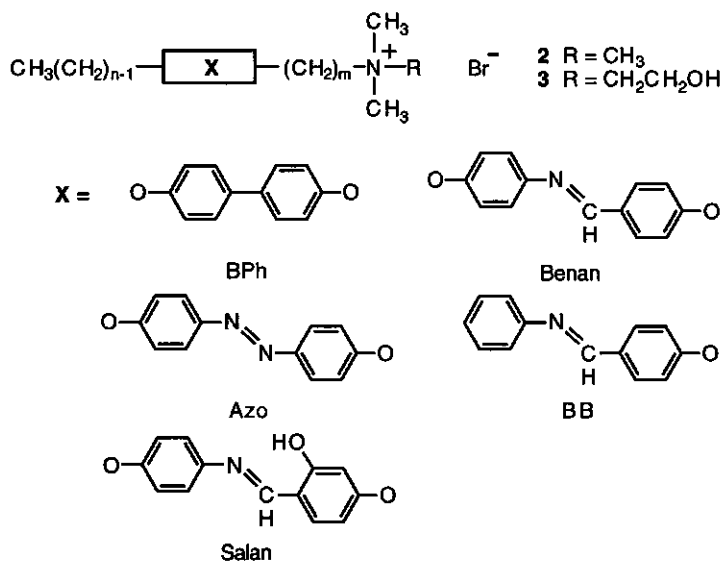
By the introduction of rod- or disk-like building blocks, which are typical of thermotropic liquid crystals, in amphiphiles the number of amphotropic compounds has increased considerably.⁷³ An example of an amphotropic compound is compound **1**.⁷⁴ In addition to being a thermotropic liquid crystal this compound forms a lyotropic lamellar phase (L_α) over the concentration range of 25–70 wt % of surfactant in water and a micellar phase (L_1) at lower surfactant concentrations. Hexagonal (H_1) and bicontinuous cubic (V_1) phases were not observed. The similar but not amphotropic compound hexadecyltriethylammonium bromide however forms the phase sequence L_1 , H_1 , V_1 , L_α on increasing surfactant concentration. The destabilization of the high curvature mesophases (H_1 , V_1) by the bulky cyanobiphenyloxy group obviously stems from the difficulty of packing to high density in these curved structures.



If a rigid π -system and an alkyl chain are covalently bound in one amphotropic molecule, it is not clear *a priori* if this molecule will spontaneously assemble into a layered structure. In order to get stable layered assemblies of amphotropic molecules several conditions must be met.⁷⁵⁻⁷⁸ The first condition is that the cross-sectional area of the aromatic part of the molecule should match with that of the alkyl part. If this requirement is not exactly met this can be compensated for by tilting or interdigitation of the alkyl chains or the aromatic units. The aromatic units tend to aggregate spontaneously in layers, usually forming herringbone structures. The alkyl chains also spontaneously assemble into layer structures which can be viewed as pseudo-hexagonally close-packed. The second condition is that the intra-assembly planes - the layered alkyl chains and the layered mesogens - will be commensurate, *i.e.* will have an epitaxial matching of the sublattices. The third condition is that the valence geometry of the bond between the aromatic part and the alkyl part must not perturb the cross-sectional match and epitaxy in the two dimensional layer. If one of these conditions is not met, one of the layers will be less close-packed and ordered, and the system will not form stable layered structures.

1.3.2 Bilayer properties

Kunitake et al. investigated a great number of amphotropes of the type tail-mesogen-spacer-headgroup with mesogenic units like biphenyl (BPh), azobenzene (Azo), diphenylazomethine (BB), benzylideneaniline (Benan) and salicylideneaniline (Salan). Cationic headgroups like trimethylammonium bromide and hydroxyethyltrimethylammonium bromide were used (2 and 3). Also anionic (phosphate), nonionic (polyoxyethylene) or zwitterionic (aminimide) headgroups were used.⁷⁹



The compounds **3** with azobenzene units form stable bilayer structures when $n = 12$, irrespective of the spacer length m .⁸⁰ When $n \leq 6$ no stable bilayers are formed, irrespective of m . For $n = 10$ with $m = 5, 6, 8$ and 10 and for $n = 8$ with $m = 10$ also bilayers are formed. The mode of molecular packing in the bilayer assembly is determined by the combination of the lengths of the spacer and the alkyl tail. As typical examples, the combination of the C_{12} tail and the C_5 spacer produces a bilayer packing with tilted molecular orientation, whereas the combination of C_8 tail and C_{10} spacer produces a parallelly interdigitated packing.^{81,82} The aggregation behavior of single chained ammonium amphiphiles containing benzilideneaniline and salicylideneaniline units is essentially identical to that of azobenzene containing amphiphiles.^{83,84}

The different modes of assembly are also reflected in the UV absorption maximum of the azobenzene units. As predicted by the molecular exciton theory of Kasha (see section 1.2.2) the tilted bilayers give rise to a red shift (J-aggregates) and the parallelly interdigitated bilayers (H-aggregates) to a blue shift of the UV absorption maximum.

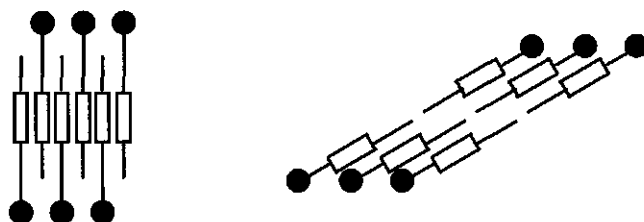


Figure 10. *interdigitated bilayer*

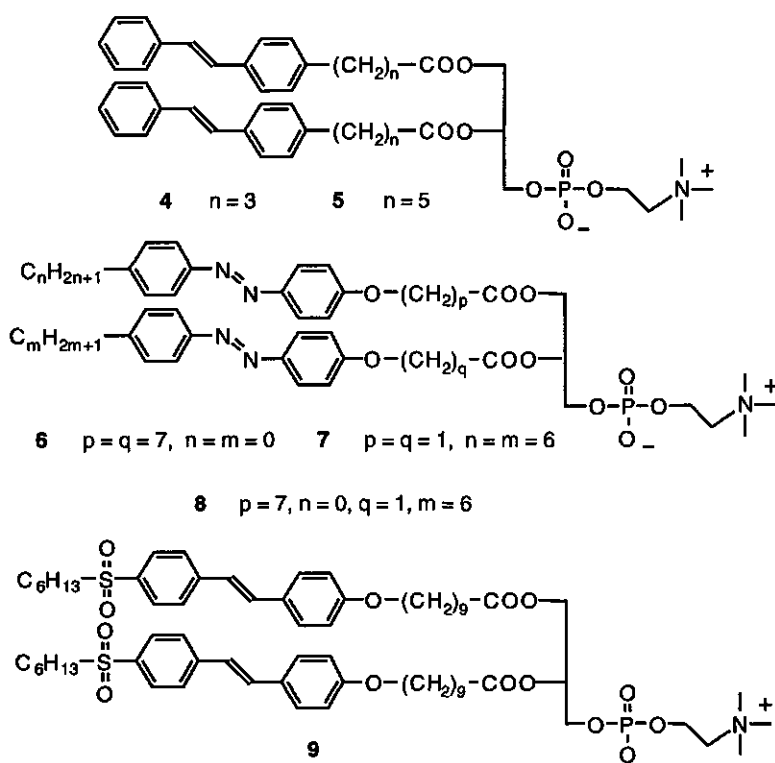
tilted bilayer

For some of the bilayers the spectral shift changes at the phase transition temperature of the bilayer. This is attributed to reduced chromophore stacking in bilayers which are in their liquid-crystalline state.^{80,83,84} When these bilayer dispersions are cast onto a solid substrate the chromophore stacking is maintained. These cast films possess regular multilayer structures.⁸¹ Apparently, vesicular or lamellar aggregates in water are transformed into macroscopically extended bilayers parallel to the substrate surface. In these films the mesogenic units are thus oriented more or less perpendicular to the surface. Upon heating or upon exposure of these cast films to moisture the molecules undergo reversible crystal packing transformations.^{85,86}

When bilayer vesicles of $C_{12}AzoC_{10}N$ (**2**) are mixed with a large excess of vesicles of didodecyltrimethylammonium bromide, the stacking of the chromophores is lost. This is monitored by the disappearance of the blue shifted absorption maximum and the appearance of the absorption maximum of the non-stacked mesogenic units. This phenomenon was attributed to a spontaneous fusion process of both types of bilayer vesicles resulting in mixed bilayers in which there is no stacking of the mesogenic units anymore.⁸⁷ The exact mechanism of the fusion process was not elucidated but in a personal communication the author stated that he did

not mean a fusion process in the sense of two vesicles merging into one big vesicle but referred to a random mixing of amphiphiles. When bilayer aggregates of $C_{12}AzoC_{10}N$ are sonicated with only a tenfold excess of didodecyldimethylammonium bromide vesicles, a part of the $C_{12}AzoC_{10}N$ molecules becomes monomerically dispersed in the didodecyldimethylammonium bromide matrix whereas the other part remains clustered. This phase separation equilibrium is strongly dependent on the physical state of the didodecyldimethylammonium bromide bilayer *i.e.* whether it is in the gel or liquid crystalline phase.⁸⁷

Extensive studies on the aggregation properties of trans stilbene and azobenzene containing amphiphiles have been performed in the group of David Whitten.⁸⁸⁻⁹⁶ The phosphatidylcholine derivatives **4** and **5** form bilayer structures in water.⁸⁸⁻⁹¹ H-aggregates are formed in compressed LB monolayers and in the bilayer aggregates. The similarity of the absorption spectra and the photophysics of LB films and of vesicles suggests similar aggregation of the stilbene units in both systems. Monte Carlo simulations show that the aromatic units of these amphiphiles most favorably pack in a herringbone structure H-aggregate.



The chirality of the headgroup induces a chiral packing of the mesogens in the bilayer as is observed by the strong induced circular dichroism (ICD) for the vesicles of **4**, **5** and **6**. This chiral superstructure is lost upon isomerization of the trans mesogens to the cis form as is seen by the loss of the ICD.⁹¹

A rapid monomer exchange equilibrium is established between aqueous dispersions of **4** or **5** and dimyristoylphosphatidylcholine (DMPC) vesicles at room temperature.⁹⁰ The absorption spectra recorded as a function of time show two isosbestic points suggesting that the H-aggregates decompose directly into isolated chromophores due to the formation of mixed bilayers.

For vesicles of **6** a larger aggregation number for the chromophores and a higher T_c was found than for vesicles of **7** and **8**. This is attributed to a better packing of chromophores when the chromophores are more decoupled from the headgroup.

The molecular packing in aggregates of **9** (with the 4,4' donor-acceptor substituents) is essentially the same as for the compound without these substituents.⁹² The dipole induced by these substituents may have been expected to have a significant effect on the two-dimensional packing and ordering of these molecules. This result however suggests that dispersive rather than electrostatic interactions are dominant aggregation forces for stilbenes incorporated in amphiphiles.

1.3.3 Metal ion binding amphotropes

The degree of phase separation of the amphotropic molecules **10** and **11** in a matrix bilayer of dihexadecyldimethylammonium bromide can be regulated by the addition of Cu^{2+} ions to the aqueous dispersion.^{97,98} By the binding of Cu^{2+} ions to the headgroups of compounds **10** and **11** phase separation is induced. The metal ion binding can be monitored by the blue shifting of the UV absorption maximum due to the phase separation. These systems can be regarded as membrane based metal ion sensors.

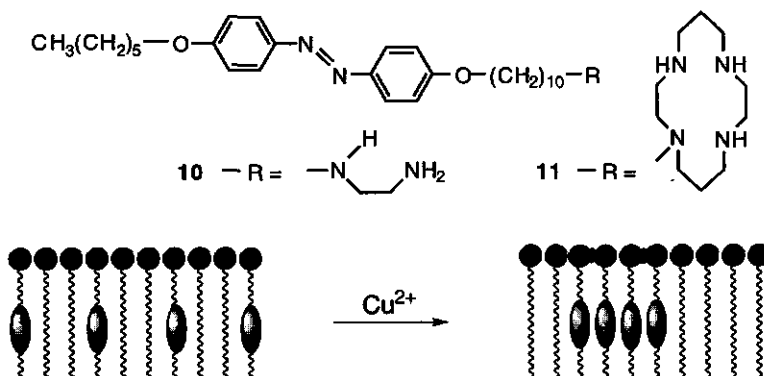
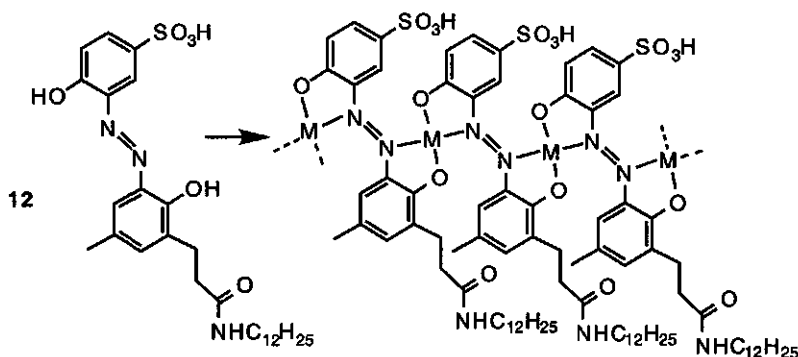


Figure 11. Phase separation induced by the binding of Cu^{2+} to the headgroup of the amphotropes.

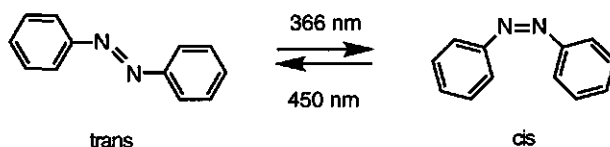
The amphotropic compound **12** which has an *o,o'*-dihydroxyazobenzene unit as headgroup forms rod-like bilayer membranes in water. This mesogenic unit binds metal ions resulting in the formation of coordinatively polymerized bilayers.⁹⁹ The binding of metal ions is accompanied by changes in the UV absorption spectrum and in the aggregate morphology. The Co(II) complex forms helical superstructures.



1.3.4 Effects of trans-cis isomerization

When azobenzene mesogens are incorporated in amphiphiles, the lyotropic behavior of these compounds is strongly influenced by the trans-cis isomerization state of the azobenzene unit.

The isomerization of $C_{12}AzoC_nN$ (**2**) with $n = 2, 4$ and 10 is accompanied by a change in aggregate morphology.¹⁰⁰ The trans isomer forms globular bilayer aggregates in water with diameters of 20 nm. Upon irradiation with light of 366 nm the globular aggregates are transformed into short rods with diameters of 5-7 nm. Further irradiation at 450 nm restored the original globular morphology.



Trans-cis photoisomerization of similar azobenzene containing surfactants also increases the critical aggregation concentration and reduces the degree of counterion binding.^{15,16} This is attributed to a difference in aggregation mode of the trans surfactant and of the trans-cis mixture. The effects are most pronounced when the azobenzene unit is located in the middle of the molecule, where isomerization results in the most drastic change in the shape of the molecule.

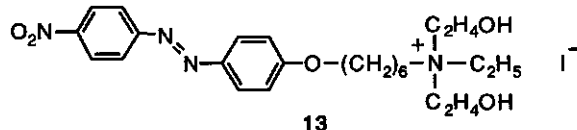
Incorporation of azobenzene containing amphiphiles in dimyristoylphosphatidylcholine (DMPC) and dipalmitoylphosphatidylcholine (DPPC) vesicle membranes results in membranes

whose permeability can be regulated by photoisomerization of the azobenzenes.^{101,102} These membranes can be regarded as simple model systems for photoreceptors in living systems.

The rate of isomerization is very dependent on the physical state of the bilayer. It is faster in a liquid crystalline bilayer than in a rigid gel bilayer.¹⁰³ In the liquid crystalline phase the so-called frictional force against photoisomerization is smaller.

1.3.5 Amphrotrope-polyelectrolyte complexes

Ionic surfactants and oppositely charged polyelectrolytes spontaneously form addition complexes which precipitate from aqueous solution. A highly cooperative zipper mechanism is usually observed which begins to operate already at very low concentrations and complexes with a 1:1 stoichiometry are usually observed.¹⁰⁴ Recently, the solid state structure and material properties of these complexes have become focus of interest. It turned out that these complexes can easily be redissolved in organic solvents and cast to films of high homogeneity and mechanical stability. The lamellar bilayer structure is usually preserved in the bulk and the polymer acts as an external stabilizer.¹⁰⁴⁻¹⁰⁹ One might say that these complexes combine the ability of surfactants for self-organization with the excellent stability and mechanical properties of polymers.



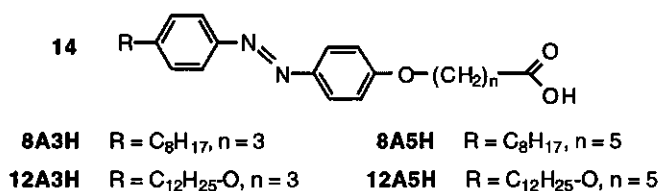
Complexation of amphotropic molecules with oppositely charged polyelectrolytes usually results in a stabilization of the liquid crystalline phase with respect to the uncomplexed molecule. Compound 13 for example is in a smectic phase from 40 to 170 °C whereas the 1:1 complex with poly(vinylsulfonate) is smectic from 50 to 235°C.¹¹⁰ Amphotropic monomers which do not show a liquid crystalline phase by themselves have also been shown to form stable mesophases after complexation to polyelectrolytes.¹¹¹ This forms a new concept in the design of polymeric liquid crystalline materials.

1.3.6 Langmuir-Blodgett films

Fukuda et al.^{112,113} performed a detailed study on the orientation of the chromophores in mono- and multilayers of azobenzenes containing one or two stearyl amino groups at different positions of the aromatic system. It was found that the orientation of the azobenzenes depends on the number and position of the long chain substituents.

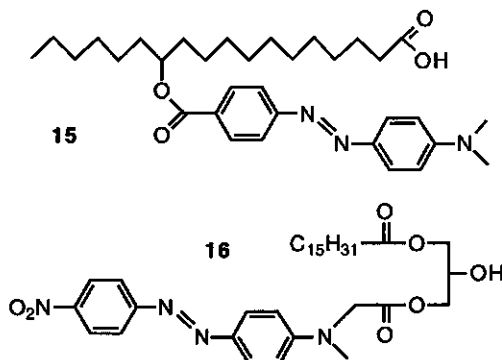
The monolayer and multilayer properties of azobenzene containing long chain fatty acids 14 have also been studied in detail.^{114,115} By the blue shifting of the UV absorption maximum of

the spread monolayers it was found that **8A3H** and **8A5H** and their barium salts undergo a liquid crystalline to gel phase transition upon compression of the monolayer. On the other hand, spread monolayers of **12A3H** and **12A5H** and their barium salts directly form H-aggregates in the gel phase without a phase transition. The molecular ordering of **8A3H** and **8A5H** in the transferred LB film was not as high as in the spread monolayer. For **12A3H** and **12A5H** the molecules have the same degree of order in the spread monolayers and in the LB film irrespective of the number of monolayers.¹¹⁵ Polyion complexation of the monolayer can either modify or stabilize the structures in the monolayers.^{114,116}

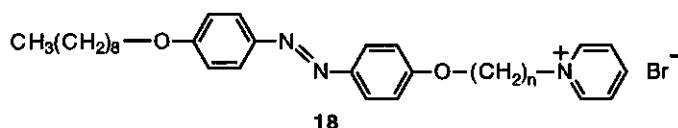
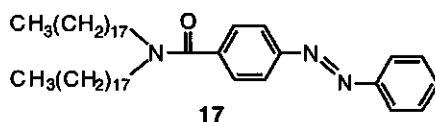


Heesemann^{117,118} showed that for monolayers of compounds **15** and **16** the chromophores lie flat on the water surface at low surface pressures. The plateau region in the isotherms was attributed to a change of the orientation of the chromophore axis (horizontal to vertical) and an aggregation process of the chromophores (monomers to H-aggregates).

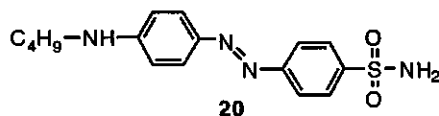
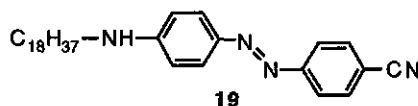
The photoisomerization of the azobenzene moiety is usually more restricted in condensed monolayers or LB films^{119,120} than in bilayer structures. Efficient isomerization in LB films is found when the azobenzene unit has enough space to isomerize. Compound **17** can efficiently be isomerized in a LB film because the cross section of the two alkyl tails is larger than for the azobenzene unit giving it enough space to isomerize.¹²⁰ The monoalkyl analog of **17** resists isomerization in LB films. Monolayers of **18** ($n = 20$) mixed with DMPA (dimyristoylphosphatic acid) also give efficient photoisomerization because the azobenzenes stick out above the DMPA molecules and thus have much freedom.¹²¹⁻¹²³



Compound **18** with $n = 6, 12$ or 14 and $(\text{TCNQ})_2^{\bullet-}$ (bis-tetracyanoquinodimethane radical anion) as counterion forms conducting LB multilayers whose conductivity is influenced by the isomerization state of the azobenzene unit.¹²⁴ This is a typical example of a light induced molecular switch.



The orientation of the azobenzene containing molecules in the LB films can be influenced by irradiation of the films with (polarized) UV light of 366 nm. It is known that azobenzene units which are dispersed in or covalently bound to a matrix material will reorient themselves to an orientation perpendicular to the plane of polarization of the incident light.¹²⁵⁻¹³⁰ This is due to a so-called photoselection process. The azobenzenes which are excited undergo reversible trans-cis isomerizations resulting in a random reorientation of these molecules. When however the trans molecule happens to lie perpendicular to the plane of polarization (or parallel to the propagation direction) of the incident light, the azobenzene will not be excited anymore because there is no overlap between the electrical vector of the light and the transition moment of the azobenzene. Therefore irradiation with polarized light results in a macroscopic anisotropy.

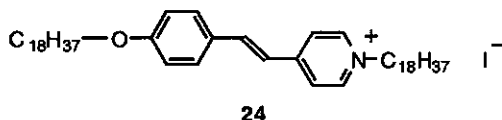
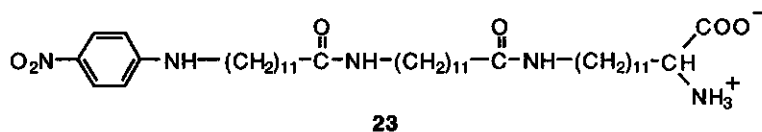
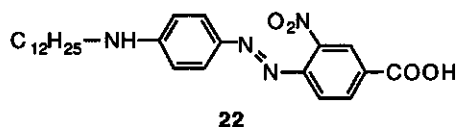
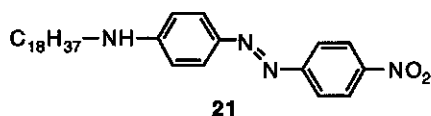


For LB films of azobenzene containing amphiphiles another mechanism for the light induced orientational changes has been proposed. When LB films of **19** are irradiated with nonpolarized light of 336 nm the molecular axes evade massively toward the surface normal accompanied by drastic structural changes of the film.¹³¹ This phenomenon was attributed to a dissipation of the excitation energy as thermal energy. The rearrangement would thus be facilitated by a local melting of the film and the surface free energy would be the driving force.

When LB films of **20** are irradiated in an electrical field, macroscopically polar films are readily obtained.¹³²

1.3.7 Second harmonic generation

It has been well established that mesogens containing an electron donor and acceptor attached to a π -conjugated system have a permanent dipole and a large second order hyperpolarizability coefficient. If these mesogens can be arranged in a non-centrosymmetric fashion, materials with high second order non-linear susceptibility can be obtained. One of the manifestations of the non-linear interaction of light with matter is Second Harmonic Generation, SGH (the emitted light has twice the frequency of the incident light). The rapid growth of the field of optoelectronics in recent years has set off an intensive effort in searching for better non-linear optical materials. For non-chiral molecules only Langmuir-Blodgett films deposited in the X- or Z-mode (head-to-tail) have the natural potential for a non-centrosymmetric structure.¹³³ Unfortunately Y-type deposition usually occurs. In addition X- or Z-type deposition usually leads to an Y-type multilayer structure due to molecular turnaround.¹³⁴



So far only a few monomeric materials have been reported to produce genuine X- or Z-type multilayers. In 1983 Aktsipetrov *et al.*¹³⁵⁻¹³⁷ published the first paper on second harmonic generation from polar LB multilayers using compound **21**. Ledoux¹³⁸ and Loulergue¹³⁹ used compound **22** which has improved amphiphilic properties due to the addition of a carboxylate headgroup (which is also an electron acceptor group). Popovitz-Biro *et al.*^{140,141} reported excellent non-centrosymmetric Z-type deposition for compound **23** with an impressive

quadratic dependence of the SHG signal on the number of layers. They used a *p*-nitroaniline group at the end of the alkyl group in order to stabilize the Z-type multilayer by head-to-tail hydrogen bonding. Ashwell *et al.*¹⁴³ showed that addition of a second hydrophobic endgroup to the hydrophilic chromophore (compound **24**) reduces the tendency of the molecules to invert during deposition and Z-type structures can readily be obtained for films containing more than 100 layers. Non-centrosymmetric LB films have also been obtained from polymers bearing pendant mesogenic units or from alternating multilayers which were prepared using a special trough.

1.4 Outline of the thesis

As shown in paragraph 1.3 a great number of amphotropic compounds has been synthesized and investigated over the last decades. Nevertheless, many aspects of the aggregation behavior of these compounds are not well understood today.

The scope of this thesis is to obtain a better understanding of the aggregation behavior of these compounds. This has been done by the design and synthesis of a series of structurally related novel amphotropes. These compounds have been investigated for their thermotropic phase behavior and their aggregation behavior in water and at the water-air interface. Focus of interest have been amphotropes with ammonium headgroups and some well known mesogenic units at the termini of the hydrophobic chains. Three classes of novel amphotropes have been synthesized *i.e.* single chained, double chained and triple chained compounds. When possible, applications of these compounds have been pointed out.

Chapters two and three deal with the single chained amphotropes. In *Chapter two* the effects of different mesogenic units based on biphenyl, stilbene and azobenzene on the thermodynamics of aggregation in water are described. Also the formation of ion-pair amphiphiles with sodium dodecylsulfate is studied. *Chapter three* describes the binding of metal ions by an ammonium amphiphile carrying an *o*-hydroxyazobenzene mesogenic unit.

The *Chapters four to nine* deal with the double chained amphotropes. In *Chapter four* the bilayer forming properties of amphotropes with one mesogen are reported. The effects of the nature and the dipole moment of the mesogen on the gel-to-liquid crystalline phase transition temperature have been investigated. *Chapter five* describes the properties of cationic and anionic amphotropes with two 4-cyanobiphenyl-4'-oxy mesogenic units. In *Chapter six* the mesogenic units are used as probes to study the molecular ordering of the molecules in the bilayers upon the introduction of polymerizable groups in the amphotropes and subsequent polymerization of the bilayers. In *Chapter seven* the mesogenic units are used as intrinsic probes to study the monomer transfer between bilayer vesicles and the solubilization of these bilayers into micelles. In *Chapter eight* the effects of the relative orientation of the dipoles of the

mesogens within the molecule on the aggregation behavior is subject of discussion. *Chapter nine* deals with complexes of poly(acrylic acid) with didodecyldimethylammonium bromide and with different amphotropes. Finally, *Chapter ten* deals with the triple chained amphotropes. The formation of monolayers at the water-air interface by these compounds with different mesogenic units and the molecular ordering in Langmuir-Blodgett films is investigated. The thesis is concluded with a *Summary* of the most relevant results and conclusions.

1.5 References

- 1 Ramadan, M.; Evans, D. F.; Lumry, R.; Philion, S. *J. Phys. Chem.* **1985**, *89*, 3405.
- 2 Evans, D. F.; Yamaguchi, A.; Wei, G. J.; Bloomfield, V. A. *J. Phys. Chem.* **1983**, *87*, 3537.
- 3 Rico, I.; Lattes, A. *J. Phys. Chem.* **1986**, *90*, 5870.
- 4 Garibi, H.; Palepu, R.; Tiddy, G. J. T.; Hall, D. G.; Wyn-Jones, E. *J. Chem. Soc., Chem. Comm.* **1990**, 115.
- 5 Reinsborough, V. C. *Aust. J. Chem.* **1970**, *23*, 1473.
- 6 Diamant, H.; Andelman, D. *Langmuir* **1994**, *10*, 2910.
- 7 Zana, R.; Benraou, M.; Rueff, R. *Langmuir* **1991**, *7*, 1072.
- 8 Danino, D.; Talmon, Y.; Zana, R. *Langmuir* **1995**, *11*, 1448.
- 9 Zana, R.; Levy, H.; Papoutsi, D.; Beinert, G. *Langmuir* **1995**, *11*, 3694.
- 10 Evans, D. F.; Wennerström, H. *The Colloidal Domain, Where Physics, Biology and Technology Meet*; VCH Publishers: New York, 1994, p 25.
- 11 Ishikawa, Y.; Kuwahara, H.; Kunitake, T. *J. Am. Chem. Soc.* **1994**, *116*, 5579.
- 12 Frank, H. S.; Evans, M. W. *J. Chem. Phys.* **1945**, *13*, 507.
- 13 Blokzijl, W.; Engberts, J. B. F. N. *Angew. Chem.* **1993**, *105*, 1610.
- 14 (a) Bijma, K. *Surfactant Structure and the Thermodynamics of Micelle Formation*, dissertation, University of Groningen, 1995. (b) Sein, A. *How a Simple Anionic Surfactant adopts a Lamellar Arrangement*, dissertation, University of Groningen, 1995.
- 15 (a) Besseling, N. A. M.; Scheutjens, J. M. H. M. *J. Phys. Chem.* **1994**, *98*, 11597. (b) Haak, J. R.; Engberts, J. B. F. N. *J. Am. Chem. Soc.* **1986**, *108*, 1705.
- 16 Israelachvili, J. N.; Mitchell, D. J.; Ninham, B. W. *J. Chem. Soc. Faraday Trans.* **1976**, *272*, 1525.
- 17 Gruen, D. W. R. *J. Phys. Chem.* **1985**, *89*, 146.
- 18 Gorter, E.; Grendel, F. *J. Exp. Med.* **1925**, *41*, 439.
- 19 Singer, S. J.; Nicolson, G. L. *Science* **1972**, *175*, 720.
- 20 Kunitake, T.; Okahata, Y. *J. Am. Chem. Soc.* **1977**, *99*, 3860.
- 21 Rank, J. L.; Mateu, L.; Sadler, D. M.; Tardieu, A.; Gulik-Krzywicki, T.; Luzatti, V. *J. Mol. Biol.* **1974**, *85*, 249.
- 22 (a) Fonteijn, T. *Asymmetric Fusion of Di-n-alkylphosphate Vesicles*, dissertation, University of Groningen, 1992. (b) Sackmann, E. *Ber. Bunsenges. Phys. Chem.* **1978**, *82*, 891. (c) Sackmann, E. *FEBS Letters* **1994**, *346*, 3.
- 23 Kunitake, T. *Angew. Chem.* **1992**, *104*, 692.
- 24 Okahata, Y.; Ando, R.; Kunitake, T. *Ber. Bunsenges. Phys. Chem.* **1981**, *85*, 789.
- 25 Blandamer, M. J.; Briggs, M. J.; Cullis, P. M.; Engberts, J. B. F. N.; Hoekstra, D. *J. Chem Soc., Faraday Trans.* **1994**, *90*, 1905.

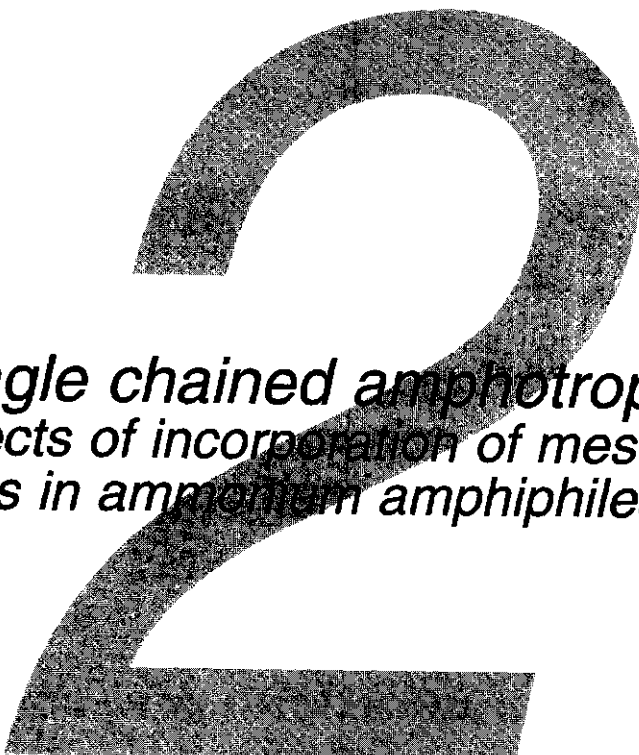
- 26 Blandamer, M. J.; Briggs, M. J.; Cullis, P. M.; Engberts, J. B. F. N. *Chem. Soc. Rev.* **1995**, 251.
- 27 Fox, S. W. *Science* **1960**, 132, 200.
- 28 Fox, S. W. *Science* **1958**, 127, 346.
- 29 Fox, S. W. *Nature* **1965**, 205, 328.
- 30 Fox, S. W.; Johnson, J. E.; Vegotsky, A. *Science* **1956**, 124, 923.
- 31 Fox, S. W.; Harada, K.; Kendrick, J. *Science* **1959**, 129, 1221.
- 32 Shinoda, K. *Pure Appl. Chem.* **1980**, 52, 1195.
- 33 Lange, H.; Schwuger, M. J. *Kolloid-Z. Z.-Polymere* **1968**, 223, 145.
- 34 Kooreman, S. *Calcium Tolerant Anionic Surfactants*, dissertation, University of Groningen, 1995.
- 35 Lasic, D. D. *Biochem. J.* **1988**, 256, 1.
- 36 Lasic, D. D. *J. Colloid Interface Sci.* **1988**, 124, 428.
- 37 Kondo, Y.; Hirota, U.; Yoshino, N.; Nishiyama, I.; Abe, M. *Langmuir* **1995**, 11, 2380.
- 38 Lasic, D. D. *J. Colloid Interface Sci.* **1990**, 140, 302.
- 39 Lasic, D. D.; Belic, A.; Valentincic, T. *J. Am. Chem. Soc.* **1988**, 110, 970.
- 40 Lasic, D. D.; Kirdic, J.; Zagork, S. *Biochim. Biophys. Acta* **1987**, 896, 117.
- 41 Engberts, J. B. F. N.; Hoekstra, D. *Biochim. Biophys. Acta* **1995**, 1241, 323.
- 42 Rupert, L. A. M.; Hoekstra, D.; Engberts, J. B. F. N. *J. Am. Chem. Soc.* **1985**, 107, 2628.
- 43 Rupert, L. A. M.; Hoekstra, D.; Engberts, J. B. F. N. *J. Am. Chem. Soc.* **1986**, 108, 3920.
- 44 Ringsdorf, H.; Schlarb, B.; Venzmer, J. *Angew. Chem.* **1988**, 100, 117.
- 45 Ringsdorf, H.; Schlarb, B. *Makromol. Chem.* **1988**, 189, 299.
- 46 Aliev, K. V.; Ringsdorf, H.; Schlarb, B. *Makromol. Chem. Rapid Commun.* **1984**, 5, 345.
- 47 Fukuda, H.; Diem, T.; Stefely, J.; Kezdy, F. S.; Regen, S. L. *J. Am. Chem. Soc.* **1986**, 108, 2321.
- 48 Lasic, D. D.; Papahadjopoulos, D. *Science*, **1995**, 267, 1275.
- 49 Lasic, D. D. *Angew. Chem.* **1994**, 106, 1765.
- 50 Lasic, D. D.; Martin, F. J.; Gabizon, A.; Huang, S. K.; Papahadjopoulos, D. *Biochim. Biophys. Acta* **1991**, 1070, 187.
- 51 Mueller, P.; Chien, T. F. *Biophys. J.*, **1983**, 44, 375.
- 52 Menger, F.; Lee, S. J. *Langmuir* **1995**, 11, 3685.
- 53 Menger, F.; Gabrielson, K. *J. Am. Chem. Soc.* **1994**, 116, 1567.
- 54 Menger, F.; Balachander, N. *J. Am. Chem. Soc.* **1992**, 114, 5862.
- 55 Menger, F.; Gabrielson, K. *Angew. Chem.* **1995**, 107, 2260.
- 56 Wick, R.; Walde, P.; Luisi, P. L. *J. Am. Chem. Soc.* **1995**, 117, 1435.
- 57 Gericke, A.; Simon-Kutscher, J.; Hühnerfuss, H. *Langmuir* **1993**, 9, 2119.
- 58 (a) Kato, T. *Langmuir* **1990**, 6, 870. (b) Kajiyama, T.; Oishi, Y.; Uchida, M.; Takashima, Y. *Langmuir* **1993**, 9, 1978.
- 59 McFate, C.; Ward, D.; Olmsted, J. *Langmuir* **1993**, 9, 1036.
- 60 a) de Mul, M. N. G.; Mann Jr.; *Langmuir* **1994**, 10, 2311. b) Honig, E. P. *J. Colloid Interface Sci.* **1973**, 43, 66.
- 61 Vertogen, G.; De Jeu, W. H. *Thermotropic Liquid Crystals, Fundamentals*, Springer-Verlag: Berlin; **1988**, part I.
- 62 Stegemeyer, H. *Topics in Physical Chemistry: Liquid Crystals*, Steinkopff: Darmstadt; **1994**.
- 63 Chandrasekhar, S. *Liquid Crystals*, Cambridge University Press: Cambridge; **1992**, p. 1-8.
- 64 Brown, C. H.; Shaw, W. G. *Chem. Rev.* **1975**, 57, 1049.
- 65 Kasha, M.; Rawls, H. R.; Ashraf El-Bayoumi, M. *Pure Appl. Chem.* **1965**, 11, 371.
- 66 Shimomura, M.; Satoshi, A. *Langmuir*, **1995**, 11, 969.

- 67 Le Breton, H.; Letard, J. F.; Lapouyade, R.; Le Calvez, A.; Maleck-Rassoul, R.; Freysz, E.; Ducasse, A.; Belin, C.; Morand, J. P. *Chem. Phys. Lett.* **1995**, 242, 604.
- 68 Hunter, C. A.; Sanders, J. K. M.; Stone, A. J. *Chem. Phys.* **1989**, 133, 395.
- 69 Gudipati, M. S. *J. Phys. Chem.* **1994**, 89, 9750.
- 70 Gray, G. W.; Winsor, O. A. *Liquid Crystals and Plastic Crystals*, Vol 1, Ellis Horwood ed.: Chichester: 1974.
- 71 Jeffrey, G. A. *Acc. Chem. Res.* **1985**, 19, 168.
- 72 Tiddy, G. J. *Phys. Rep.* **1980**, 57, 1.
- 73 Ringsdorf, H.; Schlarb, R.; Venzmer, J. *Angew. Chem.* **1988**, 100, 117.
- 74 Fuller, S.; Hopwood, J.; Rahman, A.; Shinde, N.; Tiddy, G. J.; Attard, G. S.; Howell, O.; Sproston, S. *Liquid Crystals* **1992**, 12, 521.
- 75 Ulman, A.; Scaringe, P. *Langmuir* **1992**, 8, 894.
- 76 Garnaes, J.; Larsen, N. B.; Bjornholm, T.; Jorgenson, M.; Kjaer, K.; Als-Nielsen, J. Jorgensen, J. F.; Zasadzinski, J. A. *Science* **1994**, 264, 1301.
- 77 Evans, S. D.; Urankar, E.; Ulman, A.; Ferris, N. *J. Am. Chem. Soc.* **1991**, 113, 4121.
- 78 Schnidman, Y.; Ulman, A.; Eilers, J. E. *Langmuir* **1993**, 9, 1071.
- 79 Okahata, Y.; Kunitake, T. *Ber. Bunsenges. Phys. Chem.* **1980**, 84, 550.
- 80 Shimomura, M.; Ando, R.; Kunitake, T. *Ber. Bunsenges. Phys. Chem.* **1983**, 87, 1134.
- 81 (a) Kunitake, T. *MRS Bulletin* **1995**, 22. (b) Wakayama, Y.; Kunitake, T. *Chem. Lett.* **1993**, 1425.
- 82 Shimomura, M.; Aiba, S.; Tajima, N.; Inoue, N.; Okuyama, K. *Langmuir* **1995**, 11, 969.
- 83 Nishimi, T.; Ishikawa, Y.; Ando, R.; Kunitake, T. *Recl. Trav. Chim. Pays-Bas* **1994**, 113, 201.
- 84 Ishikawa, Y.; Nishimi, T.; Kunitake, T. *Chem. Lett.* **1990**, 165.
- 85 Okuyama, K.; Ikeda, M.; Yokoyama, S.; Hamada, Y.; Shimomura, M. *Chem. Lett.* **1988**, 1013.
- 86 Nishimi, T.; Ishikawa, Y.; Kunitake, T.; Sekita, M.; Xu, G.; Okuyama, K. *Chem. Lett.* **1993**, 295.
- 87 Shimomura, M.; Kunitake, T. *Chem. Lett.* **1981**, 1001.
- 88 Chen, H.; Weiss Farahat, C.; Farahat, M. S.; Geiger, C.; Leinhos, U. W.; Liang, K.; Song, X.; Penner, T. L.; Ulman, A.; Perlstein, J.; Law, K. L.; Whitten, D. G. *MRS Bulletin* **1995**, 39.
- 89 Song, X.; Geiger, C.; Leinhos, U.; Perlstein, J.; Whitten, D. G. *J. Am. Chem. Soc.* **1994**, 116, 10340.
- 90 Song, X.; Geiger, C.; Furman, I.; Whitten, D. G. *J. Am. Chem. Soc.* **1994**, 116, 4103.
- 91 Song, X.; Perlstein, J.; Whitten, D. G. *J. Am. Chem. Soc.* **1995**, 117, 7816.
- 92 Furman, I.; Geiger, C.; Whitten, D. G.; Penner, T. L.; Ulman, A. *Langmuir* **1994**, 10, 837.
- 93 Zhao, X. M.; Perlstein, J.; Whitten, D. G. *J. Am. Chem. Soc.* **1994**, 116, 10463.
- 94 Spooner, S. P.; Whitten, D. G. *J. Am. Chem. Soc.* **1994**, 116, 1240.
- 95 Mooney, W. F.; Brown, P. E.; Russel, J. C.; Costa, S. B.; Pedersen, L. G.; Whitten D. G. *J. Am. Chem. Soc.* **1984**, 106, 5659.
- 96 Mooney, W. F.; Whitten, D. G. *J. Am. Chem. Soc.* **1986**, 108, 5712.
- 97 Shimomura, M.; Kunitake, T. *J. Am. Chem. Soc.* **1982**, 104, 1757.
- 98 Sing, A.; Tsao, L.; Markowitz, M.; Gaber, B. P. *Langmuir* **1992**, 8, 1570.
- 99 (a) Suh, J.; Lee, K. J.; Bae, G.; Kwon, O. B.; Oh, S. *Langmuir* **1995**, 11, 2626. (b) Suh, J.; Shin, H.; Shin, S. *Langmuir*, **1996**, 12, 2323.
- 100 (a) Kunitake, T.; Nakashima, N.; Shimomura, M.; Okahata, Y.; Kano, K.; Ogawa, T. *J. Am. Chem. Soc.* **1980**, 102, 6644. (b) Hayashita, T.; Kurosawa, T.; Miyata, T.; Tanaka, K.; Igawa, M. *Colloid Polym. Sci.* **1994**, 272, 1611.

- 101 Kano, K.; Tanaka, Y.; Ogawa, T.; Shimomura, M.; Okahata, Y.; Kunitake, T. *Chem. Lett.* **1980**, 421.
- 102 Tanaka, M.; Sato, T.; Yonezawa, Y. *Langmuir* **1995**, *11*, 2834.
- 103 Shimomura, M.; Kunitake, T. *J. Am. Chem. Soc.* **1987**, *109*, 5175.
- 104 Antonietti, M.; Kaul, A.; Thünemann, A. *Langmuir* **1995**, *11*, 2633 and references therein.
- 105 Antonietti, M.; Burger, C.; Effing, J. *Adv. Mater.* **1995**, *7*, 751.
- 106 Okahata, Y.; Enna, G. *J. Phys. Chem.* **1988**, *92*, 4546.
- 107 Okahata, Y.; Enna, G.; Taguchi, K.; Seki, T. *J. Am. Chem. Soc.* **1985**, *107*, 5300.
- 108 Tal'roze, R.; Kuptsov, S. A.; Sycheva, T. I.; Bezborodov, V. S.; Plate, N. A. *Macromolecules* **1995**, *28*, 8689.
- 109 Tirell, D. A.; Turek, A. B.; Wilkinson, D. A.; McIntosh, T. J. *Macromolecules* **1985**, *18*, 1512.
- 110 Ujie, S.; Iimura, K. *Macromolecules* **1992**, *25*, 3174.
- 111 Bazuin, C. G.; Tork, A. *Macromolecules* **1995**, *28*, 8877.
- 112 Nakahara, H.; Fukuda, K. *J. Colloid Interface Sci.* **1983**, *93*, 530.
- 113 Fukuda, K.; Nakahara, H. *J. Colloid Interface Sci.* **1984**, *98*, 555.
- 114 Sato, T.; Ozaki, Y.; Iriyama, K. *Langmuir* **1994**, *10*, 2363.
- 115 Kawai, T.; Umemura, J.; Takenaka, T. *Langmuir* **1989**, *5*, 1378.
- 116 Kimizuka, N.; Kunitake, T. *Colloids Surf.* **1989**, *38*, 79.
- 117 Heesemann, J. *J. Am. Chem. Soc.* **1980**, *102*, 2167.
- 118 Heesemann, J. *J. Am. Chem. Soc.* **1980**, *102*, 2176.
- 119 Moss, R. A.; Jiang, W. *Langmuir* **1995**, *11*, 4217.
- 120 Anzai, J.; Sugaya, N.; Osa, T. *J. Chem. Soc. Perkin Trans. 2* **1994**, 1897.
- 121 Maack, J.; Ahuja, R. C.; Möbius, D.; Tachibana, H.; Matsumoto, M. *Thin Solid Films* **1994**, *242*, 122.
- 122 Maack, J.; Ahuja, R. C.; Tachibana, H. *J. Phys. Chem.* **1995**, *99*, 9210.
- 123 Maack, J.; Ahuja, R. C.; Tachibana, H. *J. Phys. Chem.* **1995**, *99*, 9221.
- 124 Tachibana, H.; Azumi, R.; Nakamura, T.; Matsumoto, M.; Kawabata, Y. *Chem. Lett.* **1992**, 173.
- 125 Yokoyama, S.; Kakimoto, M.; Imai, Y. *Langmuir* **1993**, *9*, 1086.
- 126 Eich, M.; Wendorff, J. M. *Makromol. Chem., Rapid Commun.* **1987**, *8*, 59.
- 127 Yokoyama, S.; Kakimoto, M.; Imai, Y. *Mol. Cryst. Liq. Cryst.* **1993**, *227*, 295.
- 128 Hvilsted, A.; Andruzzi, F.; Kulinna, C.; Siesler, H. W.; Ramanujam, P. S. *Macromolecules*, **1995**, *28*, 2172.
- 129 Natansohn, A.; Xie, S.; Rochon, P. *Macromolecules* **1992**, *25*, 5531. Natansohn, A.; Rochon, P.; Gosselin, J.; Xie, S. *Macromolecules* **1992**, *25*, 2268.
- 130 Yokoyama, S.; Kakimoto, M.; Imai, Y. *Langmuir* **1994**, *10*, 4594.
- 131 Schönhoff, M.; Chi, F. F.; Fuchs, H.; Lösche, M. *Langmuir* **1995**, *11*, 163.
- 132 Palto, S. P.; Blinov, L. M.; Yudin, S. G.; Grewer, G.; Schönhoff, M.; Lösche, M. *Chem. Phys. Lett.* **1993**, *202*, 308.
- 133 Ulman, A. *An Introduction to Ultrathin Organic Films, from Langmuir-Blodgett to Self-assembly*, Academic Press Inc.: San Diego; 1991, chapter 5.1.
- 134 Honig, E. P. *J. Colloid Interface Sci.* **1973**, *43*, 66.
- 135 Aktsipetrov, O. A.; Akhmediev, N. N.; Mishina, E. D.; Novak, V. R. *JEPT Lett.* **1983**, *37*, 207.
- 136 Aktsipetrov, O. A.; Akhmediev, N. N.; Baranova, I. M.; Mishina, E. D.; Novak, V. R. *Sov. Tech. Phys. Lett.* **1985**, *11*, 249.

- 137 Aktsipetrov, O. A.; Akhmediev, N. N.; Baranova, I. M.; Mishina, E. D.; Novak, V. R. *Zh. Eksp. Teor. Fiz.* **1985**, *89*, 911.
- 138 Ledoux, I.; Josse, D.; Vidakovich, P.; Zyss, J.; Hann, R. A.; Gordon, P. F.; Bothwell, P. D.; Gupta, S. K.; Allen, S.; Robin, P.; Chastaing, E.; Dubois, J. C. *Europhys. Lett.* **1987**, *3*, 803.
- 139 Lelourque, J. C.; Dumont, M.; Levy, Y.; Robin, P.; Pocholle, J. P.; Papuchon, M. *Thin Solid Films* **1988**, *160*, 399.
- 140 Popovitz-Biro, R.; Hill, K.; Shavit, E.; Hung, D. J.; Lahav, M.; Leiserowitz, L.; Sagiv, J.; Hsiung, H.; Meredith, G. R.; Vanherzeele, H. *J. Am. Chem. Soc.* **1990**, *112*, 2498.
- 141 Popovitz-Biro, R.; Hill, K.; Landau, E. M.; Lahav, M.; Leiserowitz, L.; Sagiv, J. *J. Am. Chem. Soc.* **1988**, *110*, 2672.
- 142 Ashwell, G. A.; Jackson, P. D.; Crossland, W. A. *Nature* **1994**, *368*, 438.

Chapter 2



*Single chained amphotropes:
Effects of incorporation of mesogenic
units in ammonium amphiphiles*

Abstract

A number of novel single chained ammonium amphiphiles with biphenyl, stilbene and azobenzene mesogenic moieties at the terminus of the hydrophobic tail have been synthesized. These compounds form micellar aggregates in water. The critical aggregation concentration (cac) decreases from the biphenyl to the stilbene to the azobenzene containing amphiphiles. This decrease in cac does not correlate with increased hydrophobicity or dipole moment, but correlates with increasing enthalpic contributions. These are attributed to favorable π - π stacking interactions between the mesogenic units.

These amphiphiles readily form 1:1 complexes with sodium dodecyl-sulfate. These so-called ion-pair amphiphiles form unstable bilayer vesicles.

2.1 Introduction

In the early 1980s a new class of compounds was introduced which combined the structural features of amphiphiles and thermotropic liquid crystals. These molecules are composed of a polar headgroup, one or more hydrophobic chains and a mesogenic unit incorporated in the hydrophobic part. The mesogenic unit usually consists of a rigid aromatic group and owes its name to its capability to induce thermotropic liquid crystalline phases or mesophases. Being also amphiphiles, these compounds show lyotropic mesomorphism when dispersed in water. The unique combination of amphiphilic and thermotropic properties is expressed in their name of amphotropic compounds.

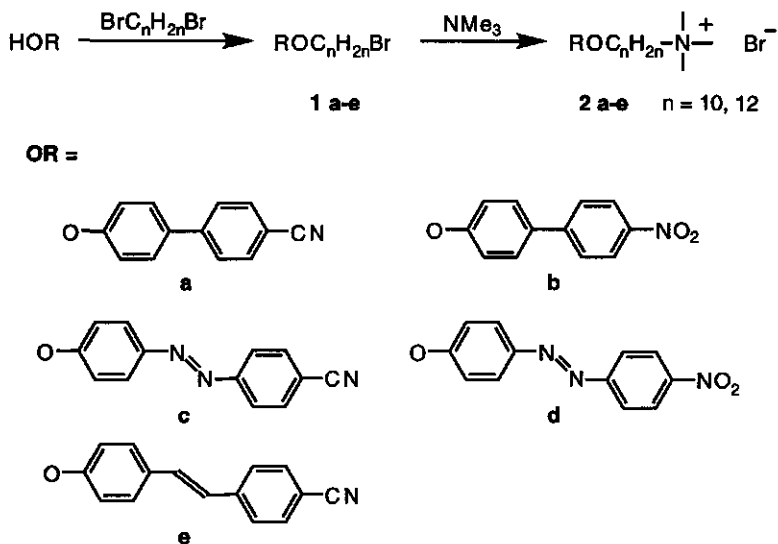
The lyotropic behavior of a series of amphotropes was first investigated by Kunitake *et al.*¹⁻⁸ They focused on single chained compounds of the type head-spacer-mesogen-tail. Later, many researchers applied amphotropic compounds in the field of Langmuir-Blodgett technology.⁹⁻¹⁶ Thin films of these compounds are promising photochromic materials for optical information storage, light induced switches and non-linear optical devices. Since then, many amphotropic monomers and polymers^{17,18} have been designed, synthesized and investigated for their physical properties.

However, to date little is known about the effect of the nature of the mesogenic units on the lyotropic mesomorphism of these compounds. We have therefore synthesized a series of novel single chained ammonium amphiphiles with different chain lengths and different mesogenic units attached at the termini of the alkyl chains.

Critical aggregation concentrations in water have been measured and thermodynamic parameters for the aggregation process have been calculated. Also the formation of ion-pair amphiphiles using sodium dodecylsulfate as the second component was investigated by UV spectroscopy and light microscopy.

2.2 Results and discussion

The synthetic pathway and molecular structures of the investigated amphotropes are given in Scheme 1. The composition and purity of the compounds was checked by 200 MHz ¹H NMR, thin layer chromatography and elemental analyses. Most compounds contained 0.5 or 1 mol of crystal water. The thermotropic phase behavior of these compounds is very complicated and often not unequivocal. This may be caused by the presence of different crystal packing modes, exhibiting different melting points. The additional presence of mesophases further complicates elucidation of the thermotropic phase behavior. Also the bound crystal water is believed to influence the phase behavior.



Scheme 1. Synthetic pathway and structures of compounds **2a-e**.

2.2.1 Lyotropic aggregation behavior

The compounds **2a-e** readily dissolve in water upon heating. The compounds **2a-d** form micellar aggregates in dilute solutions above their Krafft temperature. No bilayer structures were observed upon microscopic investigation of the solution. This is in line with the results found by Shimomura *et al.*⁴ in their investigation of molecules of the type headgroup-decyl spacer-azobenzene-tail. They found that when the tail was shorter than 8 carbon atoms no stable bilayers but micelle-like structures were formed. The stilbene containing compounds **2e** ($n=10,12$) however, form giant bilayer vesicles which can readily be observed by optical microscopy. This shows that very subtle changes in the molecular structure can result in dramatic changes of the aggregate architecture.

The Krafft temperatures of the compounds **2a-e** are all found in the range of 45-65 °C. At room temperature the stability of the undercooled aqueous dispersions varies from several minutes to several hours before crystallization is observed. Although the dispersions are meta-stable at room temperature, it is possible to determine critical aggregation concentrations (cac) at room temperature. The cac values at 20 °C are given in Table 1. From the critical aggregation concentration the change of standard Gibbs free energy for aggregation ($\Delta G^\circ_{\text{agg}}$) can be deduced. According to the 'phase separation model'¹⁹⁻²¹ which assumes 100% of counterion binding, $\Delta G^\circ_{\text{agg}}$ of a monovalent ionic surfactant, in the absence of added electrolyte is given by:

$$\Delta G^\circ_{\text{agg}} = 2RT \ln(\text{cac}) \quad (1)$$

where R is the gas constant and T the absolute temperature. The cac values are expressed in dimensionless mole fraction units. Figure 1 shows the plot of ΔG°_{agg} versus the number of methylene units in the spacer for compounds **2a-e**. Data of n -alkyltrimethylammonium bromides are also displayed.^{22,23} It is clearly seen that substitution of a terminal methyl group with a mesogenic unit drastically lowers ΔG°_{agg} .

Table 1. Critical Aggregation Concentrations for **2a-e** and Alkyltrimethylammonium Bromides ($C_{n+1}TAB$) at 293 K in water.

Compound	n^a	cac (mM)
C_{n+1}TAB^b	9	65
	11	15.3
	13	3.60
2a	10	0.70
	12	0.28
2b	10	0.64
	12	0.27
2c	10	0.27
	12	0.05
2d	10	0.26
	12	-
2e	10	0.53
	12	0.14

^a n is the number of methylene units in the alkyl chain

^b data taken from ref. 24

When Figure 1 is examined in more detail it is seen that of all amphiphiles those with the azobenzenes have the lowest cac 's and the most negative ΔG°_{agg} values. The biphenyl mesogens give rise to the highest cac values. Furthermore, it is seen that substitution of the cyano group by a nitro group in both the biphenyl and the azobenzene mesogens hardly influences the ΔG°_{agg} . From the slope of ΔG°_{agg} versus the number of methylene units $\Delta G^\circ_{CH_2}$ for these molecules can be calculated and is approximately -2.8 kJ/mol. This value is in good agreement with values reported for single chained amphiphiles of -2.7/-3.0 kJ/mol.^{24,25}

ΔG°_{agg} can be considered as composed of a summation of contributions from the various units which make up the amphiphile. If we take $\Delta G^\circ_{CH_2}$ and $\Delta G^\circ_{headgroup}$ identical for both the mesogen containing compound and the alkyltrimethylammonium bromide, the difference in ΔG°_{agg} between a mesogen containing compound and the alkyltrimethylammonium bromide with the same number of methylene units can be expressed as $(\Delta G^\circ_{mes}) - (\Delta G^\circ_{CH_3})$. $\Delta G^\circ_{CH_3}$ is the change of Gibbs free energy associated with transfer of the methyl group from the aqueous

phase to the interior of the aggregate. The value of $\Delta G^\circ_{\text{CH}_3}$ has been reported to be -9.6 kJ/mol^{24,25}. Using this method the contribution to the change of standard Gibbs free energy for aggregation of the mesogenic units ($\Delta G^\circ_{\text{mes}}$) can be calculated and the values are given in Table 2.

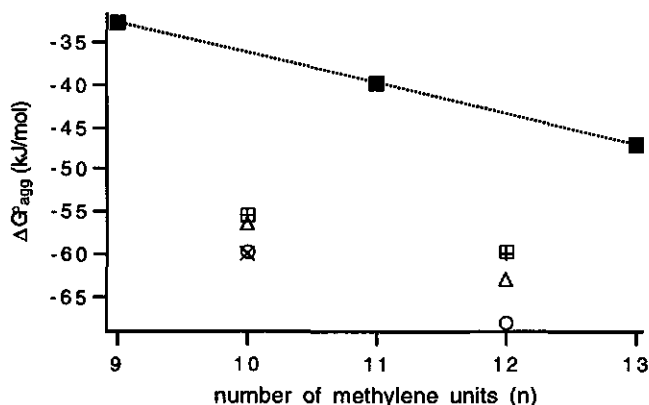


Figure 1. Plot of $\Delta G^\circ_{\text{agg}}$ (kJ/mol) at 293 K versus the number of methylene units in the alkyl spacer (n) for compounds **2a** (□), **2b** (+), **2c** (O), **2d** (X), **2e** (Δ) and alkyltrimethylammonium bromides (■).

We have tried to correlate these results with the hydrophobicity of the mesogens. The hydrophobicity of each of the mesogens can be estimated using Rekker's hydrophobic fragmental constants (Σf_i)²⁶ and the values are given in Table 2. This value is expected to predict the partitioning of a molecule in a water-octanol system. It turns out that the hydrophobicity increases from azobenzene to biphenyl to stilbene. This does not correlate with our observations. It is therefore concluded that hydrophobicity is not the only driving force for this aggregation process.

Table 2. Calculated Dipole Moments, Hydrophobicity Values (Σf_i)²⁶ and Calculated Free Energy Change of Aggregation of the Mesogens **a-e** ($\Delta G^\circ_{\text{mes}}$).

Mesogen RO	Dipole moment (Debye)	Σf_i	$\Delta G^\circ_{\text{mes}}$ (kJ/mol)
a	4.1	3.1	-27
b	6.0	3.3	-27
c	4.4	1.1	-33
d	6.8	1.2	-33
e	4.4	3.6	-28

Because all the investigated mesogens are donor- π -acceptor systems they have a permanent dipole. In order to investigate if electrostatic dipole-dipole interactions could dominate the observed aggregate stability, the dipole moment values of the mesogenic units **a-e** (in vacuum) were calculated by semi-empirical computer calculations and the results are also given in Table 2. It is clear that substitution of a cyano group by a nitro group increases the dipole moment drastically. This is due to the fact that the nitro group is a stronger electron acceptor than the cyano group. When going from the biphenyl system to the stilbene system, while maintaining the same donor-acceptor pair, the dipole moment increases slightly because of the increased distance between donor and acceptor group. The stilbene unit and the azobenzene unit have practically the same dipole moment because they have almost the same geometry.

Experimentally, it is found that substitution of a cyano group by a nitro group only slightly affects the cac. Substitution of the stilbene unit by an azobenzene unit, while keeping the same donor-acceptor pair, has a large influence on the cac, although the magnitude of the dipole moment remains the same. It is therefore concluded that the dipole moment of the mesogens does not dominate the aggregate stability.

Because neither the hydrophobicity of the mesogens nor the dipole-dipole interactions between the mesogens could account for the observed aggregate stabilities, additional experiments have been performed to elucidate the type of interactions that dominate the aggregation behavior. In principle, determination of $\Delta G^\circ_{\text{agg}}$ from cac values as a function of temperature leads to the enthalpy ($\Delta H^\circ_{\text{agg}}$) and the entropy ($\Delta S^\circ_{\text{agg}}$) of aggregation. These latter terms can provide insight into the physical nature of the aggregation process. Hydrophobic aggregation is often associated with a large positive entropy change due to solvent disordering effects. On the other hand, physical attraction between molecules results in a favorable, negative enthalpy change upon aggregation.²⁷ Therefore, the cacs of the compounds **2b**, **2c** and **2e** were measured in the temperature range between 20° and 45°C. For all measured compounds an increase in cac was found with increasing temperature (Table 3). Equation (1) can be rewritten to give equation (2).²⁷

$$\Delta G^\circ_{\text{agg}}/T = 2R\ln(\text{cac}) = (\Delta H^\circ_{\text{agg}}/T) - \Delta S^\circ_{\text{agg}} \quad (2)$$

This first order model neglects heat capacity changes ($\Delta C_p = \delta\Delta H/\delta T = 0$)^{23,25} and gives only a rough estimate of $\Delta H^\circ_{\text{agg}}$. $\Delta H^\circ_{\text{agg}}$ has been obtained from the slope of a plot of $2R\ln(\text{cac})$ versus $1/T$ (Figure 2). Some literature data of *n*-dodecyltrimethylammonium bromide and *n*-hexadecyltrimethylammonium bromide are also displayed.²³ It is clearly observed that the slopes for the compounds **2b**, **2c** and **2e** are steeper than for the alkyltrimethylammonium bromide compounds, reflecting a more favorable $\Delta H^\circ_{\text{agg}}$. Furthermore, $\Delta H^\circ_{\text{agg}}$ becomes more favorable upon going from the biphenyl to the stilbene to the azobenzene containing compound, corresponding with the decrease in cac. It is therefore concluded that favorable enthalpic

interactions, which are stronger for the azobenzene mesogens than for the stilbene or biphenyl units, play an important role in determining the aggregate stability.

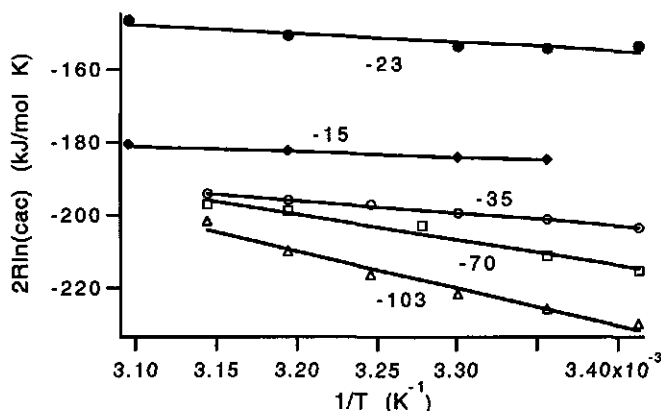


Figure 2. Plot of $2R\ln(cac)$ versus $1/T$ for compounds **2b** (○), **2c** (Δ) and **2e** (□) with $n = 12$ and for *n*-dodecyltrimethylammonium bromide (●) and *n*-hexadecyltrimethylammonium bromide (◆). The values of the slopes are given in the plot in kJ/mol.

Possibly, π - π stacking of the mesogens in the formed aggregates is an important driving force for aggregate formation. Such stacking interactions have been described as a form of Van der Waals interactions between aromatic units.²⁸ When aromatic units are depicted as positively charged σ -skeletons sandwiched between negatively charged π -electron clouds, mutual attraction between the σ -skeleton of one molecule with the π -electron cloud of an adjacent molecule can compensate the repulsion between the π -electron clouds. Therefore, the aggregated state represents a free energy minimum.²⁹ This means that azobenzene mesogens give better π - π stacking than biphenyl or stilbene mesogens, resulting in a more negative stacking enthalpy and consequently in a more negative ΔG°_{agg} . Possibly, the polarizability of the azo-bridge contributes to the stabilization of the aggregate through dispersion interactions. Our results also agree with calculations performed by Hunter³⁰ who found that hetero atoms in an aromatic compound can cause large partial atomic charges which can lead to additional intermolecular electrostatic interactions. This indicates that local dipoles within the aromatic system can favor aggregation, whereas the net dipole moment of the whole aromatic system does not dramatically affect the aggregation behavior.

The biphenyl mesogens **a** and **b** have a ΔG°_{mes} of -27 kJ/mol (Table 2). For a pentyl group, which has the same calculated hydrophobicity as the biphenyl mesogen using Rekker's hydrophobic fragmental constants, a ΔG°_{agg} value of approximately -21 kJ/mol can be deduced. This means that the aggregate stabilizing effect of the biphenyl mesogen can mainly be ascribed to the hydrophobicity of this unit and that the stacking interactions are only somewhat

stronger than the London-dispersion interactions between pentyl chains. Similar results are found for the stilbene mesogen.

The azobenzene mesogens have a $\Delta G^\circ_{\text{mes}}$ of -33 kJ/mol. This mesogenic unit however, is much less hydrophobic than the biphenyl or the stilbene mesogens. Therefore hydrophobicity is not expected to dominate the aggregate stabilizing effect of azobenzenes. This confirms that stacking or dispersion interactions play an important role in the aggregation of azobenzenes.

Table 3. Critical Aggregation Concentrations of Compounds **2b**, **2c**, and **2e** ($n=12$) and *n*-Dodecyltrimethylammonium Bromide ($C_{12}\text{TAB}$) and *n*-Hexadecyltrimethylammonium Bromide ($C_{16}\text{TAB}$) at Different Temperatures.

Compound	Temperature (K)	cac (mM)
2b ($n=12$)	293	0.27
	298	0.31
	303	0.35
	308	0.39
	313	0.43
	318	0.48
2c ($n=12$)	293	0.05
	298	0.07
	303	0.09
	308	0.13
	313	0.18
	318	0.30
2e ($n=12$)	293	0.14
	298	0.17
	305	0.28
	313	0.37
	318	0.40
C₁₂TAB^a	291	5.40
	298	5.27
	303	5.33
	313	6.40
	323	8.28
C₁₆TAB^a	298	0.82
	303	0.87
	313	0.95
	323	1.05

^a Data from ref. 23. See also ref. 31

2.2.2 Ion-pair amphiphiles

As it turns out that mesogenic units can stabilize aggregates of single chained amphotropes, the question arose whether they can also stabilize aggregates of ion-pair amphiphiles (IPAs). Single chained cations that are paired with single chained anions represent a novel class of bilayer forming surfactants. Ion-pair amphiphiles have been proposed as interesting materials for both

theoretical investigations and practical device applications. Several studies have been performed on IPAs of alkyltrimethylammonium bromides with sodium dodecylsulfate (SDS)³²⁻³⁴ and with fatty acids.^{35,36}

The geometry of a surfactant molecule is believed to play a crucial role in defining its aggregation properties.³⁷ Conical-shaped molecules pack most comfortably into spherical aggregates. In contrast cylindrical-shaped surfactants prefer to assemble into bilayers.

It is reasoned that the effective interfacial headgroup area of each partner of an IPA should be substantially smaller than for each individual surfactant, due to electrostatic attraction between the headgroups and due to a reduction of hydration. The overall effect is an increase in the cylindrical character of each ion. This contributes to the formation of bilayer structures.

For the single chained compounds **2a-e** the formation of a 1:1 complex with SDS can be followed very nicely with UV spectroscopy. Figure 4 shows the spectral changes upon addition of SDS to a solution of **2c**. The first spectrum shows monomerically dispersed **2c**, under its cac. Upon addition of SDS the absorption maximum shifts from 363 nm to 340 nm due to parallel stacking of the chromophores in the newly formed aggregates. The intensity of the absorption band also decreases. The spectrum continues to change until a 1:1 composition is reached. Upon addition of a large excess of SDS no further spectral changes occur. This means that the formed aggregates are not solubilized by an excess of SDS, which presumably forms separate micelles. A possible molecular arrangement in the IPA aggregate is given in Figure 3.

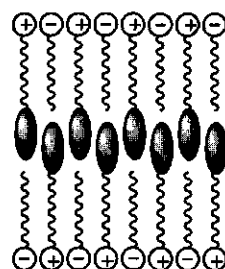


Figure 3. Possible bilayer structure of an IPA.

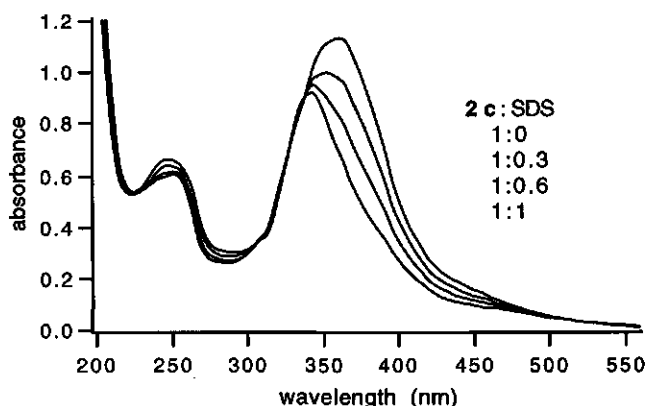


Figure 4. Changes in the UV absorption spectrum of an aqueous solution of **2c** upon addition of sodium dodecylsulfate (top to bottom).



Figure 5. Giant vesicle of an IPA of **2a** and SDS.

Upon hydration of solid **2a** and **2b** in a SDS solution at 60 °C the formation of giant liposomes was observed with optical microscopy (see Figure 5). These liposomes are not stable at room temperature and tend to crystallize very soon after preparation. Upon hydration of **2c**, **2d** and **2e** in a SDS solution no formation of giant liposomes was observed.

2.3 Conclusions

A series of novel amphotropes has been synthesized and their aggregation behavior in water has been investigated. The single chained compounds **2a-d** form micellar aggregates upon heating in water, in contrast to **2e** ($n=10$ or 12) which forms bilayer vesicles. From the decrease of the critical aggregation concentration (cac) it was deduced that the aggregate stability increases from biphenyl to stilbene to azobenzene containing amphotropes. This sequence does not correlate with the hydrophobicity as quantified by Rekker's hydrophobic fragmental constants, nor with the dipole moments of the mesogens. From temperature dependent cac determinations it was concluded that the aggregate stability is determined by hydrophobic interactions and favorable enthalpic interactions, which are attributed to π - π stacking interactions between the mesogens in the aggregate. The π - π stacking interaction contribution increases from biphenyl to stilbene to azobenzene explaining the excellent aggregate stabilizing properties of azobenzene.

Addition of SDS to the single chained amphotropes **2a** and **2b** induces the formation of bilayer vesicles by the formation of ion-pair amphiphiles. However, these bilayer structures are not very stable and crystallize soon after preparation.

2.4 Experimental section

2.4.1 Synthesis

4'-Cyano-4-hydroxybiphenyl (**a**) was obtained from Merck.

4-Hydroxy-4'-nitrobiphenyl (**b**) was synthesized as described before.^{15,16}

4'-Cyano-4-hydroxyazobenzene (**c**) and 4-hydroxy-4'-nitroazobenzene (**d**) were prepared by reaction of the diazonium salts of 4-nitroaniline or 4-aminobenzonitrile with phenol.³⁸

4'-Cyano-4-hydroxystilbene (**e**) was synthesized in a two step reaction. 5 g (20 mmol) of *p*-bromophenylacetic acid and 2.5 g (20 mmol) of *p*-hydroxybenzaldehyde together with 3 mL of piperidine were heated at 110 °C for 3 h followed by heating at 160 °C for 4 h. The reaction mixture was treated with water and the precipitate was collected. The reaction product 4'-bromo-4-hydroxystilbene was purified by column chromatography on silica gel using dichloromethane as eluent (yield 55%).

A mixture of 3 g (11 mmol) of 4'-bromo-4-hydroxystilbene and 2.2 g of CuCN was refluxed for 15 h in 10 mL of dry DMF. The mixture was allowed to cool and a solution of 4 g of FeCl₃·6H₂O and 2.5 mL of concentrated HCl solution in 10 mL of water was added. This mixture was heated at 70 °C for 25 minutes. The reaction mixture was then extracted with CHCl₃. The CHCl₃ layers were washed with 5 M HCl solution and with NaHCO₃ solution and dried on MgSO₄. The solvent was removed under reduced pressure and water was added to the residue. The crystalline precipitate was collected and purified by column chromatography on silica gel using methanol/CHCl₃ (1:100) as eluent (yield 73%).

1-Bromo- ω -RO-alkane (**1a-e**)

A mixture of 25 mmol of the appropriate phenol (**a-e**) and 50 mmol of 1, ω -dibromoalkane and 50 mmol K₂CO₃ in 100 mL of 2-butanone was refluxed for 16 h. The salt was removed by filtration and the filtrate was concentrated by evaporation of the solvent. The product was purified by column chromatography on silica gel using petroleum ether (bp. 40-60 °C)/CH₂Cl₂, 1:1 v/v as eluent (yield 60 %).

¹H-NMR (CDCl₃, TMS, δ , ppm): 1.40 (m, 2n-8 H, -(CH₂)_{n-4}-), 1.80 (m, 4 H, Br-CH₂-CH₂-, RO-CH₂-CH₂-), 3.40 (t, 2 H, Br-CH₂-), 4.00 (t, 2 H, RO-CH₂-), 7.00 - 8.30 (m, 8 H, Ar-H).

Mp: **1a** (n=10) 75 °C, **1a** (n=12) 78 °C, **1b** (n=10) 80 °C, **1b** (n=12) 84 °C, **1c** (n=10) 102 °C, **1c** (n=12) 105 °C, **1d** (n=10) 85 °C, **1d** (n=12) 90 °C, **1e** (n=10) 95 °C, **1e** (n=12) 99 °C,

N-(ω -RO-alkyl)-*N,N,N*-trimethylammonium bromide (**2a-e**)

A solution of 0.8 mmol of the bromide (**1a-e**) in 6 mL of a 20% (w/w) solution of trimethylamine in ethanol was heated at 100 °C for 20 h in a closed reaction vessel. The mixture was allowed to cool to room temperature and was then thoroughly cooled in ice. The precipitate was collected by filtration and washed with diethyl ether (yield 90%).

¹H-NMR (CDCl₃, TMS, δ , ppm): 1.40 (m, 2n-8 H, -(CH₂)_{n-4}-), 1.80 (m, 4 H, N-CH₂-CH₂-, RO-CH₂-CH₂-), 3.4 (m, 11 H, N-(CH₃)₃, -CH₂-N), 4.00 (t, 2 H, RO-CH₂-), 7.00 - 8.30 (m, 8 H, Ar-H).

1a (n=10) Mp. 163 °C. Anal. Calcd for $C_{26}H_{37}N_2OBr$ (0.5 H_2O): C, 64.61; H, 7.93; N, 5.80. Found: C, 64.67; H, 7.83; N, 5.90. **1a** (n=12) Mp. 163 °C. Anal. Calcd for $C_{28}H_{41}N_2OBr$ (0.3 H_2O): C, 66.33; H, 8.27; N, 5.53. Found: C, 66.37; H, 8.26; N, 5.80. **1b** (n=10) Mp. 151 °C. Anal. Calcd for $C_{25}H_{37}N_2O_3Br$ (3.3 H_2O): C, 54.03; H, 7.95; N, 5.07. Found: C, 54.11; H, 7.09; N, 5.34. **1b** (n=12) Mp. 128 °C. Anal. Calcd for $C_{27}H_{41}N_2O_3Br$ (0.9 H_2O): C, 60.30; H, 8.02; N, 5.21. Found: C, 60.32; H, 7.74; N, 5.20. **1c** (n=10) Mp. 189 °C. Anal. Calcd for $C_{26}H_{37}N_4OBr$ (1 H_2O): C, 60.11; H, 7.57; N, 10.79. Found: C, 60.15; H, 7.13; N, 10.81. **1c** (n=12) Mp. 194 °C. Anal. Calcd for $C_{28}H_{41}N_4OBr$ (1.1 H_2O): C, 61.21; H, 7.93; N, 10.20. Found: C, 61.13; H, 7.47; N, 10.22. **1d** (n=10) Mp. 205 °C. Anal. Calcd for $C_{25}H_{37}N_4O_3Br$ (2.3 H_2O): C, 53.34; H, 7.45; N, 9.95. Found: C, 53.28; H, 7.35; N, 9.74. **1d** (n=12) Mp. 218 °C. Anal. Calcd for $C_{27}H_{41}N_4O_3Br$ (1.6 H_2O): C, 56.07; H, 7.70; N, 9.69. Found: C, 56.05; H, 7.41; N, 9.72. **1e** (n=10) Mp. 185 °C. Anal. Calcd for $C_{28}H_{39}N_2OBr$: C, 67.33; H, 7.81; N, 5.61. Found: C, 67.42; H, 7.85; N, 5.71. **1e** (n=12) Mp. 190 °C. Anal. Calcd for $C_{30}H_{43}N_2OBr$: C, 68.24; H, 8.22; N, 5.31. Found: C, 68.13; H, 8.29; N, 5.53.

2.4.2 Methods

Critical aggregation concentrations were determined by measuring the specific conductivity of an amphotrope solution in distilled water as a function of the concentration. A Philips Digital Conductivity meter PW 9527 with a Philips PW9550/60 electrode were used. The measuring compartment was thermostatted with a Haake FE 2 thermostat. Semi-empirical calculations of the dipole moments were performed by using MOPAC 6.0 with a PM3 hamiltonian (QCPE programme nr. 455).³⁹ The energy of the input structures was first minimized using Quanta CHARMM. Giant vesicles were prepared by allowing 0.1-0.2 mg of the solid material to hydrate for several minutes in water of 70 °C.

2.5 References

- 1 Nishimi, T.; Ishikawa, Y.; Ando, R.; Kunitake, T. *Recl. Trav. Chim. Pays Bas* **1994**, *113*, 201.
- 2 Okahata, Y.; Kunitake, T. *Ber. Bunsenges. Phys. Chem.* **1980**, *84*, 550.
- 3 Shimomura, Y.; Kunitake, T.; *J. Am. Chem. Soc.* **1982**, *104*, 1757.
- 4 Shimomura, Y.; Ando, R.; Kunitake, T. *Ber. Bunsenges. Phys. Chem.* **1983**, *87*, 1134.
- 5 Nishimi, T.; Ishikawa, Y.; Kunitake, T.; Sekita, M.; Xu, G.; Okuyama, K. *Chem. Lett.* **1993**, 295.
- 6 Kunitake, T. *Angew. Chem.* **1981**, *104*, 692.
- 7 Kimizuka, N.; Kunitake, T. *Chem. Lett.* **1988**, 829.
- 8 Shimomura, Y.; Kunitake, T. *Chem. Lett.* **1981**, 1001.
- 9 Everaars, M. D.; Marcelis, A. T. M.; Sudhölter, E. J. R. *Langmuir* **1993**, *9*, 1986.
- 10 Everaars, M. D.; Marcelis, A. T. M.; Sudhölter, E. J. R. *Thin Solid Films* **1994**, *242*, 78.
- 11 Heesemann, J. *J. Am. Chem. Soc.* **1980**, *101*, 2167 and 2176.
- 12 Fukuda, K.; Nakahara, H. *J. Colloid Interface Sci.* **1984**, *98*, 555.
- 13 Nakahara, H.; Fukuda, K. *J. Colloid Interface Sci.* **1983**, *93*, 530.
- 14 Ashwell, G. J.; Jackson, P. D.; Crossland, W. A. *Nature* **1994**, *368*, 438.
- 15 Ou, S. H.; Percec, V.; Mann, J. A.; Lando, J. B. *Langmuir* **1994**, *10*, 905.

- 16 Ou, S. H.; Percec, V.; Mann, J. A.; Lando, J. B.; Zhou, L.; Singer, K. D. *Macromolecules* **1993**, *26*, 7263.
- 17 Adams, J.; Rettig, W.; Duran, R. S.; Naciri, J.; Shashidhar, R. *J. Phys. Chem.* **1993**, *97*, 2021.
- 18 Mentzel, H.; Weichart, B.; Schmidt, A.; Paul, S.; Knoll, W.; Stumpe, J.; Fisher, T. *Langmuir* **1994**, *10*, 1926.
- 19 van Os, N. M.; Daane, G. J.; Bolsman, T. A. B. M. *J. Colloid Interface Sci.* **1987**, *115*, 402.
- 20 van Os, N. M.; Smit, B.; Karaborni, S. *Recl. Trav. Chim. Pays Bas* **1994**, *113*, 181.
- 21 Bijma, K.; Engberts, J. F. B. N.; Haandrikman, G.; van Os, N. M.; Blandamer, M. J.; Butt, M. D.; Cullis, P. M. *Langmuir* **1994**, *10*, 2578.
- 22 Lianos, P.; Zana, R. *J. Colloid Interface Sci.* **1981**, *84*, 100.
- 23 Barry, B. W.; Russell, G. F. I. *J. Colloid Interface Sci.* **1972**, *40*, 174.
- 24 Evans D. F. *Langmuir* **1988**, *4*, 12.
- 25 Tanford, C. *The Hydrophobic Effect*; 2nd ed.: Wiley: New York, 1980.
- 26 Rekker, R. F. *The Hydrophobic Fragmental Constant*; 1st ed.; Elsevier scientific publishing company: Amsterdam, 1977.
- 27 Stauffer, D. A.; Barraus Jr, R. E.; Daughtery, D. A. *J. Org. Chem.* **1990**, *55*, 2762.
- 28 Hunter, C. A.; Sanders, K. M. *J. Am. Chem. Soc.* **1990**, *112*, 5525.
- 29 Zhao, X. M.; Perlstein, J.; Whitten, D. G. *J. Am. Chem. Soc.* **1994**, *116*, 10463.
- 30 Hunter, C. A. *Chem. Soc. Rev.* **1994**, 101.
- 31 The cac values for *n*-dodecyltrimethylammonium bromide at room temperature in Table 1 and Table 3 are considerably different. These data are obtained from references 22 and 23 respectively. We believe that the value from reference 22 is more reliable because of the good semilogarithmic relationship between the cac and the number of methylene units in the alkyl chain.
- 32 Kaler, E. W.; Kamalakara Murthy, A.; Rodriguez, B. E.; Zasadzinski, J. A. N. *Science* **1989**, *245*, 1371.
- 33 Herrington, K. L.; Kaler, E. W.; Muller, D. D.; Zasadzinski, J. A.; Chiruvolu, S. *J. Phys. Chem.* **1993**, *97*, 13792.
- 34 N. Filipovic-Vincekovic, N.; Skrtic, D.; Tomasic, V. *Ber. Bunsenges. Phys. Chem.* **1991**, *95*, 1646.
- 35 Chung, Y.; Regen, S. L.; Fukuda, H.; Hirano, H. *Langmuir* **1992**, *8*, 2843.
- 36 Fukuda, H.; Kawata, K.; Okuda, H.; Regen, S. L. *J. Am. Chem. Soc.* **1990**, *112*, 1635.
- 37 Israelachvili, J. N.; Mitchell, D. J.; Ninham, B. W. *J. Chem. Soc., Faraday Trans.* **1976**, *272*, 1525.
- 38 Vogel, A. I. *Textbook of Practical Organic Chemistry*; Longman Scientific & Technical: Harlow, 1989, p. 949.
- 39 Steward, J. J. P. *J. Comp. Chem.* **1989**, *10*, 209.

Chapter 3

*Metal ion binding amphotrope:
Single chained amphiphile carrying
an o-hydroxyazobenzene unit*

Abstract

A novel single chained ammonium amphiphile has been synthesized which carries an o-hydroxyazobenzene unit at the terminus of its hydrophobic chain. This compound forms ordered thread-like aggregates upon dispersion in water. These aggregates exhibit a phase transition at 56 °C. The o-hydroxyazobenzene unit binds several transition metal ions in a 2:1 stoichiometry. Binding of these metal ions results in a lowering of the critical aggregation concentration. From the changes in the UV absorption spectrum it is concluded that the Cu²⁺ complex forms more tightly packed aggregates in water than the Zn²⁺ and Ni²⁺ complexes.

3.1 Introduction

Surfactants in water form micro-heterogeneous dispersions due to their self-assembling behavior. These self-organized structures like micelles and bilayer vesicles find applications in many fields ranging from detergency to oil recovery technology. Bilayer vesicles have been used as drug delivery systems.¹⁻³ Micelles and bilayer structures from surfactants which bind metal ions in their headgroup region have shown to exhibit catalytic activity toward hydrolytic reactions.⁴⁻⁷ These systems can also be used to purify water from metal ions by removing the micelle bound metal ions by ultra filtration techniques.^{8,9} Furthermore, the binding of different metal ions to aqueous surfactant dispersions has been shown to affect the aggregate morphology in a number of cases.^{10,11}

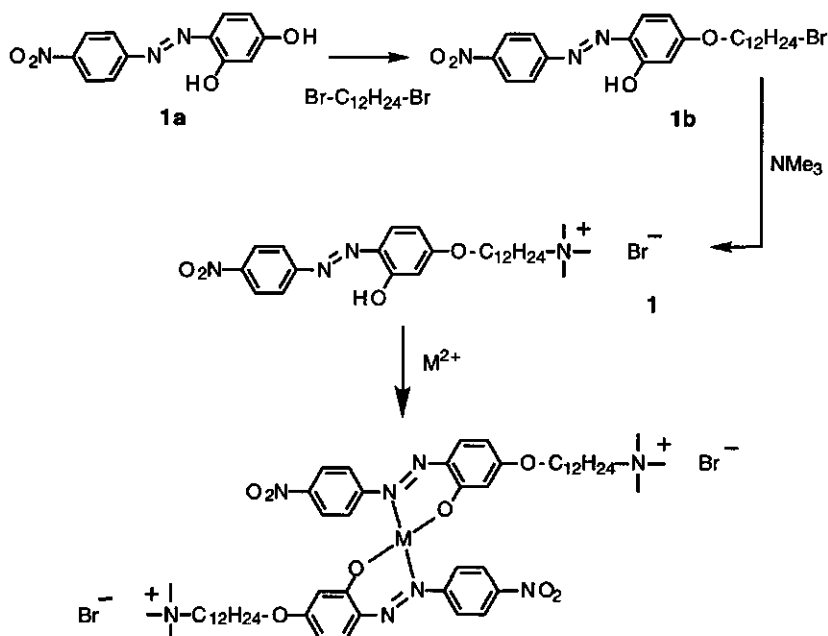
Kunitake *et al.*¹² and Singh *et al.*¹³ incorporated azobenzene units into the hydrophobic tails of single chained surfactants which can bind metal ions in their headgroup region. Binding of metal ions induces aggregation of these surfactants resulting in a blue shift of the azobenzene π - π^* absorption maximum. Recently, Suh *et al.*¹¹ have synthesized surfactants with a *o,o'*-dihydroxyazobenzene headgroup. In these surfactants two metal ions are bound by the azobenzene itself resulting in coordinatively polymerized bilayer structures.

In this chapter we report the synthesis of a novel single chained ammonium surfactant carrying an *o*-hydroxyazobenzene at the terminus of the hydrophobic chain. The aggregation behavior of this compound in water has been studied by conductometry, electron microscopy, differential scanning calorimetry, UV absorption spectroscopy and ¹H-NMR. Furthermore, the effect of metal ion binding on the aggregate stability in water has been investigated. Also the formation of ion-pair amphiphiles with sodium dodecylsulfate has been studied.

3.2 Results and discussion

A novel single chained ammonium amphiphile **1** has been synthesized containing a terminal *o*-hydroxyazobenzene unit which is able to bind transition metal ions. The synthetic pathway and the molecular structure are given in Scheme 1. The coupling of 2,4-dihydroxy-4'-nitroazobenzene with 1,12-dibromododecane results in the formation of many products. However, one of the first products to be formed is the monoalkylated compound **1b**. Therefore the reaction time should be no longer than 2 hours. Reaction of this compound with NMe₃ leads to the amphotrope **1**. At neutral pH, the Krafft point of compound **1** is found at 27 °C. In water this compound forms thread-like structures with diameters of approximately 70 Å, some of which have a strange bud at one of their ends as was observed by cryo-electron microscopy (see Figure 1). A phase transition is observed at 56 °C with DSC and with ¹H-NMR (see Figure 2). From the increase in the sharpness of the peaks in the NMR spectrum it is concluded

that the molecules undergo a transition to a more mobile state. The sharpness of the peaks in the NMR spectrum at elevated temperatures is comparable to that of cetyltrimethylammonium bromide micelles. Possibly, a transition from thread-like structures to spherical micelles occurs. Upon addition of $\text{Ni}(\text{OAc})_2$ to a dispersion of **1** at 70 °C, the NMR signals broaden considerably indicating that binding of Ni^{2+} reduces the molecular mobility.



Scheme 1. Synthetic pathway and molecular structure of compound **1** and its metal ion complex.

At neutral pH the critical aggregation concentration (cac) is found around 0.1 mM at 20 °C as was determined by conductivity measurements. The concentrations used for UV absorption spectroscopy are far below the cac and a spectrum with an absorption maximum at 395 nm is observed. The same spectrum is observed in ethanol indicating that the molecules are present as monomers. When the concentration in water is increased to far above the cac, the absorption maximum is seen to shift to 350 nm. This blue shifted absorption maximum is indicative for the presence of azobenzene aggregates with (anti)parallel transition dipoles, so-called H-aggregates.^{15,16} This means that the formed aggregates are highly ordered.

When copper(II)acetate is added to an aqueous solution of **1** under its cac, aggregation is immediately induced as is observed by the appearance of a blue shifted absorption maximum at 350 nm (see Figure 3a). Apparently, the binding of Cu^{2+} results in a concomitant supramolecular aggregation. Electron microscopy shows that the same thread-like aggregates are formed as in concentrated dispersions without Cu^{2+} . When $\text{Cu}(\text{OAc})_2$ is added to an

ethanolic solution of **1** two maxima at 366 and at 462 nm are observed (see Figure 3b) which is attributed to binding of Cu^{2+} ions without supramolecular aggregation.

The blue shift of the absorption maximum in water is almost complete when 0.6 equivalent of Cu^{2+} ions has been added. This means that Cu^{2+} binds almost quantitatively in a 1:2 stoichiometry. A complexation constant of $9 \cdot 10^9 \text{ M}^{-2}$ can be calculated from the UV absorption spectra. The proposed structure of the formed complex is given in Scheme 1. The Zn^{2+} and Ni^{2+} ions bind less strongly to **1** and a tenfold excess of $\text{Ni}(\text{OAc})_2$ or $\text{Zn}(\text{OAc})_2$ is needed to obtain the spectrum of the aggregated species. The complexation constants for Zn^{2+} and Ni^{2+} are $2 \cdot 10^8 \text{ M}^{-2}$. It is a fairly general phenomenon that the equilibrium constant for the formation of analogous complexes of divalent cations with ligands containing a nitrogen donor decreases when going from Cu^{2+} to Ni^{2+} or Zn^{2+} .¹⁶

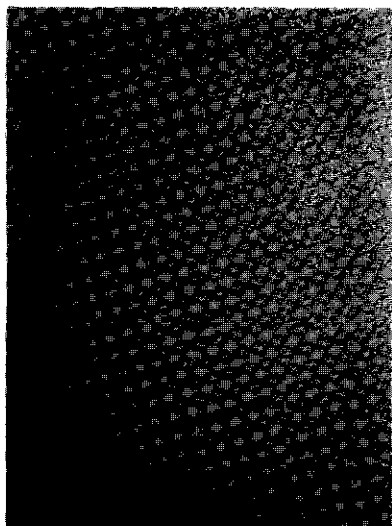


Figure 1. Cryo-electron micrograph of an aqueous dispersion of **1**. The bar represents 85 nm.

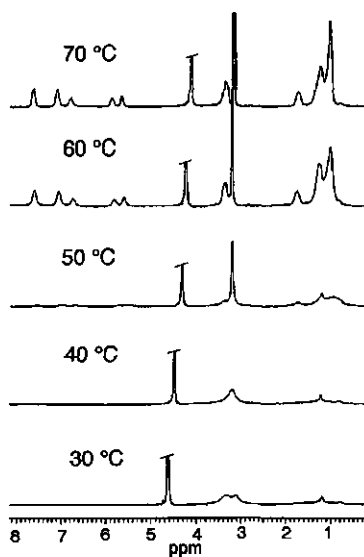


Figure 2. 200 MHz ^1H -NMR spectra of dispersions of **1** in D_2O at different temperatures. The residual HDO signal at about 4.5 ppm has been cut off.

It cannot be excluded that the acetate ions also induce aggregation by screening the headgroup repulsions. However, the great difference observed between addition of $\text{Cu}(\text{OAc})_2$ and $\text{Ni}(\text{OAc})_2$ indicates that binding of the metal ion is the dominant process in promoting the aggregation. Addition of sodium acetate also has a relatively minor effect on the aggregation in water.

Furthermore, it is observed that the extent of the blue shift is different for the three complexes. For Cu^{2+} , Ni^{2+} and Zn^{2+} the blue shifted absorption maxima lie at 350 nm, 364 nm and 378 nm respectively (see Figure 3c). According to the exciton theory proposed by Kasha¹⁵ the

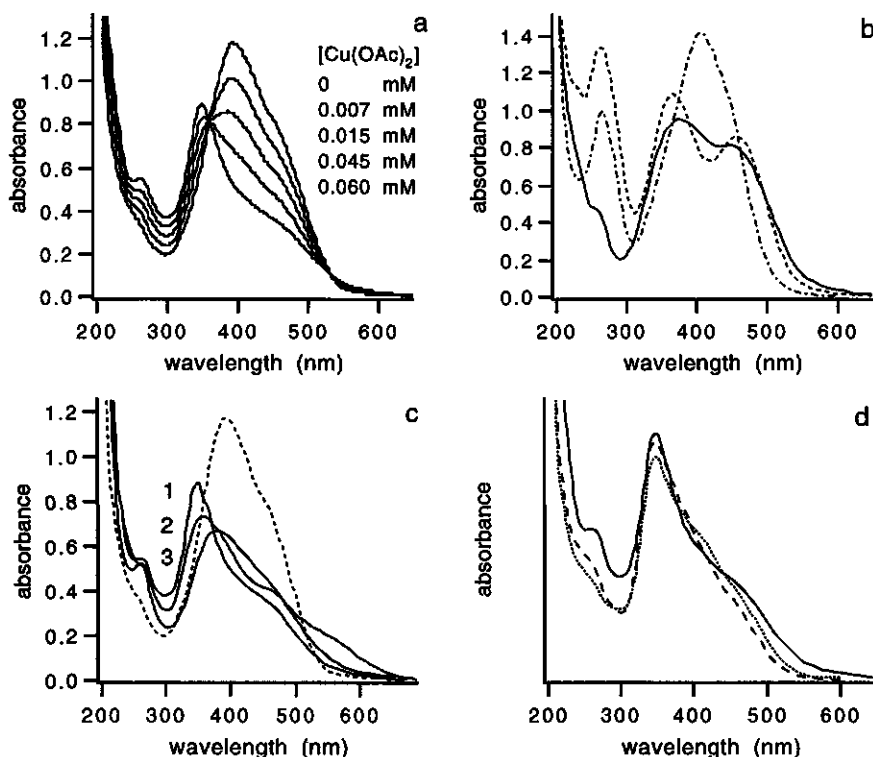


Figure 3. (a) UV absorption spectra of an aqueous dispersion of **1** (0.075 mM) before and after the addition of $\text{Cu}(\text{OAc})_2$. (b) UV absorption spectra of ethanol solutions of **1** (0.075 mM) without metal ions (---) and after the addition of $\text{Cu}(\text{OAc})_2$ (---) and after the addition of $\text{Ni}(\text{OAc})_2$ (—). (c) UV absorption spectra of aqueous dispersions of **1** (0.075 mM) before (---) and after the addition of excess $\text{Cu}(\text{OAc})_2$ (1), $\text{Ni}(\text{OAc})_2$ (2), and $\text{Zn}(\text{OAc})_2$ (3). (d) UV absorption spectrum of an aqueous dispersion of **1** at 0.3 mM, a concentration far exceeding the cac (---). UV absorption spectra at low concentrations (0.075 mM) in the presence of $\text{Cu}(\text{OAc})_2$ (---) and in the presence of SDS (---).

extent of the blue shift of the UV absorption maximum is strongly dependent on the distance between the azobenzene units and on their relative orientation. The observed differences in absorption maximum for the investigated metal ions might therefore reflect the different stacking distances between the azobenzenes in the formed aggregates. This would mean that the 1-Cu^{2+} complex forms the most ordered supramolecular aggregates.¹⁷ This is not surprising since Cu^{2+} has the strongest complexation constant.

The aggregates of the 1-Cu^{2+} complex have the same blue shifted absorption maximum as the aggregates of pure **1**. This means that incorporation of Cu^{2+} ions does not alter the average azobenzene-azobenzene distances in the aggregate. The binding of Zn^{2+} and Ni^{2+} however results in a reduction of the blue shift with respect to that of the aggregates of pure **1**. This

indicates that the binding of these ions hampers the optimal the packing of the azobenzenes in the aggregates.

When a large excess of vesicles of didodecyldimethylammonium bromide (DDAB) is added to a solution of 1-Cu^{2+} aggregates, no spectral changes occur indicating that the 1-Cu^{2+} aggregates are very stable and no mixing of monomers occurs. When vesicles of DDAB are added to 1-Zn^{2+} or 1-Ni^{2+} aggregates, the blue shift is immediately lost due to the formation of mixed aggregates in which there is no stacking of the azobenzenes anymore, even when a small excess of DDAB is used. This demonstrates that the 1-Zn^{2+} or 1-Ni^{2+} aggregates are indeed less stable than the 1-Cu^{2+} aggregates.

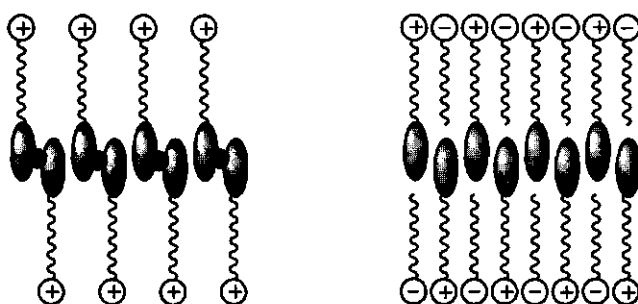


Figure 4. Schematic representation of possible aggregate structures of **1** in the presence of Cu^{2+} (left) and SDS (right).

The spectral shift caused by the aggregation induced by the binding of Cu^{2+} forms an effective means to detect very low concentrations of Cu^{2+} in water. When a concentration $50\text{ }\mu\text{M}$ of compound **1** is present in the cuvette, a concentration of $10\text{ }\mu\text{M}$ of Cu^{2+} can easily be detected. Furthermore, the Cu^{2+} ions are captured in the interior of the aggregates. This would offer a possibility to remove Cu^{2+} ions from an aqueous solution by ultra filtration techniques.

The addition of one equivalent of sodium dodecylsulfate (SDS) to a sub-micellar solution of **1** also results in a blue shift of the absorption maximum from 395 nm to 350 nm due to the formation of ion-pair amphiphiles. These ion-pair amphiphiles have a lower critical aggregation concentration than the parent amphiphiles. This is caused by the electrostatic attraction between the headgroups.^{18,19}

Interestingly, the UV absorption spectrum which is obtained for **1** in the presence of Cu^{2+} is rather similar to the spectrum obtained in the presence of sodium dodecylsulfate or for the pure compound **1** at concentrations far exceeding the *cac* (see Figure 3d). In the presence of Cu^{2+} ions the azobenzenes are forced in an antiparallel interdigitated configuration. This suggests that in the absence of metal ions the azobenzenes are also interdigitated in the formed aggregates. This interdigitation of azobenzenes in self-aggregated structures has been reported before.^{15,20} The interdigitation of the azobenzenes results in an increased distance between the alkyl chains (which might induce tilting of the alkyl chains). SDS probably fills these empty spaces very

well and therefore these ion-pair aggregates give the same spectral blue shift as the aggregates of pure **1** and the **1**-Cu²⁺ complex.

If the azobenzenes are actually interdigitated, it is difficult to imagine how these molecules form the thread-like structures, since the molecules cannot pack as conventional surfactants in a rod-like micelle. Possibly, these thread-like structures consist of narrow bilayer ribbons with the lateral edges exposed to the aqueous phase. This would expose part of the polar azobenzene units in aggregate to the water. This might compensate the unfavorable interaction of the exposed alkyl spacers.

3.3 Conclusions

The novel *o*-hydroxyazobenzene containing ammonium amphiphile **1** forms thread-like aggregates in water which exhibit a phase transition at 56°C. Aqueous dispersions of **1** exceeding the critical aggregation concentration show a blue shifted absorption maximum due to the formation of H-aggregates of the azobenzene units. It has been shown that binding of metal ions can occur in the interior of the formed aggregates. This does not seem to alter the aggregate morphology. Binding of Cu²⁺ ions results in a strong decrease of the cac and a strong stabilization of the formed aggregates. Ni²⁺ and Zn²⁺ are less strongly bound by this amphiphile and binding of these ions results in the formation of less stable and less ordered aggregates. Compound **1** readily forms ion-pair amphiphiles with sodium dodecylsulfate. The azobenzene units in the ion-pair aggregates are probably similarly interdigitated as in the Cu²⁺ ion complexed aggregates and as in the aggregates of pure **1**.

3.4 Experimental section

3.4.1 Synthesis

2,4-Dihydroxy-4'-nitroazobenzene (**1a**) was prepared by reaction of the diazonium salt of 4-nitroaniline with resorcinol.¹⁴

12-Bromo-1-[[[(4-nitrophenyl)azo]-2'-hydroxyphenyl]-4'-oxy]dodecane (**1b**)

A mixture of 25 mmol of 2,4-dihydroxy-4'-nitroazobenzene, 50 mmol of 1,12-dibromododecane and 50 mmol of K₂CO₃ in 100 mL of 2-butanone was refluxed for 2 h. The salt was removed by filtration and the filtrate was concentrated by evaporation of the solvent. The product was purified by column chromatography on silica gel using petroleum ether (bp. 40-60 °C)/CH₂Cl₂, 1:1 v/v as eluent (yield 10 %). ¹H-NMR (CDCl₃, TMS, δ, ppm): 1.40 (m, 16 H, -(CH₂)₈-), 1.80 (m, 4 H, Br-CH₂-CH₂-, RO-CH₂-CH₂-), 3.40 (t, 2 H, Br-CH₂-), 4.00 (t, 2 H, RO-CH₂-), 6.36 - 8.30 (m, 7 H, Ar-H), 12.43 (s, 1 H, HO-Ar).

***N*-{12-[[*(*4-Nitrophenyl)azo]-2'-hydroxyphenyl-4'-oxy}dodecyl}-*N,N,N*-trimethylammonium bromide (1)**

A solution of 0.8 mmol of the 12-bromo-1-[[*(*4-nitrophenyl)azo]-2'-hydroxyphenyl-4'-oxy]dodecane (**1b**) in 6 mL of a 20% (w/w) solution of trimethylamine in ethanol was heated at 100°C for 1 h in a closed reaction vessel. The mixture was allowed to cool to room temperature and was then thoroughly cooled on ice. The precipitate was collected by filtration and washed with diethyl ether. The product was purified by column chromatography on aluminum oxide (activity grade III) using CH₂Cl₂/MeOH (100:3 v/v) as eluent. Yield 80%. Mp. 198 °C.

¹H-NMR (CDCl₃, TMS, δ, ppm): 1.40 (m, 16 H, -(CH₂)₈-), 1.80 (m, 4 H, N-CH₂-CH₂-, RO-CH₂-CH₂-), 3.4 (m, 11 H, N-(CH₃)₃-, -CH₂-N-), 4.00 (t, 2 H, RO-CH₂-), 6.30 - 8.50 (m, 7 H, Ar-H), 12.43 (s, 1 H, HO-Ar). Anal. Calcd for C₂₇H₄₁N₄O₄Br: C, 57.34; H, 7.31; N, 9.91. Found: C, 57.91; H, 7.61; N, 9.91.

3.4.2 Methods

Aqueous dispersions were prepared by slightly heating and shaking of the solid material in water. The water was purified by filtration through a Seralpur pro 90C purification system. For the Differential Scanning Calorimetry (DSC) measurements (Perkin Elmer DSC 7) 1% (w/w) sample solutions were prepared. A scan rate of 10 °C/min was used. The critical aggregation concentration was determined by measuring the specific conductivity of the solution of **1** as a function of the concentration. A Philips Digital Conductivity meter PW 9527 with a Philips PW 9550/60 electrode was used. The UV absorption spectra were recorded on a Lambda 18 spectrophotometer from Perkin Elmer.

3.5 References

- 1 Lasic, D. D.; Papahadjopoulos, D. *Science* **1995**, *267*, 1275.
 - 2 Lasic, D. D.; Martin, F. J.; Gabizon, A.; Huang, S. K.; Papahadjopoulos, D. *Biochim. Biophys. Acta* **1991**, *1070*, 187.
 - 3 Lasic, D. D. *Angew. Chem.* **1994**, *106*, 1765.
 - 4 Weijnen, J. G. J.; Koudijs, A.; Engbersen, J. F. J. *J. Chem. Soc., Perkin Trans. 2* **1991**, 1121.
 - 5 Weijnen, J. G. J.; Koudijs, A.; Schellekens, G. A.; Engbersen, J. F. J. *J. Chem. Soc., Perkin Trans. 2* **1992**, 829.
 - 6 Weijnen, J. G. J.; Koudijs, A.; Engbersen, J. F. J. *J. Mol. Catal.* **1992**, *73*, L5.
 - 7 Menger, F. M. *Angew. Chem.* **1991**, *103*, 1104.
 - 8 Van Zanten, J. H.; Chang, D. S. W.; Stanish, I.; Monbouquette, H. G. *J. Membr. Sci.* **1995**, *99*, 49.
 - 9 Hebrant, M.; Bouraine, A.; Tondre, C.; Brembilla, A.; Lochon, P. *Langmuir* **1994**, *10*, 3994.
 - 10 Van Esch, J. H.; Stols, A. L. H.; Nolte, R. J. M. *J. Chem. Soc., Chem Commun.* **1990**, 1658.
 - 11 Suh, J.; Lee, K. J.; Bae, G.; Kwon, O.; Oh, S. *Langmuir* **1995**, *11*, 2626.
 - 12 Shimomura, M.; Kunitake, T.; *J. Am. Chem. Soc.* **1982**, *104*, 1757.
 - 13 Singh, A.; Tsao, L.; Markowitz, M.; Gaber, B. P. *Langmuir* **1992**, *8*, 1570.
 - 14 Vogel, A. I. *Textbook of Practical Organic Chemistry*; Longman Scientific & Technical: Harlow, 1989, p. 949.
 - 15 Kasha, M.; Rawls, H. R.; Ashraf El-Bayoumi, M. *Pure Appl. Chem.* **1965**, *11*, 371.
 - 16 Shimomura, M.; Aiba, S.; Tajima, N.; Inoue, N.; Okuyama, K. *Langmuir* **1995**, *11*, 969.
- Cotton, F. A.; Wilkinson, G.; Gaus, P. L. *Basic Inorganic Chemistry*; John Wiley & Sons: Singapore, 1987, p. 470.

- 17 Gordon, P. F.; Gregory, P. *Organic Chemistry in Colour*, Springer-Verlag: Berlin, 1987, p 116.
- 18 Kaler, E. W.; Kamalakara Muthry, A.; Rodriguez, B. E.; Zasadzinski, J. A. N. *Science* **1989**, *245*, 1371.
- 19 Herrington, K. L.; Kaler, E. W.; Miller, D. D.; Zasadzinsky, J. A.; Chiruvolu, S. *J. Phys. Chem.* **1993**, *97*, 13792.
- 20 Everaars, M. D.; Marcelis, A. T. M.; Kuijpers, A. J.; Laverdure, E.; Koronova, J.; Koudijs, A.; Sudhölter, E. J. R. *Langmuir* **1995**, *11*, 3705.

Chapter 4

*Double chained amphiphiles
carrying one mesogen*

Abstract

A number of double chained ammonium amphiphiles with biphenyl, azobenzene and stilbene mesogenic moieties at the terminus of one of the hydrophobic tails has been synthesized. These compounds form stable bilayer vesicles upon dispersion in water. In the bilayers the mesogens from molecules of opposite leaflets of the bilayer are interdigitated. Bilayers of the azobenzene containing double chained amphiphiles (4) exhibit a gel-to-liquid crystalline phase transition. The nature of the 4'-substituent at the azobenzene unit influences the phase transition temperature T_c . The T_c increases in the order $F < H < NO_2 < CN < OCH_3 < N=N-Ph$. This sequence cannot be correlated with the electron withdrawing or donating properties of the substituents. It is therefore concluded that dispersion rather than dipole-dipole interactions between the azobenzene units are important.

In the bilayers the azobenzene mesogens form H-aggregates as is observed by the blue shift of the UV absorption maximum. This blue shift is not affected by the 'gel-to-liquid crystalline' phase transition. Vesicles of 4-N=N-Ph do not exchange monomers with vesicles of didodecyldimethylammonium bromide whereas vesicles of the other compounds do. Compound 4-N=N-Ph forms monolayers at the water-air interface which are much more stable than the monolayers of any of the other investigated compounds. The amphotrope 5 which contains one perfluorinated alkyl chain forms vesicles which exhibit a high T_c and a peculiar monomer exchange behavior.

4.1 Introduction

In recent years much attention has been paid to the development of new organic materials containing azobenzene units. Being a potential mesogenic unit, the incorporation of azobenzene moieties can induce the formation of thermotropic liquid crystalline phases in both monomeric and polymeric compounds. Another attractive property of azobenzenes is their photoinduced trans-cis isomerization¹⁻⁴ so that the physical properties of azobenzene containing materials can be simply altered by irradiation with UV light.

Kunitake *et al.*⁵⁻¹² incorporated azobenzene units into the hydrophobic tails of single chained ammonium amphiphiles. Some of these compounds form bilayer membranes whose permeability can be altered by isomerizing the azobenzene units. The stacking of the azobenzenes in the bilayer results in a shift of the π - π^* absorption maximum. This shift is a direct measure for the degree of molecular order in the bilayer.

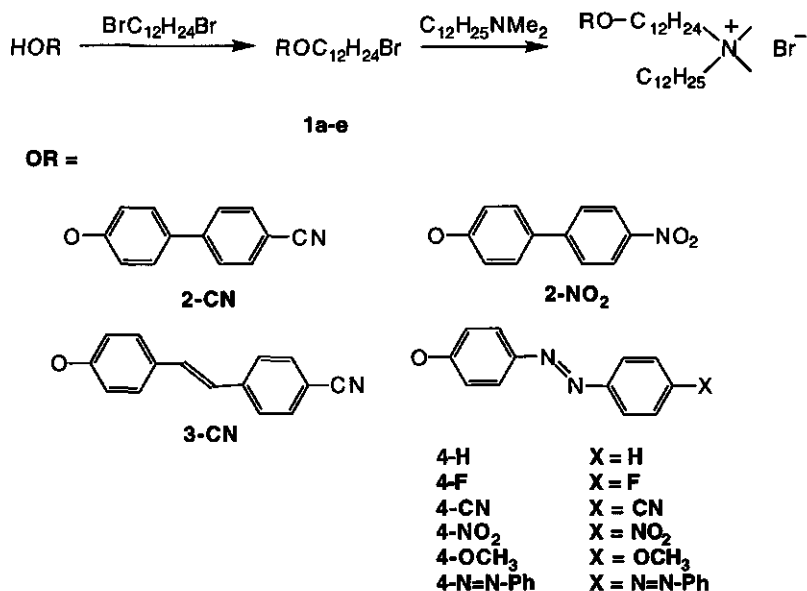
Substituents at the mesogenic units are important in determining the dipole moment of the mesogen and therefore its self-organizing properties.^{13,14} In this chapter the synthesis of a series of novel double chained ammonium surfactants carrying different biphenyl, stilbene and azobenzene mesogenic units at the terminus of one of the hydrophobic chains is described. The effect of different substituents at the azobenzene moiety on the aggregation behavior of these compounds in water and at the water-air interface has been studied. Also the effect of the introduction of a perfluorinated alkyl chain has been investigated.

The aggregate morphology was investigated by means of optical and electron microscopy. The bilayer spacing was obtained from X-ray reflectivity measurements. The aggregate stability was judged by differential scanning calorimetry experiments and monomer exchange experiments. The stability of monolayers at the water-air interface was studied by using a Langmuir trough.

4.2 Results and discussion

4.2.1 Thermotropic properties

The compounds **2** and **3** exhibit a complicated thermotropic phase behavior due to the presence of different crystal types and the presence of monotropic liquid crystalline phases. Compound **4-N=N-Ph** is the only compound in the investigated series to exhibit an enantiotropic smectic phase. Upon cooling from the isotropic phase the liquid crystalline phase appears first as bâtonettes which develop into a fan-shaped focal-conic texture typical of a smectic A phase. This compound also has a considerably higher isotropization temperature than any of the other compounds **4** (see Table 1, p. 64). This shows that this double azobenzene unit has stronger mesogenic properties than the other investigated azobenzene moieties. This is probably due to stronger interactions between these more extended aromatic units.



Scheme 1. Synthetic pathway and structures of compounds 1-4.

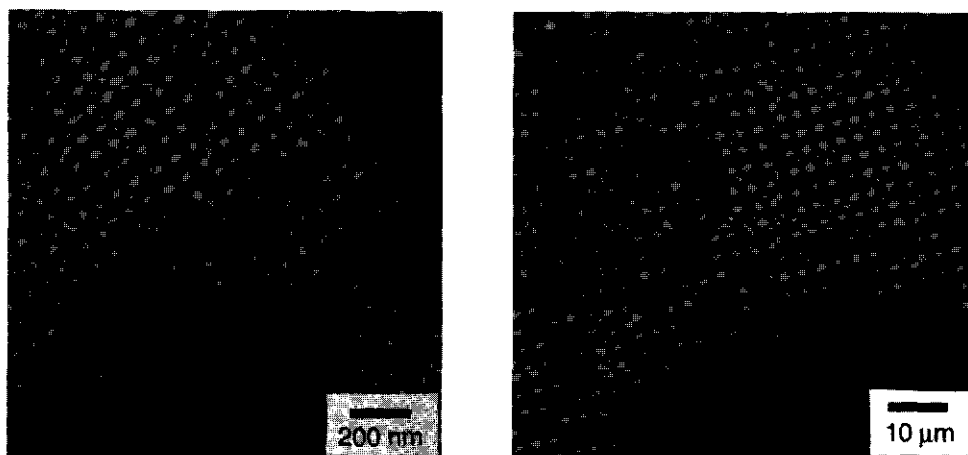


Figure 1. (a) Electron micrograph of vesicles of **4-NO₂** prepared by sonication and subsequently stained with uranyl acetate. (b) Optical micrograph of a hydrated crystal of **4-CN** in water at 60 °C.

4.2.2 Aggregate morphology and phase behavior

Compounds **2**, **3** and **4** which possess two hydrophobic tails of which one carries a mesogenic unit, form small unilamellar bilayer vesicles upon sonication (Figure 1a). Giant unilamellar vesicles¹⁵⁻¹⁷ of these compounds are formed when crystals are immersed in water of 60°C and allowed to hydrate. Hydration starts instantly as is seen by the formation of worm-like tubuli at

the surface of the crystals (Figure 1b). It is important that the sample of the hydrated crystals is not mechanically agitated, because this enhances the formation of smaller vesicles. After about 10 minutes, the formation of giant liposomes is observed which are formed by detachment of the bilayer tubules. These giant liposomes can reach diameters of 20 μm and can easily be observed by light microscopy.

Because the Krafft temperatures of compounds **2** and **3** lie around 40–50°C, the vesicles are not stable at room temperature. In the undercooled state these vesicles are usually stable for 6–8 hours before precipitation occurs.

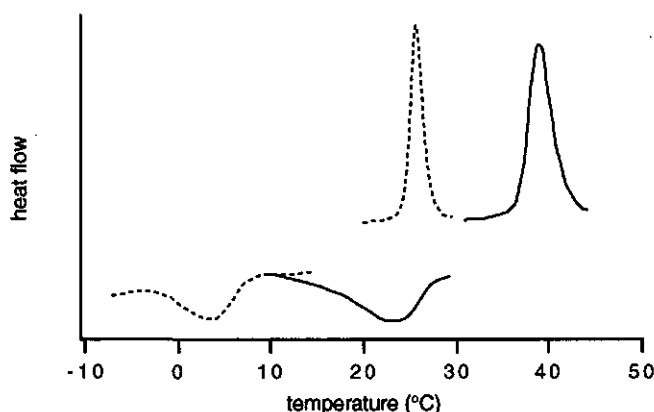


Figure 2. DSC thermograms of vesicle dispersions of **4-CN** (solid line) and **4-NO₂** (dashed line). The upper traces are heating curves and the lower traces are cooling curves.

Figure 2 shows the DSC thermograms of 2 % w/w vesicle dispersions of **4-CN** and **4-NO₂** in water. Phase transitions are seen at 39°C and at 27°C respectively. These transitions are reversible upon cooling and are attributed to the gel-to-liquid crystalline phase transition of the bilayers (T_c). For **4-CN** this phase transition has been confirmed by temperature dependent $^1\text{H-NMR}$ measurements (see Figure 3). The sharpening

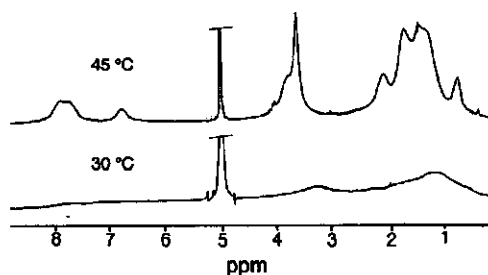


Figure 3. $^1\text{H-NMR}$ spectra of bilayer vesicles of **4-CN** in D_2O ($T_c = 39^\circ\text{C}$).

of the NMR peaks above T_c indicates increased molecular mobility in the bilayers.

When vesicle dispersions of **4-CN** and **4-NO₂** are frozen and subsequently allowed to melt, turbid dispersions of hydrated microcrystals are obtained. DSC measurements of these dispersions show phase transitions at 52 °C and 42 °C respectively. These are attributed to the

crystal to bilayer transition (which corresponds to the Krafft point).¹⁸ Upon subsequent cooling to 5°C, followed by heating, the original vesicle thermograms are restored.

For the vesicle dispersions of compounds **2-CN**, **2-NO₂** and **3-CN** no gel-to-liquid crystalline phase transitions are observed by DSC (on 2 % w/w samples). The transition temperatures are expected to lie below those of the azobenzene compounds **4-CN** and **4-NO₂** because of the lower aggregate stabilizing effect of the biphenyl and stilbene mesogens with respect to the azobenzene mesogens (see chapter 2). This will cause the bilayers to be less ordered and the phase transitions, if they occur at all, will probably be accompanied by a much smaller heat effect. These results agree well with the results for the dialkyldimethylammonium bromide series.¹⁹ Didodecyldimethylammonium bromide also has no detectable gel-to-liquid crystalline phase transition by DSC (on 2 % w/w samples¹⁹) whereas compounds with longer chains do have measurable phase transitions. For the shorter chains the driving force for aggregation is reduced, resulting in less ordered bilayers with lower phase transition enthalpies.

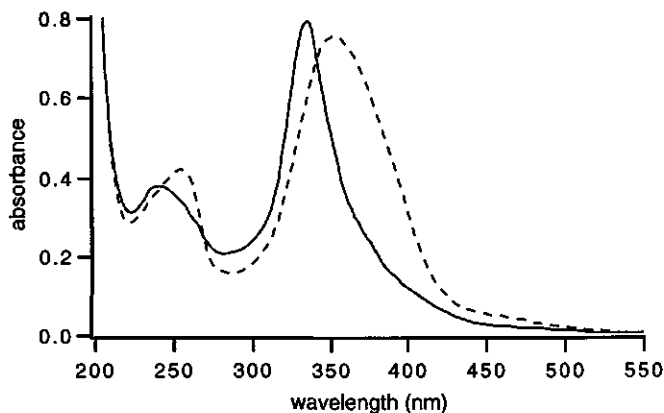


Figure 4. UV absorption spectra of compound **4-CN** as monomers in ethanol (dashed line) and as vesicles in water (solid line). The concentrations are $3 \cdot 10^{-5}$ M and $4 \cdot 10^{-5}$ M respectively.

Figure 4 shows the UV spectrum of an aqueous vesicle dispersion of **4-CN** together with the monomer spectrum observed in ethanol. The absorption maximum of the monomeric species lies at 363 nm and for the vesicle dispersion at 334 nm. Similar blue shifts of the absorption maximum are observed for vesicles of the other compounds **4** (Table 1, p. 64) and for **3-CN**. The main absorption band for the azobenzene and stilbene chromophore is the π - π^* transition for which the transition moment is oriented along the long axis of the aromatic moiety.²⁰ According to the molecular exciton model proposed by McRae and Kasha²¹ the blue shift of the absorption maximum for the vesicle dispersion is indicative of linear chromophore aggregates with their transition moments (anti)parallel to each other and ordered perpendicular to the

stacking direction (so-called H-aggregate^{22,23}). For vesicle dispersions of **2-CN** and **2-NO₂** no blue shifted absorption maxima are observed. This may be due to the relatively high *cac* values of these compounds so that at UV measuring concentrations (10^{-4} - 10^{-5} M) predominantly the molecularly solubilized species is present. An indication for this is the fact that blue shifts of a few nanometers are observed upon increasing the concentrations of these compounds.

Because the blue shift in the absorption spectrum due to the formation of H-aggregates is very sensitive to the mesogen-mesogen distance, it was expected that the gel-to- liquid crystalline phase transition would influence this spectral shift. Interestingly, the extent of the blue shift of the UV absorption maxima is not altered by the phase transition. This was tested by measuring the UV absorption spectra of 0.2 mM vesicle dispersions in a 1 mm cuvette at different temperatures. This means that although the molecules have increased mobility, as was confirmed by ¹H-NMR, the average stacking distance between the mesogens remains the same above the phase transition temperature. This suggests that the phase transition is primarily associated with the melting of the alkyl chains.

When lower concentrations of vesicles are used (0.07 mM), the blue shift disappears at higher temperatures. This is attributed to a dissolution of the bilayers into monomers as a result of the increased critical bilayer concentration.

In order to obtain more information about the structure of the bilayer, the bilayer thickness of vesicles of **4-CN** was measured by X-ray reflectivity measurements⁷ on cast films of vesicles of **4-CN**. The measurements gave a bilayer thickness of 40.8 Å. It is known that the bilayer structure is maintained in the cast films.²⁴ Taking into consideration that the calculated length of a molecule is 31 Å, this probably means that in the bilayer structure interdigitation

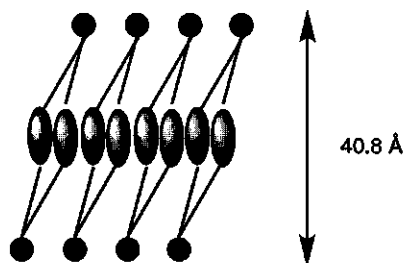


Figure 5. Schematic representation of a bilayer from **4-CN**.

of the mesogens occurs accompanied by tilting of the alkyl chains, as illustrated in Figure 5. For compound **4-CN** which has both a C₁₂ spacer and a C₁₂ tail we can obtain a perfectly ordered bilayer structure in which the mesogens of oppositely positioned molecules are interdigitated. From the blue shift in the UV spectra of the vesicles it is known that the mesogens are more or less parallelly stacked. It is therefore assumed that the alkyl chains are tilted with respect to the mesogens. The fact that the aggregate peak in the UV spectrum is very narrow ($w_{1/2}$ =30 nm) and bell-shaped indicates that there is a high degree of order in these bilayers.

Interdigitation of mesogens is very commonly encountered for thermotropic liquid crystals both in their crystalline state and in their mesophases. By interdigitation unfavorable interactions between the dipoles of the mesogens can be minimized.^{25,26}

When the C₁₂ tail of compound **4-CN** is replaced with a C₁₆ tail the UV absorption maximum of the vesicle dispersion is also blue shifted but the peak is broader ($w_{1/2}$ = 65 nm) and less symmetrical. This shows that if the alkyl tail is longer than the spacer this hampers the formation of ordered structures. DSC also shows no measurable phase transition for vesicles of this compound.

When vesicles of **3-CN** are irradiated with UV light of 366 nm, the absorption maximum at 295 nm disappears within a few minutes. This is attributed to a [2+2]-photocycloaddition of the double bonds of two adjacent stilbene mesogens (Figure 6). This results in the loss of the conjugation between the two phenyl rings of the stilbene moiety and in the formation of a cyclobutane ring. In this way it is possible to covalently connect both sides of the bilayer.

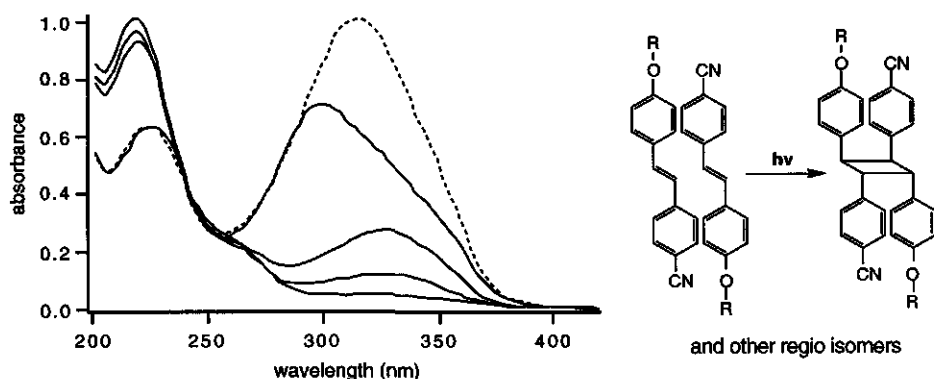


Figure 6. Time dependent decrease of the π - π^* absorption band of vesicles of **3-CN** in water upon irradiation with UV light of 366 nm (dashed line is the monomer spectrum in ethanol). [**3-CN**] = $5 \cdot 10^{-5}$ M.

4.2.3 Substituent effects on the phase transition temperatures

The Krafft temperatures of the compounds **4** are given in Table 1 (p. 64) and lie all above room temperature (the Krafft point is the temperature at which the hydrated crystals are transformed into bilayer structures). Compounds **4-H** and **4-N=N-Ph** have the highest Krafft temperatures (80° and 65 °C). This means that these compounds fit very well in a crystal lattice and therefore have a poor tendency to get hydrated and to form bilayer structures. The compounds **4-CN**, **4-NO₂** and **4-OCH₃** have Krafft temperatures around 50 °C indicating that hydration of the molecules in the crystal to give bilayer structures occurs more easily. Compound **4-F** has the lowest Krafft point. Probably, the unfavorable miscibility between fluorocarbon and hydrocarbon segments destabilizes the molecular packing in the crystal lattice.

The stability of the vesicle dispersions at room temperature varies from a few hours for **4-H** to months for **4-N=N-Ph** and **4-F**. Although the vesicles are not thermodynamically stable at room temperature, crystallization is kinetically controlled at room temperature.

All the investigated bilayer vesicles of **4**, except those of **4-N=N-Ph**, show a gel-to-liquid crystalline phase transition (T_c) by DSC. The DSC thermograms are given in Figure 7. The phase transition temperatures as observed upon heating are also given in Table 1. Scan rates of 10 °C/min were used for the DSC experiment. Using lower scan rates did not affect the observed phase transition temperatures much. Upon cooling the phase transitions are usually observed at lower temperatures. The vesicles of **4-H** exhibit two phase transitions at 24° and 28 °C. The phase transition temperatures of didodecyldimethylammonium bromide ($C_{12}C_{12}N^+$) and dioctadecyldimethylammonium bromide ($C_{18}C_{18}N^+$) bilayers are found at 17 °C²⁷ and at 45 °C²⁸ respectively. These compounds are structurally related to the compounds **4** but lack the azobenzene unit.

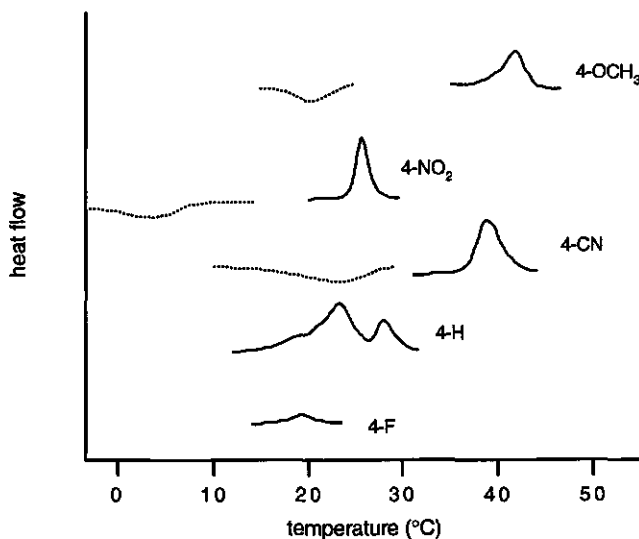


Figure 7. DSC thermograms of 1 % w/w vesicle dispersions of compounds **4**. The solid traces are the heating curves, the dashed traces are the cooling curves.

When the T_c s of vesicles of the compounds **4** are compared with that of $C_{12}C_{12}N^+$ vesicles it is seen that the introduction of the azobenzene unit with the fluorine substituent ($T_c = 19$ °C) hardly affects the phase transition temperature. All the other azobenzenes cause an increase in T_c with respect to that of $C_{12}C_{12}N^+$. Vesicles of **4-OCH₃** ($T_c = 42$ °C) have a T_c almost as high as that of $C_{18}C_{18}N^+$ bilayers. This shows that very subtle structural changes in the compounds **4** cause changes in T_c which can only be realized in the dialkyldimethylammonium bromide bilayers by drastic elongation of the alkyl chains.

Table I. Melting Points (T_m), Krafft Temperatures (T_{Krafft}) and Phase Transition Temperatures (T_c) for Compounds **4**. Also the UV Absorption Maxima of the Vesicles in Water (λ_{ves}) and the Monomers in Ethanol (λ_{EtOH}) are given.

Compound	T_m (°C)	T_{Krafft} (°C)	T_c (°C)	λ_{EtOH} (nm)	λ_{ves} (nm)
4-H	132	80	24;28	346	324
4-F	105	29	19	347	326
4-CN	151	52	39	363	334
4-NO₂	119	42	27	375	341
4-OCH₃	135	50	42	357	338
4-N=N-Ph	151-S*-182	65	†	381	368

† not observed under the employed experimental conditions

* an enantiotropic smectic liquid crystalline phase is observed

The T_c thus increases in the series **4-F** < **4-H** < **4-NO₂** < **4-CN** < **4-OCH₃**, reflecting increasing azobenzene-azobenzene interactions. The nature of the terminal group is important in determining the dipole moment of the azobenzene unit and therefore its self-organizing properties. Because the alkoxy spacer at the 4-position is an electron donating group, electron withdrawing substituents at the 4'-position give rise to mesogens with high overall dipole moments. For side chain liquid crystalline polymers it has been found that apolar substituents on the mesogen tend to induce nematic phases. Polar electron withdrawing (-CN or -NO₂) substituents induce the formation of more ordered smectic phases.^{13,14} This has been ascribed to the tendency of these mesogens with large dipole moments to form antiparallel dimers caused by the favorable dipolar interactions.

The observed trend does however not fit with the picture of bilayer stabilization by increased dipole-dipole interactions between the mesogenic units. Other parameters like the polarizability of the substituents and the precise packing mode probably also contribute to the stabilization through dispersion interactions. Bilayers of **4-F** have the lowest T_c . Possibly, the mesomeric electron donating property of the F-substituent results in reduced dipolar interactions between the mesogens. Alternatively, the unfavorable miscibility between fluorocarbon and hydrocarbon segments might destabilize the bilayer. Bilayers of **4-OCH₃** have a T_c which is relatively high although the methoxy substituent is also a mesomerically electron donating substituent. This shows that specific mesogen-mesogen interactions, which are not necessarily dependent on the dipole of the mesogen, stabilize lyotropic lamellar mesophases.

The compounds **4-H**, **4-CN**, **4-F** and **4-OCH₃** undergo facile trans-cis isomerization in the bilayer state upon irradiation with UV light of 366 nm as could be monitored with UV spectroscopy. The fact that these bilayers are in their gel phase at room temperature does not seem to hamper the isomerization. The thermal back isomerization from the cis to the trans form

is very slow at room temperature. For **4-NO₂** and **4-N=N-Ph** no cis isomer is detected upon irradiation at this wavelength. This means that either the cis isomer is not formed or that it isomerizes back to the trans isomer very rapidly. Figure 8 shows the effect of trans-cis isomerization on the gel-to-liquid crystalline phase transition of vesicles of **4-H**. For bilayers in the trans state two phase transitions are observed at 24 °C and 28 °C. After irradiation the high temperature transition is lost. This shows that the isomerization affects the molecule packing in the bilayer.

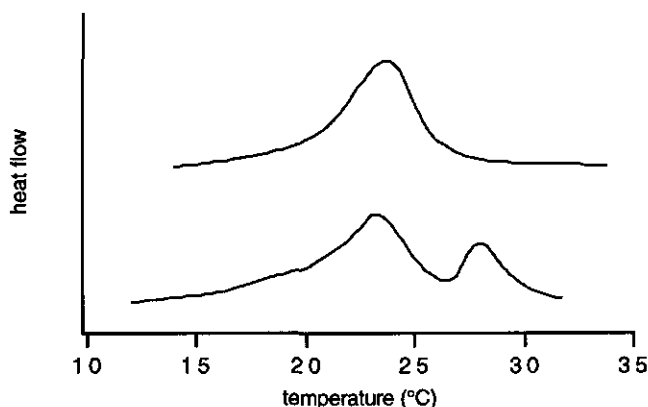


Figure 8. DSC thermograms of a 1 % w/w vesicle dispersion of **4-H** before (lower trace) and after irradiation (upper trace) with UV light of 366 nm.

4.2.4 Monomer exchange experiments

When vesicles of **4-H**, **4-NO₂**, **4-CN**, **4-OCH₃** or **4-F** are mixed with an equimolar amount of vesicles of didodecyldimethylammonium bromide (C₁₂C₁₂N⁺), the blue shifted absorbance maximum immediately returns to its monomer value. This is due to the formation of mixed bilayers in which the azobenzenes loose their stacking interaction. This process is too fast to be followed in time with our experimental set-up. In Chapter 7 it will be shown that this mixing occurs via a monomer transfer mechanism.²⁹ When vesicles of **4-N=N-Ph** are mixed with a large excess of vesicles of didodecyldimethylammonium bromide, no spectral changes are observed in the UV absorption maximum at all. Therefore it is concluded that any form of monomer mixing is absent. The penetration of the **4-N=N-Ph** bilayers by didodecyldimethylammonium bromide monomers is probably hampered by the strong interactions between the molecules of **4-N=N-Ph**. On the other hand, the monomer concentration of **4-N=N-Ph** must be very low so that the **4-N=N-Ph** monomers do not escape their bilayers to migrate towards the didodecyldimethylammonium bromide bilayers.

It can thus be concluded that **4-N=N-Ph** must have a much lower critical bilayer concentration than any of the other compounds **4**. When the hydrophobicities of **4-N=N-Ph** and **4-H** are

calculated using Rekker's hydrophobic fragmental constants³⁰, both compounds have approximately the same hydrophobicity. The low critical bilayer concentration of **4-N=N-Ph** as compared to that of **4-H** can thus not be caused solely by the hydrophobic effect. Probably, the larger aromatic system results in stronger mesogen-mesogen stacking interactions resulting in a lower critical bilayer concentration and poor miscibility with other cationic surfactants.

4.2.5 Monolayer stability

The monolayer forming properties of compounds **4** have also been investigated in order to get information about the monolayer stabilizing effects of the different azobenzene mesogens. The π -A isotherms of the compounds **4-H**, **4-CN** and **4-N=N-Ph** are given in Figure 9.

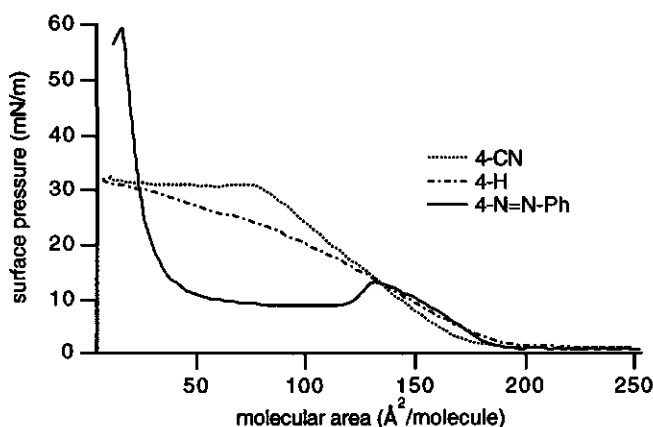


Figure 9. π -A Isotherms of compounds **4-CN**, **4-H** and **4-N=N-Ph**.

The isotherm of **4-F** is similar to that of **4-H** and those of **4-NO₂** and **4-OCH₃** are similar to that of **4-CN**. In all the isotherms an initial rise of the surface pressure is observed at an area of about 200 Å²/molecule. At this molecular area the molecules start to interact. This area corresponds to a situation in which the molecules have their azobenzene-carrying tail flat on the water surface. This orientation would be favored by a positive interaction between the azobenzenes and the water surface and has been found before by Heesemann.³⁷ Upon further compression the surface pressure rises until a plateau value is reached (at 33 mN/m for **4-CN**). At this pressure the interaction between the azobenzene unit and the water subphase is broken and the azobenzene-carrying tails are lifted from the surface. The transition to the plateau is sharp for **4-CN**, **4-NO₂** and **4-OCH₃** and smooth for **4-H** and **4-F**. This is ascribed to a better interaction with the subphase caused by the more polar substituents. This could result in a greater ordering of the molecules in the monolayer of the former three compounds resulting in a more cooperative (sharp) phase transition. Subsequently, the molecules can be compressed until the chains are in a close packed arrangement (at ± 40 Å²/molecule). Further compression

would cause the surface pressure to rise but the monolayers collapse almost immediately after this point has been reached. Monolayers of $C_{18}C_{18}N^+$ do not collapse below 50 mN/m.³⁶ Obviously the close packed arrangement of the molecules **4** in the monolayer is not a very stable one. These azobenzene units are thus not able to stabilize the monolayer through azobenzene-azobenzene interactions.

The monolayer of **4-N=N-Ph** shows a quite different π -A isotherm. The plateau value is reached at a lower surface pressure. This means that either the interaction of this azobenzene unit with the subphase is weaker or that the configuration in which the azobenzene-tail is perpendicular to the surface is more favorable than for **4-CN**, **4-NO₂** and **4-OCH₃**. Before the plateau is reached an overshoot is observed in the isotherm. This means that the relaxation time of the molecules is slow compared to the rate at which the pressure is exerted on them (compression speed of 1000 cm²/hour). Usually, these overshoots decrease when lower compression rates are used. When the close packed arrangement is obtained at 40 Å²/molecule the surface pressure rises until a surface pressure of 60 mN/m is reached. Upon expansion the isotherm is largely reversible but the overshoot is missing. Upon recompression the initial isotherm is recovered. At 25 mN/m the compressed monolayer is fairly stable in time.

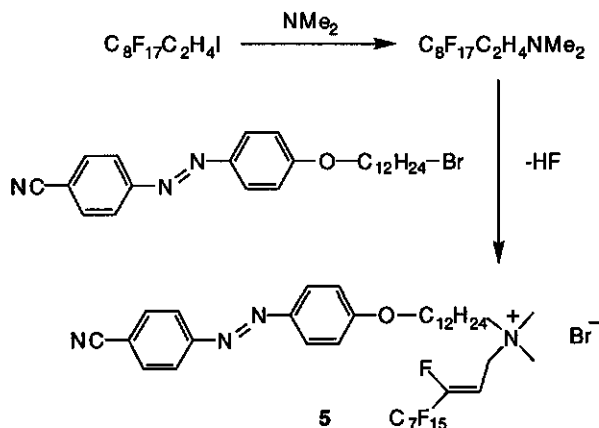
It is obvious that the larger aromatic unit of **4-N=N-Ph** results in a strong stabilization of the monolayer, probably due to enhanced azobenzene-azobenzene interactions between these larger mesogenic units. These interactions are also held responsible for the bilayer stabilizing effect of this azobenzene unit.

4.2.6 Perfluorinated amphotrope

It is known that the mixing of perfluorinated alkyl chains with hydrocarbon chains is an unfavorable process.³¹⁻³³ This tempted us to synthesize amphiphile **5** carrying one perfluoroalkyl chain and one hydrocarbon tail and a cyano-substituted azobenzene unit to monitor the ordering of these molecules in the aggregated state.

The Z-double bond in the perfluoroalkyl chain was introduced during the reaction by the trans elimination of HF.³⁴ In the ¹H-NMR spectrum strong trans coupling of 40 Hz is observed between the olefinic proton and the fluorine atom at the double bond. This compound forms a smectic phase above 132 °C and decomposes at about 200 °C.

Compound **5** forms bilayer vesicles upon sonication in pure water which have been observed with transmission electron microscopy (see Figure 11). These bilayer vesicles show a phase transition at 64 °C which is 25 °C higher than the T_c of **4-CN** vesicles. The UV absorption maximum of the azobenzene unit is blue shifted from 363 nm for monomers to 331 nm for the vesicles in water at 20 °C. This blue shift is almost the same as observed for vesicles of **4-CN**. This means that the molecular packing is not affected much by the presence of the perfluorinated tail or by the double bond.



Upon mixing of vesicles of **5** (0.05 mM) with a 70-fold molar excess of vesicles of didodecyldimethylammonium bromide ($\text{C}_{12}\text{C}_{12}\text{N}^+$) at room temperature, the blue shifted absorption maximum slowly disappears and the absorption maximum of the non-stacked azobenzenes appears due to the monomer exchange process (see Figure 10). The whole process takes several hours to complete whereas for **4-CN** vesicles the monomer transfer process is almost instantaneous (see Chapter 7). This is a direct consequence of the lower critical bilayer concentration of **5** as compared to **4-CN**. This is caused by the fact that perfluoroalkyl chains are more hydrophobic than the hydrocarbon chains.³⁰

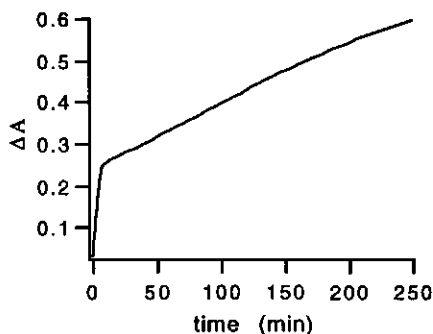


Figure 10. Change in absorbance at 366 nm after mixing vesicles of **5** with an excess of $\text{C}_{12}\text{C}_{12}\text{N}^+$ vesicles (23 °C) .

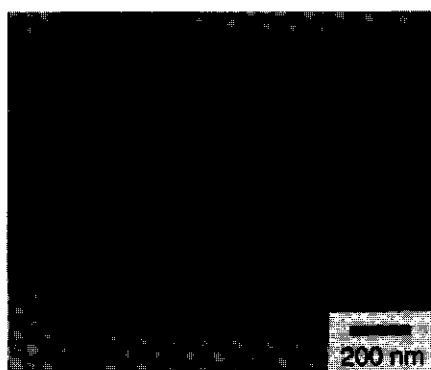


Figure 11. Transmission electron micrograph of vesicles of **5**, negatively stained with 1 % w/w uranyl acetate.

In the plot of the absorbance at 366 nm versus time at 23 °C it is seen that the monomer exchange process consists of two processes. One process is fast and occurs within the first 5 minutes after mixing. The other is slow and has a half time of several hours. This phenomenon

is tentatively explained by assuming that the fast process is caused by a dilution of the molecules of **5** due to fast penetration of the $C_{12}C_{12}N^+$ molecules in the bilayers of **5**. The molecules of **5** will however remain aggregated in smaller clusters in which the perfluoroalkyl chains are facing each other. In this way the contact between the perfluorinated and the hydrocarbon chains is minimized. These smaller clusters still cause some blue shift of the absorbance maximum. The slow process is attributed to a migration of the molecules of **5** to the excess of $C_{12}C_{12}N^+$ vesicles yielding the absorption maximum of the non-stacked azobenzene. This idea was supported by the fact that for the monomer exchange between vesicles of **5** and $C_{18}C_{18}N^+$ bilayers only the slow exchange process is observed. The low free monomer concentration of $C_{18}C_{18}N^+$ as compared to $C_{12}C_{12}N^+$ causes the penetration of these monomers into the bilayers of **5** to be slow. Therefore the migration of the monomers of **5** to the bilayers of $C_{18}C_{18}N^+$ becomes the dominant process. A detailed investigation of these and other monomer transfer processes is given in Chapter 7.

4.3 Conclusions

A series of novel double chained ammonium amphiphiles have been synthesized which carry biphenyl (**2**), stilbene (**3**) or azobenzene (**4**) mesogenic units at the terminus of one of the alkyl chains. These compounds all form bilayer vesicles. Azobenzene mesogens give a better stabilization of the formed bilayers than stilbene or biphenyl mesogens. This is due to stronger intermolecular interactions between azobenzene mesogens. For these bilayer vesicles a blue shifted absorption maximum is observed in the UV spectrum as compared to the monomer spectrum. This is caused by (anti)parallel π - π stacking of the mesogens in the bilayer (so-called H-aggregation). A layer spacing of 40.8 Å is observed for cast vesicle films of **4-CN** which indicates that the mesogens from opposite sides of the bilayer are interdigitated and that the methylene spacers are tilted with respect to the normal of the bilayer plane.

The effect of different substituents at the azobenzene unit on the 'gel-to-liquid crystalline' phase transition temperature (T_c) has also been investigated. The T_c increases in the order **4-F** < **4-H** < **4-NO₂** < **4-CN** < **4-OCH₃** < **4-N=N-Ph**, reflecting increasing azobenzene-azobenzene interactions in the bilayer. The strength of the azobenzene-azobenzene interaction does not correlate with the azobenzene dipole moment. Possibly, the different substituents contribute to the mesogen-mesogen interactions through dispersion interactions rather than through electrostatic interactions between the permanent dipoles of the mesogens.

The bilayer vesicles of **4-N=N-Ph** do not exchange monomers with bilayer vesicles of didodecyldimethylammonium bromide whereas all the other compounds **4** give a very rapid monomer exchange. This different behavior of the vesicles of **4-N=N-Ph** is caused by the extra stabilization of the bilayer by this extended azobenzene system.

All the compounds **4** give monolayers at the water-air interface which collapse at surface pressures around 33 mN/m, except **4-N=N-Ph** which gives more stable monolayers due to stronger azobenzene-azobenzene interactions.

The amphotrope **5**, containing a perfluorinated alkyl tail, forms stable bilayer vesicles in water. The molecules in the bilayers are similarly packed as the molecules of **4-CN**. The phase transition temperature is higher and monomer exchange rates are considerably slower than for compound **4-CN**.

4.4 Experimental section

4.4.1 Synthesis

4-Hydroxyazobenzene, 4'-fluoro-4-hydroxyazobenzene, 4'-cyano-4-hydroxyazobenzene, 4-hydroxy-4'-nitroazobenzene and 4-hydroxy-4'-methoxyazobenzene were prepared by reaction of the diazonium salts of aniline, 4-fluoroaniline, 4-nitroaniline, 4-aminobenzonitrile and 4-methoxyaniline respectively with phenol.³⁵

Benzeneazobenzeneazophenol was prepared by reaction of the diazonium salt of 4-phenylazoaniline with phenol. This compound was purified by column chromatography on silica gel using MeOH/CH₂Cl₂ 5:100 (v/v) as eluent.

12-Bromo-1-RO-dodecane (1)

A mixture of 25 mmol of the appropriate hydroxy-mesogen and 50 mmol of 1,12-dibromododecane and 50 mmol of K₂CO₃ in 50 mL of 2-butanone was refluxed for 16 h. The salt was removed by filtration and the filtrate was concentrated by evaporation of the solvent. The product was purified by column chromatography on silica gel using petroleum ether (bp. 40-60 °C)/CH₂Cl₂, 1:1 v/v as eluent (yield 60 %). ¹H-NMR (CDCl₃, TMS, δ, ppm): 1.40 (m, 16 H, -(CH₂)₈-), 1.80 (m, 4 H, Br-CH₂-CH₂-, RO-CH₂-CH₂-), 3.40 (t, 2 H, Br-CH₂-), 4.00 (t, 2 H, RO-CH₂-), 7.00 - 8.40 (m, 8 H, Ar-H). In case of methoxy substituent: 3.78 (s, 3H, Ar-OCH₃).

N-(12-RO-dodecyl)-N,N-dimethyl-N-dodecylammonium bromide (2, 3, 4)

A solution of 0.8 mmol of the 12-bromo-1-RO-dodecane and a fourfold excess of N,N-dimethyl-N-dodecylamine in 2-butanone was refluxed for 16 h. The mixture was allowed to cool and the solvent was removed under reduced pressure. The residue was dissolved in a small amount of dichloromethane and precipitated by addition of diethyl ether. The precipitate was collected and recrystallized from acetone (yield 60 %).

¹H-NMR (CDCl₃, TMS, δ, ppm): 0.90 (t, 3 H, CH₃-), 1.40 (m, 34 H, -(CH₂)₈-, -(CH₂)₉-), 1.80 (m, 6 H, N-CH₂-CH₂-, RO-CH₂-CH₂-), 3.40 (s, 6 H, -CH₂-N-(CH₃)₂), 3.50 (m, 4 H, -CH₂-N-(CH₃)₂-), 4.00 (t, 2 H, RO-CH₂-), 7.00 - 8.40 (m, 8 H, Ar-H). In case of 4-OCH₃ 3.78 (s, 3H, Ar-OCH₃).

2-CN: Mp 114 °C. Anal. Calcd for C₃₉H₆₃BrN₂O : C, 71.41; H, 9.68; N, 4.27. Found: C, 71.36; H, 9.82; N, 4.34. **2-NO₂**: Mp 98 °C. Anal. Calcd for C₃₈H₆₃BrN₂O₃ (0.8 H₂O): C, 66.12; H, 9.43; N, 4.06. Found: C, 66.10; H, 9.53; N, 4.00. **3-CN**: Mp 131 °C. Anal. Calcd for C₄₁H₆₅BrN₂O : C, 68.71; H, 9.80; N, 6.33. Found: C, 68.70; H, 9.77; N, 6.20. **4-H**: Mp 132 °C. Anal. Calcd for C₃₈H₆₄BrN₃O (0.3 H₂O): C, 68.71; H, 9.80; N, 6.33. Found: C, 68.70; H, 9.77; N, 6.20. **4-F**: Mp 105 °C. Anal. Calcd for C₃₈H₆₃BrFN₃O : C, 67.43; H, 9.38; N, 6.21. Found: C, 67.67; H, 9.51; N, 5.92. **4-CN**: Mp 151 °C. C₃₉H₆₃BrN₄O (1.2 H₂O): C, 66.39; H, 9.34; N, 7.74. Found: C, 66.34; H, 9.16; N, 7.88. **4-NO₂**: Mp 119 °C. Anal. Calcd for C₃₈H₆₃BrN₄O₃ (0.4 H₂O): C, 58.82; H, 9.22; N, 7.22. Found: C, 58.83; H, 9.07; N, 6.96. **4-OCH₃**: Mp

135 °C. Anal. Calcd for $C_{39}H_{66}BrN_3O_2$: C, 67.64; H, 9.67; N, 6.07. Found: C, 67.54; H, 9.74; N, 5.98. **IV-N=N-Ph**: Mp 151 °C. A smectic phase is formed which turns isotropic at 182 °C. Anal. Calcd for $C_{44}H_{68}N_5OBr$: C, 70.75; H, 9.18; N, 9.38. Found: C, 71.77; H, 9.31; N, 9.02.

***N*-[2-*Z*-(3,4,4,5,5,6,6,7,7,8,8,9,9,10,10,10-Hexadecafluorodeceny)]-*N*-[12(4-cyanoazobenzene-4'-oxy)dodecyl]-*N,N*-dimethylammonium bromide (5)**

An amount of 1 g of 3,3,4,4,5,5,6,6,7,7,8,8,9,9,10,10,10-heptadecafluoro-10-iododecane was dissolved in 20 mL of a 20 wt% solution of dimethylamine in chloroform. The solution was kept at room temperature for one night. The solvent was removed under reduced pressure and the residue was dissolved in dichloromethane and extracted with water. The organic layers were dried with $MgSO_4$. Yield 100% of *N*-(3,3,4,4,5,5,6,6,7,7,8,8,9,9,10,10,10-heptadecafluorodecyl)-*N,N*-dimethylamine.

One equivalent of *N*-(3,3,4,4,5,5,6,6,7,7,8,8,9,9,10,10,10-heptadecafluorodecyl)-*N,N*-dimethylamine and one equivalent of 12-bromo-1-(4-cyanoazobenzene-4'-oxy)dodecane were dissolved in acetonitrile and refluxed for 24 h. During the reaction trans elimination of hydrogen fluoride occurred, yielding the trans double bond. After cooling, the solvent was evaporated and the residue was purified by column chromatography on aluminum oxide (activity grade III) using $MeOH/CH_2Cl_2$ 3:100 v/v as eluent. Yield 65 %. Mp 132 °C, a smectic phase is formed until decomposition occurs at 200 °C.

1H -NMR ($CHCl_3$, TMS, δ , ppm) 1.40 (m, 16 H, $O-CH_2-CH_2-(CH_2)_8-CH_2-CH_2-N$), 1.80 (m, 4H, $O-CH_2-CH_2-(CH_2)_8-CH_2-CH_2-N$), 3.47 (s, 6 H, $N-(CH_3)_2$), 3.60 (m, 2 H, $-CH_2-CH_2-N$), 4.04 (t, 2 H, $O-CH_2-$), 4.82(d, 2 H, $=CH-CH_2-N$), 6.15 (dt, 1 H, $=CH-$, $J_{H-F} = 40$ Hz), 7.00-8.00 (m, 8 H, Ar-H). Anal. Calcd for $C_{37}H_{41}BrF_{16}N_3O$: C, 47.20; H, 4.39; N, 5.95. Found C, 47.93; H, 4.37; N, 5.85.

4.4.2 Methods

Vesicles were prepared by sonication of the solid compounds in ultra pure water until clear solutions were obtained using a Vibracell sonifier from Sonics and Materials Inc. Giant unilamellar vesicles were prepared by allowing 0.1-0.2 mg of crystals of the compounds to hydrate for several minutes in 200 μ l of water at 70-80 °C. The Krafft temperature was determined by heating an aqueous dispersion of the crystalline material. The temperature at which the formation of bilayer structures was observed by light microscopy was taken as the Krafft point. The sample solutions for the Differential Scanning Calorimetry (DSC) measurements (Perkin Elmer DSC 7) consisted of a 1 % (w/w) vesicle dispersion in water prepared by sonication. Scanning rates of 10 °C/min were used. X-ray reflectivity patterns were obtained from films which were prepared by casting a vesicle solution onto silicon wafers. The measurements were carried out with a Philips PW1710 diffractometer equipped with a Cu LFF X-ray tube at 40 kV and 55 mA. Electron microscopy was carried out for samples that were negatively stained with a 1 % aqueous uranyl acetate solution.

Monomer transfer experiments were performed by mixing sonicated vesicle dispersions of the amphotropes (0.05 mM) with vesicle dispersions of didodecyldimethylammonium bromide in thermostatted cuvettes at 23 °C. The rate of the monomer transfer was monitored by the changes in the UV absorption spectrum at 366 nm as a function of time.

The monolayer experiments were performed using a Lauda FW2 trough filled with ultrapure water. The monolayers were spread from chloroform solutions (ca. 1 mg/ml) using a Hamilton syringe. After spreading the monolayer was allowed to equilibrate for 5 minutes. A compression rate of 1000 cm^2/h was used.

4.5 References

- 1 Asano, T.; Furuta H.; Sumi, H. *J. Am. Chem. Soc.* **1994**, *116*, 5545.
- 2 Liu, Z. F.; Morigaki, K.; Enomoto, T.; Hashimoto, K.; Fujishima, A. *J. Phys. Chem.* **1992**, *96*, 1875.
- 3 Xie, S.; Natansohn, A.; Rochon P. J. *Chem. Mat.* **1993**, *5*, 403.
- 4 Eisenbach, C. D. *Makromol. Chem.* **1978**, *179*, 2489.
- 5 Kimizuka, N.; Kunitake, T. *Chem. Lett.* **1988**, 827.
- 6 Shimomura, M.; Ando R.; Kunitake T. *Ber. Bunsenges. Phys. Chem.* **1983**, *87*, 1134.
- 7 Nishimi, T.; Ishikawa, Y.; Ando, R.; Kunitake, T. *Recl. Trav. Chim. Pays Bas* **1994**, *113*, 201.
- 8 Nishimi, T.; Ishikawa, Y.; Kunitake, T.; Sekita, M.; Xu, G.; Okuyama, K. *Chem. Lett.* **1993**, 295.
- 9 Shimomura, M.; Kunitake, T. *J. Am. Chem. Soc.* **1982**, *104*, 1757.
- 10 Shimomura, M.; Kunitake, T. *J. Am. Chem. Soc.* **1987**, *109*, 5175.
- 11 Kimizuka, N.; Kawasaki, T.; Kunitake, T. *Chem. Lett.* **1994**, 1399.
- 12 Kano, K.; Tanaka, Y.; Ogawa, T.; Shimomura, M.; Okahata, Y.; Kunitake, T. *Chem. Lett.* **1980**, 421.
- 13 Richard, H.; Mauzac, M.; Nguyen, H. T.; Sigaud, G.; Achard, M. F.; Hardouin, F.; Gasparoux, H. *Mol. Cryst. Liq. Cryst.* **1988**, *155*, 141.
- 14 Schleele, T.; Imrie, C. T.; Rice, D. M.; Karasz, F. E.; Attard, G. S. *J. Pol. Sci. Part A: Pol. Chem.* **1993**, *31*, 1859.
- 15 Mueller, P.; Chien, T. F.; Rudy, B. *Biophys. J.* **1983**, *44*, 375.
- 16 Lasic, D. D. *J. Colloid Interface Sci.* **1990**, *140*, 302.
- 17 Menger, F. M.; Gabrielson, K. *J. Am. Chem. Soc.* **1994**, *116*, 1567.
- 18 Kunieda, H.; Shinoda, K. *J. Phys. Chem.* **1978**, *82*, 1710.
- 19 Okahata, Y.; Ando, R.; Kunitake, T. *Ber. Bunsenges. Phys. Chem.* **1981**, *85*, 789.
- 20 Usnanski, P.; Kryszewski, M.; Thulstrup, E. W. *Spectrochimica Acta*, **1990**, *46*, 23.
- 21 McRae, E. G.; Kasha, M. *Physical Processes in Radiation Biology*; Academic Press: New York, 1977.
- 22 Fukuda, K.; Nakahara, H. *J. Colloid Interface Sci.* **1984**, *98*, 555.
- 23 Nakahara, H.; Fukuda, K. *J. Colloid Interface Sci.* **1983**, *93*, 530.
- 24 Wakayama, Y.; Kunitake, T. *Chem. Lett.* **1993**, 1425.
- 25 Vertogen, G.; De Jeu, W. H. *Thermotropic Liquid Crystals, Fundamentals*; Springer-Verlag: Berlin, 1988; p. 36.
- 26 Zugenmaier, P.; Heiske, A. *Liq. Cryst.* **1993**, *15*, 835.
- 27 Menger, F. M.; Gabrielson, K. *Angew. Chem.* **1995**, *107*, 2260.
- 28 Okahata, Y.; Ando, R.; Kunitake, T. *Ber. Bunsenges. Phys. Chem.* **1981**, *85*, 789.
- 29 Everaars, M. D.; Marcelis, A. T. M.; Sudhölter, E. J. R. *Langmuir* **1996**, *12*, 3463.
- 30 Rekker, R. F. *The Hydrophobic Fragmental Constant*, 1st ed.; Wiley: New York, 1980.
- 31 Funasaki, N.; Hada, S. *J. Phys. Chem.* **1985**, *87*, 342.
- 32 Mukerjee, P.; Yang, A. Y. S. *J. Phys. Chem.* **1976**, *80*, 1388.
- 33 Furuya, H.; Moroi, Y.; Sugihara, G. *Langmuir* **1995**, *11*, 774.
- 34 Walker, F. H.; Pavlath, A. E.; *J. Org. Chem.* **1965**, *30*, 3284.
- 35 Vogel, I. A. *Textbook of Practical Organic Chemistry*; Longman Scientific & Technical: Harlow, 1989, p. 949.
- 36 Fukuda, H.; Diem, T.; Stefely, J.; Kezdy, F. J.; Regen, S. L. *J. Am. Chem. Soc.* **1986**, *108*, 2321.
- 37 Heesemann, J. *J. Am. Chem. Soc.* **1980**, *102*, 2167.

Chapter 5

*Double chained amphiphiles
carrying two mesogens*

Abstract

A series of novel double chained amphiphiles carrying two cyanobiphenyloxy mesogenic units at the termini of both alkyl chains and ammonium, phosphate and sulfonate headgroups were synthesized. All these new compounds show thermotropic liquid crystalline behavior. Several of these compounds form bilayer aggregates in water. From UV spectroscopy and small angle X-ray reflectivity it is inferred that the mesogenic units form interdigitated H-aggregates in the bilayer assemblies. These bilayers exhibit a gel-to-liquid crystalline phase transition as can be observed by Differential Scanning Calorimetry. The cyanobiphenyloxy unit is found to be a good fluorescent probe for the micropolarity and molecular mobility in the various lyotropic phases.

Upon spreading these molecules at the water-air interface of a Langmuir-Blodgett trough an unusual high lift-off area of about 200-250 Å²/molecule is observed in the surface pressure-area isotherms. This is associated with a situation in which the molecules lie flat on the surface. When the available area is reduced to about 40 Å²/molecule a situation is obtained in which the tails are in a close-packed arrangement.

5.1 Introduction

Amphiphiles in water can exist in various forms such as molecular dispersions, micelles, bilayers and microcrystals. Furthermore, they may form monolayers at the water-air interface. Usually amphiphiles containing one alkyl chain form micelles whereas those with two alkyl chains form bilayer aggregates.

Shimomura¹ and Okahata² have shown that single chained amphiphiles which possess a rigid aromatic group are able to form bilayers. For good bilayer forming properties these amphiphiles must have the aromatic moiety somewhere in the middle of the alkyl chain or near the headgroup and in addition a sufficiently long alkyl tail is required.

Until now only a few studies have been performed on the aggregation behavior of double chained amphiphiles with rigid aromatic groups at the termini of both alkyl chains. Therefore, we have initiated a study to explore the aggregation behavior of a series of novel compounds having this structural characteristic.

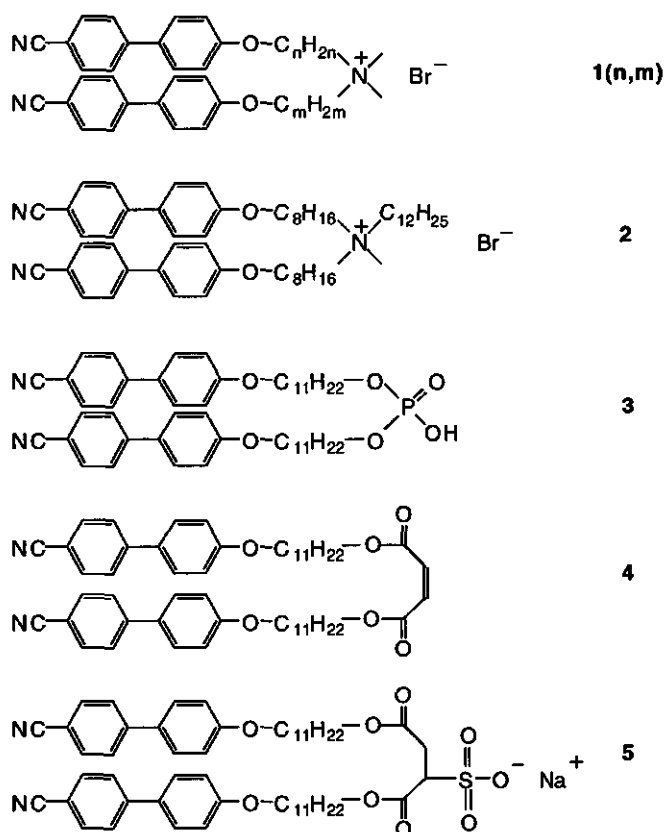
As a rigid segment the 4-cyanobiphenyl-4'-oxy moiety was chosen because of its special spectroscopic properties. Consisting of a donor- π -acceptor system this chromophore shows extensive solvatochromic shifts in its fluorescence and UV absorption maximum which makes it useful for intrinsically probing the micropolarity of various lyotropic phases. Furthermore, the 4-cyanobiphenyl-4'-oxy unit is a conventional thermotropic moiety (mesogenic unit).

In this chapter a study on the thermotropic phase behavior and aggregation behavior in water and at the water-air interface of these novel double chained amphiphiles with incorporated 4-cyanobiphenyl-4'-oxy units is presented.

5.2 Results and discussion

5.2.1 Thermotropic properties

The compounds were synthesized and purified by conventional methods (see Experimental section) and their molecular structures are given in Scheme 1. The thermotropic phase transition temperatures of these compounds were investigated by hot-stage polarization microscopy and differential scanning calorimetry (Table 1). All the compounds **1** exhibit a monotropic liquid crystalline (LC) phase upon cooling from the isotropic phase. From the observed thread-like and Schlieren textures between crossed polarizers the liquid crystalline phase is assigned to be nematic for all the compounds **1** except for **1**(12,12). Compound **1**(12,12) shows a fan-shaped focal-conic texture which is typical of a smectic A phase. Probably, the longer alkyl chains induce the formation of the more ordered smectic phase. For all compounds **1** the liquid crystalline to isotropic transition lies around 110 °C. This temperature seems to be dominated by the mesogenic units. The melting point (crystal to isotropic transition) is however strongly affected by the length of the alkyl chains.



Scheme 1. Investigated compounds 1-5.

Table 1. Melting points (Mp) and liquid crystalline to isotropic (LC-I) phase transition temperatures of the compounds 1-5. (N) = nematic, (S) = smectic A.

Compound	Mp (°C)	LC-I (°C)	Compound	Mp (°C)	LC-I (°C)
1(6,6)	198	107 (N)	1(10,12)	120	109 (N)
1(8,8)	145	110 (N)	2	110	47 (N)
1(10,10)	117	111 (N)	3	60	111 (S)
1(12,12)	142	108 (S)	4	110	78 (N)
1(6,12)	169	107 (N)	5	75	189 (S)
1(8,12)	137	107 (N)			

The phosphate amphotrope **3** and the sulfonatesuccinyl amphotrope **5** both show enantiotropic smectic A phases. The maleic acid diester **4**, which is the precursor of **5**, however shows a

monotropic nematic phase. The introduction of the ionic headgroup therefore induces the formation of a layered smectic phase.

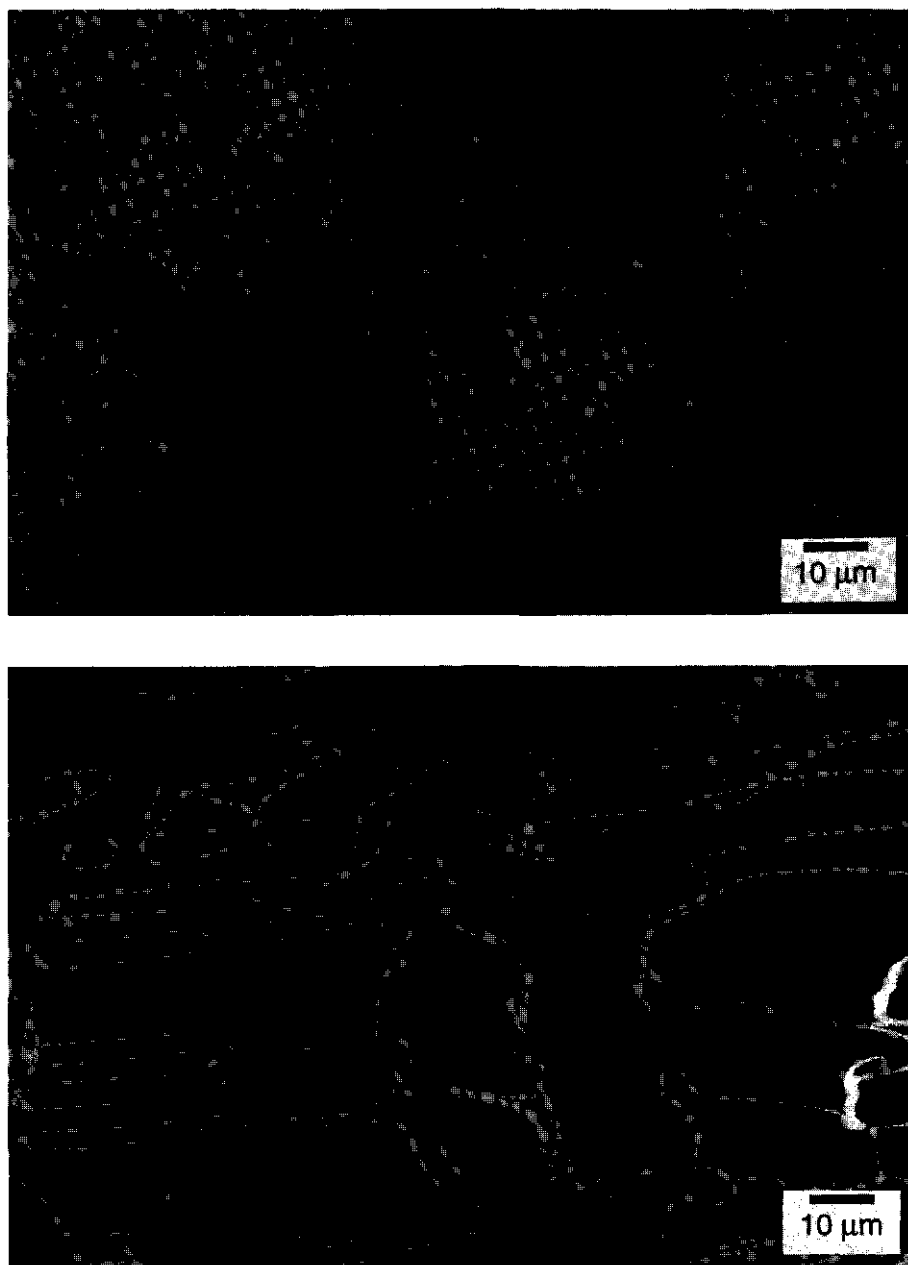


Figure 1. Optical polarizing micrographs of a smectic A phase of **5** (above) and the monotropic nematic phase of **1(10,10)** (below) .

5.2.2 Aggregation behavior in water

When compounds **1(6,6)** and **1(8,8)** are sonicated in water no clear dispersions are obtained. Compounds **1(6,12)** and **1(8,12)** do give translucent dispersions by this method but crystallization is observed within a few hours standing at room temperature. Only **1(10,10)**, **1(10,12)** and **1(12,12)** give stable, clear dispersions upon sonication. The presence of bilayer vesicles in these dispersions has been observed by electron microscopy (see Figure 4).

The bilayer thickness of **1(12,12)** is 47.7 Å as was determined by small angle X-ray reflectivity of vesicle dispersions cast onto silicon wafers. The length of the molecules, as deduced from space filling models, is 29 Å. This could mean that interdigitation of the aromatic units occurs in the bilayer, because the bilayer thickness is less than twice the molecular length. Interdigitation of mesogenic units is frequently found for thermotropic liquid crystals both in their crystal structure and in their liquid crystalline phase.³ A schematic representation of this structure is given in Figure 2.

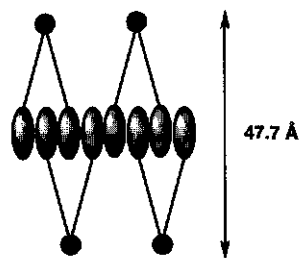


Figure 2. Schematic representation of the bilayer structure of **1(12,12)**.

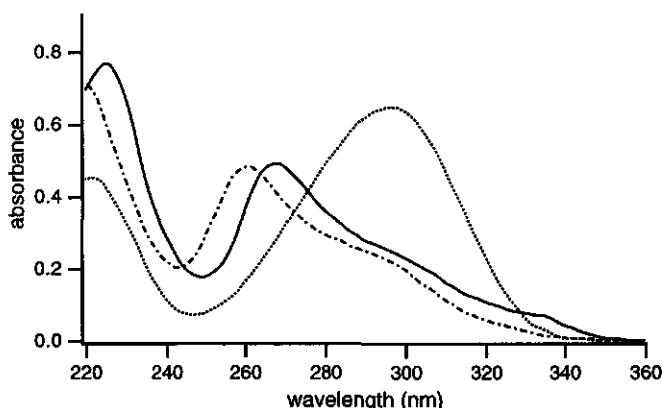


Figure 3. UV absorption spectra of **1(10,10)** (—) and **1(12,12)** (---) as vesicles in water and as monomers in ethanol (····). Concentration = 0.05 mM at 23 °C.

Figure 3 shows the UV absorption spectra of **1(10,10)** and **1(12,12)** as vesicles in water and as monomers in ethanol. As can be seen the monomer absorption is found at 297 nm whereas the vesicle absorption maxima of **1(10,10)** and **1(12,12)** are found at 267 and 259 nm respectively. According to the molecular exciton model proposed by McRae and Kasha⁴ this blue shift of the π - π^* absorption band is indicative of linear chromophore aggregates with their transition moments (anti)parallel to each other and perpendicular to the stacking direction, so-called H-

aggregates (see chapter 1.2.2). Vesicles of **1**(12,12) show a blue shift of 38 nm whereas vesicles of **1**(10,10) show a shift of 30 nm. This difference is probably due to a tighter packing of the chromophores in the bilayers of the former compound. This might be caused by the stronger Van der Waals interactions between dodecyl spacers than between decyl spacers, which results in a closer approach of the aromatic units in the interior of the bilayers. Another explanation could be that with longer alkyl spacers the mesogens are more decoupled from the headgroups which allows a better packing of the mesogens.

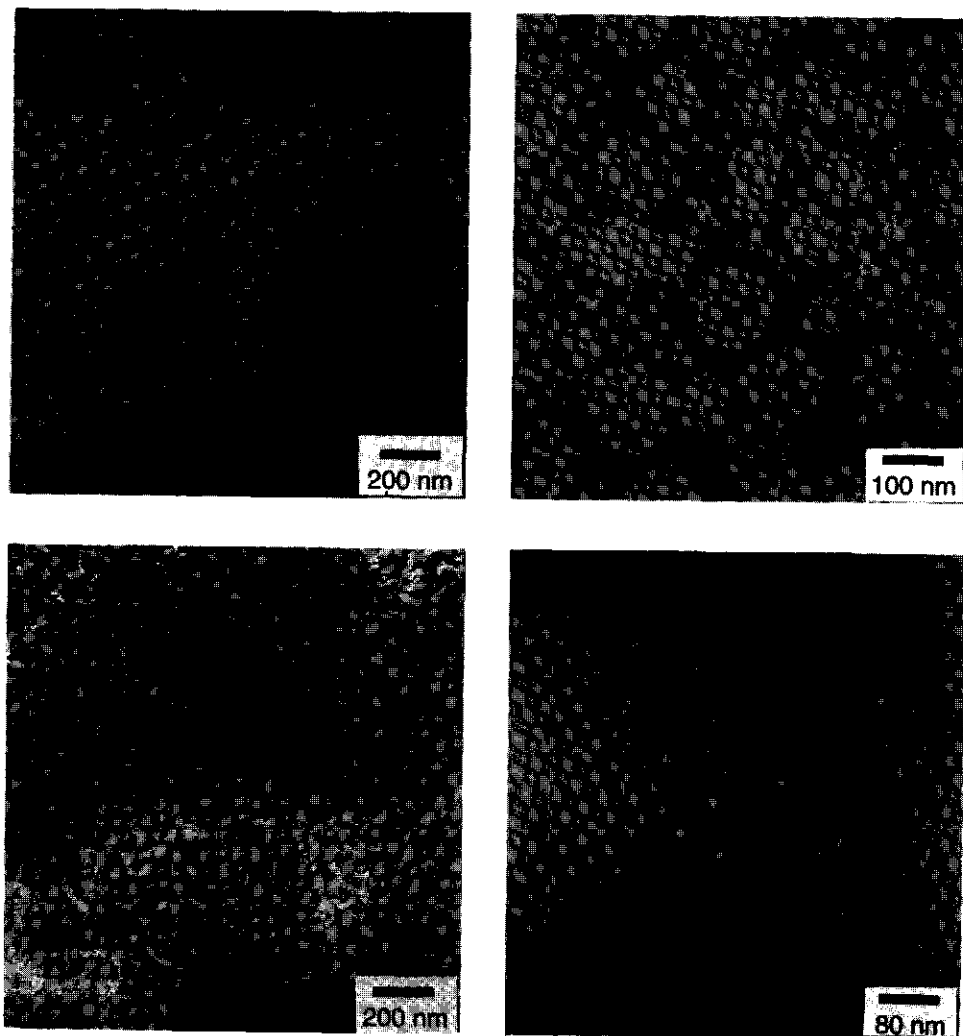


Figure 4. (a) Electron micrograph of vesicles of **1**(10,10); (b) *idem*; (c) curved bilayer fragments of **5** (d) *idem*, after ageing for one month. All samples were stained with uranyl acetate.

Like biomembranes, the bilayers of these novel compounds exhibit a gel to liquid crystalline phase transition (at a temperature T_c) as was observed by differential scanning calorimetry (DSC). Bilayers of 1(10,10), 1(10,12) and 1(12,12) show phase transitions at 55, 49 and 65 °C respectively. The transitions are reversible since upon cooling exothermic transitions are observed at 19, 20 and 12 °C respectively. The lower T_c of 1(10,12) as compared to that of 1(10,10) might be caused by a less favorable packing of the mesogens in the bilayer of this compound due to the unequal spacer lengths.

Additional evidence for the formation of bilayer vesicles was obtained from the following experiments. When clear vesicle dispersions from 1(10,10) and 1(10,12) are frozen to -20 °C and subsequently allowed to melt, the dispersions become very turbid and the presence of micro-crystalline material can be readily observed by light microscopy. When these turbid suspensions are subsequently heated to 55 °C and 49 °C respectively, while stirring, they become translucent again and remain clear even after cooling to room temperature.

This phenomenon has already been reported and is considered to be strong evidence for the presence of bilayer structures.^{1,5} What probably happens is that by freezing the vesicle dispersion the bilayer structure is disrupted by the formation of ice crystals causing crystallization of the amphiphilic material. Upon heating the bilayer aggregates are reconstituted.

Also from DSC experiments it is learned that upon heating frozen solutions of 1(10,10) and 1(10,12) the endothermic peaks at 55 and 49 °C (turbid to translucent) show an increased enthalpy change, with respect to an unfrozen vesicle solution. Subsequent cooling and heating experiments on the same sample (temperature not below 0 °C) show a restoration of the original thermogram.

Compound 3 does not give clear solutions upon sonication in water of neutral or high pH. Compound 5 gives translucent solutions upon sonication in distilled water. The UV absorption maximum lies at 259 nm indicating the presence of H-aggregates of the mesogenic units. Electron microscopy shows the presence of small curved bilayer fragments which exhibit a T_c at 60 °C (see Figure 4).

5.2.3 Mixed amphiphile systems

The anionic amphotrope 5 readily forms 1:1 complexes with dodecyltrimethylammonium bromide. The blue shifted absorption maximum observed for the bilayer fragments of 5 at 259 nm shifts to 270 nm upon stepwise addition of an equimolar amount of the cationic surfactant (Figure 5). This is attributed to the fact that the average distance between the mesogenic units in the bilayer increases as a result of the penetration of the dodecyltrimethylammonium bromide molecules. The blue shift is even further reduced upon addition of didodecyldimethylammonium bromide instead of dodecyltrimethylammonium bromide. This is due the fact that the double chained cationic amphiphile causes the mesogenic units to be separated even more.

The absorption maximum then lies at 287 nm whereas the absorption maximum of the non-aggregated cyanobiphenyloxy units lies at 297 nm. Addition of the nonionic surfactant polyoxyethylene(23) lauryl ether ($C_{12}E_{23}$) to bilayer aggregates of **5** does not result in any spectral changes. Not even when a large excess of the nonionic surfactant is added. Either the nonionic amphiphiles do not penetrate into the bilayers of **5** or the penetration does not disturb the packing of the cyanobiphenyloxy units in the bilayers. Mixing of these amphiphiles would reduce the electrostatic repulsion between the headgroups of **5** and is hence expected to be a favorable process.

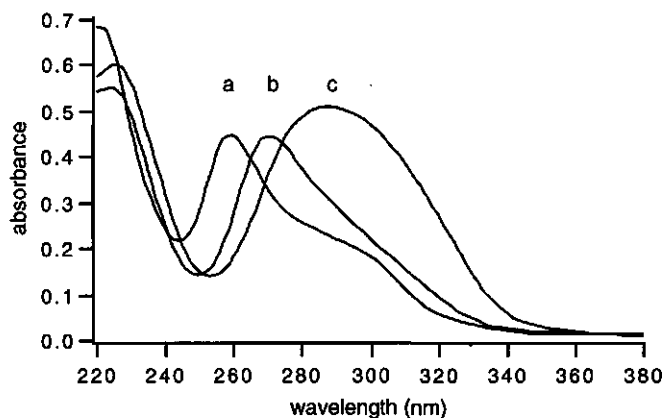


Figure 5. UV absorption spectra of bilayer aggregates of **5** in water; (a) the pure compound (b) in the presence of one equivalent of dodecyltrimethylammonium bromide; (c) in the presence of one equivalent of didodecyldimethylammonium bromide.

Addition of one equivalent of the anionic surfactant sodium dodecylsulfate to bilayer vesicles of **1**(12,12) or **1**(10,10) causes only minor changes in absorption spectrum. This surfactant probably fits well between the cationic surfactants in the bilayer without disturbing the molecule packing too much. Addition of several equivalents of the nonionic surfactant $C_{12}E_{23}$ to bilayer vesicles of **1**(12,12) or **1**(10,10) causes an instantaneous disappearance of the blue shifted absorption maximum and an appearance of the absorption maximum of the non-stacked mesogenic units. This is attributed to the formation of mixed micelles of **1**(12,12) or **1**(10,10) and $C_{12}E_{23}$.

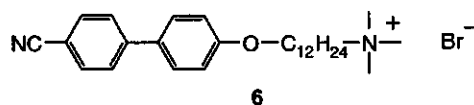
The different behavior of the cationic bilayers of **1** and the bilayer lamellae of the anionic amphiphile **5** upon addition of $C_{12}E_{23}$ remains not well understood. A possible explanation might be given by the fact that the oligoethyleneoxide part of the nonionic surfactants forms complexes with the cationic ammonium headgroups and not with anionic sulfonate groups. However, additional studies using titration microcalorimetry are required to verify this hypothesis.

5.2.4 Fluorescence studies

The fluorescence spectra of the cyanobiphenyloxy fluorophore in a series of different solvents are given Figure 6. These solvents have different dielectric constants ranging from 78 for water to 24.3 for ethanol, 3.4 for chloroform and 1.9 for hexane and PE_{40/60}. The emission maxima in these solvents are found at 396, 370, 340 and 336 nm respectively. The large solvatochromic shifts are due to the fact that the cyanobiphenyloxy unit can attain a charge transfer (CT) state upon excitation. This CT state is better stabilized in more polar solvents resulting in a red shift of the emission maximum. It is observed that the fluorescence yield is not very dependent on the polarity of the solvent.

The fluorescence spectrum of compound **6** (0.01 mM) in a 100 mM aqueous hexadecyltrimethylammonium bromide solution (C₁₆TAB, cmc = 1mM) is equal to the spectrum in water with an emission maximum at 396 nm. This means that **6** either hardly enters the CTAB micelles or that the cyanobiphenyloxy units stick out of the micellar core. Also no quenching of the fluorescence by the bromide ions was observed. In an aqueous 3 mM C₁₂E₂₃ solution an emission maximum at 369 nm is observed. This means that the mesogen experiences an environment which has a polarity comparable to that of ethanol. Probably, the mesogenic units reside in or near the ethyleneoxide region of the C₁₂E₂₃ micelle.

In 35 mM vesicle dispersions of the dialkyldimethylammonium bromides C₁₂C₁₂N⁺ and C₁₈C₁₈N⁺ the emission maxima of **6** are found at 363 nm and 371



nm respectively. This means that in these bilayer systems the mesogens experience also a fairly polar environment comparable to the polarity of ethanol. From polarity probing studies with pyrene, it is known that pyrene resides in the pallisade layer, just beneath the Stern layer of the bilayer.⁶⁻⁹ Usually an I₃/I₁ value is observed corresponding to the polarity of ethanol.¹⁰ This suggests that the cyanobiphenyloxy mesogen also resides near the Stern layer. Thus a picture emerges in which the molecules of **6** lie flat in the pallisade layer, more or less parallel to the Stern layer or that they span part of the bilayer. Actually, it is not surprising that the cyanobiphenyloxy unit likes a polar environment because of the presence of hydrophilic oxy and cyano substituents. It has also been shown that the compounds **1** preferentially lie flat on the water-air interface (see section 5.2.5). This conformation is favored by a positive interaction of the mesogens with the aqueous subphase.

The fact that in bilayers of C₁₂C₁₂N⁺ a slightly more apolar environment is found than in C₁₈C₁₈N⁺ bilayers, might be attributed to the fact that these latter bilayers are in their gel state at room temperature whereas C₁₂C₁₂N⁺ bilayers are in their liquid crystalline state. Therefore, in the C₁₈C₁₈N⁺ bilayers the mesogens might be pressed more toward the Stern layer. This has also been found with pyrene probing studies.⁹

When compound **6** is dissolved in a 40 mM SDS (sodium dodecylsulfate) solution, the fluorescence is quenched with respect to the fluorescence in water and has an emission maximum of 371 nm. This is attributed to the formation of ion-pair amphiphiles. These are 1:1 complexes of **6** and SDS which form very ordered structures, probably bilayers (see section 2.2.2). In these bilayers the mesogens are parallelly stacked resulting in a quenching of the fluorescence. This quenching is predicted for H-aggregates by the exciton theory.

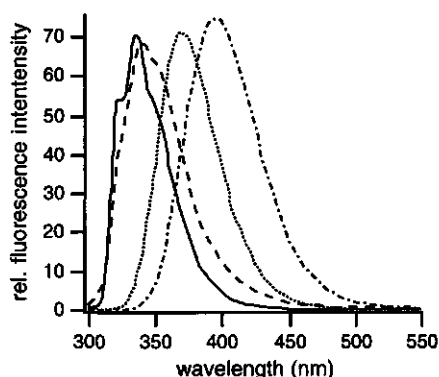


Figure 6. Fluorescence spectra of the cyanobiphenyloxy unit in petroleum ether 40/60 (—), chloroform (---), ethanol (···) and in water (— · —). $\lambda_{exc} = 270$ nm, $OD_{270} = 0.1$.

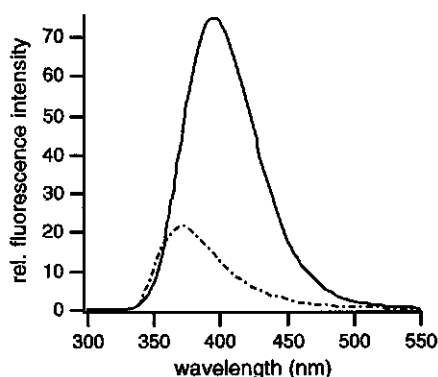


Figure 7. Fluorescence spectra of 1(10,10) as vesicles in water (---) and of **6** as monomers in water (—). $\lambda_{exc} = 270$ nm, $OD_{270} = 0.1$.

The fluorescence spectra of compounds 1(10,10) and **6** in water are given in Figure 7. The critical bilayer concentration of 1(10,10) is so low that under the employed experimental conditions, vesicles are present in the aqueous dispersion in the cuvette. This is confirmed by the presence of a blue shifted UV absorption maximum which is caused by the stacking of the mesogens in the bilayer. In ethanol an emission spectrum is observed which is similar to the spectrum of **6** in ethanol. In water the fluorescence of 1(10,10) is considerably quenched with respect to that of **6**. The emission wavelength maximum lies at 371 nm. This is the emission of the H-aggregated fluorophores, also called the exciton emission.

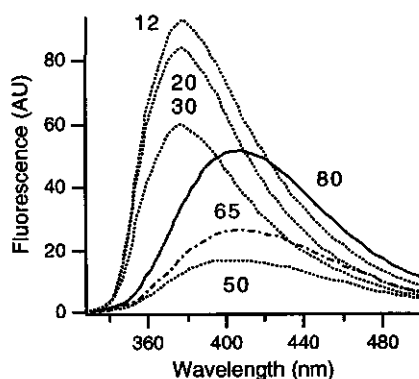


Figure 8. Temperature dependence of the fluorescence spectra of 1(10,10) as vesicles in water. The temperatures are given in °C.

The fluorescence of the vesicle dispersion of compound **1**(10,10) is very temperature dependent (Figure 8). Upon increasing the temperature, the emission is further quenched. A strong decrease in fluorescence is observed between 30 and 50 °C. For the emission of **6** in water there is no temperature dependence so that the observed spectral changes for **1**(10,10) are not due to changes in polarity or viscosity of the solvent. Possibly, the increased molecular mobility of **1**(10,10) at higher temperatures facilitates the formation of nicely stacked structures in the excited state causing the emission from the lowest S_1 level to become more inhibited.¹¹⁻¹⁴ Increasing the temperature above 50 °C results in the appearance of monomer emission in aqueous environment. At these high temperatures the bilayers start to dissolve into water as monomers. This is also seen in the UV absorption spectra.

When molecules of **1**(10,10) are solubilized in micelles of $C_{12}E_{23}$ or CTAB or in $C_{12}C_{12}N^+$ bilayers, there is no interaction between the mesogens in the ground state as is observed by the monomer absorption maximum (see also Chapter 7). The fluorescence is however still quenched with respect to the fluorescence in ethanol with a maximum at 371 nm. This can be attributed to an excimer emission.¹¹⁻¹⁴ Because the dilution of **1**(10,10) is very strong, the excimer is probably formed intramolecularly. The excimer formation can be explained because the two chains of the molecule will tend to remain closely together. Then, the mesogens are also situated relatively close to one another resulting in an increased probability of excimer formation during the lifetime of the excited species. Compound **1**(10,10) in ethanol does not show excimer emission indicating that both tails are completely solvated which reduces the encounter probability during the lifetime of the excited state.

5.2.5 Formation of monolayers

The new amphotropes are hardly soluble in water and are therefore suitable compounds for Langmuir-Blodgett (LB) studies. The surface pressure-area (π -A) isotherms of the symmetric compounds **1** are shown in Figure 9.

Interestingly, these molecules show a high lift-off area of 200-260 Å²/molecule (except for **1**(6,6)). At this point the molecules start to interact. According to model studies this indicates that these molecules lie flat on the water surface. This conformation is probably favored by the interaction of the hydrophilic cyanobiphenyloxy substituents with the aqueous subphase.^{15,16} When the area is reduced the surface pressure increases until a plateau is reached. At this point the cyanobiphenyloxy substituents are forced out of the water and the area per molecule can be reduced without further increase in pressure. When all molecules have adopted the close-packed arrangement in which the cyanobiphenyloxy containing hydrocarbon chains are pointing towards the air, the surface pressure rises again upon further reduction of the area.

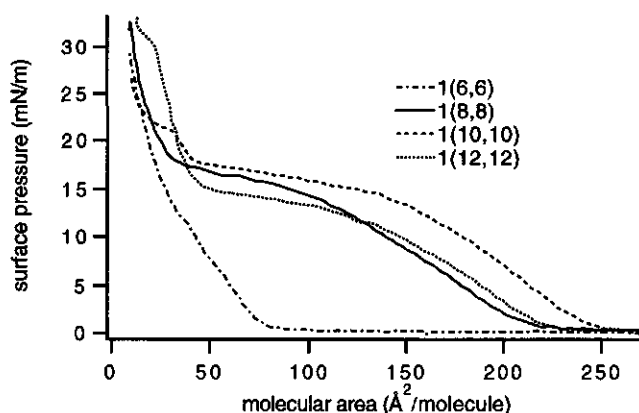


Figure 9. Surface pressure-area isotherms of the symmetric compounds **1**.

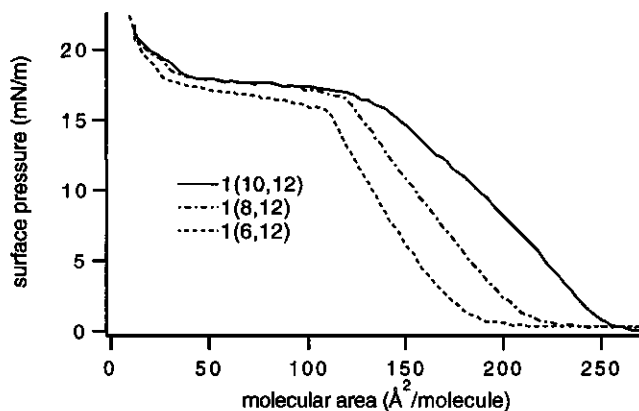


Figure 10. Surface pressure-area isotherms of the asymmetric compounds **1**.

A minimal spacer length of eight methylene units is required for these molecules to lie flat on the water surface as is deduced from absence of a plateau in the isotherm of **1**(6,6). Furthermore, it would be expected that compound **1**(12,12) would show a larger lift off area than **1**(10,10). That this is not observed may be due to the possibility of the dodecyl spacers to bend away from the subphase thus reducing contact area of the molecules with the water surface. This result is confirmed by measurements of the headgroup area of gemini surfactants.¹⁷ In this study a maximum headgroup area is observed for a spacer between the headgroups of eleven methylene units. Using longer spacers results in a backfolding of the spacer thus reducing the headgroup area.

The monolayer of **1**(8,8) in the close-packed arrangement finally collapses at a surface pressure ($\pi_c = 19$ mN/m) slightly above the plateau value, when a compression speed of 15 cm²/min is used. The monolayer of **1**(10,10) is somewhat more resistant and has a $\pi_c = 22$ mN/m. The monolayer of **1**(12,12) is the most stable having a π_c of 30 mN/m. Addition of salt (0.1 M NaBr) to the subphase results in a substantial increase of π_c , probably caused by screening of the headgroup repulsions. At the collapse point the area per molecule is reduced to approximately 15 Å²/molecule followed by a increase in surface pressure. This corresponds to an organized folding over of the monolayer to give a triple layer.^{18,19} Subsequent expansion-recompression experiments show that the π -A isotherms are reversible after the collapse has occurred.

The asymmetric compounds **1**(6,12), **1**(8,12) and **1**(10,12) were also subjected to π -A measurements (Figure 10). An obvious increase in lift-off area is observed with increasing spacer length. All monolayers have a π_c that lies slightly above the plateau value. The asymmetry of the molecules obviously reduces the physical stability of the monolayer.

When the molecules **1** are in the close-packed arrangement they occupy an area of approximately 40 Å²/molecule. This area is in the same range as that of double chained amphiphiles without aromatic moieties in their alkyl chains. This means that the cross section of a cyanobiphenyloxy unit is not much larger to that of an alkyl chain segment. Because the shape of the molecule is not affected much by the incorporation of these rigid segments the morphology of the aggregates in aqueous environment is not expected to be altered much either. Indeed, as discussed above, these molecules are found to form stable bilayer vesicles in water.

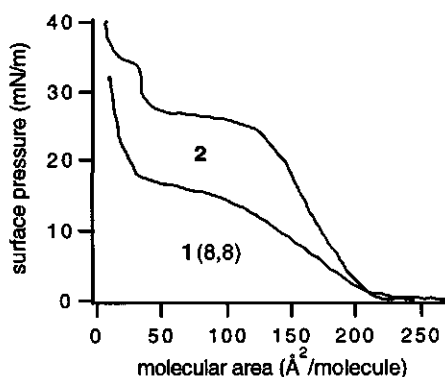


Figure 11. π -A Isotherms of **1**(8,8) and **2**.

Compound **2**, which has octyl spacers and an extra dodecyl chain, has the same lift-off area as compound **1**(8,8) in its π -A isotherm (Figure 11). This means that the dodecyl chain probably points into the air when the molecules start to interact. The plateau value of the surface pressure lies however much higher for **2** than for **1**(8,8). This means that a higher pressure is needed to remove the mesogens from the subphase. This is explained by assuming that the dodecyl tail, which points away from the subphase,

forces the mesogen carrying tails on the water, because the tails are tetrahedrally positioned around the central nitrogen atom.

The amphotropes **3** and **5** also lie flat on the water surface. The monolayers however collapse in an early stage of the compression process. Addition of salts or changing of the pH of the subphase does not stabilize these monolayers.

5.3 Conclusions

Introduction of mesogenic 4'-cyanobiphenyl-4-oxy units into double chained amphiphiles renders these molecules amphotropic. All ammonium compounds **1** show monotropic liquid crystalline behavior. Changing the spacer length affects the melting point whereas the isotropic to liquid crystalline transition temperature is almost unaffected. The phosphate (**3**) and sulfonatosuccinate (**5**) compounds show enantiotropic smectic A phases.

Upon sonication of the new amphotropic molecules **1** (n or $m > 8$) and **5** in water bilayer aggregates are formed. Compounds **1** form vesicles whereas **5** forms curved bilayer fragments. UV absorption spectroscopy indicates the formation of H-aggregates of the mesogenic units in these bilayer structures. The penetration of oppositely charged surfactants into these bilayers can disturb the aggregation of the cyanobiphenyloxy units. Fluorescence studies show that when these amphotropes are dissolved into micelles or bilayers of other surfactants, the mesogenic units preferentially lie close to the Stern layer. Also the formation of excimers of the double chained amphotropes **1** is observed.

Upon spreading the amphotropic molecules **1** at the water-air interface, the molecules are initially completely stretched on the water surface favored by a three point interaction of the ammonium headgroup and both cyanobiphenyloxy moieties with the subphase. Upon compression the cyanobiphenyloxy-alkyl chains are lifted from the interface and finally a close-packed arrangement is obtained at an area of about $40 \text{ \AA}^2/\text{molecule}$.

The phosphate and sulfonate amphotropes **3** and **5** do not give stable monolayers.

5.4 Experimental Section

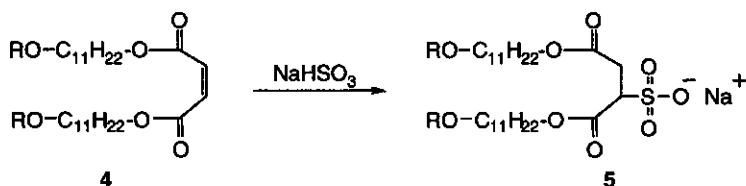
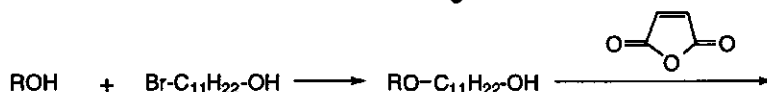
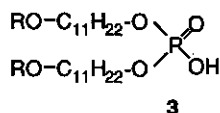
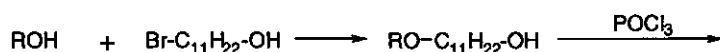
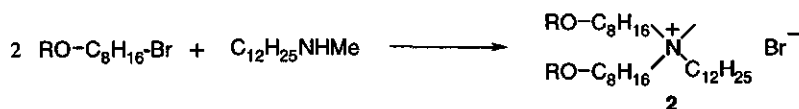
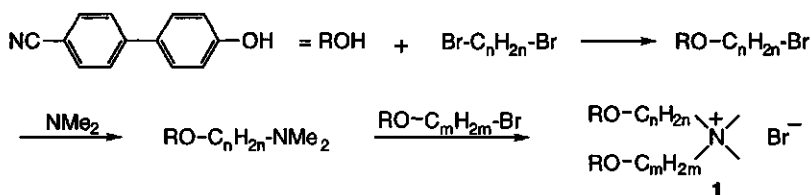
5.4.1 Synthesis

The synthesis of the amphiphiles is outlined in Scheme 1.

4-Hydroxy-4'-cyanobiphenyl was obtained from Merck and used without further purification. ω -Bromo-1-(4-cyanobiphenyl-4'-oxy)alkanes were synthesized as described in chapter 2.

N-[ω -(4-Cyanobiphenyl-4'-oxy)alkyl]-*N,N*-dimethylamine

15 mmol of dimethylamine was added as a 20% (w/v) solution of dimethylamine in chloroform to a solution of ω -bromo-1-(4-cyanobiphenyl-4'-oxy)alkane (3 mmol) in 5 mL of chloroform. After 21 h at room temperature the solvent was evaporated. The residue was dissolved in 50 mL of diethyl ether and extracted with $2 \times 100 \text{ mL}$ of 1 M aqueous HCl solution. The acidic water layers were made alkaline by addition of a concentrated NaOH solution. The water layers were extracted with $3 \times 100 \text{ mL}$ of diethyl ether and the collected organic layers were dried on MgSO_4 , filtered and the diethyl ether was evaporated. The residue was recrystallized from hexane (-20°C). Yield 10-50%.



***N,N*-Di[ω-(4-cyanobiphenyl-4'-oxy)alkyl]-*N,N*-dimethylammonium bromide (1)**

0.5 mmol of ω-bromo-1-(4-cyanobiphenyl-4'-oxy)alkane and 0.7 mmol of *N*-[ω(4-cyanobiphenyl-4'-oxy)alkyl]-*N,N*-dimethylamine were dissolved in 10 mL of acetone. This solution was refluxed for 20 h. A white precipitate was formed which was collected and washed with diethyl ether. Yield 60-70 %. **1**(6,6) Mp. 197 °C. T_L-LC 107° C. Anal. Calcd for C₄₀H₄₆N₃O₂Br: C, 70.57; H, 6.81; N, 6.17. Found C, 70.76; H, 6.80; N, 6.46. **1**(8,8) Mp. 145 °C. T_L-LC 110 °C. Anal. Calcd for C₄₄H₅₄N₃O₂Br (1H₂O): C, 70.00; H, 7.47; N, 5.56. Found: C, 70.08; H, 7.52; N, 5.54. **1**(10,10) Mp. 117 °C. T_L-LC 111 °C. Anal. Calcd for C₄₈H₆₂N₃O₂Br (1H₂O): C, 71.08; H, 7.95; N, 5.18. Found: C, 71.30; H, 7.95; N, 5.28. **1**(12,12) Mp. 142 °C. T_L-LC 108 °C. Anal. Calcd for C₅₂H₇₀N₃O₂Br (1H₂O): C, 72.02; H, 8.37; N, 4.84. Found: C, 72.21; H, 8.39; N, 4.89. **1**(6,12) Mp. 169 °C. T_L-LC 107 °C. Anal. Calcd for C₄₆H₅₈N₃O₂Br (1H₂O): C, 70.56; H, 7.72; N, 5.36. Found: C, 70.31; H, 7.75; N, 5.06. **1**(8,12) Mp. 137 °C. T_L-LC 107 °C. Anal. Calcd for C₄₈H₆₂N₃O₂Br: C, 72.70; H, 7.88; N, 5.29. Found: C, 72.37; H, 8.04; N, 5.19. **1**(10,12) Mp. 120 °C. T_L-LC 109 °C. Anal. Calcd for C₅₀H₆₆N₃O₂Br (0.5H₂O): C, 72.35; H, 8.13; N, 5.06. Found: C, 72.45; H, 8.40; N, 4.91.

***N,N*-Di[8-(4-cyanobiphenyl-4'-oxy)octyl]-*N*-dodecyl-*N*-methylammonium bromide (2)**

A mixture of *N*-dodecyl-*N*-methylamine and a twofold excess of 8-bromo-1-(4-cyanobiphenyl-4'-oxy)octane and NaHCO₃ in ethanol was heated for 72 h at 100 °C in a closed reaction vessel. The solvent was removed under reduced pressure and the residue was dissolved in CH₂Cl₂ and the salt was removed by filtration. The filtrate was concentrated to a small volume and the product was precipitated in diethyl ether. The product was purified by column chromatography on silica gel using CH₂Cl₂-MeOH 100:15 (v/v) as eluent. Yield 70 %. Mp. 110 °C.

T₁-LC 47 °C.

¹H-NMR (CDCl₃, TMS, δ, ppm): 0.90 (t, 3 H, C₁₁H₂₂-CH₃), 1.20 (m, 16 H, CH₃-(CH₂)₈-CH₂-N), 1.40 (m, 16 H, O-CH₂-CH₂-(CH₂)₄-CH₂-CH₂-N), 1.70 (m, 10 H, -CH₂-CH₂-N, O-CH₂-CH₂), 3.30 (s, 3 H, N-CH₃), 3.40 (m, 6 H, -CH₂-N), 3.96 (t, 4 H, O-CH₂-), 6.90-7.78 (m, 16 H, Ar-H).

Anal. Calcd for C₅₅H₇₆N₃O₂Br: C, 74.13; H, 8.60; N, 4.72. Found: C, 73.75; H, 8.72; N, 4.44.

11-(4-Cyanobiphenyl-4'-oxy)undecanol

One equivalent of 4'-cyano-4-hydroxybiphenyl and one equivalent of 11-bromoundecanol, one equivalent of KOH and a catalytic amount of KI in ethanol was refluxed for 16 h. The solvent was removed under reduced pressure. The residue was treated with dichloromethane and the salt was removed by filtration. The filtrate was reduced to a small volume and the product was precipitated in petroleum ether (bp. 40-60 °C). Yield 95%. Mp. 92 °C.

¹H-NMR (CDCl₃, TMS, δ, ppm): 1.49 (m, 14 H, CH₂-CH₂-(CH₂)₇-CH₂-CH₂), 1.60-2.00 (m, 4 H, CH₂-CH₂-(CH₂)₇-CH₂-CH₂), 3.45 (t, 2 H, -CH₂-OH), 4.00 (t, 2 H, O-CH₂-), 6.9-7.8 (m, 16 H, Ar-H).

Di[11-(4-cyanobiphenyl-4'-oxy)undecyl]phosphoric acid (3)

A mixture of 0.5 g (3.3 mmol) of POCl₃ and 2.4 g (6.6 mmol) of 11-(4-cyanobiphenyl-4'-oxy)undecanol in 100 mL of benzene was refluxed for 16 h. The solvent was removed under reduced pressure and the residue was treated with an aqueous 2 M NaOH solution. The mixture was stirred until the sticky substance became powdery. The solid was washed several times with water and with acetone. The compound was dissolved in dichloromethane and an equal volume of 1 M HCl solution was added. The mixture was stirred for 1 h. The organic layer was separated and dried on MgSO₄ and the solvent was evaporated. The solid was purified by column chromatography on silica gel using CH₂Cl₂/MeOH 4:1 (v/v) as eluent. The compound was redissolved in dichloromethane and stirred for 1 h with an equal volume of 1 M HCl solution. The organic layer was separated and dried on MgSO₄ and the solvent was evaporated. Yield 10 %. Mp. 60 °C, T₁-LC 111 °C.

¹H-NMR (CDCl₃, TMS, δ, ppm): 1.49 (m, 28 H, CH₂-CH₂-(CH₂)₇-CH₂-CH₂), 1.60-2.00 (m, 8 H, CH₂-CH₂-(CH₂)₇-CH₂-CH₂), 4.00 (m, 8 H, O-CH₂-), 6.9-7.8 (m, 16 H, Ar-H). Anal. Calcd for C₄₈H₆₁N₂O₆P: C, 72.70; H, 7.72; N, 3.53. Found: C, 72.58; H, 7.78; N, 3.62.

Di[11-(4-cyanobiphenyl-4'-oxy)undecyl]maleate (4)

A mixture of 8 g (22 mmol) of 11-(4-cyanobiphenyl-4'-oxy)undecanol, 0.88 g (9 mmol) of maleic acid anhydride and 0.3 g of *p*-toluenesulfonic acid in chloroform was refluxed for one night. The water was trapped by continuous extraction in a Soxhlet apparatus with aluminum oxide as desiccant. The solvent was evaporated and the crude product was purified by column chromatography on aluminum oxide (activity grade III) using CH₂Cl₂/petroleum ether (bp. 40-60 °C) 1:1 v/v as eluent. Yield 80 %. Mp. 110 °C, T₁-LC 78 °C.

¹H-NMR (CDCl₃, TMS, δ, ppm): 1.3 (m, 28 H, CH₂-CH₂-(CH₂)₇-CH₂-CH₂), 1.56-1.90 (m, 8 H, CH₂-CH₂-(CH₂)₇-CH₂-CH₂), 4.00 (t, 4 H, O-CH₂-), 4.20 (t, 4 H, CH₂-OOC-), 6.22 (2, 2 H, H-C=C-H), 6.9-7.8 (m, 16 H, Ar-H). Anal. Calcd for C₅₂H₆₂N₂O₆: C, 77.00; H, 7.71; N, 3.45. Found: C, 76.79; H, 7.77; N, 3.33.

Sodium di[11-(4-cyanobiphenyl)-4'-oxy]undecyl]-2-sulfonatosuccinate (5)

A mixture of 0.8 g (1 mmol) of 4 and a tenfold excess of NaHSO_3 was suspended in 2-propanol/water/THF 4:1:1 and refluxed for 24 h. The solvent was evaporated and the residue was dissolved in 50 mL of CH_2Cl_2 and an equal volume of water was added. This mixture was stirred for a few minutes. The organic layer was separated and dried over MgSO_4 . The product was purified by column chromatography on silica gel using $\text{CH}_2\text{Cl}_2/\text{MeOH}$ 20:1 v/v as eluent. Yield 30 %. Mp. 75 °C. $T_{\text{LC-1}}$ 189 °C.

$^1\text{H-NMR}$ (CDCl_3 , TMS, δ , ppm): 1.3 (m, 28 H, $\text{CH}_2\text{-CH}_2\text{-(CH}_2\text{)}_7\text{-CH}_2\text{-CH}_2$), 1.56-1.90 (m, 8 H, $\text{CH}_2\text{-CH}_2\text{-(CH}_2\text{)}_7\text{-CH}_2\text{-CH}_2$), 3.15 (dd, 2 H, $\text{OOC-CH}_2\text{-}$), 3.96 (t, 4 H, Ar-O-CH_2), 4.06 (t, 2 H, $\text{-CH}_2\text{-OCO-CHSO}_3\text{Na}$) 4.21 (t, 2 H, $\text{-CH}_2\text{-OCO-C-}$), 4.35 (t, 1 H, $\text{CH}_2\text{-OOC-CH(SO}_3\text{H)}$), 6.9-7.8 (m, 16 H, Ar-H).

Anal. Calcd for $\text{C}_{52}\text{H}_{63}\text{N}_2\text{O}_9\text{S Na}\cdot(2\text{H}_2\text{O})$: C, 65.66; H, 7.10; N, 2.95. Found: C, 65.44; H, 6.86; N, 2.87.

5.4.2 Methods

Vesicle solutions were prepared by sonication of the insoluble compounds in ultrapure water using a vibracell sonifier by Sonics and Materials Inc. Electron microscopy (Jeol 1200 EX II electron microscope) was carried out for samples that were negatively stained with 1% uranyl acetate. Polarization microscopy was performed using an Olympus BH-2 microscope equipped with a Mettler FP82HT hot stage and a FP80HT temperature controller. The sample solutions for the DSC measurements (Perkin Elmer DSC 7) consisted of a 0.5 % (w/w) vesicle suspension prepared by sonication. A scan rate of 10 °C/min was used. The fluorescence spectra were recorded from samples which had a optical density of 0.1 at the excitation wavelength of 270 nm. A cut-off filter of 290 nm was placed between the lamp and the sample.

The π -A isotherms were recorded on a Lauda Filmwaage FW2, which was thermostatted at 20 °C. The water used for the subphase was purified by filtration through a Seralpur pro 90C purification system. The amphiphiles were spread from chloroform solutions (1 mg/ml) onto the aqueous subphase by use of a Hamilton syringe. After spreading, the monolayer was allowed to equilibrate for 10 minutes before compression started. The area was reduced at a speed of 15 cm^2/min . All measurements were performed at least in duplo.

5.5 References

- 1 Shimomura, M.; Ando, R.; Kunitake, T. *Ber. Bunsenges. Phys. Chem.* **1983**, *87*, 1131.
- 2 Okahata, Y.; Kunitake, T. *Ber. Bunsenges. Phys. Chem.* **1980**, *81*, 550.
- 3 Vertogen, G.; de Jeu, W. H. *Thermotropic Liquid Crystals, Fundamentals*: Springer-Verlag; Berlin, 1988.
- 4 Kasha, M.; Rawls, H. R.; Ashraf El-Bayoumi, M. *Pure Appl. Chem.* **1965**, *11*, 371.
- 5 Okahata, Y.; Ando, R.; Kunitake, T. *Ber. Bunsenges. Phys. Chem.* **1981**, *85*, 789.
- 6 Turro, N. J.; Kuo, P. *J. Phys. Chem.* **1986**, *90*, 4205.
- 7 Abuin, E.; Lissi, E.; Aravena, D.; Zanocci, A.; Macuer, M. *J. Colloid Interface Sci.* **1988**, *122*, 201.
- 8 Matsui, K.; Nakazawa, T.; Morisaki, H. *J. Phys. Chem.* **1991**, *95*, 976.
- 9 Lissi, E.; Abuin, E.; Saez, M.; Zanocco, A.; Disalvo, A. *Langmuir* **1992**, *8*, 348.
- 10 Dong, D. C.; Winnik, M. A. *Can. J. Chem.* **1984**, *62*, 2560.
- 11 Ikeda, T.; Kurihara, S.; Tazuke, S. *J. Phys. Chem.* **1990**, *94*, 6550.
- 12 Kurihara, S.; Ikeda, T.; Tazuke, S. *Macromolecules* **1993**, *26*, 1590.
- 13 Tamai, N.; Yamazaki, I.; Masuhara, H.; Mataga, N. *Chem. Phys. Lett.* **1984**, *104*, 485.
- 14 Subramanian, R.; Patterson, L. K.; Levanon, H. *Chem. Phys. Lett.* **1982**, *93*, 578.
- 15 Heesemann, J. *J. Am. Chem. Soc.* **1980**, *102*, 2167.
- 16 Heesemann, J. *J. Am. Chem. Soc.* **1980**, *102*, 2176.
- 17 Diamant, H.; Andelmann, D. *Langmuir* **1994**, *10*, 2910.
- 18 McFate, C.; Ward, D.; Olmsted, J. *Langmuir* **1993**, *9*, 1036.
- 19 de Mul, M. N.; Mann Jr, J. A. *Langmuir* **1994**, *10*, 2311.

Chapter 6

Polymers and phototropes

Abstract

Two novel polymerizable double chained ammonium amphiphiles carrying mesogenic cyanobiphenyloxy units have been synthesized containing methacrylate in the headgroup or diacetylene units in the hydrophobic tails. These compounds form (bilayer) aggregates upon sonication in water. Polymerization increases the stability of these aggregates towards solubilization by a nonionic surfactant. The stacking of the cyanobiphenyloxy units in the aggregates is directly monitored by the extent of the blue shift of the absorption maximum. Upon polymerization a decrease in blue shift is observed reflecting a decrease in the ordering of the amphiphile molecules. This effect is stronger when polymerization occurs in the hydrophobic tails than in the headgroup region.

6.1 Introduction

A wide range of natural lipids and synthetic amphiphiles form bilayer vesicles in water. These vesicles have attracted much attention as potential drug delivery systems.¹⁻³ A problem encountered in the application of vesicles is their instability. The stability of vesicles can however be increased by using polymerizable amphiphiles and subsequent polymerization of the formed bilayer vesicles. Especially Ringsdorf *et al.* developed several methods to polymerize vesicles.⁴⁻⁷ Photopolymerization has been proven to be a convenient way to stabilize bilayer structures.

The previous chapter describes a study on double chained ammonium amphiphiles carrying terminal cyanobiphenyloxy units.⁸⁻¹⁰ These compounds form bilayer vesicles in which the aromatic units form H-aggregates resulting in a blue shift of the UV absorption maximum. The blue shift is very sensitive to the distance between the aromatic units and their mutual orientation.^{11,12} It can therefore be used as a probe to monitor the stacking of the cyanobiphenyloxy units in the bilayers. The degree of stacking is directly related to the ordering of the amphiphiles in the bilayer.

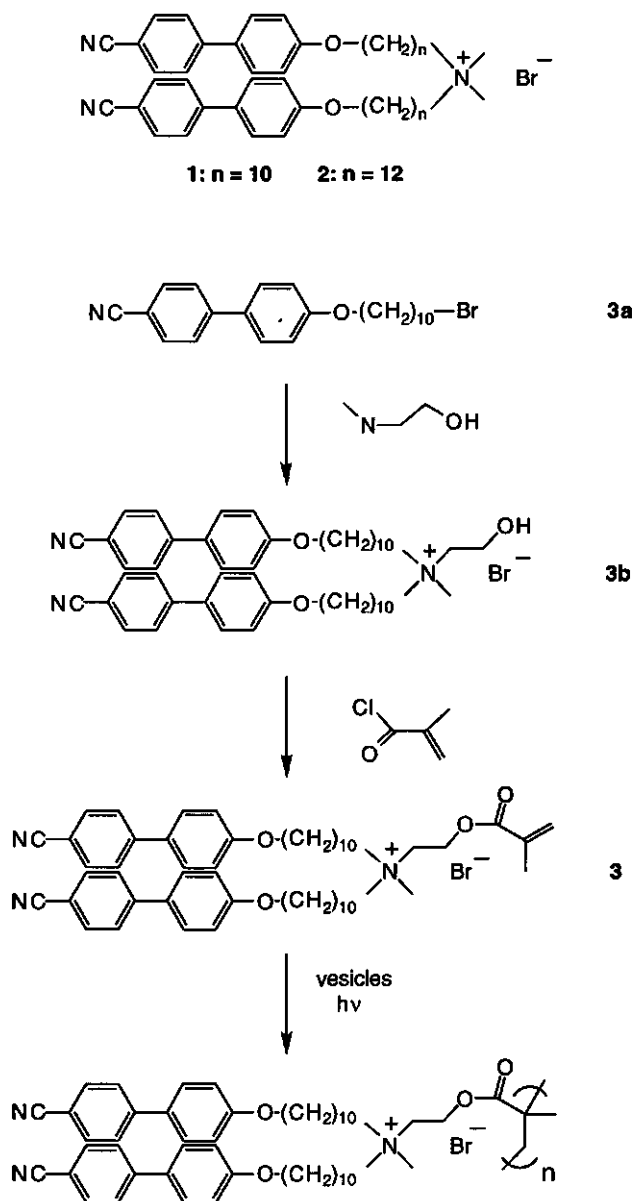
This chapter presents the synthesis of novel amphiphiles carrying terminal cyanobiphenyloxy units and polymerizable methacrylate or diacetylene units. The change in the ordering of the molecules in the (bilayer) aggregates upon polymerization has been monitored with UV spectroscopy and differential scanning calorimetry. Also the stability of the aggregates towards solubilization by nonionic surfactants was investigated using UV spectroscopy.

6.2 Results and Discussion

The investigated compounds and synthetic routes are given in Schemes 1 and 2. In compound 3 a polymerizable methacrylate ester was introduced in the headgroup of the molecule. Compound 4 contains polymerizable diacetylene units in the hydrophobic tails of the molecule. The aggregation properties of these compounds have been compared with those of the non-polymerizable molecules 1 and 2.

6.2.1 Thermotropic properties

All the investigated compounds exhibit thermotropic liquid crystalline phases of the smectic A type except for 1 which is nematic, as was observed by polarization microscopy (see also Chapter 5). Compounds 1 and 2 show monotropic liquid crystalline phases and have melting points at 117 °C and 142 °C respectively. Upon cooling from the isotropic phase the liquid crystalline phases are formed at 111 °C and 108 °C respectively.

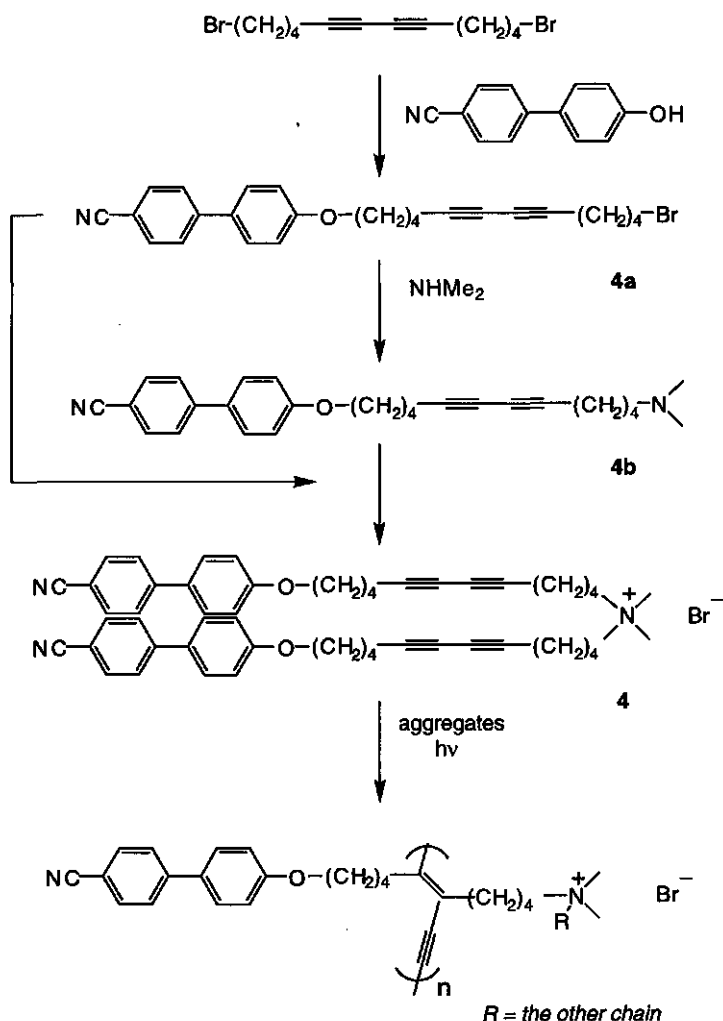


Scheme 1. Molecular structures of compounds **1** and **2** and the synthetic route to **3** and its polymer.

Compounds **3b** and **3** exhibit an enantiotropic smectic A phase with melting points at 86 °C and 60 °C and clearing points at 109 °C and 104 °C respectively. This shows that the melting point is strongly lowered by the introduction of a bulky group in the headgroup region. The liquid crystalline to isotropic phase transition temperature is however hardly affected by this

modification and seems to be dominated by the mesogenic cyanobiphenyloxy units and the alkyl spacers. Compound **4** melts at 63 °C and goes through a very short (1-2 °C) smectic trajet before it turns isotropic. Upon cooling from the isotropic phase the smectic A phase is formed at 63 °C (see also Table 1 on page 101).

After lyophilizing the polymerized aqueous dispersions of **3** and **4**, the clearing points of the solid materials had increased considerably. For compound **3** the clearing point increased from 104 °C to 143 °C and for compound **4** from 63 °C to 140 °C.



Scheme 2. Molecular structure and synthetic route to compound **4** and its polymer.

6.2.2 Lyotropic properties

The investigated compounds **1**, **2** and **3** form bilayer vesicles in water. Upon sonication of the pure compounds in water small vesicles with diameters ranging from 50 to 200 nm are formed as can be observed by electron microscopy and by dynamic light scattering measurements. Giant vesicles can also be prepared by allowing the solid compounds to hydrate above their Krafft temperature (*i.e.* the melting point of the hydrated crystals¹⁴). The giant vesicles can easily be observed with optical microscopy. Compound **4** also forms giant vesicles upon hydration at 70 °C. The aged sonicated samples however show predominantly thread-like structures (see Figure 1). These threads have a diameter of approximately 70 Å which is close to a bilayer thickness and seem to have a helical twist. The sonicated aqueous dispersions of **3** and **4** were polymerized by irradiation with UV light of 254 nm. The cyanobiphenyloxy unit is stable towards this radiation as was confirmed by prolonged irradiation of the nonpolymerizable vesicles of **1** and **2**. Upon polymerization of vesicles of **3**, the turbidity of the vesicle dispersion increases. Upon polymerization of a dispersion of **4** the initially pale solution becomes orange due to the formation of the conjugated polymer backbone (see Scheme 2). The aggregate structure is preserved upon polymerization. Figure 2 shows micrographs of giant vesicles of **3** before and after polymerization. Upon polymerization the vesicle surface becomes more corrugated. This is probably due to the strain imposed on the system by the formation of the polymer backbones.

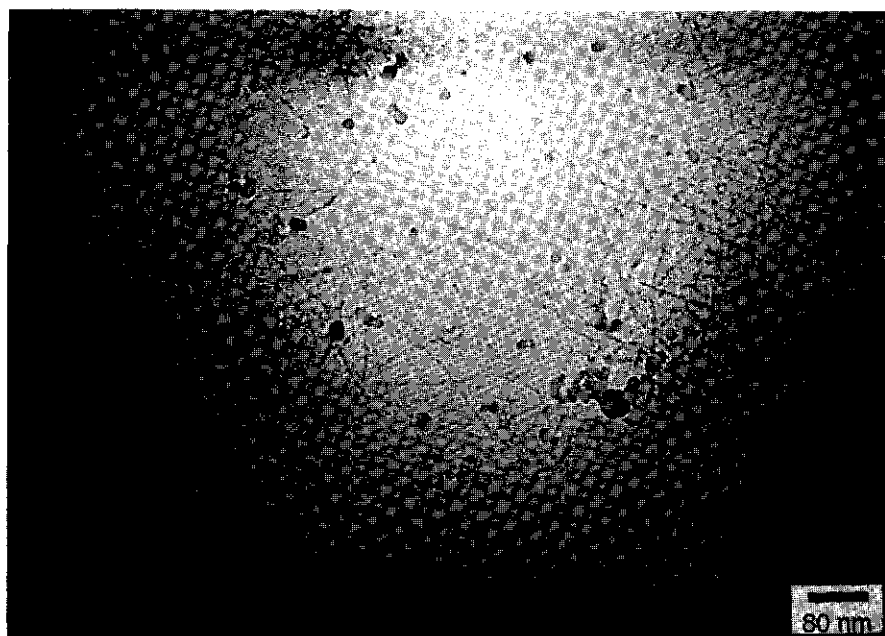


Figure 1. Cryo-electron micrograph of a sonicated dispersion of **4** in water.

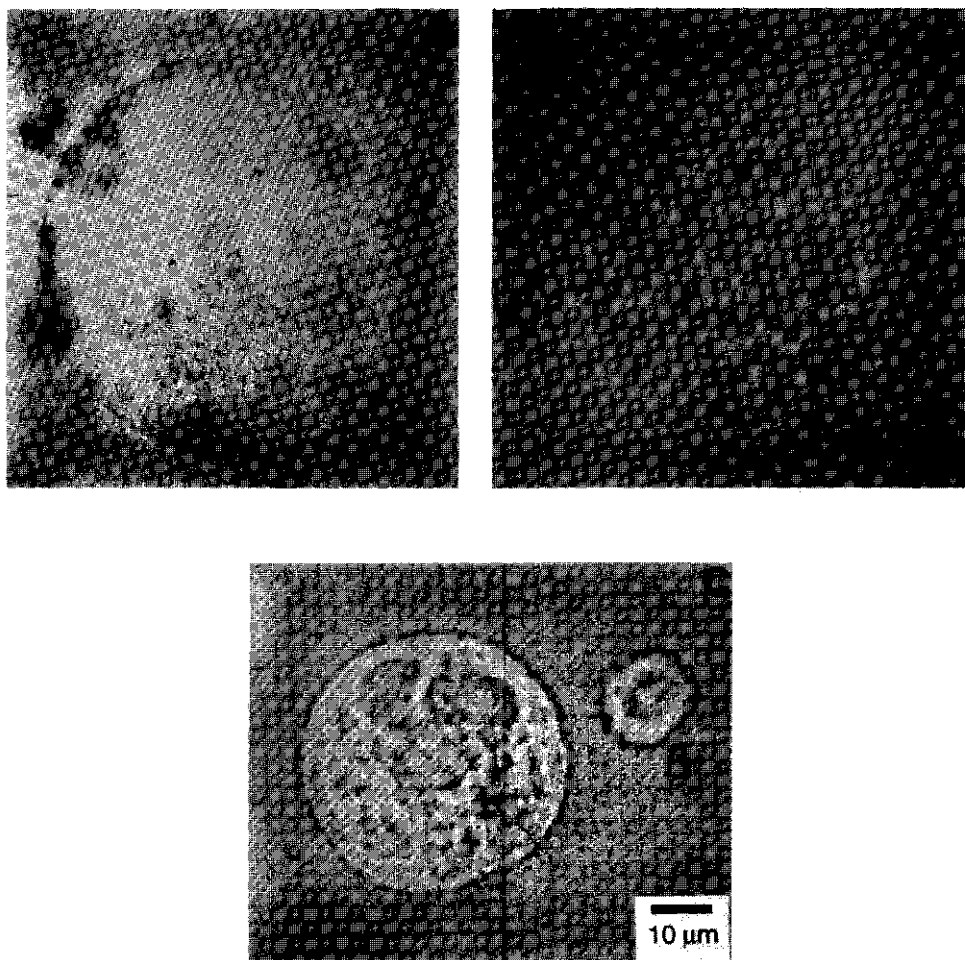


Figure 2. Optical micrographs of different giant vesicles of **3** before (a) and after (b) polymerization and after addition of an excess of $C_{12}E_{23}$ to the polymerized vesicles (c) .

In the previous chapter we have seen the UV absorption spectra of compounds **1** and **2** as vesicles and as monomers in ethanol (Chapter 5, Figure 3). The monomer absorption is found at 297 nm whereas the vesicle absorption maxima of **1** and **2** are found at 267 and 259 nm respectively. Furthermore, the aggregated chromophores have a somewhat lower extinction coefficient than the free chromophores. According to the molecular exciton model proposed by Kasha^{11,12}, this blue shift of the absorption maximum is indicative of linear chromophore aggregates with their transition moments dipoles parallel to each other and perpendicular to the stacking direction (so-called H-aggregates). The spectral shift (in wavenumber $\Delta\nu$) is given by:

$$\Delta\nu = \frac{2}{hc} \frac{N-1}{N} \frac{\mu^2}{r^3} (1 - 3 \cos^2 \alpha) \quad (1)$$

in which μ is the transition dipole moment of the chromophores, which lies along the long axis of the chromophores, and r is the center to center distance between the chromophores. The angle α is the angle between the transition dipole moments and the line between the chromophore centers. N is the number of interacting chromophores in the bilayer, h is Planck's constant and c the speed of light.

Previous X-ray reflectivity experiments confirmed H-aggregation of interdigitated cyanobiphenyloxy units in the bilayers of compound **2**¹⁰ (see also Chapter 5). Shimomura *et al.*¹² reported that single chained ammonium amphiphiles of the type headgroup-spacer-azobenzene-tail form bilayer structures. When the tail is short relative to the spacer H-aggregates of interdigitated azobenzene units were found. Also Song *et al.*¹⁵⁻¹⁷ reported the formation of H-aggregates in bilayers of phosphatidylcholines with azobenzene or stilbene units at the termini of the hydrophobic tails. This suggests that these terminal mesogenic units have the tendency to form interdigitated structures with the orientation of their transition dipole moments more or less perpendicular to the stacking direction.

The different blue shifts which are observed for the bilayer vesicles of **1** and **2** can be attributed to either different stacking distances or different tilt angles or different aggregation numbers. Because parallel stacking of these mesogens seems to be the most favorable configuration, the tilt angle is assumed to be approximately zero in all cases ($\alpha = 90^\circ$). Because the aggregation numbers are thought to be rather large, this parameter is expected to hardly affect the extent of blue shifting. The stacking distance therefore seems to be the most important parameter in determining the spectral differences.

This means that in the bilayers of compound **2** the cyanobiphenyloxy units are more closely packed than in the bilayers of **1** as is shown by the stronger blue shift of the absorption maximum. This could be due to a better decoupling of the aromatic units from the headgroup by the longer alkyl spacers or due to stronger Van der Waals attraction between dodecyl spacers than between decyl spacers. The better molecular ordering in the vesicle bilayers of **2** as compared to that of **1** is also exhibited by the higher 'gel to liquid crystalline' phase transition temperature (T_c) which is found at 65 °C for **2** and at 55 °C for **1**, as was measured by differential scanning calorimetry (DSC).

If we assume a closest stacking distance r of 3.5 Å for the cyanobiphenyloxy units in the bilayers of **2**, using equation (1) a stacking distance of 3.8 Å can be calculated in the bilayers of **1**, provided that the chromophores maintain their arrangement perpendicular to the stacking direction and have large aggregation numbers.

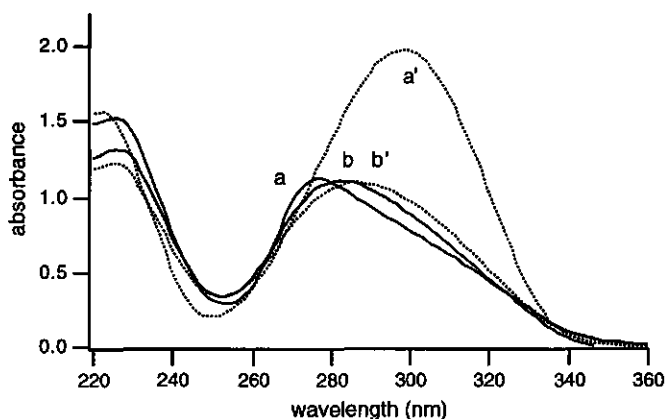


Figure 3. UV absorption spectra of vesicles of compound **3**, before (a, solid line) and after (a', dashed line) addition of $C_{12}E_{23}$. UV absorption spectra of polymerized vesicles of compound **3**, before (b, solid line) and after (b', dashed line) addition of $C_{12}E_{23}$. $[3] = 7.4 \times 10^{-5} \text{ M}$

Figure 3 shows the UV absorption spectra of vesicles of compound **3** before and after polymerization. Before polymerization the absorption maximum lies at 277 nm. This is 10 nm less blue shifted than for vesicles of compound **1**, reflecting a decreased degree of order for the bilayers of this compound. A stacking distance of 4.4 Å can be calculated for parallel chromophores, assuming that all other parameters are the same as in the vesicles of **2**. It is however realized that the increased stacking distance might induce tilting of the chromophores. This decrease in order is due to the bulky and less symmetrical headgroup of **3** as compared to that of **1**. Steric hindrance between the headgroups hampers an optimal packing of the hydrophobic chains. This is also reflected in the Krafft point of these compounds which lies around room temperature for **3** and at 55 °C for **1**. The Krafft temperature depends, amongst other factors, on the ease by which the molecules can pack in a crystal lattice.¹⁸ Also no cooperative phase transition was measured for the bilayers of **3** with DSC confirming the presence of poorly ordered bilayers.

Upon polymerization the absorption maximum shifts from 277 nm to 282 nm. This means a further disordering of the hydrophobic chains because of the strain exerted on the system by the newly formed covalent linkages. Using equation (1) a stacking distance of 4.9 Å can be calculated for parallel, non-tilted chromophores. The polymerization thus causes an increase of the average stacking distance of approximately 0.5 Å.

Figure 3 also shows the UV absorption spectra of the polymerized and non-polymerized vesicles of **3** after addition of the micelle forming surfactant polyoxyethylene(23)lauryl ether ($C_{12}E_{23}$). It was observed that the non-polymerized vesicles are immediately solubilized as indicated by the appearance of the monomer spectrum with an absorption maximum at 297 nm.

The spectrum of the polymerized vesicles on the contrary hardly changes upon addition of $C_{12}E_{23}$. There is a small shift from 282 nm to 286 nm indicating that the presence of the surfactant is felt but the stacking is not completely lost. Probably, only the non-polymerized fraction is solubilized. This shows that the polymerized vesicles are indeed much more resistant towards the solubilizing power of surfactants. Studies by optical microscopy confirmed that the structure of polymerized giant vesicles is maintained after the addition of $C_{12}E_{23}$ (see Figure 2c).

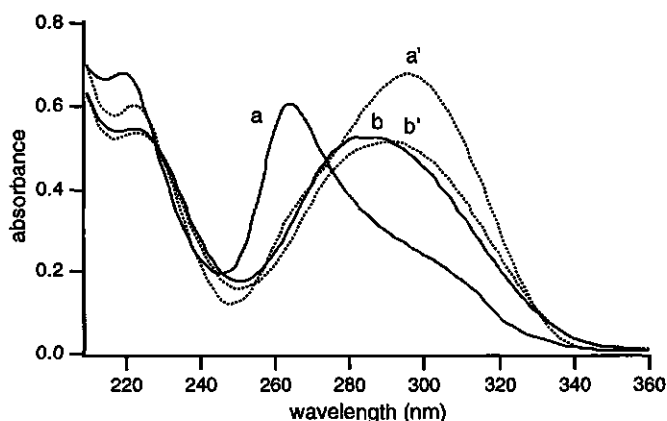


Figure 4. UV absorption spectra of aggregates of compound 4, before (a, solid line) and after (a', dashed line) addition of $C_{12}E_{23}$. UV absorption spectra of polymerized aggregates of compound 4, before (b, solid line) and after (b', dashed line) addition of $C_{12}E_{23}$. $[4] = 2.6 \times 10^{-5}$ M.

Figure 4 shows the UV absorption spectra of compound 4 as thread-like aggregates before and after polymerization. The polymerization does not affect the thread-like morphology. The absorption maximum of the non-polymerized aggregates lies at 264 nm. This is 5 nm less blue shifted than for vesicles of compound 2 which has the same structure with saturated alkyl spacers. An average stacking distance of 3.7 Å can be calculated versus a stacking distance of 3.5 Å for bilayers of 2. Apparently, the rigid diacetylene units slightly decrease the packing efficiency of this compound. This is also seen as a reduction of the Krafft temperature from 80 °C for compound 2 to 63 °C for compound 4. The T_c of these aggregates lies at 60 °C which is 5 °C lower than for bilayers of compound 2. Upon polymerization the absorption maximum shifts from 264 nm to 288 nm. This corresponds to a change in stacking distance from 3.7 Å to 5.9 Å. This dramatic change clearly shows that the molecular packing is heavily disturbed. This is of course what would be expected as a result of the diacetylene polymerization mechanism. A schematic drawing of the polymer is given in Scheme 2. The phase transition at 60 °C also disappears upon polymerization. The small shift of the absorption maximum from 288 nm to 290 nm after addition of the surfactant $C_{12}E_{23}$ (see Figure 5) shows that after polymerization these aggregates also have increased stability towards solubilization by surfactants.

Table 1. Melting Points (Mp), Liquid Crystalline-Isotropic Transition Temperatures (T_{LC-I}), Gel-to-Liquid Crystalline Phase Transition Temperatures (T_C), Krafft Temperatures (T_{Krafft}) and Absorption Maxima of Vesicles (Before and After Polymerization) of Compounds 1-4.

Compound	Mp (°C)	T_{LC-I} (°C)	T_C (°C)	T_{Krafft} (°C)	λ_{max} (nm)
1	117	111	55	55	267
2	142	108	65	80	259
3b	86	109	†	65	267
3	60	104	†	20	277 \Rightarrow 282
4	63	63	60	63	264 \Rightarrow 288

† not observed under the employed experimental conditions

6.3 Conclusions

Polymerizable double chained ammonium amphiphiles carrying terminal cyanobiphenyloxy units form bilayer vesicles or thread-like aggregates which are characterized by a blue shift of the absorption maximum of the aromatic units. This blue shift is a very sensitive probe for the packing order of the cyanobiphenyloxy units in the (bilayer) aggregates.

The introduction of a bulky group in the headgroup region of the molecule and the introduction of rigid diacetylene units in the hydrocarbon tails have a disturbing effect on the molecular packing of the molecules in the aggregates as is observed by a reduction of the blue shift.

Upon polymerization of the aggregates the molecular packing further decreases. This effect is stronger when the polymerization is carried out in the hydrocarbon spacers than in the headgroup. This result confirms what is intuitively expected. In both cases the polymerized aggregates have improved stability towards solubilization by nonionic surfactants.

6.4 Experimental section

6.4.1 Synthesis

4-Hydroxy-4'-cyanobiphenyl was obtained from Merck. The syntheses of *N,N*-di[10-(4-cyanobiphenyl-4'-oxy)decyl]-*N,N*-dimethylammonium bromide (1) and *N,N*-di[12-(4-cyanobiphenyl-4'-oxy)dodecyl]-*N,N*-dimethylammonium bromide (2) and of 10-bromo-1-(4-cyanobiphenyl-4'-oxy)decane 3a have been described before in Chapter 5.^{8,10}

***N,N*-Di[10-(4-cyanobiphenyl-4'-oxy)decyl]-*N*-hydroxyethyl-*N*-methylammonium bromide (3b)**

A mixture of 0.9 g (2.2 mmol) of **3a**^{8,10}, 70 mg (1 mmol) of 2-methylaminoethanol and 0.3 g (2.2 mmol) of K₂CO₃ in 10 mL of acetonitrile was heated at 120 °C for 16 h in a closed reaction vessel. The solvent was removed under reduced pressure and the residue was treated with dichloromethane and the salt was filtered off. The filtrate was concentrated by evaporation and the product was purified by column chromatography on silica gel using CH₂Cl₂/MeOH 100/12 (v/v) as eluent. Yield 60 %. Mp. 86 °C, a smectic A phase is formed with a clearing temperature of 109 °C.

¹H-NMR (CDCl₃, TMS, δ, ppm): 1.3 (m, 24 H, O-CH₂-CH₂-(CH₂)₆-CH₂-CH₂-), 1.8 (m, 8 H, O-CH₂-CH₂-N-CH₂-CH₂-), 3.2 (s, 3 H, N-CH₃), 3.3 (m, 4 H, N-CH₂-), 3.7 (m, 2 H, N-CH₂-CH₂-OH), 3.9 (t, 4 H, Ar-O-CH₂-), 4.6 (m, 2 H, N-CH₂-CH₂-OH), 5.0 (t, 1 H, -OH), 6.9-7.6 (m, 16 H, Ar-H).

***N,N*-Di[10-(4-cyanobiphenyl-4'-oxy)decyl]-*N*-{[(1-methylethenyl)carbonyl]oxyethyl}-*N*-methylammonium bromide (3)**

A mixture of 0.6 g (0.7 mmol) of **3b**, 0.1 g (1 mmol) of triethylamine and 1 mg of 2,6-di-*tert*-butyl-4-methylphenol (polymerization inhibitor) was dissolved in 20 mL of CH₂Cl₂ and cooled in an ice bath. To this solution was added dropwise a solution of 0.19 g (2 mmol) of methacryloyl chloride in 3 mL of CH₂Cl₂. The mixture was stirred for one night at room temperature under a N₂ atmosphere. The reaction mixture was washed with an aqueous NaHCO₃ solution and with a diluted HCl solution. The organic layer was dried over MgSO₄ and the solvent was removed under reduced pressure. The product was purified by column chromatography on silica gel using CH₂Cl₂/MeOH 100:12 (v/v) as eluent. Yield 80 %. Mp. 60 °C, a smectic A phase is formed with a clearing temperature of 104 °C.

¹H-NMR (CDCl₃, TMS, δ, ppm): 1.3 (m, 24 H, O-CH₂-CH₂-(CH₂)₆-CH₂-CH₂-), 1.8 (m, 8 H, O-CH₂-CH₂-N-CH₂-CH₂-(CH₂)₈-), 1.9 (s, 3 H, =C-CH₃), 3.4 (s, 3 H, N-CH₃), 3.5 (m, 4 H, N-CH₂-(CH₂)₉-), 3.9 (t, 4 H, Ar-O-CH₂-), 4.1 (m, 2 H, -CH₂-O-C=O), 4.6 (m, 2 H, N-CH₂-CH₂-O-(C=O)-), 5.6 (d, 1 H, C=C-H), 6.1 (d, 1 H, C=C-H), 6.9-7.6 (m, 16 H, Ar-H). Anal. Calcd. for C₅₃H₇₆N₃O₄Br: C, 71.44; H, 7.69; N, 4.72. Found: C, 71.27; H, 8.01; N, 4.56.

12-Bromo-1-(4-cyanobiphenyl-4'-oxy)-5,7-dodecadiyne (4a)

A mixture of 3.5 g (11 mmol) of 1,12-dibromo-5,7-dodecadiyne¹³, 1.5 g (8 mmol) of 4-hydroxy-4'-cyanobiphenyl and 1.4 g (10 mmol) of K₂CO₃ in 15 mL of 2-butanone was refluxed for 16 h. The solvent was evaporated and the residue was treated with CH₂Cl₂ and the salt was removed by filtration. After evaporation of the solvent, the residue was purified by column chromatography on silica gel using CH₂Cl₂/hexane 2:3 (v/v) as eluent. Yield 60 %. Mp. 97 °C.

¹H-NMR (CDCl₃, TMS, δ, ppm): 1.6 (m, 4 H, -CH₂-CH₂-C≡C-), 1.9 (m, 4 H, -CH₂-CH₂-Br, -CH₂-CH₂-O), 2.3 (dt, 4 H, -CH₂-C≡C-), 3.4 (t, 2 H, -CH₂-Br), 4.0 (t, 2 H, -CH₂-O-), 6.9-7.6 (m, 8 H, Ar-H).

***N*-[12-(4-Cyanobiphenyl-4'-oxy)-5,7-dodecadiynyl]-*N,N*-dimethylamine (4b)**

Dimethylamine (15 mmol) was added as a 20% (w/v) solution in chloroform to a solution of 1.3 g (3 mmol) of **4a** in 5 mL of chloroform. After 24 h at room temperature the solvent was evaporated to remove the excess of dimethylamine. The residue was dissolved in CH₂Cl₂ and washed with water. The organic layer was dried on MgSO₄, filtered and the CH₂Cl₂ was evaporated. Yield 95 %.

¹H-NMR (CDCl₃, TMS, δ, ppm): 1.6 (m, 4 H, -CH₂-CH₂-C≡C-), 1.9 (m, 4 H, -CH₂-CH₂-N, -CH₂-CH₂-O), 2.3 (m, 12 H, -CH₂-C≡C-, N-CH₃, N-CH₂-), 4.0 (t, 2 H, -CH₂-O-), 6.9-7.6 (m, 8 H, Ar-H).

***N,N*-Di[12-(4-cyanobiphenyl-4'-oxy)-5,7-dodecadiynyl]-*N,N*-dimethylammonium bromide (4)**

A mixture of 0.2 g (0.5 mmol) of **4b** and 0.29 g (0.7 mmol) of **4a** was dissolved in 10 mL of 2-butanone. This solution was refluxed for 20 h and the solvent was evaporated. The product was purified by column chromatography on aluminum oxide (activity grade III) using CH₂Cl₂/MeOH 100:3 (v/v) as eluent. Yield 70%. Mp 63 °C, upon cooling a smectic A phase is formed at the same temperature.

¹H-NMR (CDCl₃, TMS, δ, ppm): 1.7 (m, 8 H, -CH₂-CH₂-C≡C-), 1.9 (m, 8 H, -CH₂-CH₂-N, -CH₂-CH₂-O-), 2.4 (dt, 8 H, -CH₂-C≡C-), 3.4 (s, 6 H, N-CH₃), 3.6 (m, 4 H, N-CH₂-), 4.0 (t, 4 H, O-CH₂-), 6.9-7.6 (m, 16 H, Ar-H). Anal. Calcd. for C₅₂H₅₂N₃O₂Br (0.6 H₂O): C, 74.20; H, 6.37; N, 4.99. Found: C, 74.15; H, 6.79; N, 4.93.

6.4.2 Methods

Vesicle dispersions were prepared by sonication of the pure compound in deionized water with a Vibracell sonifier from Sonics and Materials Inc. The vesicles were polymerized by irradiation of the vesicle dispersions in a quartz cuvette with UV light of 254 nm generated by a mercury light source. The solubilization of the vesicles was carried out with an excessive amount of the nonionic surfactant polyoxyethylene(23)lauryl ether (C₁₂E₂₃). Differential scanning calorimetry (DSC) experiments were performed with 2% (w/w) vesicle dispersions using a Perkin Elmer DSC 7 apparatus. Giant vesicles were prepared by allowing a small amount of the solid compound to hydrate for one minute in a drop of water at 80 °C. The UV absorption spectra were recorded on a Lambda 18 spectrophotometer from Perkin Elmer.

6.5 References

- (1) Lasic, D. D.; Martin, F. J.; Gabizon, A. G.; Huang, S. K.; Papahadjopoulos, D., *Biochim. Biophys. Acta* **1991**, *1070*, 182.
- (2) Lasic, D. D.; Papahadjopoulos, D. *Science* **1995**, *267*, 1275.
- (3) Lasic, D. D. *Angew. Chem.* **1994**, *106*, 1765.
- (4) Ringsdorf, H.; Schlarb, B.; Venzmer, J. *Angew. Chem.* **1988**, *100*, 117.
- (5) Dorn, K.; Klingbiel, R. T.; Specht, D. P.; Tyminsky, P. N.; Ringsdorf, H.; O'Brien, D. F. *J. Am. Chem. Soc.* **1984**, *106*, 1627.
- (6) Laschewsky, A.; Ringsdorf, H.; Schmidt, G.; Schneider, J. *J. Am. Chem. Soc.* **1987**, *109*, 788.
- (7) Elbert, R.; Laschewsky, A.; Ringsdorf, H. *J. Am. Chem. Soc.* **1985**, *107*, 4134.
- (8) Everaars, M. D.; Marcelis, A. T. M.; Sudhölter, E. J. R. *Langmuir* **1993**, *9*, 1986.
- (9) Everaars, M. D.; Marcelis, A. T. M.; Sudhölter, E. J. R. *Thin Solid Films* **1994**, *242*, 78.
- (10) Everaars, M. D.; Marcelis, A. T. M.; Kuypers, A. J.; Laverdure, E.; Koronova, J.; Koudijs, A.; Sudhölter, E. J. R. *Langmuir* **1995**, *11*, 3705.
- (11) Kasha, M.; Rawls, H. R.; Ashraf El-Bayoumi, M. *Pure Appl. Chem.* **1965**, *11*, 371.
- (12) Shimomura, M.; Aiba, S.; Tagima, N.; Inoue, N.; Okuyama, K. *Langmuir* **1995**, *11*, 969.
- (13) Hammond, P. T.; Rubner, M. F. *Macromolecules* **1995**, *28*, 795.
- (14) Shinoda, K. *Pure Appl. Chem.* **1980**, *52*, 1195.
- (15) Song, X.; Perlstein, J.; Whitten, D. G. *J. Am. Chem. Soc.* **1995**, *117*, 7816.
- (16) Song, X.; Geiger, C.; Furman, I.; Whitten, D. G. *J. Am. Chem. Soc.* **1994**, *116*, 4103.
- (17) Song, X.; Geiger, C.; Leinhos, U.; Perlstein, J. *Am. Chem. Soc.* **1994**, *116*, 10340.
- (18) Evans, F. D.; Wennerström, H. *The Colloidal Domain*; VCH Publishers: New York, 1994, p. 8.

Chapter 7



*Monomer transfer and
solubilization of amphotrope
vesicles*

Abstract

Double chained ammonium amphiphiles with terminal 4'-cyano-biphenyl-4-oxy, 4'-cyanoazobenzene-4-oxy or 4'-nitroazobenzene-4-oxy moieties form vesicles upon sonication in water. The UV absorption maxima of the vesicle dispersions are blue shifted due to the formation of H-aggregates of the aromatic units in the bilayer. When these vesicles are mixed with dialkyldimethylammonium bromide vesicles, the H-aggregates disappear as can be monitored by UV spectroscopy. It was concluded that the observed spectral changes are due to a monomer exchange process instead of a vesicle fusion process, by varying the concentration of both vesicle dispersions. The same phenomenon was used to monitor the solubilization of these vesicles by hexadecyltrimethylammonium bromide micelles. For vesicles from amphiphiles with cyanobiphenyloxy units at the termini of both chains, a unidirectional diffusion of monomers to didodecyldimethylammonium bromide vesicles is found. The reverse process is hampered by the rigidity of the bilayer of the former compound due to stacking of the aromatic units. For vesicles from amphiphiles with only one azobenzene unit, the monomer exchange with didodecyldimethylammonium bromide vesicles is bidirectional, due to the reduced rigidity of these membranes. The monomer exchange with dodecyltetradecyldimethylammonium bromide and dioctadecyldimethylammonium bromide vesicles is again a unidirectional diffusion of the azobenzene containing amphiphiles. Solubilization of vesicles from amphiphiles with cyanobiphenyloxy units at the termini of both chains by hexadecyltrimethylammonium bromide micelles is an unidirectional diffusion process of monomers from the vesicles to the micelles. Solubilization of vesicles from amphiphiles with only one azobenzene unit is accompanied by penetration of hexadecyltrimethylammonium bromide monomers into the bilayers.

7.1 Introduction

In biological systems the transport of phospholipid molecules between membranes is catalyzed by phospholipid transfer proteins. In addition, non-protein-mediated transport of phospholipids has been demonstrated in artificial bilayer systems. Mainly two techniques have been used to study the spontaneous lipid transfer between vesicles.

One technique employs free flow electrophoresis.^{1,2} With this technique it is possible to separate differently charged vesicles. At the start of such an experiment, vesicles containing radioactively labeled lipid molecules are mixed with a different unlabeled vesicle dispersion. After a certain incubation time, both types of vesicles are separated by electrophoresis and the amount of radioactivity in both vesicle populations is measured.

Resonance energy transfer between fluorophores is another technique that has been used to study the kinetics of lipid transfer.^{3,4} This method employs synthetic lipids which are labeled with fluorophores. When both energy donor and energy acceptor labeled lipids are incorporated in the same vesicles this results in a considerable quenching of the fluorescence due to energy transfer. When transfer of these fluorescent lipids to other vesicles occurs, this results in a dilution of the fluorophores which reduces the probability of energy transfer and therefore the fluorescence yield increases.

A relatively new way to study monomer transfer between vesicles makes use of synthetic amphiphiles which contain aromatic units. When these amphiphiles form bilayer vesicles, the aromatic units form stacks. This is accompanied by a wavelength shift of the π - π^* absorption band⁵⁻¹² in the UV absorption spectra. During the monomer exchange process with vesicles without aromatic units, the dilution of the aromatic units causes the shifted absorption band to return to its normal value.

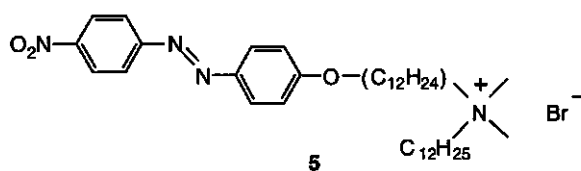
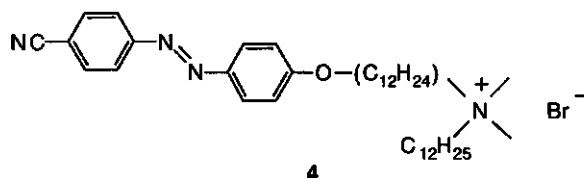
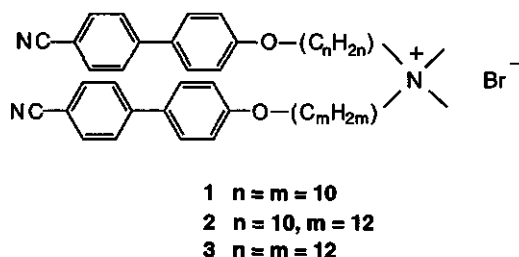
This effect was already reported in 1981 by Shimomura *et al.*¹² for mixtures of vesicles from azobenzene containing cationic surfactants and didodecyldimethylammonium bromide vesicles. They attributed the spectral changes to vesicle fusion, indicating a random mixing of monomers, but leaving the exact mechanism uninvestigated. Later studies performed by Rupert *et al.*^{13,14} showed that fusion of positively charged vesicles, *i.e.* the merging of two or more vesicles into one big vesicle, does not occur spontaneously unless fusogenic agents like dipicolinic acid are added. Only very recently, these spectral changes were attributed to monomer transfer by Song *et al.*¹⁵, who investigated monomer transfer between stilbene derivatized phosphatidylcholine vesicles and underivatized phosphatidylcholine vesicles. To our knowledge this was the first time that the rate of monomer transfer was studied by UV spectroscopy.

The previous chapters deal with the synthesis and investigation of ammonium amphiphiles which carry aromatic units¹⁶⁻¹⁹. The aromatic units are all donor- π -acceptor systems and are

well known mesogens. It was found that some of our novel vesicle forming compounds are especially suitable to investigate membrane processes.

In this chapter a study on the process of monomer transfer between vesicles of these novel compounds and dialkyldimethylammonium bromide vesicles using UV spectroscopy and differential scanning calorimetry is described. In addition, the process of vesicle solubilization, *i.e.* the formation of mixed micelles by the addition of other cationic surfactants, has also been studied in this way.

7.2 Results and Discussion



7.2.1 Vesicle forming properties

The molecular structures of the synthetic surfactants are given above. All the investigated compounds form unilamellar bilayer vesicles with diameters ranging from 50 to 200 nm upon sonication as was confirmed by electron microscopy^{16,18} (see Chapter 4 and 5). Also giant unilamellar vesicles were formed upon hydration of the crystalline material, using the technique described by Menger *et al.*²⁰ In all cases blue shifted absorption maxima are found for the vesicle dispersions.

Like biomembranes, the bilayers of these compounds exhibit a gel to liquid crystalline phase transition as was observed by differential scanning calorimetry. Bilayers from **1**, **2** and **3** show phase transitions at 55, 49 and 65 °C respectively. For vesicles from **4** and **5** phase transitions were observed at 39 and 27 °C respectively (see Chapter 4 and 5).

Previously it was found that azobenzene aromatic units have stronger mutual π - π stacking interactions than biphenyl units¹⁸ (see Chapter 2). Preliminary studies showed that bilayers of ammonium amphiphiles carrying two azobenzene units at the termini of both their chains do not readily transfer monomers and are also not solubilized by micelles of cationic surfactants. This is why in this study double chained amphiphiles are used in which only one of the alkyl chains carries an azobenzene unit. The intermolecular interactions in the bilayers of these compounds are expected to be somewhat lower than those for the compounds with two cyanobiphenyl-yloxy units, as is also reflected by the lower phase transition temperature of the bilayers of these compounds.

7.2.2 Monomer transfer between vesicles

Figure 1 shows the spectral changes which occur in time after mixing vesicles of **2** with didodecyldimethylammonium bromide ($C_{12}C_{12}N^+$) vesicles. Gradually the blue shifted absorption band disappears and the spectrum of the non-aggregated species appears showing an isosbestic point. Apparently, there is no stacking interaction between the chromophores in the mixed aggregates.

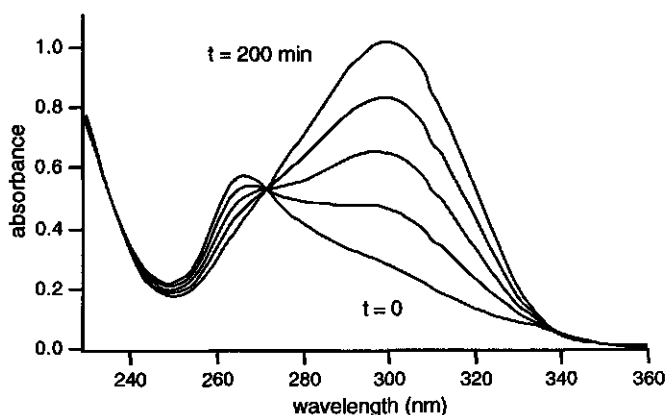


Figure 1. Spectral changes in time upon mixing vesicles of **2** (0.05 mM) with vesicles of $C_{12}C_{12}N^+$ (3.5 mM) at 23 °C.

By measuring the absorbance at 300 nm the rate of the process can be monitored. For vesicles of **1**, **2**, **4** and **5** mixed with dialkyldimethylammonium bromide vesicles the rate of the process is proportional to the concentration of the chromophore containing surfactants. The reaction rate

is independent of the concentration of dialkyldimethylammonium bromide vesicles. Therefore, the monitored process is not a fusion of vesicles and is not collision mediated, but must be a monomer transfer between vesicles.

Usually, concentrations of 0.05 mM of the chromophore-containing vesicles and 3.5 mM of the dialkyldimethylammonium bromide vesicles are used. For vesicles of **1** and **2** this excess is needed to obtain total destacking of the aromatic units. Increasing the concentration further to 10 mM has no effect on the observed transfer rates. At lower concentrations the stacking is partially maintained. For **4** and **5** equimolar concentrations of dialkyldimethylammonium bromide are sufficient to obtain complete destacking. Increasing the concentration has no effect on the transfer rates, and the measurements have been carried out with a concentration of 3.5 mM.

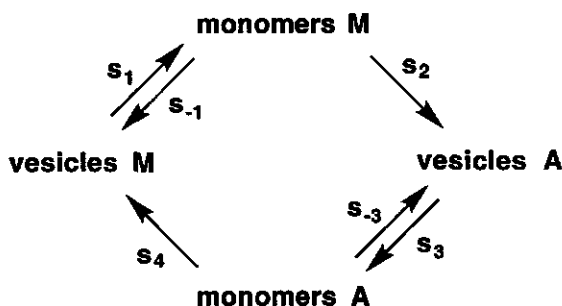


Figure 2. Possible routes for monomer transfer between a mixture of two vesicle species A and M. M represents the amphiphiles containing aromatic (Mesogenic) units at the termini of their alkyl chains.

On the basis of the experimental results the following model is proposed to explain the observations. In Figure 2 the possible routes for monomer transfer between vesicles are represented. Before mixing, the vesicles are in equilibrium with their monomers. These monomer concentrations are equal to the respective critical bilayer concentrations (*i.e.* the concentration above which bilayers are being formed). Upon mixing both vesicle dispersions, the monomers can be taken up by the vesicles of the other species. This gives two pathways ($s_1 + s_2$ and $s_3 + s_4$) via which monomer transfer can take place.

We will look now in more detail at the situation for **1** (M). As mentioned before, the transfer process is independent of the concentration of dialkyldimethylammonium bromide (A). This means that steps s_2 and s_3 can be ruled out as rate determining steps. Because of the large excess of the dialkyldimethylammonium bromide vesicles the reentry process of the mesogen-carrying amphiphiles s_{-1} is thought to be negligible. Therefore, only steps s_1 and s_4 remain as possible steps which determine which transfer pathway is followed. To determine the relative importance of step s_4 to the transfer process, the transfer reaction was performed with $C_{12}C_{12}N^+$, $C_{12}C_{18}N^+$ and $C_{18}C_{18}N^+$. In this way the free monomer concentration of

dialkyldimethylammonium bromide is changed due to the different hydrophobicity of these compounds. Figure 3 shows the change of the absorbance at 300 nm in time, reflecting the rate of the transfer processes. As can be seen the rate of the transfer process is not dramatically affected upon changing the dialkyldimethylammonium bromide species, indicating that not step s_4 but s_1 is the dominant step. The transfer process is mainly a one way process in which monomers leave the vesicles of **1** and are incorporated in the dialkyldimethylammonium bromide vesicles whereas the other route ($s_3 + s_4$) is of minor importance. This agrees with the observation that the rate of the exchange process is proportional to the concentration of vesicles of **1**. The more vesicles of **1** are present, the more monomers will be extruded from these bilayers per time unit.

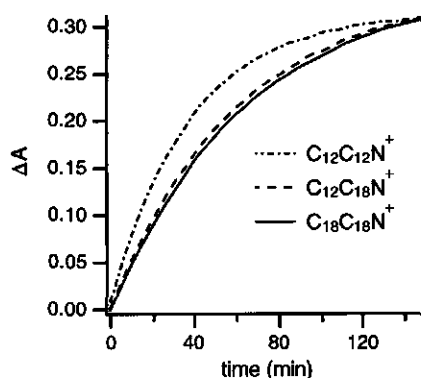


Figure 3. Rate of monomer transfer between vesicles of **1** (0.05 mM) and vesicles of $C_{12}C_{12}N^+$, $C_{12}C_{18}N^+$ and $C_{18}C_{18}N^+$ (3.5 mM) at 23 °C.

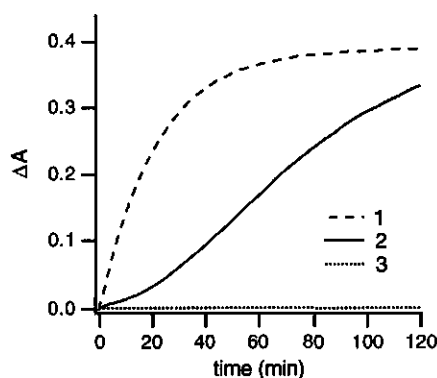


Figure 4. Rate of monomer transfer between vesicles of **1**, **2** and **3** (0.05 mM) with vesicles of $C_{12}C_{12}N^+$ (3.5 mM) at 23 °C.

In this respect the membranes of **1** differ from phospholipid biomembranes. For biological membrane vesicles unidirectional lipid diffusion is found from the most soluble lipid vesicles to the less soluble lipid vesicles.² Because **1** has a lower critical bilayer concentration¹⁷ than $C_{12}C_{12}N^+$ a migration of $C_{12}C_{12}N^+$ monomers to the vesicles of **1** would be expected. Maybe the bilayers of **1** are too rigid to allow fast entrance of dialkyldimethylammonium bromide monomers. This rigidity could be caused by π - π stacking interactions between the cyanobiphenyloxy moieties and is also reflected in the high T_c of these bilayers.

It should be remarked that $C_{12}C_{12}N^+$ and $C_{12}C_{18}N^+$ form bilayer vesicles, whereas $C_{18}C_{18}N^+$ forms bilayer lamellae.²⁴ The phase transition temperature of $C_{12}C_{12}N^+$ lies at 17 °C²⁵ so that these bilayers are in their liquid crystalline phase at room temperature. The phase transition temperature of $C_{18}C_{18}N^+$ lies at 45 °C, so these bilayers are in their gel state at room temperature.²⁴ Despite these differences the observed transfer rates are almost equal,

confirming transport of cyanobiphenyloxy containing amphiphiles to the dialkyldimethylammonium bilayers ($s_1 + s_2$) in which s_1 is rate determining.

Figure 4 shows the effects of changing the spacer length of the cyanobiphenyloxy monomers on the transfer process. When vesicles of **2** are mixed with didodecyldimethylammonium bromide vesicles (at 23°C), the absorbance plot shows a sigmoidal curve. Replacing $C_{12}C_{12}N^+$ by $C_{12}C_{18}N^+$, which has a lower critical bilayer concentration, strongly decreases the observed exchange rate (plot not shown). The release of monomers from the cyanobiphenyloxy vesicles (s_1) is probably so slow that the uptake of $C_{12}C_{12}N^+$ monomers (s_4) becomes also important. The sigmoidal shape of the curve could then be explained by assuming that the first $C_{12}C_{12}N^+$ molecules which enter the vesicles of **2** have only little effect on the degree of chromophore stacking in these vesicles and thus little effect on the UV spectrum. Only dilution of the aggregates of **2** above a certain degree results in a marked change of the UV spectrum. Figure 5 gives the temperature dependence of the monomer transfer process between vesicles of **2** and $C_{12}C_{12}N^+$. At higher temperatures a 'first order' reaction rate is observed, which could indicate that s_1 again becomes more important than s_4 .

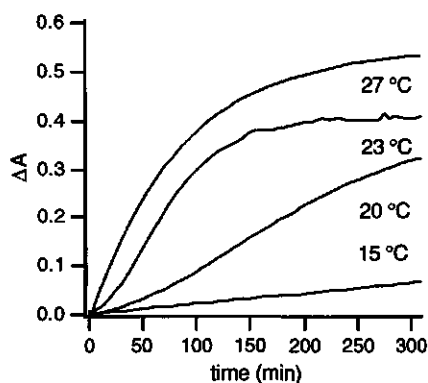


Figure 5. Rate of monomer transfer between vesicles of **2** (0.05 mM) and $C_{12}C_{12}N^+$ (3.5 mM) as a function of temperature.

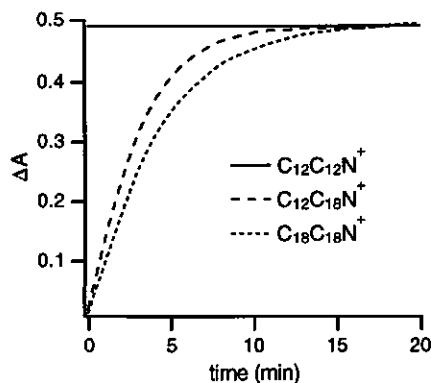


Figure 6. Rate of monomer transfer between vesicles of **4** (0.05 mM) and vesicles of $C_{12}C_{12}N^+$, $C_{12}C_{18}N^+$ and $C_{18}C_{18}N^+$ (3.5 mM) at 23°C.

Between vesicles of **3** and $C_{12}C_{12}N^+$ no detectable monomer exchange occurs (see Figure 4). For these vesicles the membranes are so rigid that $C_{12}C_{12}N^+$ monomers cannot enter them and that release of monomers of **3** is very slow.

For vesicles of both **4** and **5** the monomer transfer with $C_{12}C_{12}N^+$ is too fast to be monitored with our experimental setup. Because the transfer rate is independent of the concentration of the dialkyldimethylammonium bromide vesicles, s_2 and s_3 can again be ruled out as the rate determining processes. To test the relative importance of s_4 , the dialkyldimethylammonium

bromide species was altered from $C_{12}C_{12}N^+$ to $C_{12}C_{18}N^+$ and $C_{18}C_{18}N^+$. As can be seen in Figure 6 this results in a considerable decrease of the observed transfer rate indicating that not step s_1 but s_4 plays a major role in the monomer transfer with $C_{12}C_{12}N^+$ vesicles.

The difference between the rate of monomer transfer between the azobenzene containing vesicles and $C_{12}C_{18}N^+$ or $C_{18}C_{18}N^+$ is only small. This again suggests that step s_1 has become more important than s_4 . These findings are more in agreement with what is known for biological membranes, *i.e.* migration occurs from the most soluble vesicle species to the less soluble vesicle species. Monomers of $C_{12}C_{18}N^+$ and $C_{18}C_{18}N^+$ are expected to have an approximately equal and a lower critical bilayer concentration respectively than **4** or **5**.¹⁸

When $C_{12}C_{12}N^+$ and $C_{12}C_{18}N^+$ are both present in an equimolar ratio, the transfer rates with vesicles of **4** and **5** are the same as when only $C_{12}C_{18}N^+$ is present. This indicates that the formation of mixed bilayer vesicles of $C_{12}C_{12}N^+$ and $C_{12}C_{18}N^+$, which lowers the free monomer concentration of $C_{12}C_{12}N^+$, results in a decrease of process s_4 and allows s_1 to become more important.

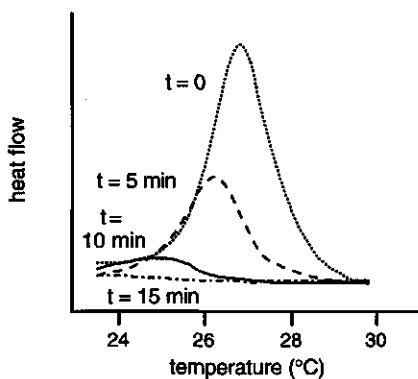


Figure 7. DSC thermograms of a mixture of vesicles of **5** and $C_{12}C_{18}N^+$ at different time intervals after mixing.

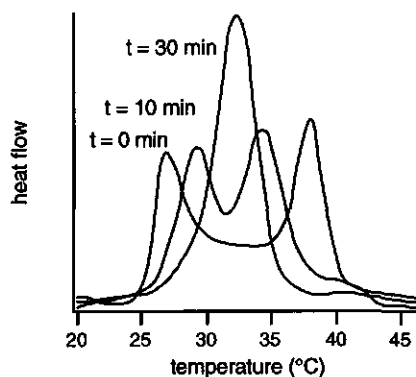


Figure 8. DSC thermograms of a mixture of vesicles of **4** and **5** at different time intervals after mixing.

The process of monomer transfer between **5** and $C_{12}C_{18}N^+$ vesicles could also be monitored by differential scanning calorimetry. Figure 7 shows how the gel to liquid crystalline phase transition peak of the vesicles of **5** disappears due to the formation of new mixed vesicles with excess of $C_{12}C_{18}N^+$, which do not exhibit a measurable phase transition. Figure 8 shows the DSC thermograms of a 1:1 mixture of vesicles of **4** and **5**. The individual phase transition peaks merge into one single phase transition peak which belongs to the mixed vesicles. This transfer process cannot be monitored by UV spectroscopy, because both vesicle species have approximately the same UV-absorption spectrum and the π - π stacking remains in the mixed vesicles.

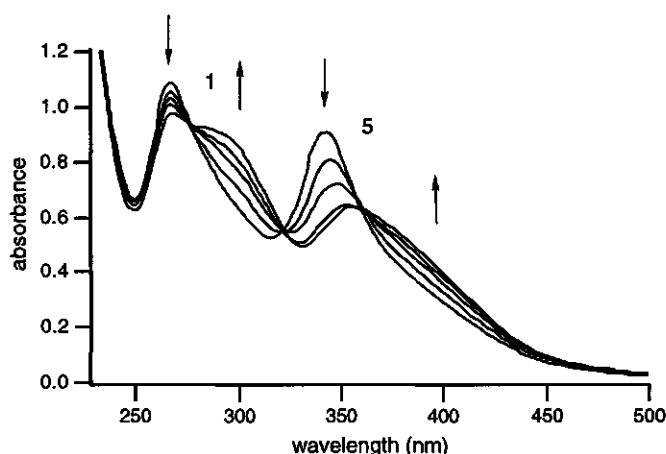


Figure 9. UV absorption spectra taken at different times after mixing equimolar vesicle dispersions of **1** and **5**. Total time span of two hours.

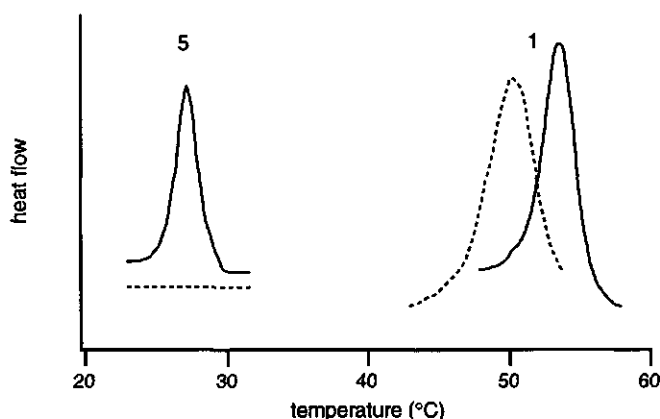


Figure 10. DSC thermograms of 1 wt% vesicle dispersions of **1** and **5** directly after mixing (solid lines) and two hours after mixing (dashed lines).

When vesicles of **1** and **5** are mixed in a 1:1 ratio, changes in the UV absorption spectrum of both compounds are found as can be seen in Figure 9. This means that mixing of both species occurs. The absorption maximum of **5** at 340 nm shifts to higher wavelengths. This is due to a reduction of the stacking interaction between the azobenzene units as a result of the mixing with molecules of **1**.

The absorption maximum of **1** remains mainly at 267 nm but a shoulder appears at 295 nm belonging to destacked cyanobiphenyloxy units. This means that the majority of the molecules of **1** remains closely packed and only a fraction mixes with the molecules of **5**. Therefore a phase separated state is maintained in which a part of the molecules **1** have diffused

into the areas with molecules **5**, but the molecules **5** hardly diffuse into the areas with molecules **1**. It is therefore concluded that the molecules **1**, which have stronger intermolecular interactions than the molecules **5**, tend to form separate domains in the mixed bilayers. This is also confirmed by DSC measurements. The phase transition of the bilayers of **5** (at 27 °C) disappears due to mixing with molecules **1**. The phase transition of the bilayers of **1** at 55 °C does not disappear but only shifts a few degrees to lower temperatures. This means that these phase separated domains have approximately the same composition as the bilayers of pure **1**.

7.2.3 Solubilization of bilayers

Single chained surfactants are known to form micelles in water above a certain critical micelle concentration. These micelles are able to solubilize hydrophobic molecules in their interior. The process of solubilization of bilayers of chromophore containing amphiphiles by cationic surfactants can be investigated in the same way as the monomer transfer process described above. Upon solubilization of the vesicles of the aromatic unit containing amphiphiles, mixed micelles are formed in which the stacking between the chromophores is lost and the UV spectrum of the non-stacked aromatic units is observed.

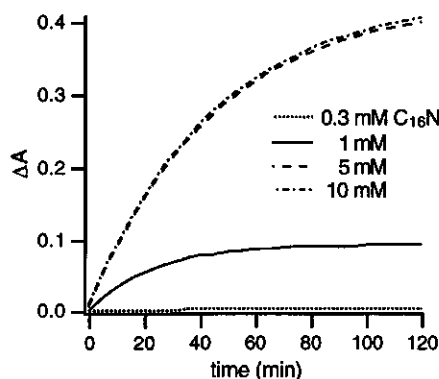


Figure 11. Rate of solubilization of vesicles of **1** (0.05 mM) with increasing concentrations of $C_{16}N^+$ at 23°C.

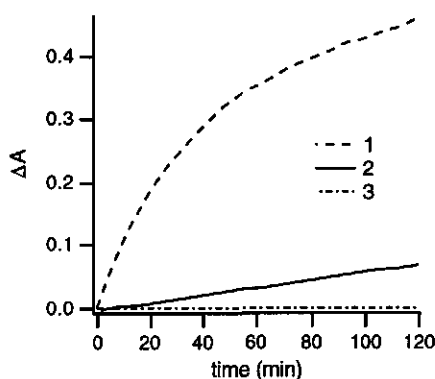


Figure 12. Rate of solubilization of vesicles of **1**, **2** and **3** (0.05 mM) by $C_{16}N^+$ (5 mM) at 23°C.

Figure 11 shows the change in UV absorption at 300 nm of vesicles of **1** due to solubilization by hexadecyltrimethylammonium bromide ($C_{16}N^+$) at different concentrations at 23°C. At this temperature the critical micelle concentration (cmc) of $C_{16}N^+$ is ~ 1 mM.²⁵ It is seen that above the cmc (5 and 10 mM) solubilization occurs with a rate which is comparable, but somewhat slower, than the monomer transfer process with dialkyldimethylammonium bromide vesicles (see Figure 3). The same solubilization rate is found with dodecyltrimethylammonium bromide ($C_{12}N^+$) which has a cmc of 25 mM at room temperature. Together with the fact that the rate is

independent of the concentration of micelles this indicates that the release of monomers from the vesicles of **1** is the dominant process. Therefore the solubilization process is also a unidirectional diffusion process of monomers going from the vesicles into the micelles. This is however, in sharp contrast to what is found for the solubilization of biomembranes. Here the micelle forming surfactant molecules are thought to enter the membranes until a saturation value is reached after which mixed micelles are formed.²⁷⁻³⁰

Figure 12 shows the solubilization curves of vesicles of **1**, **2** and **3** by $C_{16}N^+$ micelles. The rate of solubilization for vesicles of **2** is much lower than for those of **1** because of the lower critical bilayer concentration of the former compound in water. The rate of solubilization for vesicles of **2** is also lower than the rate of monomer transfer with $C_{12}C_{12}N^+$ (Figure 4). This confirms the idea that in the case of monomer transfer $C_{12}C_{12}N^+$ molecules can enter the bilayers of **2** whereas in the case of solubilization monomers only escape from the bilayers of **2** to the micelles. Vesicles of **3** are not readily solubilized by $C_{16}N^+$, probably because the free monomer concentration of **3** is very low in water.

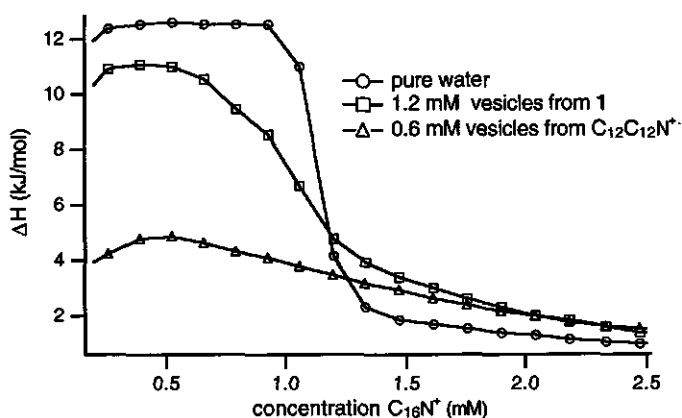


Figure 13. Enthalpy of dilution versus concentration for $C_{16}N^+$ in different aqueous media at 30 °C.

The absence of a fast penetration of $C_{16}N^+$ monomers into the bilayers of **1** can also be monitored with titration microcalorimetry. Figure 13 shows the measured enthalpies of demicellization of $C_{16}N^+$ in pure water and in a solution containing vesicles of **1**. In pure water at 30 °C the cmc of $C_{16}N^+$ is found at 1.1 mM and a demicellization enthalpy of 12 kJ/mol is found. Because the enthalpies of demicellization in pure water and in the vesicle dispersion of **1** are rather similar, it is concluded that the $C_{16}N^+$ molecules do not readily mix with the molecules of **1** in the time course of the experiment. In a solution containing vesicles of $C_{12}C_{12}N^+$ the demicellization enthalpy is drastically changed as compared to the situation in pure water. This means that a mixing of $C_{12}C_{12}N^+$ and $C_{16}N^+$ readily occurs.

All cyanobiphenyloxy containing bilayer vesicles are instantaneously solubilized by nonionic surfactants of the oligoethylene glycol alkyl ether type. These nonionic surfactants readily penetrate the cationic bilayers and the formation of mixed micelles is favored by the relief of the headgroup repulsions in the bilayers. When mixed with an anionic surfactant like sodium dodecylsulfate (SDS), only minor changes in the UV spectrum of the cyanobiphenyloxy containing bilayer vesicles are observed. This is due to the formation of ion-pair amphiphiles which form aggregates in which the π - π stacking is maintained.

Vesicles of 4 and 5 are also solubilized by $C_{16}N^+$ and $C_{12}N^+$ micelles although the process is too fast to be followed under the employed experimental conditions. This could mean that, like for monomer exchange with $C_{12}C_{12}N^+$ vesicles, $C_{16}N^+$ monomers can penetrate these vesicle bilayers. Solubilization however, only occurs above the cmc of $C_{16}N^+$. This agrees with the results of Lichtenberg³⁰ who found that solubilization of phosphatidylcholine vesicles usually does not occur when the surfactant concentration in the aqueous phase is below its cmc value. This was explained by assuming that the partition coefficient of the surfactant (s) over the lipid bilayer phase (l) and aqueous phase (a), $K = [s]_l/[s]_a$, increases strongly when the concentration of the surfactant in the aqueous phase exceeds its cmc. Thus $K_{>cmc} \gg K_{<cmc}$.

7.3 Conclusions

The bilayer properties of double chained ammonium amphiphiles which contain aromatic biphenyl or azobenzene units at the termini of their hydrocarbon chains have been investigated. These artificial amphiphiles behave like natural lipids in the sense that they form bilayer structures which exhibit phase transitions from a rigid 'gel' phase to a more fluid 'liquid crystalline' phase.

Stacking of the aromatic units in the bilayers results in a blue shift of the π - π^* absorption band. When monomer transfer between these bilayer vesicles and dialkyldimethylammonium bromide vesicles occurs, the blue shift of the absorption band disappears. This also occurs upon solubilization of these bilayer vesicles by cationic micelle forming surfactants. The rate of monomer transfer processes between bilayer vesicles and the solubilization of bilayer vesicles by cationic surfactants have been investigated by UV spectroscopy.

Ammonium amphiphiles with two cyanobiphenyloxy units at the termini of their hydrophobic tails form very rigid bilayers. This is reflected by the high T_c of these bilayers and is probably caused by π - π stacking between the aromatic units in the bilayers. Consequently, penetration of these bilayers by cationic amphiphiles is hampered. Monomer transfer between these vesicles and dialkyldimethylammonium bromide vesicles therefore becomes mainly a unidirectional process determined by the release of cyanobiphenyloxy amphiphiles from their vesicles. Also the solubilization of vesicles of these compounds by hexadecyltrimethylammonium bromide

micelles is a one way process in which the cyanobiphenyloxy amphiphiles diffuse from their bilayers into the micelles.

The bilayers formed by the ammonium amphiphiles with one azobenzene unit are less rigid than those of amphiphiles with two cyanobiphenyloxy units as reflected by their lower T_c . They allow penetration of other cationic amphiphiles. Monomer transfer with didodecyldimethylammonium bromide vesicles is now a bidirectional process. The solubilization of these bilayers by hexadecyltrimethylammonium bromide micelles is also accompanied by penetration of the surfactants into the bilayer. This however occurs only when the concentration of hexadecyltrimethylammonium bromide in the aqueous phase is above its critical aggregation concentration.

7.4 Experimental section

The synthesis and the characterization of the chromophore containing surfactants has been described before^{16,18} in chapter 4 and 5. The dialkyldimethylammonium bromides were obtained from Kodak and were used without further purification. Vesicle dispersions were obtained by sonication of the solid compounds in ultrapure water (1 wt %) until clear solutions were obtained using a Vibracell sonifier from Sonics and Materials Inc. The water was purified by a Seralpur Pro 90C purification system. The monomer transfer rate measurements were performed on a Varian Cary 13E spectrophotometer with thermostatted sample holders using cuvettes with an optical length of 1 cm. Both the sample and the reference cuvette were filled with a 3.5 mM dialkyldimethylammonium bromide vesicle dispersion. A small amount of a concentrated vesicle dispersion of amphiphiles containing aromatic units was injected into the sample cuvette to give a solution of 0.05 mM with a maximum $\pi-\pi^*$ absorbance of approximately 0.5. The cuvette was shaken manually and placed immediately in the spectrophotometer. For the cyanobiphenyloxy containing vesicles the absorbance was measured at 300 nm, for the azobenzene containing vesicles at 380 nm. The dialkyldimethylammonium bromide vesicles are present in a large excess to allow a sufficiently strong dilution of the amphiphiles carrying the aromatic units to prevent stacking of the aromatic units in the mixed bilayers. For the solubilization experiments the sample and the reference cuvette were filled with a surfactant solution of known concentration and a small amount of a concentrated vesicle dispersion of amphiphiles containing aromatic units was injected into the sample cuvette to give a solution of 0.05 mM with a maximum $\pi-\pi^*$ absorbance of approximately 0.5. Differential scanning calorimetry was carried out with mixtures of vesicle dispersions (2 % w/w) in water using a Perkin Elmer DSC 7 apparatus. The vesicle dispersions were mixed and incubated at room temperature in a series of sealed 50 μ L aluminum pans. Thermograms were recorded after every fixed time interval using a new pan. The demicellization enthalpograms were recorded using a Microcal Omega titration microcalorimeter (Microcal, Northampton, MA, USA). Ultrapure water was used and all solutions were degassed before use. The syringe contained a 10 mM $C_{16}N^+$ solution. The sample cell was filled with either ultrapure water or a vesicle dispersion. The time between the injections was 200 seconds.

7.5 References

- 1 De Cuyper, M.; Joniau, M.; Engberts, J. B. F. N.; Sudhölter, E.J.R. *Colloids Surf.* **1984**, *10*, 313.
- 2 De Cuyper, M.; Joniau, M.; Dangreau, H. *Biochemistry* **1983**, *22*, 415.
- 3 Nichols, J. W.; Pagano, R. F. *Biochemistry* **1982**, *21*, 1720.
- 4 Nichols, J. W.; Pagano, R. F. *Biochemistry* **1981**, *20*, 2783.
- 5 Nishimi, T.; Ishikawa, Y.; Ando, R.; Kunitake, T. *Recl. Trav. Chim. Pays Bas* **1994**, *113*, 201.
- 6 Okahata, Y.; Kunitake, T. *Ber. Bunsenges. Phys. Chem.* **1980**, *84*, 550.
- 7 Shimomura Y.; Kunitake, T. *J. Am. Chem. Soc.* **1982**, *104*, 1757.
- 8 Shimomura, Y.; Ando, R.; Kunitake, T. *Ber. Bunsenges. Phys. Chem.* **1983**, *87*, 1134.
- 9 Nishimi, T.; Ishikawa, Y.; Kunitake, T.; Sekita, M.; Xu, G.; Okuyama, K. *Chem. Lett.* **1993**, 295.
- 10 Kunitake, T. *Angew. Chem.* **1981**, *104*, 692.
- 11 Kimizuka, N.; Kunitake, T. *Chem. Lett.* **1988**, 827.
- 12 Shimomura, Y.; Kunitake, T. *Chem. Lett.* **1981**, 1001.
- 13 Rupert, L. A. M.; Hoekstra, D.; Engberts, J. B. F. N. *J. Am. Chem. Soc.* **1985**, *107*, 2628.
- 14 Rupert, L. A. M.; Hoekstra, D.; Engberts, J. B. F. N. *J. Am. Chem. Soc.* **1986**, *108*, 3920.
- 15 Song, X.; Geiger, C.; Furman, I.; Whitten, D. G., *J. Am. Chem. Soc.* **1994**, *116*, 4103.
- 16 Everaars, M. D.; Marcelis, A. T. M.; Sudhölter, E. J. R. *Langmuir* **1993**, *9*, 1986.
- 17 Everaars, M. D.; Marcelis, A. T. M.; Sudhölter, E. J. R. *Thin Solid Films* **1994**, *242*, 78.
- 18 Everaars, M. D.; Marcelis, A. T. M.; Kuipers, A. J.; Laverdure, E.; Koronova, J.; Koudijs, A.; Sudhölter, E. J. R. *Langmuir* **1995**, *11*, 3705.
- 19 Everaars, M. D.; Marcelis, A. T. M.; Sudhölter, E. J. R. *Colloids Surf.* **1995**, *102*, 117.
- 20 Menger, F. M.; Gabrielson, K. *J. Am. Chem. Soc.* **1994**, *116*, 1567.
- 21 Zugenmaier, P.; Heiske, A. *Liq. Cryst.* **1993**, *13*, 835.
- 22 Vertogen, G.; de Jeu, W. H. *Thermotropic Liquid Crystals, Fundamentals*; F. P. Springer Verlag: Berlin, 1988; p. 36.
- 23 McRae, E. G.; Kasha, M. *Physical Processes in Radiation Biology*; Academic Press: New York, 1964, p. 23.
- 24 Okahata, Y.; Ando, R.; Kunitake, T. *Ber. Bunsenges. Phys. Chem.* **1981**, *85*, 789.
- 25 Menger, F. M.; Gabrielson, K. D. *Angew. Chem.* **1995**, *107*, 2260.
- 26 Lianos, P.; Zana, R. *J. Coll. Int. Sci.* **1981**, *84*, 100.
- 27 Lichtenberg, D. *Biochim. Biophys. Acta* **1985**, *821*, 470.
- 28 Urbaneja, M. A.; Alonso, A.; Gonzales-Mañas, J. M.; Gofí, F. M.; Partearroyo, M. A.; Tribout, M.; Paredes, S. *Biochem. J.* **1990**, *270*, 305.
- 29 De la Maza, A.; Parra, J. L.; *Coll. Surf. A; Physiochem. Eng. Asp.* **1993**, *70*, 189.
- 30 Lichtenberg, D.; Robson, R. J.; Dennis, E. A. *Biochim. Biophys. Acta* **1983**, *737*, 285.

!

Chapter 8

*Effects of mesogen orientation
on self-organization*

Abstract

A series of novel double chained ammonium amphotropes have been synthesized which differ in the orientation of the dipoles of their mesogenic units along the molecular long axis. The mesogenic units consist of an azobenzene core which has an electron donating oxy unit at the 4 position and an electron withdrawing carboxy unit at the 4' position. This mesogenic unit has an intrinsically high dipole moment. The effects of the orientation of the dipoles of the mesogens on the thermotropic and lyotropic aggregation behavior of these compounds have been investigated. The thermotropic properties can be rationalized by assuming that the antiparallel orientation of the mesogenic units is the most favorable one. Compound 1, which has both dipoles pointing away from the headgroup, gives fully extended bilayers with parallel mesogens upon sonication in water. Compound 2, with alternating dipoles and 3, which has both dipoles pointing toward the headgroup, give interdigitated bilayers. These compounds also form monolayers at the water-air interface. Compounds 1 and 2 initially lie flat at the water-air interface whereas the mesogens of compound 3 have no interaction with the water surface.

The contribution of the dipolar mesogens to the monolayer electrical surface potential is small. The orientation of the dipole moments of the mesogenic units has only a minor effect on the lyotropic aggregation behavior of these compounds.

8.1 Introduction

In the last decade the interest in amphotropic compounds has increased enormously. This relatively new class of compounds owes its name to its potential to form both thermotropic and lyotropic liquid crystalline phases. Structurally these compounds are characterized by the presence of a polar or ionic headgroup, hydrophobic tails and mesogenic units.¹ Of special interest are amphotropes containing mesogens based on azobenzene. Azobenzenes can undergo reversible trans-cis isomerization upon irradiation with UV/VIS light. This makes it possible to alter the physical properties of these materials by simple irradiation with UV/VIS light. These compounds can be applied in electro-optical devices, in data storage devices and in molecular switches.

It is assumed that the dipole moment of the mesogenic unit is important in determining its aggregational behavior. It has been suggested that mesogens with a high dipole moment prefer to arrange themselves in an antiparallel fashion which results in the most favorable dipolar interactions.²⁻⁴ This results in the formation of interdigitated smectic phases. Mesogens with weaker dipoles would favor the formation of nematic phases.

In this chapter the synthesis of a series of three novel double chained amphotropes is described. These compounds are structural isomers which only differ in the orientation of their mesogenic units with respect to the molecular long axis. The mesogenic units are azobenzenes which contain an electron donating oxy substituent and an electron withdrawing carboxy group. This mesogen therefore has a net dipole moment. Of the three compounds one has both dipoles directed toward the tails (1), the second has one dipole pointing toward the tail and one pointing toward the headgroup (2) and the third has both dipoles pointing toward the headgroup (3).

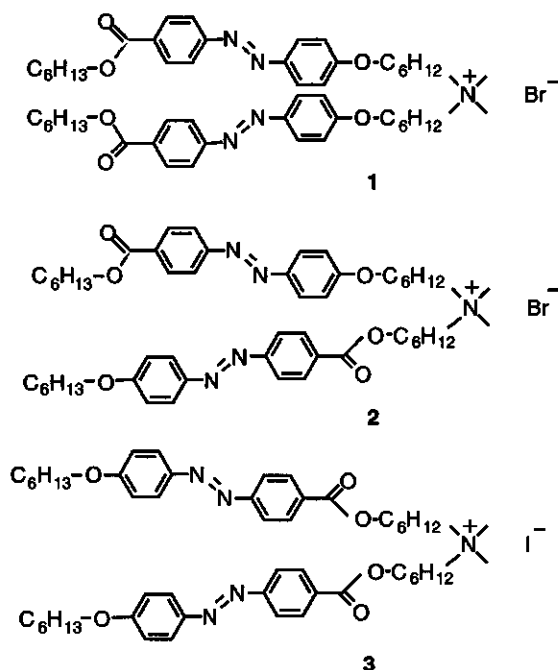
The thermotropic properties have been investigated using polarization microscopy and differential scanning calorimetry. The monolayer and bilayer properties of these compounds have been studied using UV spectroscopy, X-ray reflectivity, the Langmuir technique and surface potential measurements. The results are discussed in terms of the structural differences between the investigated compounds.

8.2 Results and discussion

8.2.1 Thermotropic properties

The purity of the compounds 1, 2 and 3 was checked by TLC, 200 MHz ¹H-NMR and elemental analyses. Compounds 1 and 2 have a bromide counter ion, whereas compound 3 has a iodide counterion. This occurred during the reaction of 13 with 14 where KI is added to enhance the reaction rate (see Scheme 1, Experimental section) Therefore, only the thermal

properties of **1** and **2** can be compared in terms of their molecular structures whereas the properties of **3** may be influenced by the different counter ion.



All the compounds **1**, **2** and **3** exhibit an enantiotropic smectic A phase. This is concluded from polarization microscopy because bâtonettes appear upon cooling the compound from the isotropic phase. The smectic phase readily adopts a homeotropic alignment which is seen as dark regions between crossed polarizers. The differential scanning calorimetry thermograms of **1** and **2** are given in Figure 1. It is seen that **2** has a melting point and isotropization temperature which are 20 and 30 °C higher respectively than those of compound **1**. Compound **3** has an intermediate isotropization temperature (**1**: C 132 S_A 173 I; **2**: C 150 S_A 204 I; **3**: C 166 S_A 180 I). This observation fits the picture that an antiparallel arrangement of the dipolar mesogens is the most favorable and stabilizes the liquid crystalline phase. However, it cannot be denied that steric factors which determine the molecular packing also play an important role in determining the thermal properties, especially of the crystalline phase.

8.2.2 Lyotropic properties

The compounds **1**, **2** and **3** form bilayer vesicles upon sonication in water. These vesicles can be visualized by electron microscopy (not shown). The bilayer thicknesses have been

determined with X-ray reflectivity⁵⁻¹⁵ of cast bilayer films (see Figure 2). For compound 1 a bilayer thickness of 51.5 Å is found whereas those for 2 and 3 are 36.8 and 34.2 Å respectively.

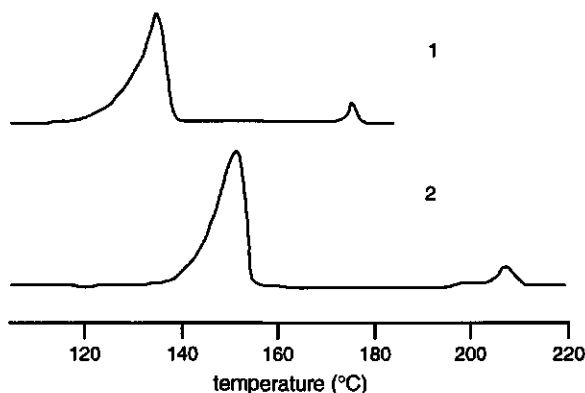


Figure 1. DSC thermograms of compounds 1 and 2. First heating curves are displayed.

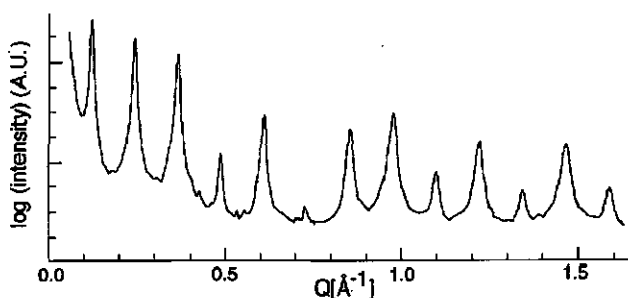


Figure 2. Small angle X-ray reflectivity data for cast bilayer films of compound 1. $Q_n = 2\pi n/d$, with d = bilayer spacing and n the order of the peaks.

The length of the molecules as determined from space filling models is 29 Å. UV absorption measurements indicate the presence of H-aggregates of the azobenzene units which means that the molecules are oriented perpendicular to the bilayer and are not tilted. This means that compound 1 forms an almost fully extended bilayer and that the bilayers of 2 and 3 are almost fully interdigitated. This is also confirmed by the electron density profiles (not shown). Schematic representations of the bilayers based on the X-ray data are given in Figure 3. These bilayer configurations cannot easily be rationalized. Intuitively, one would expect that compound 1 could also form interdigitated bilayers because that would result in more favorable intermolecular dipole compensation. The fact that no interdigitation is observed implies that a better packing is obtained in the extended bilayer configuration, despite the less

favorable mesogen-mesogen interactions. Compound 2 is not expected to have better mesogen-mesogen interactions upon interdigitation so that here probably also other forces drive the interdigitation.

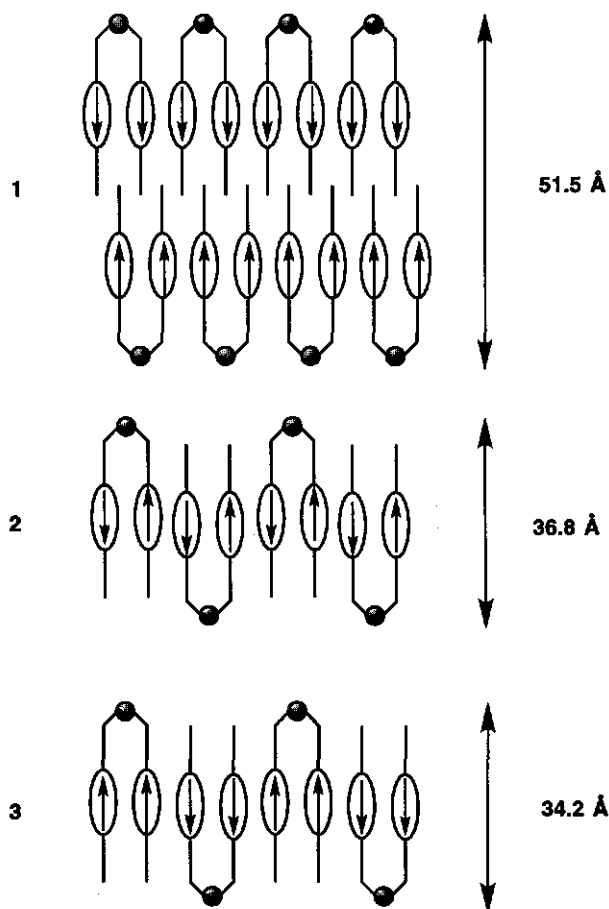


Figure 3. Schematic representation of the possible bilayer structures of compounds 1, 2 and 3.

The stacking of the mesogens in the bilayer results in a shift of the π - π^* transition in the UV absorption maximum to lower wavelengths. This blue shift is typical of (anti)parallelly aggregated chromophores ($\alpha = 90^\circ$), so-called H-aggregates. The spectral shift (in wavenumber $\Delta\nu$) is given by:

$$\Delta\nu = \frac{2}{hc} \frac{N-1}{N} \frac{\mu^2}{r^3} (1 - 3 \cos^2 \alpha)$$

in which μ is the transition dipole moment of the chromophores and r is the center to center distance between the mesogens. The angle α is the angle between the long axes of the chromophores and the line between the chromophore centers. N is the number of interacting chromophores in the bilayer, h is Planck's constant and c the speed of light.

It is seen from this formula that the extent of the blue shift is very dependent on the relative distance between the chromophores and the angle between the line connecting two chromophore centers and the long axes of the chromophores. The aggregation numbers, N , are expected to be large for all the compounds **1**, **2** and **3** and therefore to have no effect on the observed blue shift. Also the front to front distance between the azobenzenes is assumed to be approximately equal for these different bilayers. This means that probably the angle α , *i.e.* the relative position of two adjacent mesogens along the normal to the bilayer is important in determining the blue shift. In other words, one could say that the depth of the interdigitation is important.

For the bilayers of **1**, **2** and **3** the UV absorption maxima of 314, 330 and 317 nm are found (see Figure 4) whereas the monomer absorption lies at 374 nm. The strongest blue shift is found for bilayers of **1**. This can be explained because the mesogens are all perfectly parallelly stacked in the extended bilayers. For the interdigitated bilayers of **2** and **3** smaller blue shifts are found. This can be explained by assuming that the mesogens from adjacent molecules are not perfectly (anti)parallelly stacked. This would be caused by an insufficiently deep interdigitation of the molecules from both leaflets of the bilayer. The smaller blue shift for the bilayers of **2** as compared to those of **3** is in agreement with the observed larger bilayer thickness of **2**.

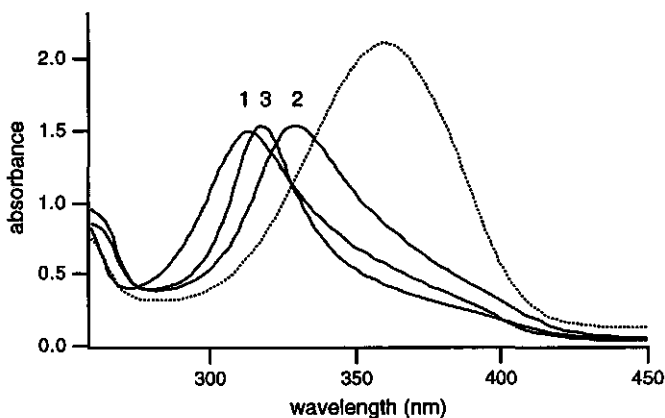


Figure 4. UV absorption spectra of the compounds **1**, **2** and **3** as vesicles in water (solid lines) and as monomers in ethanol (dashed line).

8.2.3 Monolayer behavior

The compounds **1**, **2** and **3** all form monolayers at the water-air interface. The π -A isotherms are given in Figure 5. The isotherm of **1** shows an initial rise in surface pressure at ca. 160 Å²/molecule. At this point the molecules start to interact. This area corresponds to a situation in which the molecules lie flat with their tails at the water-air interface. This is favored by the interaction of the carbonyl groups in the distal parts of the tails with the aqueous subphase. Upon compression the surface pressure rises until a plateau value is reached at 13 mN/m. At this pressure the interactions between the tails and the subphase are broken and the tails are forced away from the subphase. The monolayer can be compressed without further increase in surface pressure until the molecules are all in a close packed arrangement with their tails standing upright (at 70 Å²/molecule). Further compression results in a steep increase in surface pressure. The condensed monolayer goes through a series of phase transitions and finally collapses at 70 mN/m.

When the UV absorption spectra of this monolayer are recorded, the absorption maximum is seen to shift from 374 nm to 341 nm over the course of the plateau and shifts further to 312 nm in the steep part of the isotherm. This is due to the stacking of mesogens when the tails are forced onto each other. Interestingly, the absorbance is not seen to increase during the compression although the concentration of molecules in the monolayer increases. This is also attributed to the uplifting of the tails. The light of the spectrophotometer beam falls perpendicularly through the monolayer. The electrical vector of the light thus lies parallel to the water surface. When the mesogens are lifted up, this brings their transition moments from the plane of the water surface to a position perpendicular to the surface which reduces the light absorbance.

The isotherm of **3** lacks the plateau. This means that the tails initially do not lie completely flat on the surface. This is because the carbonyl groups lie in the proximal part of the tail, near the headgroup. Probably, a critical distance between the headgroup and carbonyl group is required in order to obtain a flat orientation of the tails.

In the isotherm of compound **2** a plateau is observed from 150 Å²/molecule at a surface pressure of 3 mN/m. This means that the interaction of the tails with the subphase is weaker for this compound than for compound **1**. This is due to the presence of one proximal and one distal carbonyl group. Interestingly, the observed isotherm is not an average of the isotherms of **1** and **3** indicating that initially not one tail stands upward and the other lies flat at the interface. Probably, both tails interact with one another and are simultaneously repelled from the interface. *In situ* UV absorption measurements of the monolayer of **2** again show a blue shift of the absorption maximum upon compression. The direction of the dipoles of the mesogens does not seem to affect the collapse pressures much. This collapse pressure can be regarded as a measure for the monolayer stability.

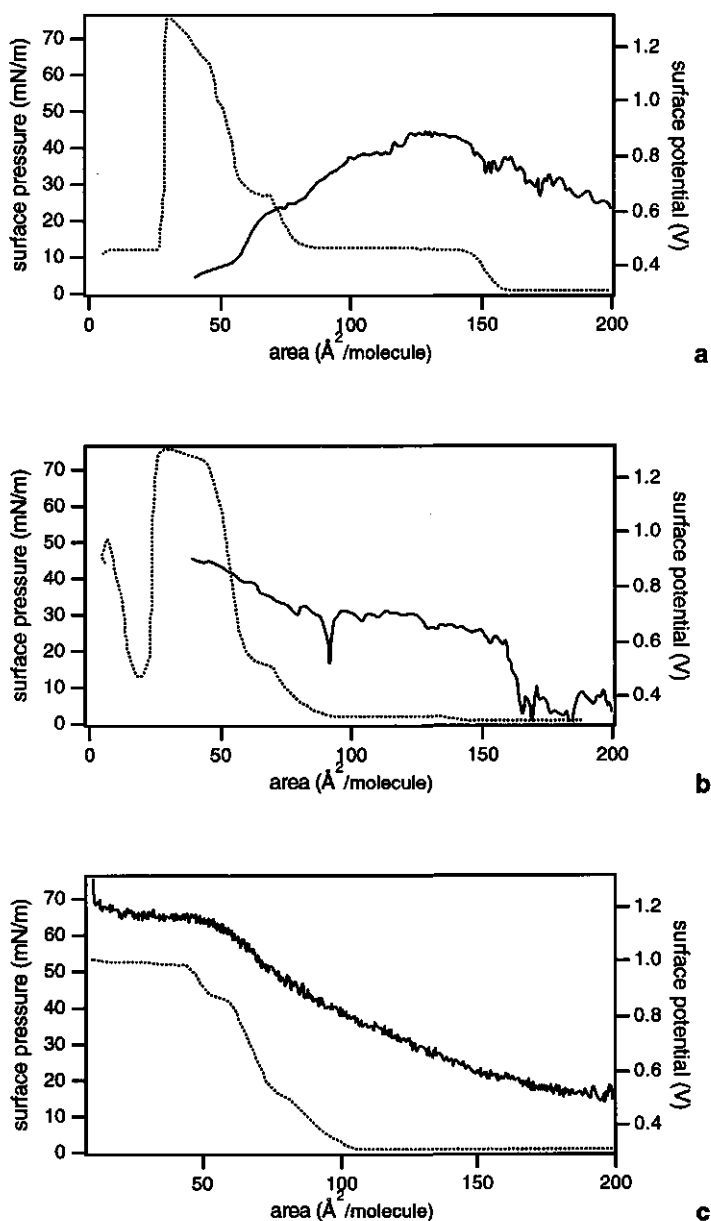


Figure 5. Surface pressure-area isotherms (\cdots) and surface potential-area (—) isotherms of compounds 1 (a), 2 (b) and 3 (c).

In order to test if the direction of the dipoles of the mesogenic units contributes significantly to the overall electrical surface potential of the monolayer, the surface potential-area isotherms were measured simultaneously with the recording of the π -A isotherms. The surface potential-area isotherms are also given in Figure 5.

The surface potential-area isotherm¹⁶⁻²⁵ of **1** shows an increase before the onset of the π -A isotherm and reaches a maximum at the onset of the plateau. Upon reduction of the molecular area in the plateau region the surface potential drops. The uplifting of the mesogens in the plateau region is expected to have a negative contribution to the surface potential (δ^+ at the water side and δ^- at the air side). However, the carbonyl group of the ester functionality also has a large ground state dipole moment which contributes negatively to the surface potential when the oxygen is directed toward the air. Studies on similar compounds carrying other dipolar mesogenic units *e.g.* the cyanobiphenyloxy unit which lacks the carbonyl group do not show a decrease in surface potential in the plateau region (data not shown). The decrease in surface potential in the plateau region might thus be ascribed to the contributions of the carbonyl group caused by the uplifting of the tails rather than to contributions of the entire mesogenic unit.²⁶

The surface potential-area isotherm of **2** shows a steep increase at the onset of the isotherm. In the plateau region the surface potential remains practically constant. This can be due to compensation of the contributions of both carbonyl groups *i.e.* one points with the oxygen upwards and one points downward.

In the isotherm of **3** there is no plateau and the alkyl chains are pointing toward the air over the whole area range of the isotherm. This results in a gradual increase in surface potential upon reduction of the available area per molecule. The carbonyl groups contribute positively to the surface potential which could explain why a higher surface potential is reached than for the monolayers of **1** or **2**.

In general, the contribution of the dipole of the mesogens in the monolayer to the measured surface potential seems small when compared to the contribution of the carbonyl group. This would mean that in the ground state no charge separated state is present in these donor- π -acceptor mesogens.

When the compressed monolayers (at 15 mN/m) of **1**, **2** and **3** are irradiated with UV light of 366 nm a steep increase in surface pressure is observed (see Figure 6). This is caused by the trans-cis isomerization of the azobenzenes in the monolayer. The bent cis molecules occupy a larger area than the linear trans molecules which causes the increase in surface pressure. After irradiation the cis molecules isomerize back to the trans form. The rate of this back isomerization process is very dependent on the amount of visible light to which the monolayer is exposed. The purely thermal cis to trans isomerization is very slow at room temperature in the compressed monolayer. This process can be repeated many times.

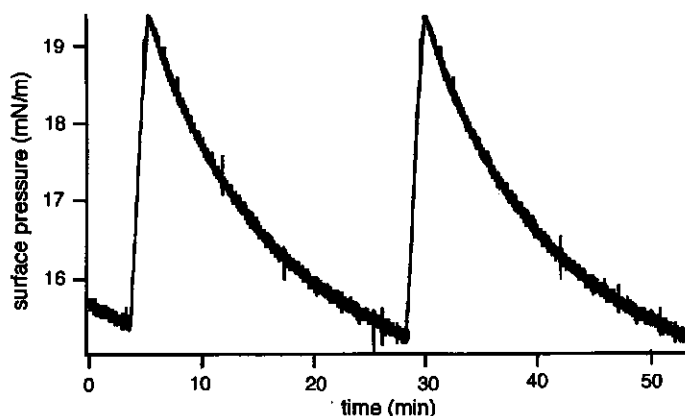


Figure 6. Increase in the surface pressure upon irradiation of a condensed monolayer of **1** with UV light of 366 nm and the decrease of the surface pressure under ambient light conditions.

Upon irradiation of the monolayer of **1** at 15 mN/m, the surface potential increases with 0.05 Volt. The isomerization changes the orientation of the carbonyl groups and therefore affects the surface potential. The carbonyls which initially point with their oxygen upward will be pointing more downward after isomerization and thus increase the surface potential. Also other parts of the molecule might contribute to the change in surface potential but the carbonyl group is expected to have by far the largest contribution.²⁶

When a condensed monolayer of **3** is irradiated with UV light, the surface potential remains constant despite the changes in surface pressure. The carbonyl groups, which are at the proximal part of the tail are not expected to reorient much upon isomerization. From the fact that no contributions from other parts of the molecules to the surface potential are measured it is concluded that only a small percentage of all molecules in the monolayer is isomerized under the employed conditions.²⁷ Probably, the isomerization is sterically hampered in this condensed monolayer.

When the surface pressure is kept constant at 10 mN/m, the movable barrier of the Langmuir trough starts to move upon irradiation of the monolayer with UV light due to expansion of the monolayer. This is a typical example of a light sensitive mechanical device.

8.3 Conclusions

This chapter describes the synthesis of a series of novel double chained amphotropic compounds which differ in the orientation of their dipolar mesogenic units. These compounds all exhibit an enantiotropic smectic A phase. The thermotropic phase behavior can be

understood with the rationalization that antiparallel mesogens have the strongest dipolar interactions and give the best stabilization of the liquid crystalline phase, although steric packing effects cannot be ignored.

The investigated amphotropic compounds form bilayer vesicles in water. Compounds **2** and **3** form interdigitated bilayers and **1** forms fully extended bilayers. Mesogen-mesogen interactions are clearly observed for all compounds by the blue shift of the UV absorption maximum. The bilayers of **1** do not have the most favorable mesogen-mesogen dipolar interactions.

The compounds **1**, **2** and **3** also form monolayers at the water-air interface of approximately equal stability. The mesogens of **1** and **2** initially have contact with the water surface whereas molecules of **3** have not. This behavior is attributed to the presence of a polar carbonyl group in the distal part of the tails of the former two compounds. The net dipole of the mesogens does hardly contribute to the monolayer surface potential. Instead a clear contribution of the carbonyl groups is found.

It can thus be concluded that in lyotropic liquid crystalline phases the orientation of the net dipole moment of the mesogens plays only a minor role in determining the aggregation behavior. Instead other Van der Waals interactions and packing constraints seem to be more important.

8.4 Experimental section

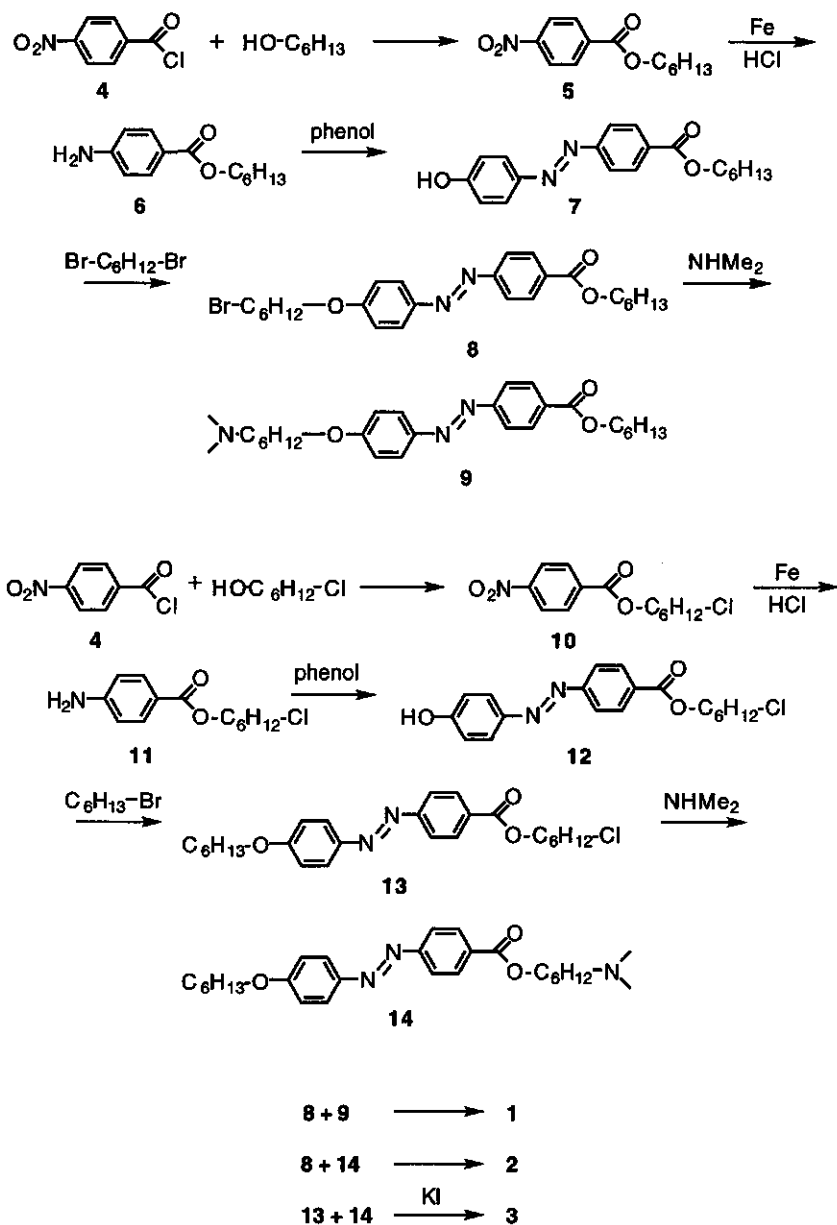
8.4.1 Synthesis

Hexyl-4-nitrobenzoate (**5**) and 6-chlorohexyl-4-nitrobenzoate (**10**)

To a stirred solution of 30 g (16 mmol) of 4-nitrobenzoylchloride (**4**) and 18 g (18 mmol) of hexanol in 200 mL of benzene was added dropwise 20 mL (0.25 mol) of pyridine at room temperature. The reaction occurs instantaneously. The reaction mixture was extracted twice with a 1 N HCl solution and with a 1 N NaHCO₃ solution. The benzene layer was dried on MgSO₄ and the solvent was removed under reduced pressure. Yield 94%. **10** was prepared in a similar manner using 24 g (18 mmol) of 6-chlorohexanol.

Hexyl-4-aminobenzoate (**6**) and 6-chlorohexyl-4-aminobenzoate (**11**)

To a rigorously stirred mixture of 40 g (170 mmol) of hexyl-4-nitrobenzoate (**5**), 250 g of iron powder and 100 mL of water was added 1.5 mL of a concentrated HCl solution. A strong evolution of heat occurred and the reaction mixture was cooled on an ice bath. When the heat evolution ceased, the reaction mixture was further heated for 1 h at 70-80 °C. The reaction mixture was extracted with dichloromethane. The organic layers were dried on MgSO₄ and the solvent was evaporated. The solid material was washed with petroleum ether (bp. 40/60 °C). Yield 90 %. Compound **11** was prepared in a similar manner using 6-chlorohexyl-4-nitrobenzoate (**10**).



Scheme 1. Synthetic pathways for the compounds 1, 2 and 3.

**Hexyl-4'-hydroxyazobenzene-4-carboxylate (7) and
6-chlorohexyl-4'-hydroxyazobenzene-4-carboxylate (12)**

An amount of 8 g (0.036 mol) hexyl-4-aminobenzoate (6) was dissolved in a hot mixture of 13 mL of a concentrated HCl solution and 13 mL of water in a 250 mL beaker. The stirred solution was cooled to 0-5 °C in an ice bath until the HCl salt of 6 precipitates. While stirring, a cold solution of 3.7 g (0.045 mol) of NaNO₂ in 8 mL of water was added dropwise. The temperature should not rise above 8 °C. This cold solution was added dropwise to an ice cold solution of 3.15 g (0.035 mol) of phenol and 7 g of NaOH in 25 mL of water. After the addition was complete concentrated HCl was slowly added until the solution was acidic. The precipitate was collected by filtration and washed with water and dried at the air. Yield 87 %. Compound 12 was prepared in a similar manner using (11).

**Hexyl-4'-(6-bromohexyloxy)azobenzene-4-carboxylate (8) and
6-chlorohexyl-4'-hexyloxyazobenzene-4-carboxylate (13)**

A mixture of 5 g (18 mmol) of 7, 8.8 g (36 mmol) of 1,6-dibromohexane and 4.9 g (36 mmol) of K₂CO₃ in 100 mL of 2-butanone was refluxed for 16 h. After cooling the salt was removed by filtration and the solvent was evaporated. The product was purified by column chromatography on silica gel using CH₂Cl₂/petroleum ether (bp. 40-60 °C) 1:1 v/v as eluent. The product was recrystallized from petroleum ether (bp. 40-60 °C). Yield 60%. Compound 13 was prepared in a similar manner using 12 and bromohexane.

(8) ¹H-NMR (CDCl₃, TMS, δ, ppm); 0.90 (t, 3 H, C₅H₁₀-CH₃), 1.20-2.0 (m, 16 H, -CH₂-(CH₂)₄-CH₂), 3.43 (t, 2 H, -CH₂-Br), 4.09 (t, 2 H, O-CH₂), 4.32 (t, 2 H, COO-CH₂), 6.90-8.20 (m, 8 H, Ar-H).

(13) ¹H-NMR (CDCl₃, TMS, δ, ppm); 0.90 (t, 3 H, C₅H₁₀-CH₃), 1.20-2.00 (m, 16 H, -CH₂-(CH₂)₄-CH₂), 3.55 (t, 2 H, -CH₂-Cl), 4.10 (t, 2 H, O-CH₂), 4.35 (t, 2 H, COO-CH₂), 6.90-8.20 (m, 8 H, Ar-H)

**N-[6-(4-Hexyloxycarboxyazobenzene-4'-oxy)hexyl]-N,N-dimethylamine (9) and
N-[6-hexyl(4'-hexyloxyazobenzene-4-carboxylate)]-N,N-dimethylamine (14)**

An amount of 1 g (2 mmol) of 8 was dissolved in 50 mL of a 20% (w/w) solution of dimethylamine in chloroform. This solution of was kept at room temperature for one night in a closed vessel. The solvent was removed under reduced pressure and the residue was dissolved in dichloromethane and extracted with water. The organic layers were dried on MgSO₄ and the solvent was evaporated. Yield 95 %. Compound 14 was prepared in a similar manner except that the solution of 13 was heated at 50 °C for several days in a closed vessel.

¹H NMR (CDCl₃, TMS, δ, ppm); 0.90 (t, 3 H, (CH₂)₅-CH₃), 1.20-2.0 (m, 16 H, -CH₂-(CH₂)₄-CH₂), 2.20 (m, 8H, -CH₂-N(CH₃)₂), 3.43(t, 2H, -CH₂-Br), 4.09 (t, 2H, O-CH₂), 4.32 (t, 2H, COO-CH₂), 6.90-8.20 (m, 8H, ArH)

**N,N-Di[6-(4-hexyloxycarboxyazobenzene-4'-oxy)hexyl]-N,N-dimethylammonium bromide (1) and
N-[6-(4-hexyloxycarboxyazobenzene-4'-oxy)hexyl]-N-[6-hexyl(4'-hexyloxyazobenzene-4-carboxylate)]-
N,N-dimethylammonium bromide (2) and**

N,N-Di[6-hexyl(4'-hexyloxyazobenzene-4-carboxylate)]-N,N-dimethylammonium iodide (3)

An amount of 0.5 g of both 8 and 9 was dissolved in 10 mL of 2-butanone and refluxed for 16 h.

After cooling, the solvent was evaporated and the residue was dissolved in a small amount of dichloromethane. The product (1) was obtained by precipitation using petroleum ether (bp. 40-60) and recrystallized from acetone. Yield 70 %. Compound 2 was prepared similarly from 8 and 14 and compound 3 from 13 and 14. In the latter case the solution was heated to 100°C in a closed reaction vessel for 48 h in the presence of an excess of KI.

¹H-NMR (CDCl₃, TMS, δ, ppm) 0.90 (t, 6H, (CH₂)₅-CH₃), 1.20-1.95 (m, 32H, -CH₂-(CH₂)₄-CH₂), 3.35 (s, 6H, N-CH₃), 3.60 (m, 4H, N-CH₂), 4.05 (t, 4H, O-CH₂), 4.32 (t, 4H, COO-CH₂), 6.90-8.20 (m, 16H, Ar-H).

- (1) Anal. Calcd for $C_{52}H_{72}O_6N_5Br(0.5 H_2O)$: C, 65.60; H, 7.73; N, 7.36. Found: C, 65.52; H, 7.76; N, 7.41.
 (2) Anal. Calcd for $C_{52}H_{72}O_6N_5Br(0.5 H_2O)$: C, 65.60; H, 7.73; N, 7.36. Found: C, 65.60; H, 7.79; N, 7.34.
 (3) Anal. Calcd for $C_{52}H_{72}O_6N_5I(0.5 H_2O)$: C, 61.41; H, 7.28; N, 6.89. Found: C, 61.15; H, 7.67; N, 6.52.

8.4.2 Methods

The thermotropic phase behavior has been investigated with a polarization microscope (Olympus BH-2) equipped with a hot stage (Mettler FP82HT) which was connected to a temperature controller (Mettler FP80HT). Differential scanning calorimetry was performed on a Perkin Elmer DSC 7.

Bilayer vesicles were prepared by sonication of the solid compounds in ultrapure water (1 wt %) until clear dispersions were obtained using a Vibracell sonifier from Sonics and Materials Inc. Bilayer thicknesses were determined by small angle X-ray reflectivity of films that were prepared by casting vesicle dispersions onto silicon wafers.

The monolayers at the water-air interface were spread from chloroform solutions (1 mg/ml) using a Hamilton syringe. The π -A isotherms were recorded on a Lauda FW2 Langmuir trough which was thermostatted at 20 °C. Compression speeds of 1000 cm²/h were used. The water used for the subphase was purified through a Seralpur Pro 90 purification system. The monolayers were irradiated with light of 366 nm using a Camag Universal UV-lampe 29230 which was positioned at 10 cm from the monolayer. The light has an intensity of approximately 0.5 mW/cm² at the monolayer. The UV absorption spectra at the water-air interface were recorded with a quartz fiber optic probe (Spectrofiip 8452, Photonetics) connected to a HP 8452 A diode array spectrophotometer.

The surface potential was recorded with a vibrating condenser voltmeter (model 320B EX from Trek Inc). The surface potential of an amphiphilic monolayer at the water-air interface can be described as a linear combination of three different terms.

$$\Delta V = \Delta V_O + \Delta V_p + \Psi_O$$

The term ΔV_O is the surface potential for a clean water-air surface and is usually -300 to -500 mV. This contribution is caused by the asymmetry of the water-air interface which leads to the orientation of the water molecules (with the oxygen pointing towards the air). The second term, ΔV_p , arises from the permanent dipole of the amphiphilic molecule. This may be further subdivided into contributions from different parts of the molecule. The third term Ψ_O , is called the double layer potential and is caused by the charges in the amphiphile headgroup. The vibrating condenser only measures the vertical components of these dipole moments. The dipolar term, ΔV_p , may be expressed as¹⁹:

$$\Delta V_p = \frac{\mu}{\epsilon_O \epsilon_A} = \left(\frac{\mu_H}{\epsilon_H} + \frac{\mu_W}{\epsilon_W} + \frac{\mu_T}{\epsilon_T} \right) / A \epsilon_O$$

where A is the mean area per surfactant molecule, μ_H is the dipole moment of the polar headgroup region, μ_W the contribution of the oriented water molecules which constitute the hydration shell of the amphiphile headgroups at the water-air interface and μ_T the dipole moment of the hydrophobic part (for aliphatic chains only the terminal -CH₃ group contributes to this term). ϵ_H , ϵ_T and ϵ_W are the local dielectric constants for the headgroup, tail and the interfacial water region respectively.

Our measurements were performed using ultrapure water as subphase. A reference electrode (copper wire) was inserted in the subphase and the vibrating plate was positioned 1-2 mm above the water surface and the surface potential was set to zero. Finally the monolayer was spread. The values of ΔV reported here are always with respect to the clean subphase interface.

Acknowledgements

We are indebted to dr. Blandine Jérôme from the FOM Institute in Amsterdam for performing the X-ray analyses. Thanks are also due to dr. Osvaldo Novais de Oliveira Junior from the Institute of Physics of São Carlos in São Paulo (Brasil) for his help with the interpretation of the surface potential measurements.

8.5 References

- 1 Ringsdorf, H.; Schlarb, B.; Venzmer, J. *Angew. Chem.* **1988**, *100*, 117.
- 2 Richard, H.; Mauzac, M.; Nguyen, H. T.; Sigaud, G.; Achard, M. F.; Harduin, F.; Gasparoux, H. *Mol. Cryst. Liq. Cryst.* **1988**, *155*, 141.
- 3 Schleck, T.; Imrie, C. T.; Rice, D. M.; Karasz, F. E.; Attard, G. S. *J. Polym. Sci. Part A: Polym. Chem.* **1993**, *31*, 1895.
- 4 Vertogen, G.; de Jeu, W. H. *Thermotropic Liquid Crystals, Fundamentals*: Springer-verlag; Berlin, 1988, p. 36.
- 5 Savronov, V. V.; Lvov, Y. M.; Budovska, L. D.; Ivanova, N. V. *Thin Solid Films* **1993**, *224*, 112.
- 6 Fenzl, W.; Sigl, L.; Richardsen, H.; Cevc, G. *Colloids Surf. A: Phys. Eng. Asp.* **1995**, *102*, 247.
- 7 Okuyama, K.; Watanabe, H.; Shimomura, M.; Hirabayashi, K.; Kunitake, T.; Kajiyama, T.; Yasuoka, N. *Bull. Chem. Soc. Jpn.* **1986**, *59*, 3351.
- 8 Sommerdijk, N. A. J. M.; Feiters, M. C.; Nolte, R. J. M.; Zwanenburg, B. *Recl. Trav. Chim. Pays Bas* **1994**, *113*, 194.
- 9 Sano, M.; Sasaki, D. Y.; Isayama, M.; Kunitake, T. *Langmuir* **1992**, *8*, 1893.
- 10 Tardieu, A.; Luzatti, V.; Reman, F. C. *J. Mol. Biol.* **1973**, *75*, 711.
- 11 McIntosh, T. J.; Simon, S. A.; Ellington, J. C.; Porter, N. A. *Biochemistry* **1984**, *23*, 4038.
- 12 Hui, S. W.; Mason, J. T.; Huang, C. *Biochemistry* **1984**, *23*, 5570.
- 13 Harlos, K.; Eibl, H. *Biochemistry* **1981**, *20*, 2888.
- 14 Nishimi, T.; Ishikawa, Y.; Ando, R.; Kunitake, T. *Recl. Trav. Chim. Pays Bas* **1994**, *113*, 201.
- 15 Shimomura, M.; Aiba, S.; Tajima, N.; Inoue, N.; Okuyama, K. *Langmuir* **1995**, *11*, 969.
- 16 Oldani, D.; Hauser, H.; Nichols, B. W.; Phillips, M. C. *Biochim. Biophys. Acta* **1975**, *382*, 1.
- 17 Demchak, R. J.; Fort Jr, T. J. *Colloid Interface Sci.* **1974**, *46*, 191.
- 18 Paltauf, F.; Hauser, H.; Phillips, M. C. *Biochim. Biophys. Acta* **1971**, *249*, 539.
- 19 Vogel, V.; Möbius, D. *J. Colloid Interface Sci.* **1988**, *126*, 408.
- 20 Taylor, D. M.; Oliveira Jr, O. N.; Morgan, H. *Chem. Phys. Lett.* **1989**, *161*, 147.
- 21 Nguyen, M. T.; Kanazawa, K.; Brock, P.; Diaz, A. F.; Yee, S. *Langmuir* **1994**, *10*, 579.
- 22 Takeo, M. *J. Colloid Interface Sci.* **1993**, *157*, 291.
- 23 Ahuja, R. C.; Caruso, P. L.; Möbius, D.; Wildburg, G.; Ringsdorf, H.; Philp, D.; Preece, J. A.; Stoddart, J. F. *Langmuir* **1993**, *9*, 1534.
- 24 Taylor, D. M.; Oliveira Jr, O. N.; Morgan, H. *J. Colloid Interface Sci.* **1990**, *139*, 508.
- 25 Kajikawa, K.; Yamaguchi, T.; Anzai, T.; Takezoe, H.; Fukuda, A.; Okada, S.; Matsuda, H.; Nakanashi, H.; Abe, T.; Ito, H. *Langmuir*, **1992**, *8*, 2764.
- 26 Prof. dr. N. O. Oliveira Jr, personal communication.
- 27 Maack, J.; Ahuja, R. C.; Möbius, D.; Tachibana, H.; Matsumoto, M. *Thin Solid Films* **1994**, *2442*, 122.

Chapter 9

9

*Surfactant-polyelectrolyte
complexes*

Abstract

The lyotropic and thermotropic phase behavior of some surfactant-polyelectrolyte complexes have been investigated.

It has been observed that upon heating the insoluble complex of didodecyldimethylammonium bromide (DDAB) and poly(acrylic acid) (PAA) in water, multivesicular superstructures are formed, which morphologically strongly resemble biological tissues. The mechanism of the formation of these multivesicular superstructures is somewhat different from the vesicle formation of pure crystalline surfactants.

The complexation of double chained ammonium amphotropes to poly(acrylic acid) results in the formation of ionically bound side chain liquid crystalline polymers. Analysis of the thermotropic phase behavior of these complexes shows broader liquid crystalline temperature ranges and higher isotropization temperatures than for the monomeric amphotropes.

9.1 Introduction

Biological tissues consist of lipid membrane cells which are inter- and intracellularly stabilized by biopolymers like proteins and polysaccharides.¹ The study of the interaction between water-soluble polymers and bilayer forming surfactants is therefore highly relevant to a better understanding of the organization of these complex structures.^{2,3} However, studies on the interactions between ionic surfactants and oppositely charged polyelectrolytes⁴⁻⁹ in aqueous solution are often hampered by the formation of precipitates.¹⁰⁻¹² Recently, the solid state structure and material properties of these complexes have become focus of interest. The lamellar bilayer structure is often preserved in the bulk and the polymer acts as an external stabilizer.¹³⁻¹⁸

This chapter presents an morphological study of the insoluble complex of didodecyldimethylammonium bromide (DDAB) and poly(acrylic acid) (PAA) in water using optical microscopy. In addition the thermotropic phase behavior of complexes of PAA with double chained ammonium amphotropes has been investigated using hot stage polarization microscopy and differential scanning calorimetry.

9.2 Results and discussion

9.2.1 Superstructures from didodecyldimethylammonium bromide and poly(acrylic acid)

A thin film of DDA-PAA complex was prepared by casting an ethanolic solution of DDAB and PAA (1:10 monomeric units) onto a microscope glass slide. After addition of water this initially clear film becomes turbid and swells but remains tightly adsorbed onto the microscope slide. Subsequent heating of the water-covered film for 1 min at 80 °C results in the spontaneous formation of immense numbers of vesicles. The vesicles are immobilized in the surrounding matrix of DDA-PAA hydrogel (Figure 1a,b). In some locations the vesicles are so closely packed that they form tissue-like superstructures (Figure 1c-f). The diameter of the vesicles varies from smaller than 1 μm to 30 μm .

Less developed superstructures can also be prepared by heating the water-covered precipitate obtained by mixing *aqueous* solutions of DDAB and PAA or by heating a cast DDAB film covered with an *aqueous* PAA solution. In the latter case sometimes spherical matrix particles including one or more vesicles detach from the surface and migrate freely through the solution (Figure 1g). The vesicles are then clearly observed in the interior of the matrix particle. Sometimes the enveloping matrix layer is very thin and the particles resemble normal giant bilayer vesicles.¹⁹⁻²¹

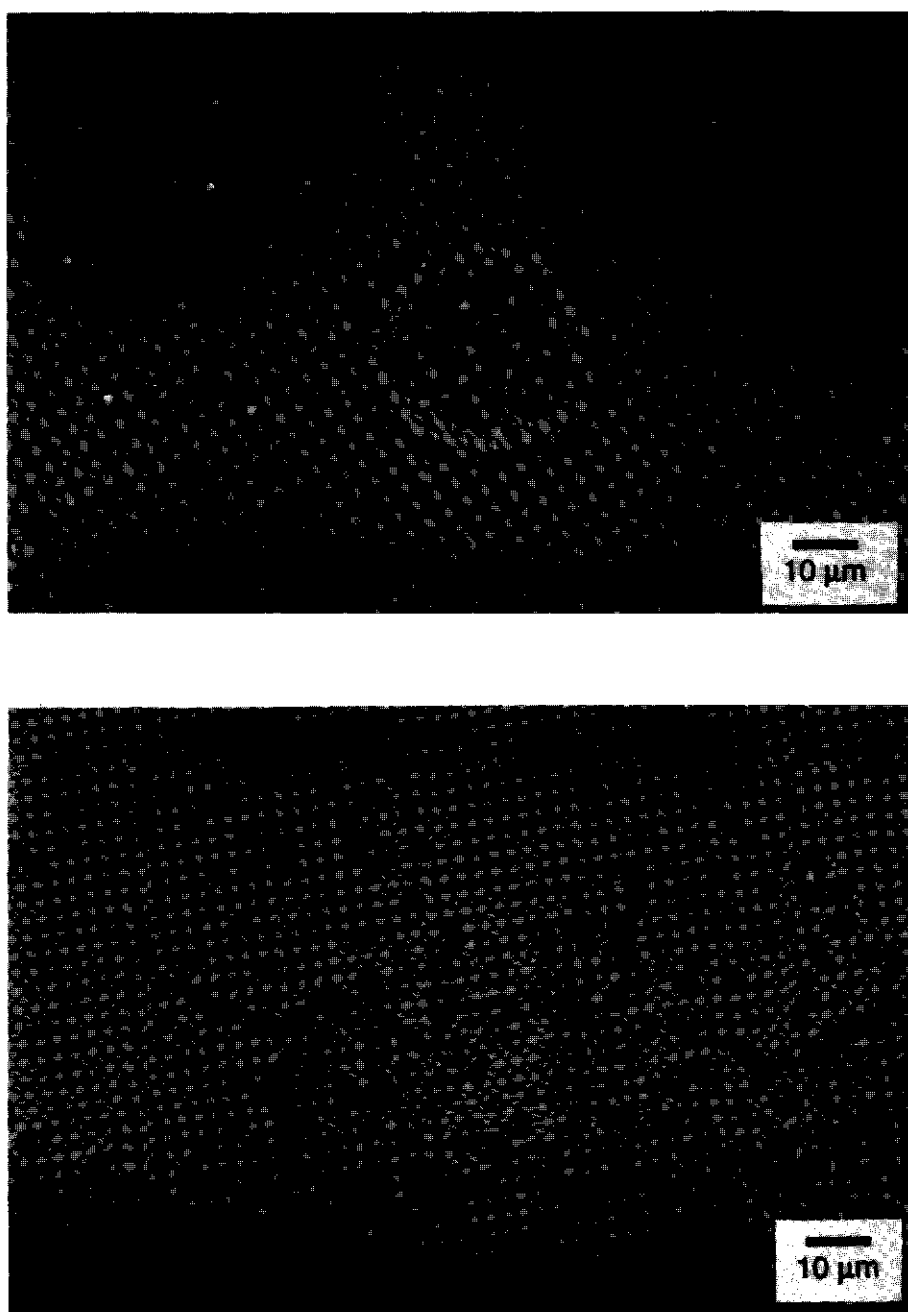
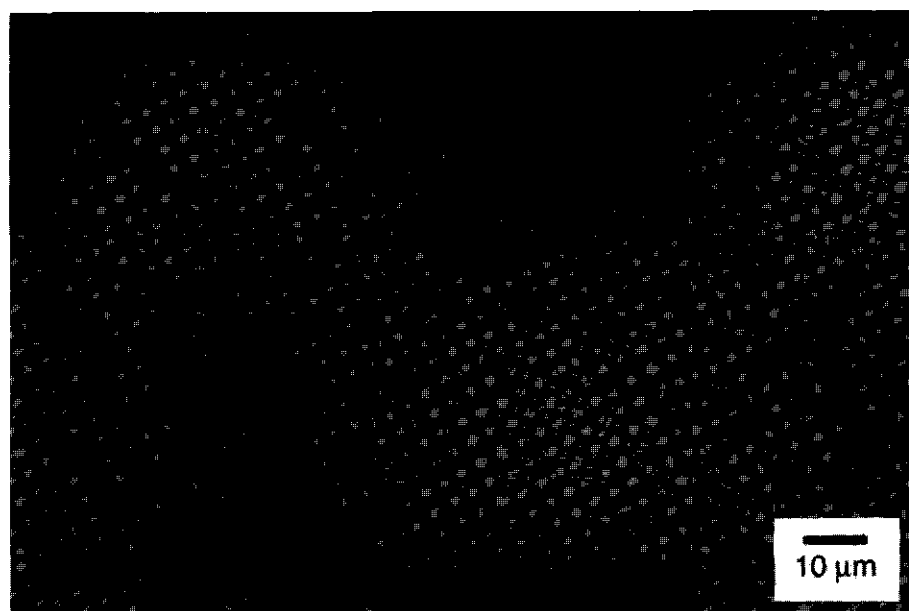
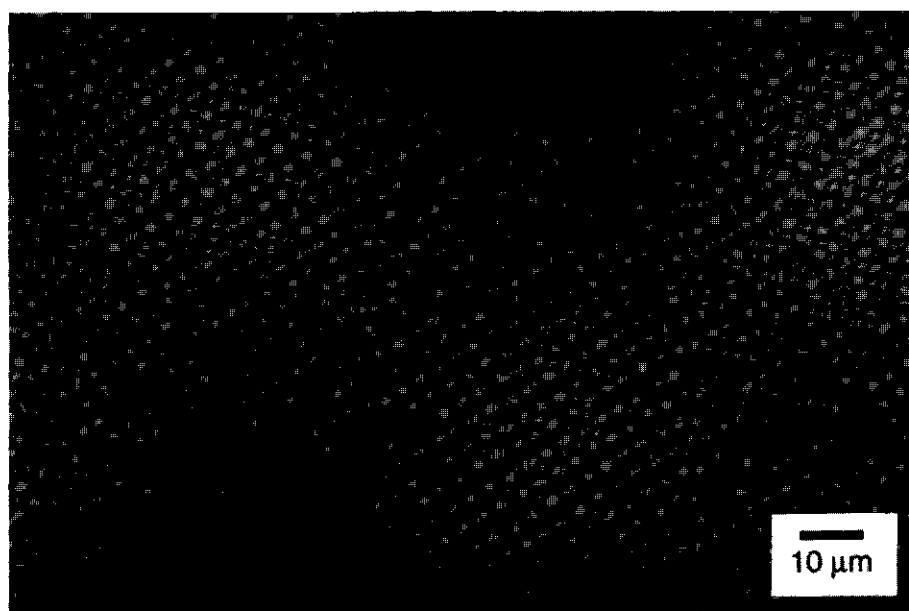
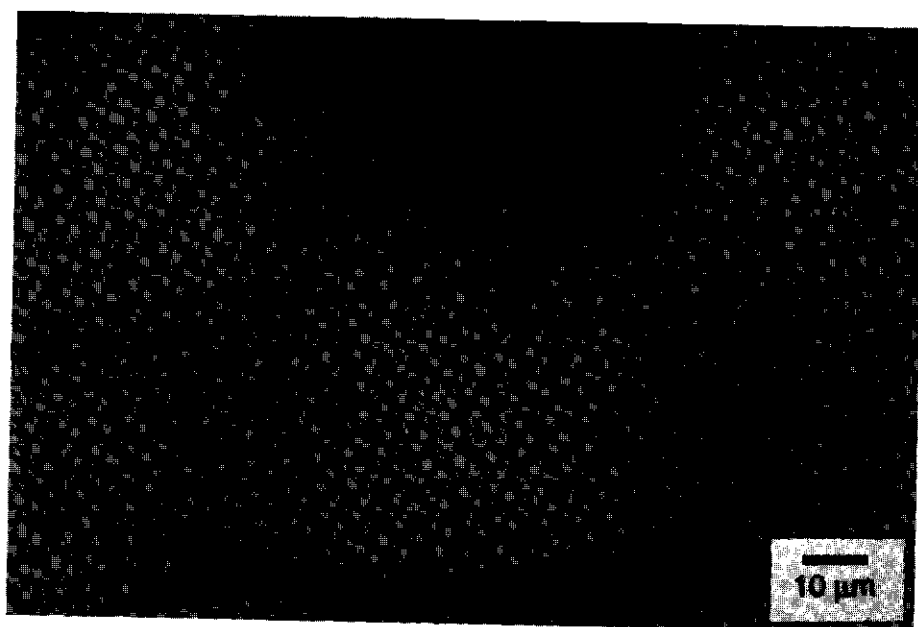
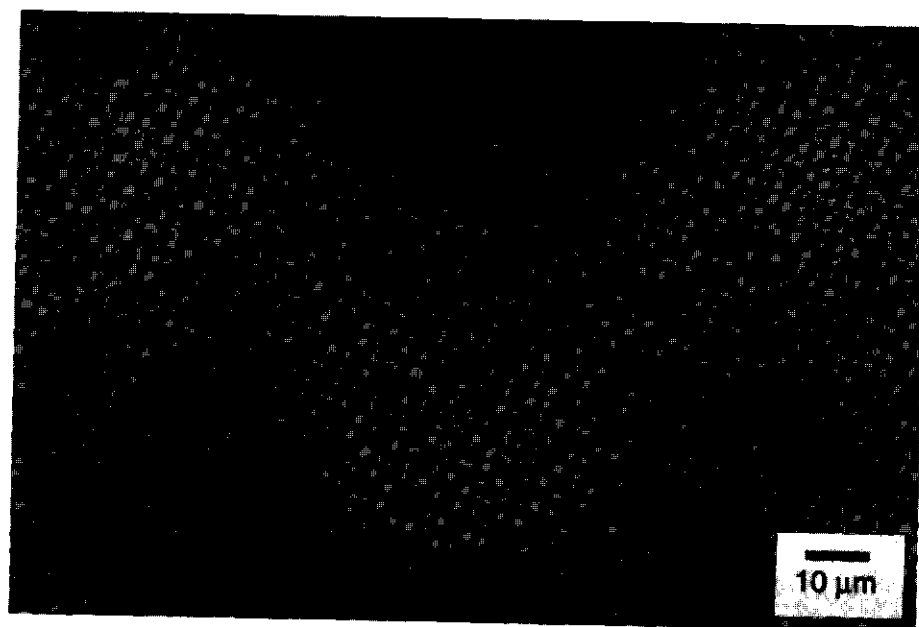


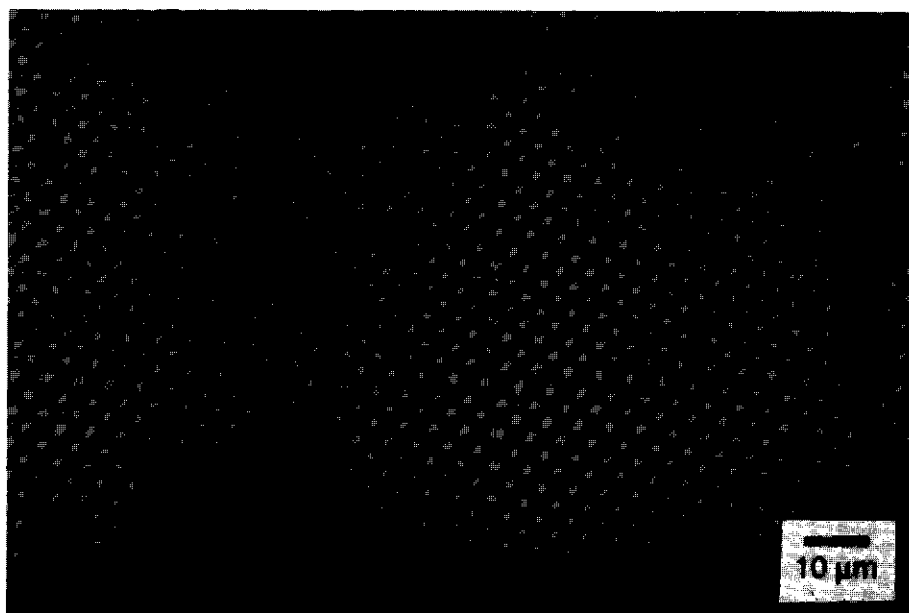
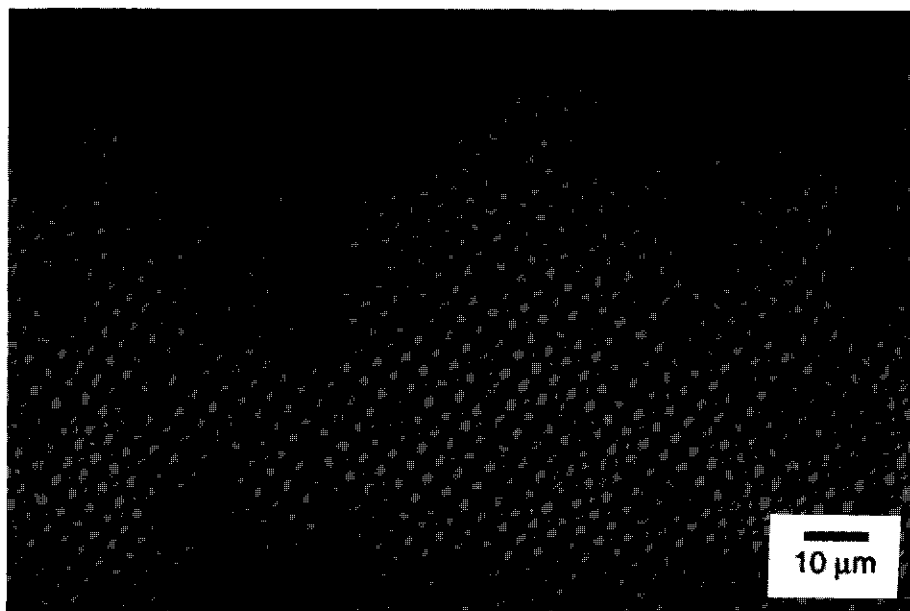
Figure 1. (a,b) Optical micrographs of vesicles embedded in a blob of DDA-PAA matrix adsorbed on a microscope slide.



(c,d) Optical micrographs of densely packed vesicles in the hydrated DDA-PAF film.



(e,f) Optical micrographs of densely packed vesicles in the hydrated DDA-PAA film.



(g) Optical micrograph showing DDA-PAA matrix particles containing one or more vesicles;

(h) Collapsed vesicles due to osmotic dehydration after the addition of a salt solution.

Proof for the presence of water containing vesicles was obtained from the following observations: (1) heating of the film in the absence of water does not result in the formation of superstructures; (2) upon evaporation of water the vesicle structures collapse; (3) Osmotic shrinkage and subsequent collapse of the larger vesicle structures are observed after addition of a hypertonic salt solution (see Figure 1h).^{22,23} The smaller vesicle structures only deteriorate under these conditions.

The formation of tissue-like superstructures is observed between pH 1 and 10 although the tissues become increasingly unstable at both extreme pH values. When stored in pure water these tissue-like structures are stable for at least several weeks. The stability of the superstructure is further enhanced by a strong adhesion of the matrix to the glass substrate.

Good quality tissue-like samples are obtained when PAA and DDAB are mixed in a ratio of approximately ten acrylate units to one DDAB molecule. Upon increasing the ratio of DDAB to PAA, the formation of myelin structures and free bilayer vesicles becomes predominant upon heating of the submersed cast film, as is also observed for pure DDAB.²² Under optimal conditions the binding sites of the polymer are only partially occupied by DDA cations. The DDA cations might thus be able to migrate along the polymer backbone, facilitating the reorganization of the material into multivesicular superstructures.

When other polyelectrolytes are used like polysulfonates,²⁴ alginic acid or hydrophobically modified poly(maleic acid),²⁵ no tissue-like structures are observed. Presumably the interaction between the surfactant and the polyelectrolyte must not be too strong in order to allow a reorganization of the material. Using dioctadecyldimethylammonium bromide instead of didodecyldimethylammonium bromide also does not result in the formation of tissue-like structures. Probably, the low monomer solubility of this compound with respect to DDAB hampers an easy reorganization of the complex. Using the single chained amphiphile hexadecyltrimethylammonium bromide however does also result in the formation of tissue like-structures. The formation of tissue-like structures therefore seems to be determined by a delicate balance of interactions.

Our observations suggest that vesicles in the DDA-PAA hydrogel are formed via a different mechanism than that observed for pure crystalline vesicle forming surfactants. In the latter case the hydrated surface of the crystalline surfactant forms myelin structures, from which the vesicles detach.²⁶⁻²⁸ In the DDA-PAA hydrogel the vesicles are formed in the hydrated bulk of the material. Upon heating, the already swollen material is probably further hydrated and the molecules are given the mobility to reorganize into the vesicular structures. The tissue-like superstructure is then stabilized by the presence of the negatively charged PAA which binds and interconnects the positively charged DDA bilayer vesicles. This concept is based on the fact that besides tissues, freely migrating vesicle structures are observed which look very similar to normal bilayer vesicles. Furthermore, the tissues show birefringence between crossed

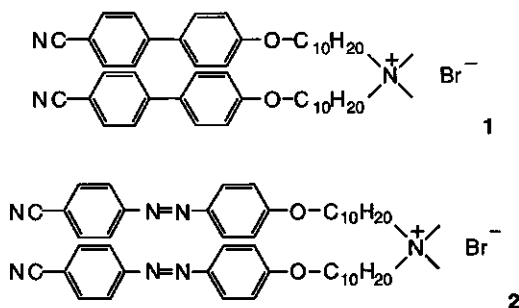
polarizers indicating the presence of ordered structures. The presence of bilayer structures in the tissues has however not been proven and no phase transition was observed by DSC.

9.2.2 Ionically bound side chain liquid crystalline polymers

Recently, the solid state structure and thermotropic properties of surfactant-polyelectrolyte complexes have become focus of interest.²⁹⁻³⁰ Electrostatic complexation of amphotropes to oppositely charged polyelectrolytes results in the formation of ionically bound side chain liquid crystalline polymers. It turns out that these complexes can easily be dissolved in organic solvents and cast to films of high homogeneity and mechanical stability.^{13,14} The smectic layer structure is usually preserved in the bulk and the polymer acts as an external stabilizer.²⁹⁻³⁰ Complexation with an oppositely charged polyelectrolyte usually results in a stabilization of the liquid crystalline phase with respect to that of the uncomplexed amphotrope.

The DSC thermogram of compound **1** is given in Figure 2. By hot stage polarization microscopy this compound is seen to melt at 112 °C and to form a monotropic nematic phase at 108 °C upon cooling. The DSC thermogram of the 1:2 complex with poly(acrylic acid) (1:PAA in monomeric units) shows that the melting peak has disappeared indicating that **1** is not present in a crystalline state. The material is however strongly birefringent which means that the complex is probably in a (undercooled) liquid crystalline state. The DSC thermogram further shows a reversible phase transition at about 160 °C. This is the isotropization temperature as was confirmed by polarization microscopy. The isotropization temperature of this complex thus lies considerably higher than for the pure compound **1**.

The DSC thermogram of compound **2** is given in Figure 3. This compound melts at about 140 °C and gives a smectic A phase and finally becomes isotropic at 175 °C. The higher isotropization temperature of this compound as compared to that of **1** is attributed to stronger stacking interactions between azobenzenes than between biphenyls which might be caused by the presence of the polarizable nitrogen atoms (see Chapter 2). In the 1:2 complex with poly(acrylic acid) the melting peak has disappeared and the isotropization temperature is seen to increase to 216 °C.



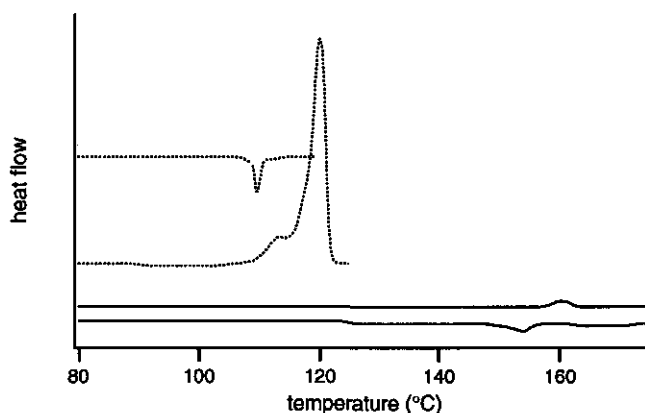


Figure 2. DSC thermograms of compound **1** as pure compound (dotted lines) and of the 1:2 (in monomeric units) mixture with poly(acrylic acid) (solid lines). Both the heating and the cooling traces are displayed. Positive peaks correspond to endothermic phase transitions.

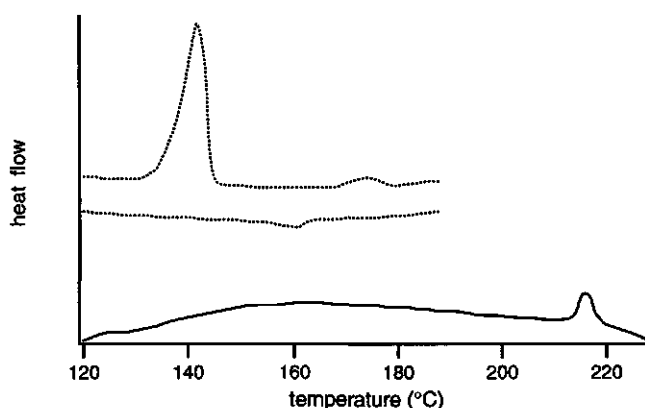


Figure 3. DSC thermograms of compound **2** as pure compound (dotted lines; heating and cooling traces) and of the 1:2 (in monomeric units) mixture with poly(acrylic acid) (solid line; heating curve). Positive peaks correspond to endothermic phase transitions.

9.3 Conclusions

The DDA-PAA complex has been shown to form ordered multivesicular assemblies in water which resemble the architecture of biological tissues. Like in biological tissues, where polypeptides and polysaccharides are known to keep the phospholipid walled cells together,¹ it is suggested that in our system DDA vesicles are held together by the PAA matrix. We have

thus made a step forward from the study of synthetic bilayer vesicles, which are model systems for single cells, to the more complex multivesicular assemblies which could be regarded as model systems for biological tissues.

Ionically bound side chain liquid crystalline polymers are readily formed by complexation of poly(acrylic acid) with double chained ammonium amphotropes. These materials have the benefits of both monomers and polymers *i.e.* a good solubility in organic solvents and broad liquid crystalline temperature ranges.

9.4 Experimental section

The lyotropic samples were prepared as follows: a solution of DDAB (0.02 M) and PAA (0.2 M in monomeric units; $M_w = 90,000$) in ethanol was cast onto a glass microscope slide to give a thin film. After drying this film was covered with pure water and subsequently heated at 80 °C for 1 minute on a Mettler FP82HT hot stage. No corrections of the pH were made (pH = 3). After cooling to room temperature the turbid films which were still covered with water were inspected by optical microscopy using an Olympus BH-2 microscope.

The amphotrope-PAA complexes were prepared by addition of an aqueous PAA solution to an aqueous vesicle dispersion of the amphotrope (2:1 in monomeric units). The precipitate was lyophilized to give a fluffy powder.

9.5 References

- 1 Darnell, J.; Lodish, H.; Baltimore, D. *Molecular Cell Biology*; Scientific American Books: New York, 1986.
- 2 Goddard, E. D. *Colloids Surf.* **1986**, *19*, 255.
- 3 Breuer, M. M.; Robb, I. D. *Chem. Ind.* **1972**, 530.
- 4 Kiefer, J. J.; Somasundaran, P.; Ananthapadmanabhan, K. P. *Langmuir* **1993**, *9*, 1187.
- 5 Hayakawa, K.; Kwak, J. C. T. *J. Phys. Chem.* **1983**, *87*, 506.
- 6 Hayakawa, K.; Santerre, J. P.; Kwak, J. C. T. *Macromolecules* **1983**, *16*, 1642.
- 7 Santerre, J. P.; Hayakawa, K.; Kwak, J. C. T. *Colloids Surf.* **1985**, *13*, 35.
- 8 Goddard, E. D. *Colloids Surf.* **1986**, *19*, 301.
- 9 Thalberg, K.; Lindman, B. *Langmuir* **1991**, *7*, 277.
- 10 Ohbu, K.; Hiraishi, O.; Kashiwa, I. *J. Am. Oil Chem. Soc.* **1982**, *59*, 108.
- 11 Goddard, E. D.; Hannan, R. B. *J. Am. Oil Chem. Soc.* **1977**, *54*, 561.
- 12 Seki, M.; Morishima, Y.; Kamachi, M. *Macromolecules* **1992**, *25*, 6540.
- 13 Antonetti, M.; Kaul, A.; Thünnemann, A. *Langmuir* **1995**, *11*, 2633.
- 14 Antonetti, M.; Burger, C.; Effing, J. *Adv. Mater.* **1995**, *7*, 751.
- 15 Okahata, Y.; Enna, G. J. *J. Phys. Chem.* **1988**, *92*, 4546.
- 16 Okahata, Y.; Enna, G. J.; Taguchi, K.; Seki, T. *J. Am. Chem. Soc.* **1985**, *107*, 5300.
- 17 Tal'roze, R.; Kuptsov, S. A.; Sycheva, T. I.; Bezborodov, V. S.; Platé, N. A. *Macromolecules* **1995**, *28*, 8689.
- 18 Tirelli, D. A.; Turek, A. B.; Wilkinson, D. A.; McIntosh, T. J. *Macromolecules* **1985**, *18*, 1512.
- 19 Brady, J. E.; Evans, D. F.; Kachar, B.; Ninham, B. W. *J. Am. Chem. Soc.* **1984**, *106*, 4279.
- 20 Regen, S. L.; Shin, J. S.; Yamaguchi, K. *J. Am. Chem. Soc.* **1984**, *106*, 2446.

- 21 Fukuda, H.; Diem, T.; Stefely, J.; Kezdy, F. J.; Regen, S. L. *J. Am. Chem. Soc.* **1986**, *108*, 2321.
- 22 Carmona-Ribeiro, A. M.; Chaimovich, H. *Biophys. J.* **1986**, *50*, 621.
- 23 Menger, F. M.; Balachander, N. *J. Am. Chem. Soc.* **1992**, *114*, 5862.
- 24 poly(2-acrylamido-2-methyl-1-propane sulfonic acid) was used.
- 25 poly(maleic acid-co-alkyl vinyl ether) II-6 was used.
Nieuwkerk, A. C.; Marcelis, A. T. M.; Sudhölter, E. J. R. *Macromolecules* **1995**, *28*, 4986.
- 26 Lasic, D. D. *Biochem. J.* **1988**, *256*, 1.
- 27 Lasic, D. D. *J. Colloid Interface Sci.* **1988**, *124*, 428.
- 28 Lasic, D. D. *J. Colloid Interface Sci.* **1990**, *140*, 302.
- 29 Ujie, S.; Iimura, K. *Macromolecules* **1992**, *25*, 3174.
- 30 Bazuin, C. G.; Tork, A. *Macromolecules* **1995**, *28*, 8877.

Chapter 10

10

Triple chained amphotropes

Abstract

A number of triple chained ammonium amphotropes has been synthesized with cyano- and nitrobiphenyl and azobenzene mesogenic moieties at the termini of their hydrophobic chains. These compounds exhibit thermotropic liquid crystalline behavior and form stable monolayers at the water-air interface. The monolayers give Z-type transfer onto hydrophilic quartz. However, the transferred material reorganizes and the morphology of the film appears to depend on the thermotropic properties of the material. For the azobenzene containing Langmuir-Blodgett multilayers molecular reorganization is observed upon irradiation with UV light or upon heating to give well ordered, centrosymmetric, homeotropically aligned films.

10.1 Introduction

In recent years, the interest in Langmuir-Blodgett (LB) technology for the preparation of thin organic films has increased enormously.¹⁻⁴ Organic molecules have the advantage that they can easily be modified and designed to exhibit a specific function. The idea of 'tailor made' molecules that would form mono- and multilayers with special, desired properties has inspired many researchers. However, the relationship between the molecular structure of compounds and the properties of their assemblies in mono- and multilayers is still poorly understood.

For example, there is great interest in non-centrosymmetric LB-multilayer assemblies.^{5,6} These assemblies show great potential as materials with piezoelectric or non-linear optical (NLO) properties. For non-chiral compounds only X- or Z-type multilayers are non-centrosymmetric. Unfortunately, X- and Z-type multilayers are often not stable and rearrange into Y-type structures by molecular turnaround.⁷ So far only few monomeric materials have been reported to produce genuine X- and Z-type multilayers.⁸⁻¹⁴

In the chapters 4, 5^{15,16} and 8 we have reported on the monolayer formation of double chained ammonium amphiphiles containing one or two mesogenic moieties. These so-called amphotropic molecules combine lyotropic and thermotropic mesomorphism and are promising candidates for the formation of non-centrosymmetric multilayer assemblies because of their bolaform structure. Furthermore, it is envisaged that it should be possible to influence the order within the layers of these amphiphiles by bringing the layers in a liquid crystalline phase and exposing them to strong electric or magnetic fields.

However, it was found that these compounds do not give stable LB-monolayers or satisfactory deposition to multilayers. We have therefore extended our work to triple chained ammonium amphiphiles with terminal mesogenic groups. Hydroxyethyl groups were introduced in the headgroup region and nitro groups at the termini to favor head-to-tail hydrogen bonding between successive layers in order to stabilize possible Z-type structures.

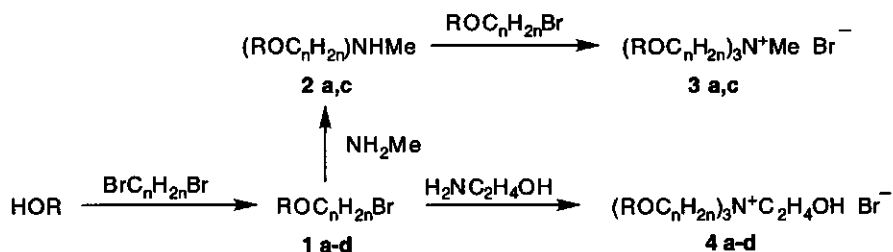
All mesogens consist of a donor- π -acceptor system. This creates the possibility to investigate the films with UV and fluorescence spectroscopy and by second harmonic generation. Besides the biphenyl mesogens, azobenzene mesogens were also investigated. The effect of the light induced trans-cis isomerization process on the organization of the individual molecules in the film has been studied.

10.2 Results and discussion

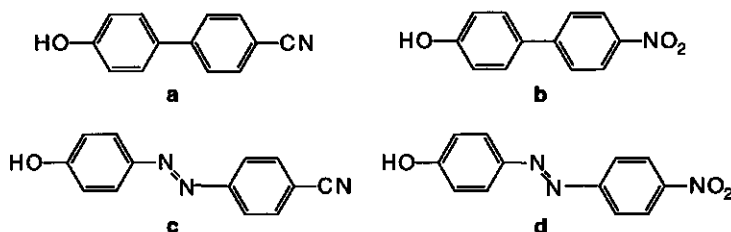
10.2.1 Thermotropic properties

The synthesis of the amphiphiles is represented in Scheme 1. The compounds **4a-d** are synthesized in a two step reaction starting from the phenols **a-d**. The synthesis of **3a** and **3c**

requires an additional step. Because monomethylamine is a gas at room temperature, direct quaternization of the amine is difficult. The monomethyl amine is therefore first alkylated with one molecule of **1a** or **1c**. The non-volatile reaction products (**2a,c**) are subsequently subjected to quaternization with two equivalents of **1a** or **1c**.



HOR =



$n = 12$ for **4 a-d** and **3 a**
 $n = 10$ for **3 c** and **2 c**

Scheme 1. Synthetic pathways and structures of compounds **3a**, **3c** and **4a-d**.

The molecular structures and the purity of the intermediates and the final products were confirmed by $^1\text{H-NMR}$ spectroscopy, thin layer chromatography (TLC) and elemental analyses. Most of the amphiphiles contained 0.5-1 mol of crystal water.

All these novel compounds show liquid crystalline phases which are probably smectic A as judged from their fan-shaped focal-conic textures as observed by polarization microscopy (Figure 1). Table 1 gives the melting points (Mp) and the phase transition temperatures of the liquid crystalline (LC) phase to the isotropic (I) phase. The phase transition enthalpies as determined by DSC are also given.

Compound **3a** shows a monotropic LC phase. Compound **4a**, on the other hand, has an enantiotropic LC phase. In this case the substitution of one methyl group for a hydroxyethyl group in the headgroup lowers the melting point below the LC-I transition temperature which itself is not affected. Upon comparing **3c** and **4c** it is again seen that the LC-I transition

temperature is not strongly influenced by a change in the headgroup region and alkyl chain length. The LC-I transition temperature seems to be determined by the mesogenic units.

It is interesting to note that for **4d** the enthalpy change for the crystalline to liquid crystalline transition is lower than for the LC-I transition. Usually this transition enthalpy is several times higher than for the LC-I transition. This may indicate that the intermolecular forces within the crystal lattice are only slightly stronger than in the LC phase. For compound **4b** no crystalline phase could be observed. This compound is isolated in a viscous smectic phase as deduced from the observed focal-conic textures (Figure 1).

Table 1. Melting Points (Mp) and Liquid Crystalline-Isotropic Phase Transition Temperatures (LC-I) and the corresponding Phase Transition Enthalpies (ΔH).

Compound	Mp (°C)	LC-I (°C)	ΔH^{mp} (kJ/mol)	ΔH^{LC-I} (kJ/mol)
3a	130	108 ^a	21	6.1
3c	94,105 ^b	172	18	7.2
4a	74	108	9	5.5
4b	- ^c	120	-	9.6
4c	145	172	25	10
4d	60	191	4	13

^a monotropic liquid crystalline phase

^b two transitions were observed in the DSC experiment

^c not observed starting from 20 °C

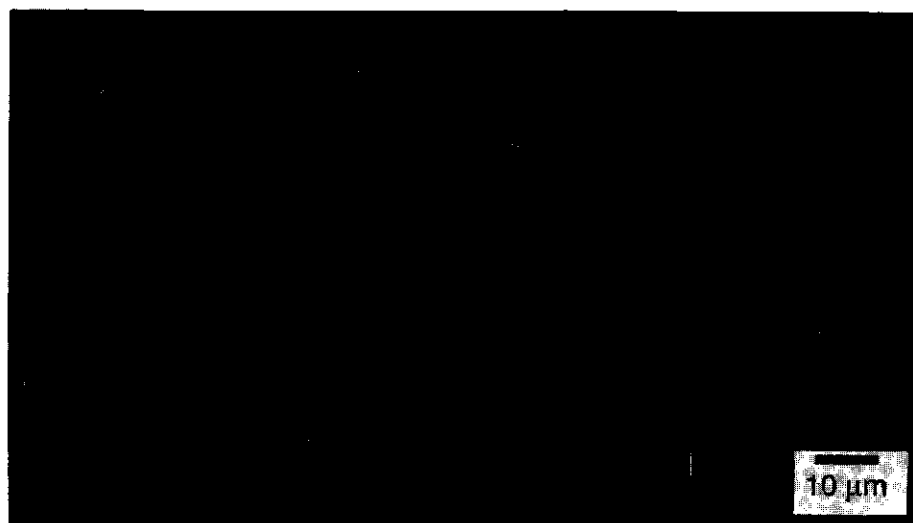


Figure 1. Polarizing optical micrograph of a smectic phase of **4b** at room temperature.

The presence of mesogenic units in these molecules enhances their tendency to form liquid crystalline phases. This might be advantageous for obtaining highly ordered LB multilayers. Apparently, the polar headgroup has a strong influence on the melting point but not on the liquid crystallinity.

10.2.2 Monolayer properties

All compounds **3** and **4** form monolayers at the water-air interface. In Figure 2 the surface pressure-area isotherms of the biphenyl compounds **3a**, **4a** and **4b** are presented. The large lift off areas of the π -A isotherms indicate that these molecules initially lie flat at the water surface.^{15,16} This orientation is favored by the positive interaction between the hydrophilic parts of the mesogens and the aqueous subphase.¹⁸⁻²⁰ Upon compression the surface pressure increases until a plateau region is reached. This can be interpreted as the point where the interaction between the mesogen part and the aqueous subphase is broken and the hydrophobic tails are lifted from the interface. The monolayer can now be compressed until all molecules are oriented with their tails toward the air. At this point, where the molecules are in a close packed arrangement, further compression leads to a steep increase in surface pressure. Ultimately, the monolayers collapse at pressures of about 25 mN/m.

The shape of the isotherms is not affected much by the rate of compression or the temperature of the subphase. Furthermore, the isotherms are reproducible upon expansion and subsequent recompression.

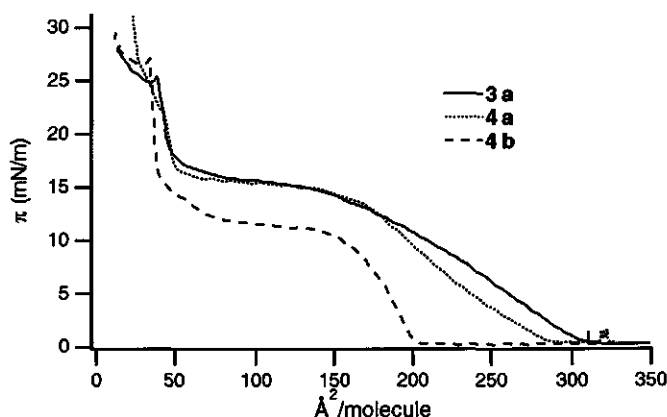


Figure 2. π -A isotherms of compounds **3a**, **4a** and **4b**.

Looking in more detail at the isotherms of **3a** and **4a**, it is seen that substitution of the methyl group by an hydroxyethyl group does not dramatically affect the π -A isotherms. This can be expected because even at the collapse area, the size of the headgroup is not large enough to influence the π -A isotherm. Surprisingly, substitution of a cyano group by a nitro group in the

mesogen has a large effect on the lift-off area and the plateau value of the surface pressure as is seen upon comparing **4a** and **4b**. This supports the rationalization that the mesogen has an interaction with the aqueous subphase, although the different mesogens might have different interactions.

The π -A isotherms of the azobenzene compounds **4c** and **4d** are given in Figure 3. Substitution of the biphenyl unit for an azobenzene moiety results in an increased lift off area because each molecule now takes up more space when it lies on the water-air interface. As for the biphenyl compounds substitution of the cyano group for a nitro group in the azobenzene unit results in a reduction of the lift off area.

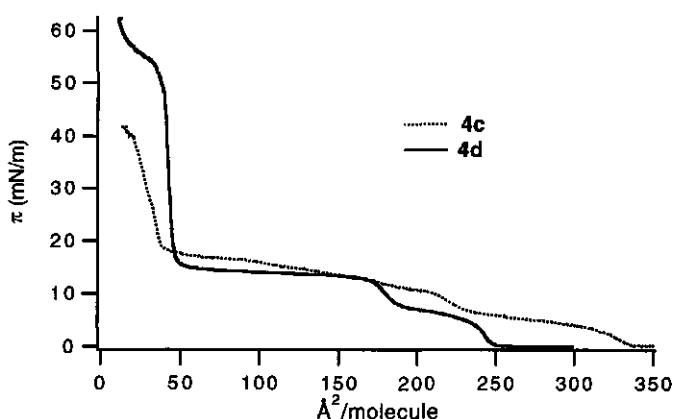


Figure 3. π -A Isotherms of compounds **4c** and **4d**.

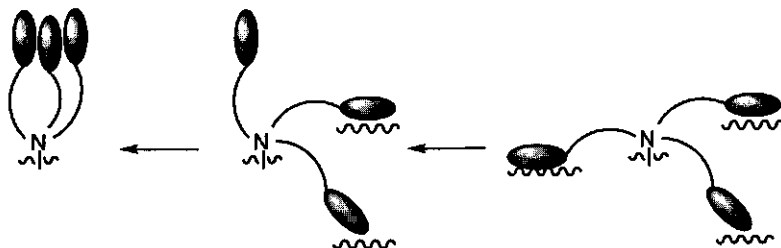


Figure 4. Schematic representation of the sequential repulsion of the hydrophobic tails from the water-air interface.

It is interesting to note that for the molecules with azobenzene mesogens two plateau regions in the π -A isotherms are observed, whereas for the biphenyl compounds only one plateau is found. This result can be tentatively explained by assuming that at the lower plateau one of the hydrophobic chains is selectively repelled from the interface and that at the second plateau both

other tails are rejected from the interface, as illustrated in Figure 4. This implies that for the biphenyl compounds there is no preference for consecutive removal of the hydrophobic chains from the interface. This difference in behavior might be related to the degree of order within the monolayer. It is suggested that the higher the degree of order, the more the molecules will experience the same lateral pressure and they will cooperatively reject their first tail. When there is less order this will cause pressure inhomogeneities within the monolayer. Consequently, not all molecules will rearrange cooperatively.

Additionally, higher collapse pressures are observed for the azobenzene containing compounds than for the biphenyl containing compounds. This is again attributed to stronger interactions between azobenzenes than between biphenyls which result in the formation of a more stable monolayer.

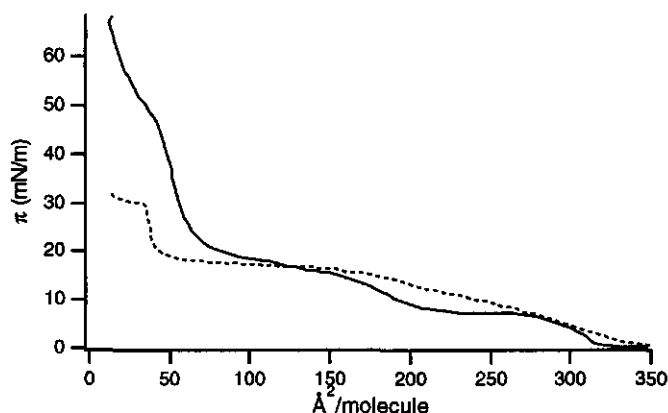


Figure 5. π -A Isotherms of **3c** before (solid line) and after irradiation (dashed line) of the spreading solution with light of 366 nm until the photostationary state is reached.

Figure 5 shows the π -A isotherms of **3c** before and after irradiation of the spreading solution with UV light (366 nm). By irradiation a part of the azobenzene moieties is converted from the linear trans isomer to the bend cis isomer. The spontaneous isomerization of these cis azobenzenes to the energetically favored trans form is slow at room temperature. We can thus be sure that a considerable amount of cis azobenzenes is present in the monolayer during the recording of the π -A isotherm. This is expected to reduce the local order within the monolayer. The effect is that the two plateaus are not distinguishable anymore. Another result of the irradiation is the lowering of the collapse pressure. Because of the different shape of the mesogens in the trans and the cis form, the mesogens no longer pack efficiently, leading to a destabilization of the monolayer.

10.2.3 Langmuir-Blodgett films

The monolayers of **3a**, **3c** and **4b** and **4d** can be transferred onto hydrophilic quartz in a Z-type (head-to-tail) deposition with transfer ratios of approximately unity. Compounds **4a** and **4c**, which have a hydroxyethyl group in combination with a cyano group, give lower transfer ratios. After deposition of the first layer during upstroke movement of the substrate the surface remains hydrophilic owing to the presence of terminal hydrophilic cyano or nitro groups. Therefore, both the advancing and receding contact angles of the water meniscus are $< 90^\circ$, resulting in Z-type transfer.

Inspection of the transferred layers of **3a** with Atomic Force Microscopy (AFM) reveals a surface covered with microcrystals (data not shown). This suggests that crystallization of the transferred material occurs after or during the deposition. Deposited films (ten monolayers) of **3c** are also not flat, showing altitude differences of 20-50 nm, indicating that here also reorganization has taken place. However, no crystallites are seen which could mean that the material is in an undercooled liquid crystalline state.

Compounds **4b** and **4d** have a hydroxyethyl group, which is a hydrogen bond donor, in the headgroup and nitro groups, which are hydrogen bond acceptors, at their termini. Despite the possibility for stabilization of Z-type multilayer assemblies by head-to-tail hydrogen bonding, no significant second harmonic generation was found for the transferred multilayers of either of these compounds. This means that stable Z-type structures are not obtained. It seems that for these compounds the driving force for molecular turnaround cannot be compensated by this type of head-to-tail hydrogen bonding.

The UV absorption spectrum of multilayers of **3c** transferred onto quartz is given in Figure 6. The absorption band at 370 nm is somewhat distorted with respect to the monomer spectrum (not shown) because of the aggregated state of the molecules. When the quartz slide is positioned at different angles with respect to the propagation direction of the light beam, the UV spectra of these layers are identical. This means that the aggregates are randomly oriented in the transferred material.

When the transferred material is irradiated with (non polarized) UV light, the intensity of the absorption band at 370 nm decreases as shown in Figure 6. As can be seen in Figure 7, now a blue shifted absorption band at 330 nm appears when the angle between the propagation direction of the light and the normal to the quartz slide is increased (60°). The appearance of a blue-shifted band indicates the presence of parallel chromophore stacks (so-called H-aggregates).²³⁻²⁵ The fact that this absorption band is not seen when the propagation direction of the light is perpendicular to the quartz slide (0°) means that the transition dipole moments of the H-aggregates are directed perpendicular to the quartz surface. In this case there is no overlap between the electronic vector of the irradiated light and the transition dipole moment of the mesogens, which lies approximately parallel to the long axis of the mesogen.²⁶ By irradiation we have thus obtained a homeotropic smectic phase in which layers of molecules lie parallel to

the quartz surface. This was also confirmed by polarized UV absorption measurements. This homeotropically aligned phase does not show any second harmonic generation indicating that the structure is fully centrosymmetric (head-to-head, tail-to-tail).

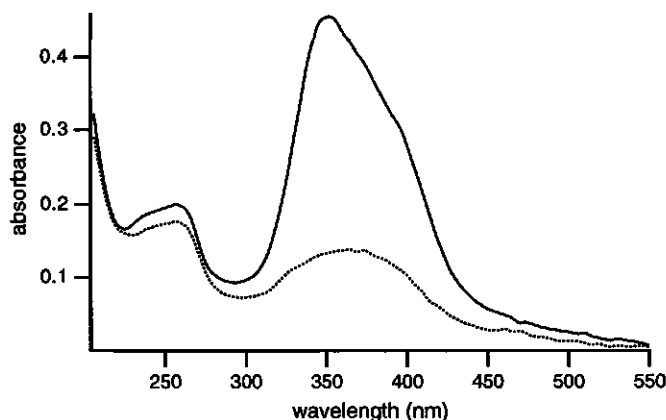


Figure 6. UV absorption spectra of LB-multilayers of compound **3c** transferred onto quartz (15 monolayers on each side): immediately after transfer (solid line) and after 10 minutes of irradiation at 366 nm with an intensity of 10-20 mW/cm² (dashed line).

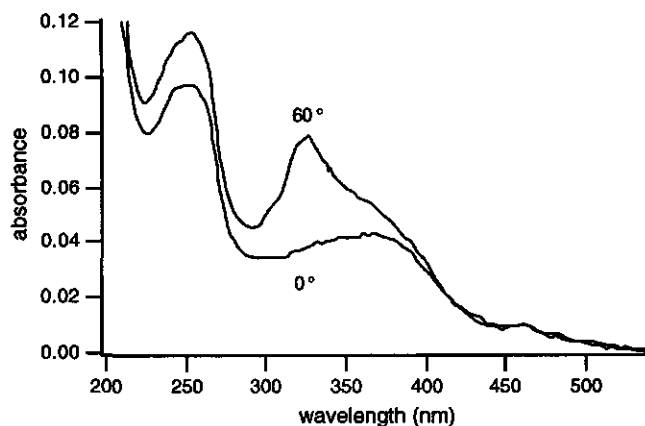


Figure 7. UV absorption spectra of transferred LB-monolayers of compound **3c** (5 monolayers on each side) after 10 minutes of irradiation at 366 nm with an intensity of 10-20 mW/cm². The angle between the light beam and the normal of the quartz slide is varied (0° and 60°).

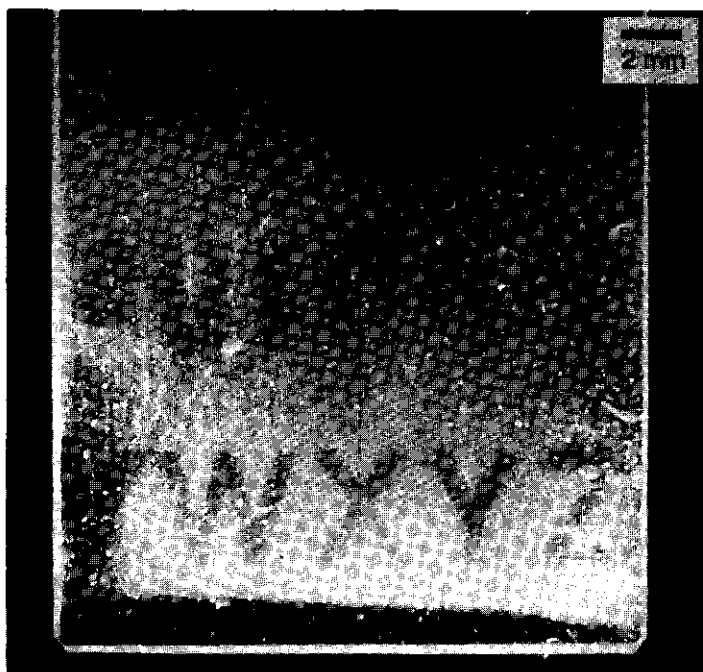


Figure 8. Image of a quartz slide which is covered with ten LB monolayers of **3c**. The clear (dark) patterns are obtained by irradiation of the film with UV light of 366 nm (no contrast amplification).

The same homeotropic arrangement could be obtained by heating the transferred material (not irradiated) to approximately 90 °C. This suggests that in the transferred material the molecules are in a thermodynamically unstable situation where an energy barrier prevents the formation of the more stable homeotropic phase. This homeotropic smectic phase is probably stabilized by the possibility of extensive π - π stacking and a positive alignment interaction with the substrate. Upon heating the material the molecules are given the energy to form the aligned phase.

It is known that irradiation of disordered films of azobenzene containing materials can lead to photoinduced optical anisotropy.²⁷⁻³¹ The irradiated light causes trans-cis isomerization of the azobenzene units followed by a reorientation (the probability for the molecular axis returning to the original position is small). This sequence of absorption, isomerization and reorientation will be repeated until the transition dipole moment of the trans azobenzene lies parallel to the propagation direction (or perpendicular to the polarization direction) of the light. This photoselection process can induce a macroscopic anisotropy. The obtained situation is usually not thermodynamically stable.

In most cases described in the literature, the anisotropy is lost upon heating of the irradiated layers.²⁷⁻³¹ For LB-layers of **3c** an anisotropic order is spontaneously attained upon heating

which remains even after cooling, indicating that the formation of the homeotropic phase is energetically favorable. Because photoselection is based on statistical reorganization of the molecules, it would be very unlikely that structures in which the mesogens are all perfectly stacked would be formed. It is therefore assumed that for **3c** the irradiation induced anisotropy is not caused by photoselection but that upon irradiation the molecules are given enough energy to surpass the energy barrier to form the energetically favored homeotropic phase. Spincoated films of **3c** behave in the same way as the LB-films, although upon spincoating a portion of the molecules immediately enters the homeotropic phase.

Recently, Schönhoff *et al.*³² have observed a similar phenomenon upon irradiation of LB films of azobenzene containing molecules. They speculated that the excitation energy is not able to induce trans-cis isomerization which is sterically hindered in these films. Instead, the excitation energy will be dissipated as thermal energy. This causes the irradiated material to melt locally. The subsequent reorganization of the material will be driven by a reduction the total surface energy.

Because irradiation of these LB-films leads to a fading of the color (see also Figure 6) and reduction of the turbidity due to reorganization of the molecules, it is possible to write in these layers by means of UV light. The written patterns are stable for at least several months (Figure 8). Unfortunately, the layers are not thermally stable, because upon heating above 90 °C the remaining molecules also assume the homeotropic alignment and the patterns disappear. After heating the molecules cannot be reoriented anymore, because even after bringing the molecules into the isotropic phase, the homeotropic phase is reformed upon cooling.

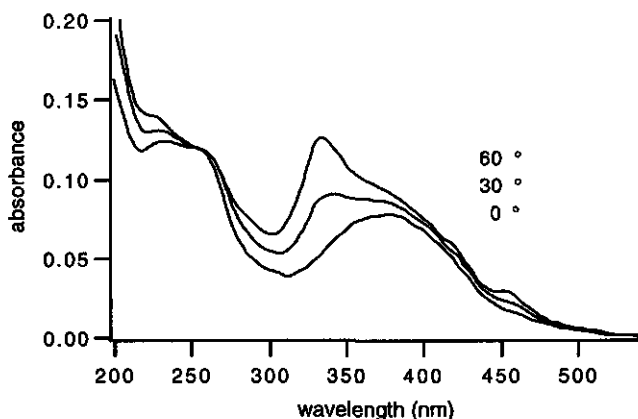


Figure 9. UV absorption spectra of LB-monolayers of compound **4d** transferred onto quartz (7 monolayers on each side). The angle between the light beam and the normal of the quartz slide is varied (0°, 30° and 60°).

Compound **4d** gives a homeotropic phase (head-to-head, tail-to-tail) directly after LB transfer or spincoating. X-ray diffraction analysis suggests that the mesogenic units are interdigitated in this phase. This compound has a lower melting point than **3c**, which could be the reason that the homeotropic phase can be reached at room temperature, whereas for **3c** it is kinetically limited at room temperature. Figure 9 shows the UV spectra of LB multilayers of **4d** at three different angles of incidence. The presence of H-aggregates perpendicular to the substrate is clearly seen.

Compound **4b** does not give a homeotropic phase upon LB transfer or spincoating. Not even after heating. Instead a smectic bulk phase is formed which shows identical UV spectra under different angles. This shows the importance of the azobenzene mesogen in inducing the homeotropic phase.

10.3 Conclusions

A series of novel triple chained ammonium amphiphiles containing terminal biphenyl and azobenzene mesogens has been synthesized. All these novel compounds form stable monolayers at the water-air interface. The molecules initially lie flat at the water surface but upon compression the hydrophobic tails are lifted from the interface. The compounds with the azobenzene mesogens give π -A isotherms with two plateaus and high collapse pressures, whereas the compounds with biphenyl mesogens give only one plateau and relatively low collapse pressures. This is explained by a greater ordering in the monolayers of the azobenzene compounds caused by the stronger interaction between azobenzenes than between biphenyls. Substitution of a cyano group for a nitro group in the mesogen has a major influence on the π -A isotherms indicating that the mesogens play an important role in the different interactions at the aqueous subphase. These novel compounds show Z-type transfer (head-to-tail) onto quartz, but the multilayers are not stable and reorganize, despite of the possibility of head-to-tail hydrogen bonding. This reorganization probably already occurs during the transfer process. None of the transferred layers shows second harmonic generation. The final aggregation form that is obtained after Z-type transfer depends on the thermotropic properties of the compounds and the nature of the mesogen. Compound **3a**, which has a high melting point and a monotropic LC phase is found to crystallize after deposition. For **4b**, which is liquid crystalline at room temperature the transferred layers show no homeotropic alignment. The azobenzene containing compound **4d**, which has a low melting point (60 °C) forms a homeotropic smectic phase after LB deposition or spincoating. At room temperature this compound has enough kinetic energy to form the head-to-head, tail-to-tail homeotropic phase. The azobenzene containing compound **3c** (Mp = 96 °C) gives an undercooled LC phase. During the transfer process molecular turnaround occurs toward the favored homeotropic alignment, but this process stops

prematurely probably because it is kinetically inhibited. Only by irradiation with UV light or by heating above 90° C the molecules are given enough energy to form the homeotropic smectic phase. This phenomenon can be applied in the field of optical data-storage because we can write patterns in these layers using UV light.

10.4 Experimental section

10.4.1 Synthesis

4'-Cyano-4-hydroxybiphenyl (**a**) was obtained from Merck. 4-Hydroxy-4'-nitrobiphenyl (**b**) was synthesized as described previously.^{5,6} 4'-Cyano-4-hydroxyazobenzene (**c**) and 4-hydroxy-4'-nitroazobenzene (**d**) were prepared by reaction of the diazonium salts of 4-nitroaniline or 4-aminobenzonitrile with phenol.¹⁷

12-Bromo-1-RO-dodecane (**1a-d**)

A mixture of 25 mmol of the appropriate phenol (**a-d**) and 50 mmol of 1,12-dibromododecane and 50 mmol K₂CO₃ in 100 mL of 2-butanone was refluxed for 16 h. The salt was removed by filtration and the filtrate was concentrated by evaporation of the solvent. The product was purified by column chromatography on silica gel using petroleum ether (bp. 40-60 °C)/CH₂Cl₂, 1:1 (v/v) as eluent. Yield 60 %.

¹H-NMR (CDCl₃, TMS, δ, ppm): 1.40 (m, 16 H, -(CH₂)₈-), 1.80 (m, 4 H, Br-CH₂-CH₂-, RO-CH₂-CH₂-), 3.40 (t, 2 H, Br-CH₂-), 4.00 (t, 2 H, RO-CH₂-), 7.00- 8.30 (m, 8 H, Ar-H).

N-(12-RO-dodecyl)-*N*-methylamine (**2a**)

A solution of 0.5 g of the bromide **1a** in 20 mL of a solution of monomethylamine in CHCl₃ (25% w/w) was kept for 16 h at room temperature. The solvent and the excess of monomethylamine were distilled off and the residue was dissolved in CHCl₃ and extracted with water. The organic layers were dried on MgSO₄ and the pure product was obtained by removal of the solvent. Yield 100 %.

¹H-NMR (CDCl₃, TMS, δ, ppm): 1.40 (m, 16 H, -(CH₂)₈-), 1.82 (m, 4 H, N-CH₂-CH₂- and RO-CH₂-CH₂-), 2.65 (s, 3 H, N-CH₃), 2.98 (m, 2 H, -CH₂-N), 4.00 (t, 2 H, RO-CH₂-), 7.00- 8.30 (m, 8 H, Ar-H).

Compound **2c** was synthesized with a decyl spacer by the same method as used for **2a**.

N,N,N-Tris(12-RO-dodecyl)-*N*-methyllumonium bromide (**3a**)

A mixture of 0.1 g of **2a** and a twofold excess of the appropriate bromide (**1a**) and a twofold excess of NaHCO₃ in 10 mL of acetonitrile was heated at 130 °C for 48 h in a closed reaction vessel. The solvent was distilled off and the residue was treated with CH₂Cl₂ and filtered to remove the salts. The product was purified by column chromatography on silica gel with CH₂Cl₂/MeOH 10/1 (v/v) as eluent. Yield 50 %.

¹H-NMR (CDCl₃, TMS, δ, ppm): 1.40 (m, 48 H, -(CH₂)₈-), 1.80 (m, 12 H, N-CH₂-CH₂-, RO-CH₂-CH₂-), 3.32 (s, 3 H, N-CH₃), 3.43 (m, 6 H, -CH₂-N), 4.00 (t, 6 H, RO-CH₂-), 7.00-8.30 (m, 24 H, Ar-H).

Compound **3c** was synthesized with a decyl spacer by the same method as used for **3a**.

3a: Anal. Calcd for C₇₇H₁₀₁N₄O₄Br (1 H₂O): C, 75.15; H, 8.38; N, 4.16. Found: C, 75.27; H, 8.29; N, 4.83. **3c**: Anal. Calcd for C₇₀H₈₇N₁₀O₄Br (1.3 H₂O): C, 68.92; H, 7.40; N, 11.48. Found: C, 68.92; H, 7.16; N, 10.97. Melting points are given in Table 1.

***N,N,N*-tris(12-RO-dodecyl)-*N*-hydroxyethylammonium bromide (4a-d)**

A mixture of 10 mg (0.16 mmol) of ethanolamine, a threefold excess of a bromide (1a-d) and a threefold excess of NaHCO₃ in 10 mL of acetonitrile was heated for 48 h at 130 °C in a closed reaction vessel. The solvent was distilled off and the residue was treated with CH₂Cl₂ and filtered to remove the salt. The product was purified by column chromatography on neutral aluminum oxide (activity grade III) with CH₂Cl₂/MeOH 100/3 (v/v) as eluent. Yield 50 %.

¹H-NMR (CDCl₃, TMS, δ, ppm): 1.40 (m, 48 H, -(CH₂)₈-), 1.80 (m, 12 H, N-CH₂-CH₂- and RO-CH₂-CH₂), 3.40 (m, 6 H, (-CH₂)₃N-CH₂-CH₂-OH), 3.48 (m, 2 H, (-CH₂)₃N-CH₂-CH₂-OH), 4.00 (t, 6 H, RO-CH₂-), 4.13 (m, 2 H, (-CH₂)₃N-CH₂-CH₂-OH), 5.44 (t, 1 H, -OH), 7.00-8.30 (m, 24 H, Ar-H).

4a: Anal. Calcd for C₇₇H₁₀₁N₄O₄Br (1.3 H₂O): C, 73.98; H, 8.35; N, 4.48. Found: C, 73.93; H, 8.22; N, 4.53. 4b: Anal. Calcd for C₇₄H₁₀₂N₄O₁₀Br (1 H₂O): C, 68.13; H, 7.96; N, 4.30. Found: C, 68.10; H, 7.81; N, 4.26. 4c: Anal. Calcd for C₇₇H₁₀₁N₁₀O₄Br (1 H₂O): C, 70.56; H, 7.77; N, 10.69. Found: C, 71.42; H, 7.84; N, 10.87. 4d: Anal. Calcd for C₇₄H₁₀₁N₁₀O₁₀Br (1 H₂O): C, 64.85; H, 7.43; N, 10.22. Found: C, 65.14; H, 7.33; N, 10.21. Melting points are given in Table 1.

10.4.2 Methods

The π-A isotherms were recorded on a Lauda FW2 Filmwaage, which was thermostatted at 20 °C. The water used for the subphase was purified by filtration through a Seralpur Pro 90C purification system. The amphiphiles were spread from chloroform solutions (1 mg/mL) onto the aqueous subphase by use of a Hamilton syringe. After spreading, the monolayer was allowed to equilibrate for 5 minutes before compression started. A compression speed of 15 cm²/min was used.

Monolayers were transferred onto hydrophilic quartz at a constant surface pressure of 20 mN/m with vertical dipping speeds of 1 mm/min, except monolayers of 3e which were transferred at a pressure of 35 mN/m. The quartz substrates were thoroughly cleaned before usage by sonication in dichloromethane followed by treatment with chromic acid. The slides were rinsed with ultrapure water and dried in a stream of nitrogen.

The azobenzene samples were irradiated with a CAMAG, Universal UV-Lampe 29230 at 366 nm. The samples were positioned at a distance of 2-3 cm from the UV-source where the radiation has an estimated intensity of 10-20 mW/cm². The UV spectra were recorded on a Varian, Cary 13E spectrophotometer. Polarization microscopy was performed using an Olympus BH-2 microscope equipped with a Mettler FP82HT hot stage and a FP80HT temperature controller. Differential scanning calorimetry measurements were performed on a Perkin Elmer DSC 7 apparatus. Atomic Force Microscopy measurements were carried out on a Digital Instruments Nanoscope II FM instrument.

10.5 References

- Swalen, J. D.; Allara, D. L.; Andrade, J. D.; Chandross, E. A.; Garoff, S.; Israelachvili, J.; McCarthy, I. J.; Murray, R.; Paese, R. F.; Rabolt, J. F.; Wynne K. J.; Yu, H. *Langmuir* **1987**, *3*, 932.
- Ulman, A. *An Introduction to Ultrathin Films*; Academic Press: San Diego, 1991.
- MacRitchie, F. *Chemistry at Interfaces*; Academic Press: San Diego, 1990.
- Tredgold, R.H. *Order in Thin Organic Films*; Cambridge University Press: Cambridge, 1994.
- Ou, S. H.; Percec, V.; Mann, J. A.; Lando, J. B.; Zhou, L.; Suger, K. D. *Macromolecules* **1993**, *26*, 7263.
- Ou, S. H.; Percec, V.; Mann, J. A.; Lando, J. B. *Langmuir* **1994**, *10*, 905.
- Honig, E. P. *J. Colloid Interface Sci.* **1973**, *43*, 66.

- 8 Popovitz-Biro, R.; Hill, K.; Shavit, E.; Hung, D. J.; Lahav, M.; Leiserowitz, L.; Sagiv, J.; Hsiung, H.; Meredith, G. R.; Vanherzeele, H. *J. Am. Chem. Soc.* **1990**, *112*, 2498.
- 9 Popovitz-Biro, R.; Hill, K.; Lahav, M.; Leiserowitz, L.; Sagiv, J.; Hsiung, H.; Meredith, G. R.; Vanherzeele, H. *J. Am. Chem. Soc.* **1988**, *110*, 2672.
- 10 Ledoux, I.; Josse, D.; Vidakovi, P.; Zyss, J.; Hann, R. A.; Gordon, P. F.; Bothwell, B. D.; Gupta, S. K.; Allen, S.; Robin, P.; Chastaing, E.; Dubois, J. C. *Europhys. Lett.* **1987**, *3*, 803.
- 11 Ashwell, G. J.; Jackson, P. D.; Crossland, W. A. *Nature* **1994**, *368*, 438.
- 12 Senoh, T.; Sanui, K.; Ogata, N. *Chem. Lett.* **1990**, 1849.
- 13 See reference 2 p 339-363 and references herein.
- 14 Watakabe, A.; Okada, H.; Kunitake, T. *Langmuir* **1994**, *10*, 2722.
- 15 Everaars, M. D.; Marcelis, A. T. M.; Sudhölter, E. J. R. *Langmuir* **1993**, *9*, 1986.
- 16 Everaars, M. D.; Marcelis, A. T. M.; Sudhölter, E. J. R. *Thin Solid Films* **1994**, *78*, 242.
- 17 Furniss, B. S.; Hannaford, A. J.; Smith, P. W. G.; Tachell, A. R. *Vogel's Textbook of Practical Organic Chemistry*; Longman Scientific & Technical: Harlow, 1989, p. 949.
- 18 Heesemann, J. *J. Am. Chem. Soc.*, **1980**, *101*, 2167.
- 19 Heesemann, J. *J. Am. Chem. Soc.*, **1980**, *101*, 2176.
- 20 Menger, F. M.; Richardson, S. D.; Wood, M. G.; Sherrod, M. J. *Langmuir* **1989**, *5*, 833.
- 21 Ulman, A.; Scaringe, R. P. *Langmuir* **1992**, *8*, 894.
- 22 Shnidman, Y.; Ulmann, A.; Eilers, J. E. *Langmuir* **1993**, *9*, 1071.
- 23 Fukuda, K.; Nakahara, N. *J. Colloid Interface Sci.* **1984**, *98*, 555.
- 24 Mentzel, H.; Weichart, B.; Schmidt, A.; Paul, S.; Knoll, W.; Stumpe, J.; Fisher, T. *Langmuir* **1994**, *10*, 1926.
- 25 Sato, T.; Ozaki, Y. *Langmuir* **1994**, *10*, 2363.
- 26 Uznanski, P.; Kryszewski, M.; Thulstrup, E. W. *Spectrochimica Acta* **1990**, *46 A*, 23.
- 27 Yokoyama, S.; Kakimoto, M.; Imai, Y. *Langmuir* **1993**, *9*, 1086.
- 28 Gibbons, W. M.; Shannon, P. J.; Sun, S. T.; Swetlin, B. J. *Nature* **1991**, *351*, 49.
- 29 Hank, G.; Koswig, H. D.; Ruhmann, R.; Rübner, J.; Stumpe, J.; Müller, L.; Kreysig, D. *Makromol. Chem., Rapid Commun.* **1991**, *12*, 81.
- 30 Wiesner, U.; Reynolds, N.; Boeffel, C.; Spiess, H. W. *Makromol. Chem., Rapid Commun.* **1991**, *12*, 8.
- 31 Ivanov, S.; Yakovlev, I.; Kostromin, S.; Shibaev, V. *Makromol. Chem., Rapid Commun.* **1991**, *12*, 709.
- 32 Schönhoff, M.; Chi, L. F.; Fuchs, H.; Lösche, M. *Langmuir* **1995**, *11*, 163.

Summary

When the structural characteristics of amphiphiles and thermotropic liquid crystals are combined in one molecule *i.e.* a polar headgroup with apolar tails and mesogenic units, compounds are obtained which can exhibit both thermotropic and lyotropic mesomorphism. This class of compounds is called amphotropic liquid crystals.

This thesis deals with the study of new amphotropic compounds. The majority of the new amphotropes consist of a cationic ammonium headgroup with one, two or three hydrophobic tails containing different mesogenic units, although some compounds with anionic headgroups have also been investigated. The goal of this thesis is to correlate the molecular structure with the self-assembling behavior of these compounds. Special attention has been given to the effect of different mesogenic units on the aggregation behavior of these compounds in water and at the water-air interface.

The single chained amphotropes form micellar aggregates in water. Interestingly, these aggregates are better stabilized by azobenzene mesogens than by biphenyl or stilbene mesogens, despite the more hydrophilic character of azobenzene. This is attributed to stronger π - π stacking interactions between azobenzene mesogens than between biphenyl and stilbene mesogens. The polarizable azo-group might give rise to extra dispersion interactions between the mesogens thus favoring self-aggregation (Chapter 2).

The formation of ion-pair amphiphiles from these amphotropic ammonium compounds and sodium dodecylsulfate as second component can directly be monitored by UV absorption spectroscopy and fluorescence spectroscopy. These ion-pair amphiphiles form bilayer vesicles which precipitate shortly after preparation (Chapter 2).

When an *o*-hydroxyazobenzene unit is incorporated into a single chained ammonium amphiphile, a molecule is obtained which can effectively complex Cu^{2+} ions. This results in an extra stabilization of the formed aggregates in water and this complexation can be monitored by optical spectroscopy. This system is a very sensitive probe for the quantitative detection of minor concentrations of Cu^{2+} ions in water (Chapter 3).

The double chained amphotropes all form bilayer vesicles in water (Chapter 4 and 5). These bilayer membranes show a phase transition from a rigid gel phase at low temperatures to a more mobile liquid crystalline phase at higher temperatures, as is also known to occur in biomembranes. The phase transition temperature is very dependent on the nature of the substituents at the mesogenic units. The phase transition temperature is however not related to the net dipole moment of the mesogenic units. Therefore, dispersion interactions rather than electrostatic interactions between the permanent dipoles of the mesogens determine the strength of the mesogen-mesogen interactions (Chapter 4).

The 4-cyanobiphenyl-4'-oxy mesogenic unit shows large solvatochromic shifts of its fluorescence maximum. Amphotropes carrying this mesogen are therefore good probes to

monitor the micropolarity in all kinds of lyotropic aggregates. The obtained results are in good agreement with previous studies using pyrene as a probe (Chapter 5).

In the bilayer membranes of these amphotropes the mesogenic units form H-aggregates which results in a blue shift of the UV absorption maximum of the mesogenic units. The extent of this blue shift is a direct measure for the ordering of the molecules in the bilayer. This offers the possibility to study a great number of membrane processes in detail. The process of monomer transfer between bilayer vesicles of these amphotropes and bilayer vesicles of nonmesogenic double chained amphiphiles has been studied in this way (Chapter 6). This transfer process is sometimes a one-way migration of the amphotropes to the bilayer vesicles of the other amphiphile. Depending on the nature of the amphotrope the reverse process can also occur. For the solubilization of bilayers of amphotropes in micelles of other surfactants the same processes were found. Additionally, these transfer processes have also been studied by differential scanning calorimetry and titration microcalorimetry (Chapter 6).

The effect of polymerization of the bilayer membrane on the ordering of the molecules in the bilayer has also been studied. The molecular ordering is clearly reduced upon polymerization. The stability of the membrane however increases (Chapter 7).

The orientation of the mesogenic units along the long axis of the molecule influences the aggregation behavior in water and at the water-air interface. This is not due to contributions of the dipole moments of the mesogenic units but can rather be attributed to steric effects. (Chapter 8).

Complexes of these double chained ammonium amphotropes or didodecyldimethylammonium bromide with poly(acrylic acid) form tissue-like structures in water which can be regarded as model systems for biological tissues. Complexes of double chained ammonium amphotropes with poly(acrylic acid) can be considered to be ionically bound liquid crystalline side chain polymers and they exhibit very broad liquid crystalline temperature ranges (Chapter 9).

The triple chained amphotropes form stable monolayers at the water-air interface. These molecules initially lie flat at the water surface and upon compression the hydrophobic chains are one by one expelled from the water surface. The compressed monolayers can be transferred onto solid substrates. Subsequent layers are transferred in a head-to-tail mode. These transferred layers are however not stable and reorganize to a head-to-head and tail-to-tail packing. Eventually a thin film of (liquid) crystalline material is obtained. In the case of the compound with azobenzene mesogens, the orientation of the molecules in the film can be influenced by irradiation with UV light. This offers the possibility to write patterns in these films; an optical data storage device (Chapter 10).

Samenvatting

Wanneer de structuurkenmerken van amfifielen en thermotrope vloeibare kristallen worden verenigd in één molecuul d.w.z. een polaire kopgroep met apolaire staarten en mesogene eenheden, dan worden stoffen verkregen die zowel thermotroop als lyotroop mesomorfisme kunnen vertonen. Dit type verbindingen noemen we amfotrope vloeibare kristallen of kortweg amfotropen.

In dit proefschrift wordt een studie aan een serie nieuwe amfotrope verbindingen beschreven. Het merendeel van deze nieuwe amfotropen bevat een kationische ammoniumkopgroep en één, twee of drie apolaire staarten met verschillende typen aromatische mesogene eenheden, hoewel ook enkele verbindingen met anionische kopgroepen zijn onderzocht. De doelstelling van het onderzoek is het correleren van de moleculaire structuur met de zelfordenende eigenschappen van deze verbindingen. Vooral is gekeken naar het effect van verschillende mesogene eenheden op het aggregatiegedrag van deze verbindingen in water en aan het water-lucht grensvlak.

De enkelstaartige amfotropen vormen micellaire structuren in water. Opvallend is dat deze aggregaten beter worden gestabiliseerd door azobenzeenmesogenen dan door bifenyl- of stilbeenmesogenen, ondanks het meer hydrofiele karakter van azobenzeen. Dit wordt toegeschreven aan sterkere π - π stacking interacties tussen azobenzenen dan tussen bifenylen of stilbenen. De polariseerbare azogroep zou kunnen zorgen voor extra dispersie interacties tussen de mesogenen wat de zelfaggregatie ten goede komt (Hoofdstuk 2).

De vorming van ionpaaramfifielen van deze amfotrope ammonium verbindingen met natrium dodecylsulfaat als tweede component kan direct worden gevolgd met UV absorptie-spectroscopie en fluorescentiespectroscopie. Deze ionpaaramfifielen vormen bilaagvesikels, maar deze kristalliseren kort na de bereiding uit (Hoofdstuk 2).

Wanneer een *o*-hydroxyazobenzeeneenheid wordt geïncorporeerd in een enkelstaartige amfifiel, dan wordt een verbinding verkregen die zeer efficiënt Cu^{2+} ionen kan binden. Dit resulteert in een extra stabilisatie van de gevormde aggregaten in water en kan optisch worden gedetecteerd. Dit systeem is zeer gevoelig voor de kwantitatieve detectie van Cu^{2+} ionen in water (Hoofdstuk 3).

De dubbelstaartige verbindingen vormen allen bilaagvesikels in water (Hoofdstuk 4 en 5). Deze bilaagmembranen vertonen een faseovergang van een rigide gelfase bij lage temperatuur naar een vloeibaar-kristallijne fase bij hogere temperatuur, net zoals bekend is voor biomembranen. De faseovergangstemperatuur is erg afhankelijk van het type substituent aan de mesogene eenheid (Hoofdstuk 4). De faseovergangstemperatuur is echter niet gerelateerd aan het netto dipoolmoment van de mesogene eenheid. Het zijn blijkbaar eerder dispersie interacties dan dipolaire interacties tussen de permanente dipolen van de mesogenen die de sterkte van de mesogeen-mesogeen interactie bepalen.

De 4-cyanobiphenyl-4'-oxy mesogene eenheid vertoont aanzienlijke solvatochrome verschuivingen van haar fluorescentiemaximum. Amfotrope verbindingen met deze

mesogene eenheid zijn dan ook geschikt om the micropolariteit in allerlei lyotrope systemen te bepalen. De resultaten komen goed overeen met polariteitsstudies uitgevoerd met pyreen (Hoofdstuk 5).

In bilaagmembranen van amfotrope verbindingen liggen de mesogene eenheden netjes gestapeld hetgeen resulteert in een blauwverschuiving van het UV-absorptiemaximum van de mesogenen. De mate van deze verschuiving is een directe maat voor de ordening van de moleculen in de bilaag. Dit biedt de mogelijkheid om een groot aantal membraanprocessen in detail te bestuderen. Zo is het proces van monomeeruitwisseling tussen bilaagmembranen van deze amfotrope verbindingen en gewone dubbelstaartige amfifielen in detail bestudeerd (Hoofdstuk 6). Dit uitwisselingsproces is soms een éénrichtingsverkeer van de amfotrope verbindingen naar de bilagen van het andere amfifiel. Afhankelijk van de aard van de amfotrope verbinding kan soms ook het omgekeerde proces optreden. Hetzelfde geldt voor het oplossen van bilaagmembranen van deze amfotrope verbindingen in micellen van andere surfactanten. Deze processen zijn daarnaast ook bestudeerd met differential scanning calorimetry en titratie microcalorimetrie (Hoofdstuk 6).

Verder is gekeken naar het effect van polymerisatie van de membraan op de ordening van de moleculen in de bilaag. De moleculaire ordening neemt duidelijk af als gevolg van polymerisatie. De stabiliteit van de membraan wordt daarentegen wel groter (Hoofdstuk 7).

De richting van de mesogene eenheid langs de lengte-as van het molecuul beïnvloedt het aggregatiegedrag in water en aan het water-lucht grensvlak. Dit lijkt niet te worden veroorzaakt door het dipoolmoment van de mesogene eenheden maar eerder door sterische effecten (Hoofdstuk 8).

Complexen van sommige dubbelstaartige amfotrope ammoniumverbindingen of didodecyldimethylammonium bromide met polyacrylzuur vormen complexe microstructuren in water die kunnen worden beschouwd als een modelsysteem voor biologische weefsels. Complexen van dubbelstaartige amfotrope ammoniumverbindingen met polyacrylzuur kunnen worden beschouwd als ionisch gebonden vloeibaar-kristallijne zijketenpolymeren en vertonen uitgebreide vloeibaar-kristallijne temperatuurtrajecten (Hoofdstuk 9).

De driestaartige amfotrope verbindingen vormen stabiele Langmuir monolagen aan het water-lucht grensvlak. Deze moleculen liggen aanvankelijk plat op het water maar bij compressie worden de staarten één voor één uit het water gedrukt. De gecomprimeerde monolagen kunnen worden getransfereerd op vaste substraten. De opeenvolgende lagen worden kop-naar-staart overgedragen. Deze getransfereerde multilagen zijn echter niet stabiel en reorganiseren naar een kop-naar-kop en staart-naar-staart pakking. Uiteindelijk wordt een ultradunne film (vloeibaar) kristallijn materiaal verkregen (1 tot 20 monolagen). In het geval van de verbinding met de azobenzenemesogenen kan de oriëntatie van de moleculen in de film worden beïnvloed door de laag te bestralen met UV licht. Op deze manier kan in deze ultradunne lagen worden geschreven; een optisch dataopslagsysteem dus (Hoofdstuk 10).

Curriculum Vitae

Marcel Dialma Everaars werd geboren op 22 juni 1970 te Asola (Italië). In 1988 behaalde hij het VWO diploma aan het Christelijk Lyceum Arnhem. In datzelfde jaar werd begonnen met de studie Moleculaire Wetenschappen aan de Landbouwniversiteit Wageningen. Tijdens de doctoraalfase werden de afstudeervakken Fysisch-Organische Chemie en Moleculaire Fysica gevolgd. In augustus 1992 werd het doctoraalexamen *cum laude* afgelegd. In de periode van 1 oktober 1992 tot 1 oktober 1996 was hij als assistent in opleiding verbonden aan de vakgroep Organische Chemie van de Landbouwniversiteit Wageningen, alwaar het in dit proefschrift beschreven onderzoek werd uitgevoerd.

Sinds 16 oktober 1996 is hij werkzaam als research-chemicus bij Océ-Nederland in Venlo.

List of publications

The contents of most chapters of this thesis has been published in article form.

- 1) M. D. Everaars, A. T. M. Marcelis, E. J. R. Sudhölter
Aggregation Behavior of Double Chained Ammonium Amphiphiles Containing
Cyanobiphenyloxy Units
Langmuir **1993**, *9*, 1986-1989 (Chapter 5)
- 2) M. D. Everaars, A. T. M. Marcelis, E. J. R. Sudhölter
Monolayer Formation of Synthetic Ammonium Amphiphiles Carrying Cyanobiphenyloxy
Mesogens
Thin Solid Films **1994**, *242*, 78-82 (Chapter 5)
- 3) M. D. Everaars, A. T. M. Marcelis, E. J. R. Sudhölter
Molecular Ordering in Langmuir-Blodgett Films of Triple Chained Ammonium Amphiphiles
Containing Mesogenic Moieties
Colloids Surf. A: Physicochem. Eng. Asp. **1995**, *102*, 117-126 (Chapter 10)
- 4) M. D. Everaars, A. T. M. Marcelis, A. J. Kuijpers, E. Laverdure, J. Koronova, A. Koudijs,
E. J. R. Sudhölter
Effects of Introduction of Mesogenic Units in Ammonium Amphiphiles on the Aggregation
Behavior in Water
Langmuir **1995**, *11*, 3705-3711 (Chapters 2 and 4)
- 5) M. D. Everaars, A. T. M. Marcelis, E. J. R. Sudhölter
Monomer Transfer and Solubilization of Bilayer Vesicles from Double Chained Ammonium
Amphiphiles Carrying Aromatic Units
Langmuir **1996**, *12*, 3462-3467 (Chapter 7)
- 6) M. D. Everaars, A. C. Nieuwkerk, S. Denis, A. T. M. Marcelis, E. J. R. Sudhölter
Superstructures from Didodecyldimethylammonium Bromide and Polyacrylic Acid
Langmuir **1996**, *12*, 4042-4043 (Chapter 9)
- 7) M. D. Everaars, A. T. M. Marcelis, E. J. R. Sudhölter
Effect of Polymerization on Chromophore Stacking in Bilayer Membranes
Langmuir **1996**, *12*, 3964-3968 (Chapter 7)

- 8) M. D. Everaars, A. T. M. Marcelis, E. J. R. Sudhölter
Monolayer and Bilayer Stability of Ammonium Amphiphiles Carrying Azobenzene Units;
Effects of Substituents at the Azobenzene Units
Recl. Trav. Chim. Pays Bas, accepted (Chapter 4)
- 9) M. D. Everaars, A. T. M. Marcelis, E. J. R. Sudhölter
Metal Ion Complexation by an Ammonium Amphiphile Carrying an *o*-Hydroxyazobenzene
Unit
to be submitted (Chapter 3)
- 10) M. D. Everaars, A. T. M. Marcelis, E. J. R. Sudhölter
Effects of Mesogen Orientation in Double-Chained Amphotropic Ammonium Compounds on
their Self-Aggregation
to be submitted (Chapter 8)

